Total synthesis and biochemical evaluation of azumamides A–E and analogs

Villadsen, Jesper

Publication date:
2015

Document Version
Publisher's PDF, also known as Version of record

Total synthesis and biochemical evaluation of azumamides A–E and analogs

PhD Thesis by Jesper Villadsen

Technical University of Denmark

Department of Chemistry

2800 Kgs. Lyngby

Preface

The work presented in this thesis was performed during a three year Ph.D. study in the Department of Chemistry at the Technical University of Denmark (DTU). The project was financed by the Lundbeck Foundation and the work was carried out under the competent supervision of Associate Professor Christian Adam Olsen. This thesis is submitted in agreement with the requirements presented for obtaining the Ph.D. degree at DTU. The work is divided into six chapters, where the first chapter is aimed at introducing the reader to the research area and at the same time presenting the background for the projects. Chapter two and three cover the experimental efforts and results related to the work done on the azumamide projects. Chapter two describes the total synthesis of azumamides A–E and the preparation of two epimeric analogs, whereas chapter three is focused on the synthesis of azumamide analogs. Finally, chapter four presents the research conducted during my three months stay abroad at the Institute for Research in Biomedicine (IRB), at the University of Barcelona. At IRB, I had the pleasure of working in the group of Professor Fernando Albericio.

First, I would like to thank Christian for giving me the opportunity to do research in his group and for introducing me to the fascinating area of chemical biology. I am grateful for our collaboration through the last three years and I have enjoyed our scientific discussions. Furthermore, I would like to thank the rest of my colleagues in the Olsen group for creating an outstanding and inspiring place to work. Especially, Dr. Andreas Stahl Madsen for proofreading this thesis and Helle Esbjørn Kristensen for conducting the biochemical profiling of azumamides A–E and the epimeric analogs. A special thanks to Alex Maolanon, for sharing thoughts and ideas on the azumamide projects and Associate Professor Pernille Harris is acknowledged for performing the X-ray experiments. Charlotte H. Gotfredsen and Casper Hoeck are gratefully acknowledged for their efforts on producing NMR solution structures. I would like to thank all the technicians in building 201. Brian Ekman-Gregersen and Janne Rasmussen are acknowledged for ordering of all the chemicals, Tina Gustafsson for assistance during HPLC, LC-MS, or GC-MS problems, and Anne E. Hector for support on NMR experiments. The rest of the staff in building 201 is also gratefully acknowledged for sharing knowledge and being good co-workers. Professor Fernando Albericio deserves special thanks for inviting me into his excellent research group and for giving me the opportunity to discover Spain and Barcelona.

Finally, I would like to thank my family and friends for providing support through the last three years. I am forever indebted to my dear girlfriend, Marie, for her love, support, and guidance throughout my studies.

Jesper Villadsen

Kgs. Lyngby, December 2013

Abstract

Histone deacetylases (HDAC) are a family of enzymes, which serve as epigenetic modulators. Their biological function has been related to DNA transcription and regulation of various biochemical pathways. Development of isoform selective HDAC inhibitors could be useful for dissecting the individual biochemical pathways associated with each HDAC isoform and these compounds could potentially serve as anti-cancer drugs. Macrocyclic peptides and depsipeptides is an interesting class of HDAC inhibitors, which are found in Nature. These compounds are characterized by being highly potent and moderate selective HDAC inhibitors and we turned our attention to a class of cyclic tetrapeptides, known as azumamides. We developed a synthetic route, which allowed us to complete the total synthesis of azumamides A–E. This is the first reported total synthesis of azumamide B–D and our results validate the proposed structures. The key step in this route is a diastereoselective Mannich reaction, which enabled us to prepare two site-specifically edited epimeric azumamide analogs, where the stereochemistry in the unique β-amino acid was inverted. The two epimeric homologs were screened together with azumamide A–E against the entire panel of recombinant HDAC isoforms. Thus, providing the first full profiling of the azumamides. The epimers were inactive against the full panel of HDAC enzymes and show that the β-amino acid scaffold is highly sensitive to modifications in the stereochemistry. The profiling of the natural products showed that the azumamides are poor inhibitors of class IIa HDACs, but potent inhibitors of HDAC1–3, 10, and 11 (IC_{50} values between 14 to 67 nM). Furthermore we showed that carboxylic acid containing compounds (azumamide C and E) were more potent than their carboxyamide counterparts (azumamide A and B). Isoform selectivity was observed in class I and class IIb. In class I, azumamides C and E were 60–350-fold more potent towards HDAC1–3 over HDAC8 and in class IIb they were >200-fold more potent against HDAC10 over HDAC6. Finally, we found that azumamide C was ~2-fold more potent than azumamide E, which indicate having a tyrosine residue in the macrolactam ring increase the activity compared to the phenylalanine homolog.

The synthetic route was elaborated to produce structurally edited azumamide analogs. A series of β^2-desmethylated compounds were synthesized in parallel to a series of β^2-dimethylated analogs. Having observed the importance of the aromatic amino acid in the azumamides, a tryptophan-series was also prepared. The synthesis of these compounds underline the broad perspective and flexibility of the developed Mannich strategy. The dimethylated analogs were found to be poor HDAC inhibitors and only the tryptophan-containing compound showed activity below 20 μM. The removal of the β^2-methyl group induced a 1.5–18-fold loss in potency across the different isoforms. The methyl group was found to be less important for inhibition of HDAC 6 and 8 (1.5–3-fold decrease in activity). Based on NMR solution structures we hypothesize that the β^2-methyl group, found in the natural products, guides the β^3-side chain towards the active site. Judging from the biochemical data on the desmethylated series, this directing feature is important for the activity of this type of inhibitors. Furthermore, a β^3-propyl azumamide C analog was developed in order to investigate the effect of the zinc-binding moiety. Preliminary testing showed that this compound was active against HDAC3 with an IC_{50} of 3 μM. The straight forward synthesis of the β-amino acid required for this analog also illustrate the effectiveness of the developed Mannich reaction.

On a different project, a promising Bsmoc-based scaffold was probed to serve as a linker in anti-body drug conjugates (ADC) and preliminary results encourage further investigations of this strategy.

Resumé

Histone deacetylaser (HDAC) er en familie af enzymer, der fungerer som epigenetiske modulatorer. Deres biologiske funktion er blevet relateret til transskription af DNA og regulering af forskellige biokemiske processer. Udviklingen af isoform selektive HDAC inhibitorer kunne være nyttig i forhold til at identificere de biokemiske processer, som er forbundet med de enkelte HDAC isoformer og disse inhibitorer kunne have potentiale som anti-cancer lægemidler. Makrocykliske peptider er en interessant klasse af HDAC inhibitorer. Disse molekyler er karakteriseret ved at være potente og moderate selektive HDAC inhibitorer og vi fokuserede på en klasse af naturligt forekommende cykliske tetrapeptider, kendt som azumamider. Vi udviklede en syntesevej som gjorde os i stand til at syntetisere azumamid A–E. Dette er den første totalsyntese af azumamid B–D og vores resultater bekræfter de originale strukturer. Det vigtigste trin i vores syntesevej er en diastereoselektiv Mannich-reaktion, som gjorde det muligt at syntetisere to azumamid epimere, hvor vi har vendt stereokemien i den unikke β-aminosyre. Disse to epimere blev screenet sammen med azumamid A–E mod alle 11 HDAC enzymer. Dette resulterede in den første fyldestgørende HDAC karakterisering af azumamiderne. De to epimere var inaktive mod samtlige HDAC enzymer og illustrerer at β-aminosyren er følsom for modifikationer i stereokemien. Karakteriseringen af azumamid A–E viste a azumamiderne er svage inhibitorer af klasse I enzymerne, men potente mod HDAC1–3, 10 og 11 med IC50-værdier mellem 14 nM til 67 nM. Derudover viste vores resultater at de azumamider, som indeholder carboxylsyrer (azumamid C og E) er mere potente end de azumamider som indeholder et amid (azumamid A og B). Vi observerede isoform-selektivitet i klasse I og IIb. I klasse I var azumamid C og E mellem 60 og 350 gange mere potente mod HDAC1–3 i forhold til HDAC8 og i klasse II var de mere end 200 gange mere potente mod HDAC10 i forhold til HDAC6. Vores resultater indikerede også at det er mere favorabelt at have tyrosin i det cykliske peptid i forhold til phenylalanin.

Vi har anvendt vores fleksible og robuste syntesevej til at syntetisere en række azumamid analoger. Vi syntetiserede både en serie af β^2-desmethylerede og β^2-dimethylerede analoger. På baggrund af resultaterne med azumamiderne valgte vi også at syntetisere en serie af analoger, hvor vi introducerer tryptophan i stedet for tyrosin og phenylalanin. Syntesen af disse analoger viser at vores syntesevej er fleksibel og kan anvendes til at producere nye azumamid analoger. De dimethylerede analoger viste sig at være dårlige HDAC inhibitorer og kun det molekyle som indeholdt tryptophan var aktivt ved koncentrationer under 20 µM. De desmethylerede analoger var mellem 1,5 og 18 gange dårligere en naturstofferne til at inhibere de fleste enzymer. De isoformer som var mindst påvirkede af demethyleringen var HDAC6 og 8. Baseret på NMR strukturer af disse molekyler foreslår vi at β^2-methyl gruppen, som er til stede i azumamiderne, kan dirigerer den zink-bindende β^3-sidekæde mod det aktive site. Ud fra den biokemiske screening af de desmethylerede analoger ser det ud til a denne dirigering er vigtig for aktiviteten af disse molekyler.

For at undersøge effekten af den zink-bindende gruppe, fremstillede vi også en β^3-propyl azumamid C analog. Denne analog blev testet på HDAC3 og viste sig at være aktiv med en IC50 på 3 µM. Denne analog kunne også syntetiseres ved hjælp af vores Mannich strategi og bekræftede endnu en gang den brede anvendelse af vores syntesevej.

Jeg har også arbejdet på at udvikle en ny linker til fremstillingen af anti-body drug conjugates. I et forsøg på at validere konceptet bag denne linker, syntetiserede jeg en række forskellige molekyler med baggrund i Bsmoc-beskyttelsesgruppen. Stabilitetstestning af disse molekyler indikerede at denne strategi kunne danne baggrund for udviklingen af nye linkere.

Abbreviations

aa	Amino acid
Ac	Acetyl
ADC	Antibody-drug conjugates
ADP	Adenosine diphosphate ribose
Ala	Alanine
AMC	4-amino-4-methylcoumarin
Aoda	2-amino-8-oxodecanoic acid
Asp	Aspartic acid
BAIB	Bis(acetoxy)iodobenzene
BAK	Bcl-2 homologous antagonist/killer
Bcl	B-cell lymphoma
Bcl-xl	B-cell lymphoma extra large
BINAP	2,2'-bis(diphenylphosphino)-1,1'-binaphthyl
Bn	Benzyl
Boc	tert-butyloxycarbonyl
Boc	*Tert*-butyloxycarbonyl
BSA	Bovine serum albumine
Bsmoc	1,1-dioxobenzo[b]thiophene-2-ylmethyloxycarbonyl
Cbz	Carboxybenzyl
CDI	Carbonyldiimidazole
CHAP	Cyclic hydroxamic acid-containing peptide
CNS	Central nervous system
CTCL	Cutaneous T-cell lymphoma
dr	Diastereoisomeric ratio
DBU	1,8-diazabicyclo[5.4.0]undec-7-ene
DDQ	2,3-Dichloro-5,6-dicyano-1,4-benzoquinone
DFT	Density function theory
DIC	N,N´-diisopropylcarbodiimide
DMAP	4-dimethylaminopyridine
DMF	N,N-dimethylfromamide
DMP	Dess–Martin periodinane
DMSO	Dimethylsulfoxide
DNA	Deoxyribonucleic acid
DPPA	Diphenylphosporyl azide
DR	Death receptor
DTS	Diverted total synthesis
ee	Enatiomeric excess
EDC	1-Ethyl-3-(3-dimethylaminopropyl)carbodiimide
equiv	Equivalent
FDA	Food and Drug Administration
FDPP	Pentafluorophenyl diphenylphosphinate
Fmoc	9-flourenylmethyloxycarbonyl
GSH	Glutathione
h	Hour
HAT	Histone acyltransferase
HATU	1-[Bis(dimethylamino)methylene]-1H-1,2,3-triazolo[4,5-b]pyridinium 3-oxid hexafluorophosphate

HCT-116	Human colon adenocarcinoma
HDAC	Histone deactylase
HDAH	(HDAC)-like amidohydrolase
HDLP	Histone deacetylase-like protein
His	Histidine
HMBA	Hexamethylenebisacetamide
HMPA	Hexamethylphosphoramide
HOBt	1-hydroxy-7-benzotriazole
HOBt	1-Hydroxybenzotriazole
HPLC	High performance liquid chromatography
IC	Inhibitory concentration
*i*Pr	Isopropyl
KDAC	Lysine deacetylase
KDM	Lysine demethylases
KHMDS	Potasiumhexamethyldisilazide
KMT	Lysine methyltransferase
LC-MS	Liquid chromatography mass spectrometry
LDA	Lithium diisopropylamide
LTMP	Lithium 2,2,6,6-tetramethyl piperidide
MBD	Methyl binding domain
mCPBA	*meta*-chloroperoxybenzoic acid
MeCpG2	Methyl CpG binding protein 2
MEF2	Myocyte enhance factor
MELC	Murine-virus-infected erythroleukemia cells
min	Minutes
MMPP	Magnesium monoperoxyphtalate
mp	Melting point
MsCl	Methanesulfonyl chloride
NAD	Nicotinamide adenine dinucleotide
N-CoR	Nuclear receptor corepressor
NMI	*N*-methyl imidazole
NMO	*N*-methylmorpholine-*N*-oxide
NMR	Nuclear magnetic resonance
p53	Tumor protein 53
PDB	Protein data bank
PG	Protection group
Phe	Phenylalanine
PMB	Paramethoxybenzyl
PMB	*para*-methoxybenzyl
PMP	*para*-methoxyphenyl
rt	Room temperature
SAHA	Suberoylanilide hydroxamic acid
SAR	Structure activity relationship
Sir	Sirtuin
SMRT	Silencing mediator for retinoid or thyroid-hormone receptors
SPPS	Solid-phase peptide synthesis
TBAF	Tetrabutylammonium fluoride
TBAI	Tetrabutylammonium iodide
TBSCl	*tert*-Butyl(chloro)dimethylsilane
^{t}Bu	*tert*-butyl

Tce	Trichloroethane
TEMPO	2,2,6,6-Tetramethylpiperidin-1-yl)oxy
Tf	Trifluoromethanesulfonyl
TFA	Trifluoroacetic acid
THF	Tetrahydrofuran
TMS	Trimethylsilyl
TNF	Tumor necrosis factor
TPSCl	2,4,6-Triisopropylbenzenesulfonyl chloride
TRAIL	TNF-related apoptosis-inducing ligand
Trp	Tryptophan
TS	Transition state
TSA	Trichostatin
TSCl	4-Toluenesulfonyl chloride
Tyr	Tyrosine
Val	Valine
VLC	Vacuum Liquid Chromatography

Publications

Publications

Villadsen, J. S.; Stephansen, H. M.; Maolanon, A. R.; Harris, P.; Olsen, C. A., Total Synthesis and Full Histone Deacetylase Inhibitory Profiling of Azumamides A–E as Well as β^2- epi-Azumamide E and β^3-epi-Azumamide E. *Journal of Medicinal Chemistry* **2013,** *56* (16), 6512-6520.

Publications in preparation

Maolanon, A. R; Villadsen, J. S.; Hoeck, C.; Gotfredsen, C. H.; Harris, P; Olsen, C. A., Structural editing of the azumamide scaffold: Synthesis and structure–activity relationships. (manuscript in preparation for submission to Chemical Science)

Contents

1 Introduction

1.1 Epigenetics

In living organisms the hereditary information is stored in the DNA, which exist as a double-stranded helical structure. DNA pass on the genetic information from one generation to another and it determines which proteins that are available to the organism. DNA is transcribed into mRNA by the RNA polymerase and subsequent translation by the ribosome creates the target protein. Cells within an organism contain the same DNA and therefore have the potential to differentiate into many different specialized cell types. The differentiation of a specific cell is regulated by transcription and translation of specific DNA regions. These DNA regions code for proteins that are specific for a given cell phenoptype. The underlying mechanism that regulates and controls cell differentiation, is complex. In order to understand the different factors involved, it is advantageous to examine how the DNA is organized and stored within the cells. The double-stranded DNA is wrapped around core histone proteins to create the nucleosome. The nucleosome particle is build up of 145 bp of DNA, which is coiled 1.7 times around one histone protein octamer.[1] These octamers consist of two copies of each of the four core histone proteins: H2A, H2B, H3, and H4. The nucleosomes are anchored to the DNA strand by H1.[2, 3] The histone proteins organize on the DNA strand like "beads on a string" and fold up to produce chromatin 30 nm fibers (Figure 1-1). Kornberg[4] and Olins[5] were the first to report this ordered structure using electron microscopy. The 30 nm fibers are condensed into loops (around 300 nm in length), which are further folded into larger fibers (250 nm wide). The coiling and compression of the 250 nm wide fiber results in a chromatid, which make up one-half of the chromosome during cell division.

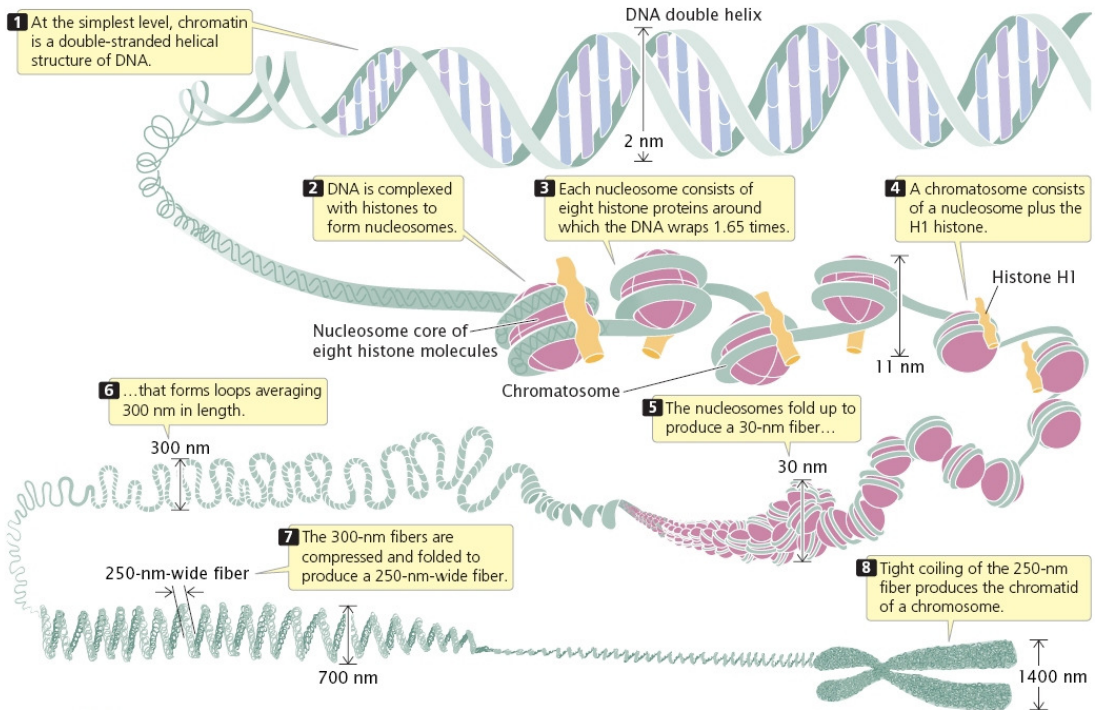

Figure 1-1. Illustration of DNA packaging in cells. (Adapted from Annunziato, A.)[6]

The transcription and translation of specific genes can be regulated by external modifications, which do not change the DNA sequence. The study of these modifications is termed epigenetics. One of the most studied epigenetic modifications is DNA-methylation. Methylation of DNA occurs on two nucleobases, cytosine (C) and adenine (A), and is catalyzed by DNA methyl transferases. The primary target for methylation of the DNA is the cytosine component of CpG islands, where a cytosine is found next to a guanine (G). These CpG islands

are often found in promoter regions on the DNA and in general the methylation of CpG islands is associated with gene silencing. When the CpG dinucleotide is methylated the different transcription factors are unable to recognize the DNA, leading to gene silencing. Furthermore, it is believed that methylated CpG islands attract proteins called methyl-CpG-binding domains (MBD), which are involved in transcriptional repression.[7] Another well described epigenetic mechanism is acetylation of lysine side chains in proteins which interact with the DNA. There is an abundance of lysine residues in the amino-terminal tail of all four core histone proteins. Post-translational modifications of these tails, and in particular of the lysine residues, play a key role in gene expression as well as histone assembly and deposition.[8,9]

A variety of post-translational modifications can occur on the *N*-terminal tails of histones. The most important modifications are acetylation and methylation, however phosphorylation and adenosine diphosphate ribose (ADP)-ribosylation have also been found.[9] Histone methylation occurs primarily on the side chain of lysine residues, but methylation of arginine side chains have also been observed.[10] The methylation state is controlled by histone lysine methyltransferases (KMTs) and demethylases (KDMs). Lysine residues can be either mono-,di- or tri-methylated and the different methylation degrees can lead to either transcriptional activation or repression. Furthermore, methylation is mostly found in H3 and H4 on specific lysine residues. For instance, methylation of H3K4, H3K36, and H3K79, found in the coding region or around the transcription start site of the gene, is associated with gene activation. In contrast, methylation of H3K9 and H3K27 in the promoter region results in silencing of the gene.[11] The methyl group functions as a recruiter of either repressive proteins or activator proteins, depending on which lysine it is located on. Therefore, the methylation state is closely related to the transcriptional balance in the cell. Tight regulation of the KMT and KDM activities is essential to maintain the transcriptional balance and misregulation is believed to promote cancer.[12, 13] The mechanisms and biological pathways responsible for cancer development in cells with a poorly regulated histone methylation state is not clear. However, activation of oncogenes and silencing of tumor-suppressor genes is likely to be involved.[13]

1.2 Histone acetyltransferases (HATs) and histone deacetylases (HDACs)

The acetylation/deactylation of histones takes place on the *ε*-amino groups of the lysine residues and the equilibrium is regulated by histone acetyl transferases (HATs) and histone deacetylases (HDACs). HATs catalyze the acetylation of the amino groups and the HDACs catalyze the reverse reaction (Scheme 1-1).

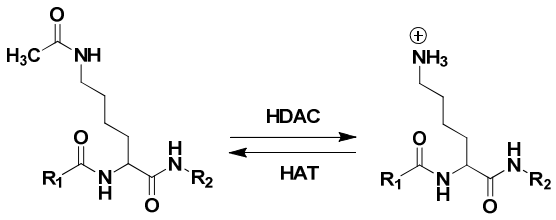

Scheme 1-1. Lysine modifications catalyzed by HDACs and HATs.

HDACs also target non-histone proteins and currently these enzymes are often referred to as lysine deactylases (KDACs), as to describe their function rather than their target.[14] Deacetylation of the *ε*-amino group results in a positive charge on the nitrogen at physiological pH. This positive charge can interact strongly with the negative charges on the DNA backbone and the DNA–histone complex will adapt a compact and folded structure that impairs transcription.[15, 16] In the acetylated form, the nitrogen atom will be neutral and the interaction between the histones and the DNA is significantly weaker. This reduced interaction allows a more flexible and unfolded DNA–histone complex and the DNA can be accessed by the transcriptional machinery (Figure 1-2).

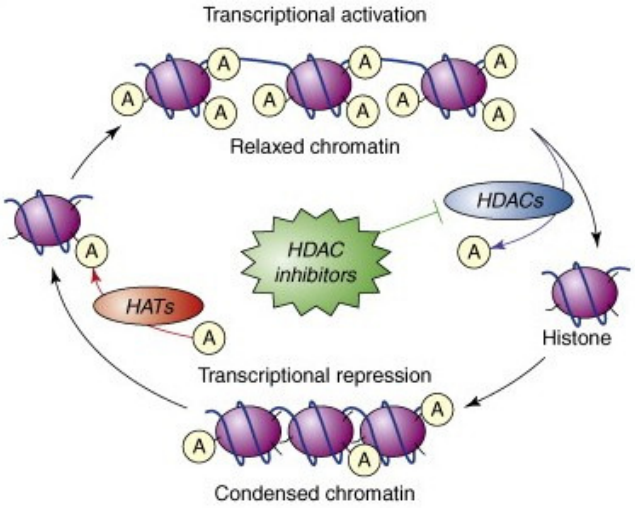

Figure 1-2. The roles of HATs and HDACs in DNA transcription. (Adapted from Chiu et al.)[17]

The first mammalian HDAC was isolated by Stuart Schreiber in 1996[18] and in the same year David Allis cloned the first HAT.[8] Today, the HDAC family consists of 18 isoforms where HDAC11 was the last enzyme to enter the family.[19] The HDACs are categorized into four classes (Table 1-1). The grouping of isoforms is based on the structural resemblance to the homologous yeast proteins.[20] Class I (HDAC1, 2, 3, and 8), class II (HDAC4, 5, 6, 7, 9, and 10) and class IV (HDAC11) are Zn^{2+} dependent enzymes, whereas class III, called sirtuins (SIRT1–7)[21] are nicotinamide adenine dinucleotide (NAD)-dependent.[22] Class II HDACs are further divided into two sub classes, class IIa (HDAC4, 5, 7, and 9) and class IIb (HDAC6 and 10).

Table 1-1. Classification of the KDAC family.

Class	HDAC isoform	Catalytic requirements
I	HDAC1-3, HDAC8	Zn^{2+}
IIa	HDAC4, 5, HDAC7, HDAC9	Zn^{2+}
IIb	HDAC6, HDAC10	Zn^{2+}
III	SIRT1-7	NAD^{+}
IV	HDAC11	Zn^{2+}

1.2.1 Class I HDACs

Gregoretti and co-workers have performed phylogenetic analysis on HDAC and shown that HDAC1 and 2 may originate from a single metazoan HDAC1/2 protein.[22] This hypothesis is supported by the evidence that HDAC1 and 2 both exist in similar complexes *in vivo*, including NurD[23], CoREST[24], and Sin3.[25, 26] The enzymes are similar in function and sequence, but if HDAC1 is removed in embryonic mouse cells, the cell growth is impaired and proliferation is disturbed.[27] This result shows that HDAC2 is unable to perform all the functions performed by HDAC1. The major structural difference between HDAC1 and 2, is a region found in the *C*-termini of HDAC2. This region is predicted to form *α*-helical coils, which could mediate interaction with other proteins. In HDAC1, the same region is not believed to have the same preference for formation of *α*-helical coils. This structural variance could explain some of the functional differences observed between the two isoforms. Interestingly HDAC1 has been found to form dimers with itself and HDAC2.[28, 29] A HDAC association domain (HAD), which is located in the *N*-terminus of HDAC1, was reported to be essential for dimerization. HDAC1 and 2 are primarily found in the nucleus of the cell in contrast to HDAC3, which is able to translocate to the cytoplasm.[30, 31] Translocation of HDAC3 to the cytoplasm can indicate that this isoform, at least in part,

has non-nuclear substrates. The translocation can to some extent be attributed to interaction of HDAC3 with chromosome region maintenance 1 (CRM1), which is believed to bind a region between residue 180–313 and direct the enzyme to the cytoplasm. HDAC3 forms homo-dimers and trimers *in vivo* and participate in multiprotein complexes.[30] Key complexes have been found to be N-CoR1, N-CoR2, (Nuclear Receptor Corepressor 1 or 2) and SMRT (Silencing Mediator for Retinoid or Thyroid-hormone receptors).[32, 33] Analogous to HDAC1 and 2, the domain associated with self-assembly is found within the first 122 residues in the *N*-terminal. Interestingly, the SMRT/NCoR HDAC3 complex interacts with the class II enzymes: HDAC4, 5, 7, and 10.[34] The last member of class I is HDAC8, which seems to be different in terms of function and the ability for form complexes. HDAC8 is phylogenetic distinct from the remaining class I enzymes and displays a lower preference for acetylated substrates. Furthermore, inhibitors of HDAC1–3, are often less active against HDAC8.[35]

1.2.2 Class II HDACs

Class II HDACs are divided into two subclasses as shown in Table 1-1. Class IIa include HDAC4, 5, 7, and 9. All four proteins contain a highly conserved C-terminal catalytic domain.[36] Interestingly, the expression of class IIa HDAC has been found to be tissue-specific. These enzymes are primarily found in muscle cells, and in particular in skeletal and heart muscle cells, whereas class I HDACs are ubiquitously expressed.[36] In terms of cellular distribution, the class IIa HDACs shuttle between the nucleus and the cytoplasm and the activity of the enzymes is controlled by the cellular localization.[37, 38] The shuttling of class II HDACs is mediated through binding to a family of proteins, known as 14-3-3 proteins. The 14-3-3 proteins facilitate the transport of the enzymes from the nucleus to the cytoplasm and is associated with transcriptional repression. The phosphorylation of three serine residues, found in the *N*-terminal of the HDAC enzymes, is essential for binding to 14-3-3 proteins.[39] Similar to HDAC3, class IIa HDACs also interact with SMRT and N-CoR1/2 through domains found in the *C*-terminal (Figure 1-3). Interestingly, class II enzymes only display deacetylase activity when bound to the SMRT/NCoR–HDAC3 complex, but no activity is observed *in vitro* when bound to SMRT/NCoR alone. Thus, class IIa HDACs may not be functional enzymes on their own, but contribute to the recruitment of the SMRT/NCoR–HDAC3 complex.[36] HDAC4 has been shown to self-associate through a 17 residue domain found in the *N*-terminal.[40] A similar domain is found in HDAC5 and 9, but currently the self-assembly of these isoforms has not been reported. The same *N*-terminal domain is involved in the interaction between class IIa HDACs and one of their major targets: myocyte enhancer factor 2 (MEF2)(Figure 1-3). MEF2 proteins are key players in the functional delivery of class IIa HDACs to their DNA targets. MEF2 recognize specific promoter regions on the DNA and thus carry the HDACs to their site of action.[41] MEF2 delivery to specific promoter regions is critical for myocyte development and disturbance of this pathway is associated with defects in myocyte differentation.[36] In a similar manner class IIa enzymes can associate with methyl CpG binding protein 2 (MeCP2), which also recruit the HDAC complexes to their DNA targets. Both MEF2 and MeCP2 directed delivery of class IIa HDACs results in transcriptional repression.[42]

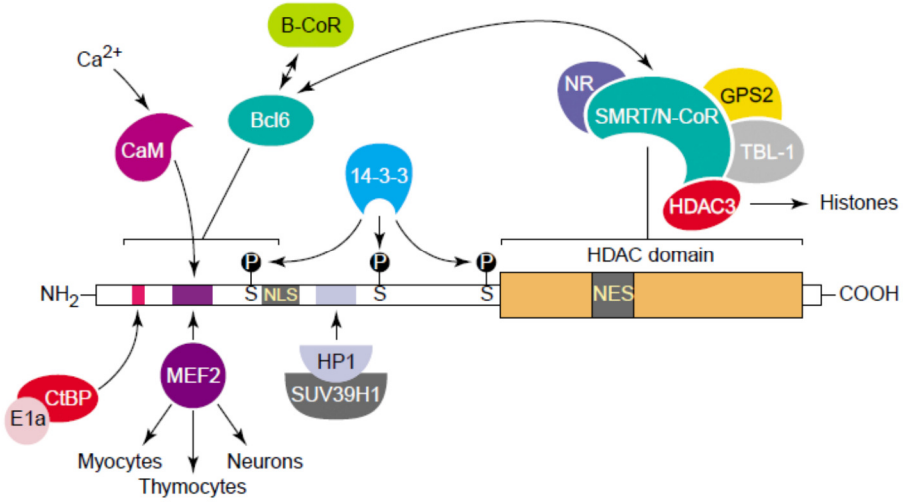

Figure 1-3. Schematic representation of the different proteins which interact with class II HDACs. (Adapted from Kasler and co-workers)[36]

HDAC6 and 10 constitute class IIb and it is believed that HDAC10 originates from a HDAC6-like protein.[22] In spite of this common ancestor, HDAC6 and 10 are structurally and functionally different. In terms of subcellular localization, HDAC6 is primarily cytosolic, but is known to shuttle to the nucleus. HDAC10 shuttle between the nucleus and the cytoplasm, with a slight preference for the nucleus. HDAC6 and 10 are characterized by two identical HDAC domains, however in HDAC10 the *C*-terminal domain is truncated and catalytic inactive.[43] HDAC10 interacts with HDAC3 and SMRT, which connects it to class IIa. In contrast, HDAC6 does not show this HDAC3/SMRT interaction and instead has been found to associate with HDAC11.[19] In 2002, Yao and co-workers reported that HDAC6 can deacetylate α-tubulin.[44] This non-histone substrate is associated with cell motility and this result indicate that posttranslational modifications are involved in a broad variety of cellular functions.

1.2.3 Class III HDACs – Sirtuins

Class III HDACs (SIRT1–7) are different from the remaining three HDAC classes as they do not require a zinc atom for their catalytic activity. In contrast, these enzymes require NAD to deacetylate lysine residues. The mammalian family has seven members and the NAD-dependent activity was first investigated by Frye in 1999[45], who showed that SIRT2 was able to transfer a radioactive labeled phosphor from NAD to bovine serum albumin (BSA). The functional activity was elaborated to include ADP-ribosyltransferase to histones and eventually to deactylation of histones at lysine 16 in H4.[46] However, the sirtuins are weak deacetylases of histone substrates compared to HDAC1–11. The target scope for the sirtuins has recently been expanded to include removal of crotonyl, malonyl, and succinyl groups from the lysine side chains in histones and other proteins (reviewed by Olsen).[47] As NAD is involved in the energy balance of the cell it was quickly hypothesized that sirtuins could be involved in cell metabolism. Subsequent studies have shown that sirtuins are indeed key players in ageing, nutritional balance, and metabolism.[48, 49] The known molecular target for sirtuins are slightly different from the other HDACs. Sirtuins seem to be more involved in post-translational modifications of non-histone proteins than class I, II, and IV HDACs, which primarily target histones. The interesting biochemistry of SIRT1–7 has not been studied in this work and these enzymes will not be discussed further in this thesis.

1.2.4 Class IV HDAC11

Class IV only include HDAC11, which was isolated in 2002.[19] This enzyme is the smallest member of the HDAC family and the catalytic domain constitute most of the peptide sequence. As mentioned in section 1.2.2 HDAC11 interacts with HDAC6, but is has not been shown to interact with complexes associated with class I and IIa enzymes. HDAC11 is believed to be a nuclear protein and it displays some deacetylase activity. However, the biological target has not yet been identified and little is known about the cellular function.

1.2.5 Concluding remarks

It is important to note that HDAC inhibitors may display different activities in experiments with isolated recombinant enzymes compared to experiments performed in cells or *in vivo*. When HDACs are found as a part of multiprotein complexes, the overall folding and structure of the enzyme may change compared to the recombinant purified version. However, functional assay data and cell experiments seem to correlate well for HDAC enzymes.[50, 51, 52]

1.3 Histone deacetylases as anticancer agents

The acetylation level of the histone tails has been correlated to cancer development and HDAC inhibitors have proven to be promising anticancer agents. [53, 54, 55] Numerous mechanisms have been proposed to explain this observation. First, HDAC inhibitors can induce apoptosis in a broad variety of cancer cell lines. HDAC inhibitors are believed to modulate a variety of cellular pathways. The most important extrinsic pathway, is the death receptor pathway, which is triggered by TNF-related apoptosis-inducing ligand (TRAIL).[56] Studies have shown that HDAC inhibitors increase expression of death receptors (DR4 and DR5) and sensitize malignant cells to TRAIL-mediated apoptosis. [57, 58, 59] The intrinsic apoptotic pathway (mitochondrial mediated), which is associated with cell stress, free radical generation, and misfolding of proteins, also plays a key role in the apoptotic properties of HDAC inhibitors. When subjected to stress or abnormal growth, the normal cell will activate pro-apoptotic proteins (BAD and BAK), which sets off a cascade of reactions resulting in activation of caspase 3 and apoptosis. This self-destructing "protection mechanism" is impaired in many cancer cells.[60, 61, 62] There is evidence that the level of HDACs is elevated in these cancer cells and this increased HDAC activity favors the condensed and compact chromatin structure (Figure 1-2).[63] This leads to transcriptional repression of the genes coding for pro-apoptotic proteins. HDAC inhibitors can shift the chromatin structure towards the relaxed form and promote transcription of the pro-apoptotic genes. [64,57, 65] Furthermore, anti-apoptotic proteins (Bcl-2 and Bcl-xL) are down regulated by HDAC inhibitors, leading to an overall pro-apoptotic state in the cell.[64] Finally, p53-mediated activation of p21, which results in G1 arrest in the cell cycle, seems to be induced by HDAC inhibitors.[66] Several of the above mentioned pathways indirectly induce p53, but recent studies also suggest that the acetylation level of p53, which is regulated by HDACs and HATs, is a critical factor in the induction of apoptosis.[67, 68] HDAC inhibitors exhibit many other interesting biological functions and it is important to remember that HDACs modulate many non-histone targets as well. This activity might be the key to many of the observed cellular effects. Mann and co-workers reported the acetylation of 1750 proteins and the presence of 3600 lysine acetylation sites by high-resolution mass spectrometry (HRMS).[69] The acetylated proteins were not restricted to the nucleus of the cell as many cytoplasmic proteins also were found to be acetylated. Generally, proteins involved in all aspects of the cellular function was acetylated, but acetylation was especially abundant in proteins involved in the cell cycle, RNA splicing, chromatin remodeling, ribosomal proteins, and DNA damage repair. Interestingly, KMTs and HDMs were found to be extensively acetylated, which suggest a direct link between the two major post-translational histone modifications. In order to evaluate the effect of HDAC inhibitors on the acetylation pattern of the proteins, two different HDAC inhibitors were tested (SAHA (**1.01**) and MS-275 (**1.08**), Figure 1-4). Remarkably, only 10% of the available acetylation sites were up-regulated by the inhibitors, suggesting a highly site specific activity of the inhibitors. The two inhibitors also resulted in increased acetylation of

different proteins, which could reflect that the two inhibitors inhibit different HDAC isoforms. In relation to cancer, it was shown that many oncogene or tumor-suppressor proteins were acetylated. The specific biochemical functions associated with acetylation of the majority of these non-histone proteins are not yet understood, but it is likely that these proteins are somehow involved in the development of cancer. Overexpression of different HDAC isoforms has been associated with different cancer types and an overview is presented in Table 1-2.

Table 1-2. Proposed correlation between overexpression of HDAC isoforms and various cancers. (Adapted from Bertrand, P.)[70]

HDAC isoform	Cancers associated with overexpression
HDAC1	Lung, breast, prostate, gastric, colorectal
HDAC2	Colorectal, gastric
HDAC3	Lung, solid tumors
HDAC4	Unknown
HDAC5	Downregulated in colon and acute myeloid leukaemia
HDAC6	Breast
HDAC7	Unknown
HDAC8	Several cancer forms
HDAC9	Unknown
HDAC10	Unknown
HDAC11	Unknown

Even though the mechanism is not fully understood, it is well established, that HDAC inhibitors are efficient molecules for inducing apotosis and targeting cancer cells. The major concern associated with HDAC inhibitors as drugs, is the destructive phenotype observed with deletion of HDAC genes.[71, 72] However, HDAC inhibitors are remarkably well tolerated *in vivo*. A plausible explanation is that HDACs participate in multiprotein transcriptional complexes (Sin3, NurD, CoREST). Complete removal of the HDAC from such complexes may render them completely inactive, whereas inhibition with small molecules will leave the complexes intact and somewhat functional.[73] Another interesting aspect is the shortage of isoform selective HDAC inhibitors. Most of the compounds developed so far are primarily defined as class specific inhibitors. The development of isoform selective HDAC inhibitors, would be an extremely important tool for understanding the individual biological roles of the different isoforms, and such compounds have great potential as drugs.[74, 54]

The therapeutic potential of HDAC inhibitors is not limited to cancer treatment. The anti-epileptic and mood-stabilizing drug, valproic acid (**1.04**, Figure 1-4) is identified as HDAC1 inhibitor, thus linking these nervous system disorders to histone acetylation.[75, 76] Transcriptional dysregulation is central to the pathogenesis of Huntington`s disease, which is initiated by mutations in the hutingtin gene. HDAC inhibitors have been shown to be effective in a mouse model of Huntigton`s disease and epigenetic modification could be effective in treatment of Huntington`s disease.[77] Nestler and co-workers studied gene expression and chromatin remodeling in mice subjected to chronic defeat stress and subsequent treatment with the anti-depressant drug, imipramine. [78] Chronic defeat stress is a well-established mimic of depression and it was observed that imipramine administration increased histone acetylation in promoters regions, which were repressed before imipramine treatment. The increase in histone acetylation was associated with downregulation of HDAC5. Interestingly, viral-mediated expression of HDAC5 abolished the anti-depressant effect of imipramine, which underscore the importance of histone acetylation pattern, and hence chromatin remodeling, in the pathogenesis of depression.

In summary, HDAC inhibitors have great potential as drugs, within a widespread of diseases and medical conditions. However, the mechanisms involved in the observed therapeutic benefits are complex and poorly understood. The emergence of potent and selective HDAC inhibitors, as well as improved disease models, have founded a solid background for understanding the complex roles of HDACs.

1.4 HDAC inhibitors

HDAC inhibitors can be classified in many different ways, but in this work, they have been classified according to their chemical structure and divided into four major classes: hydroxamic acids, cyclic peptides, short-chain fatty acids, and benzamides (Figure 1-4).[79]

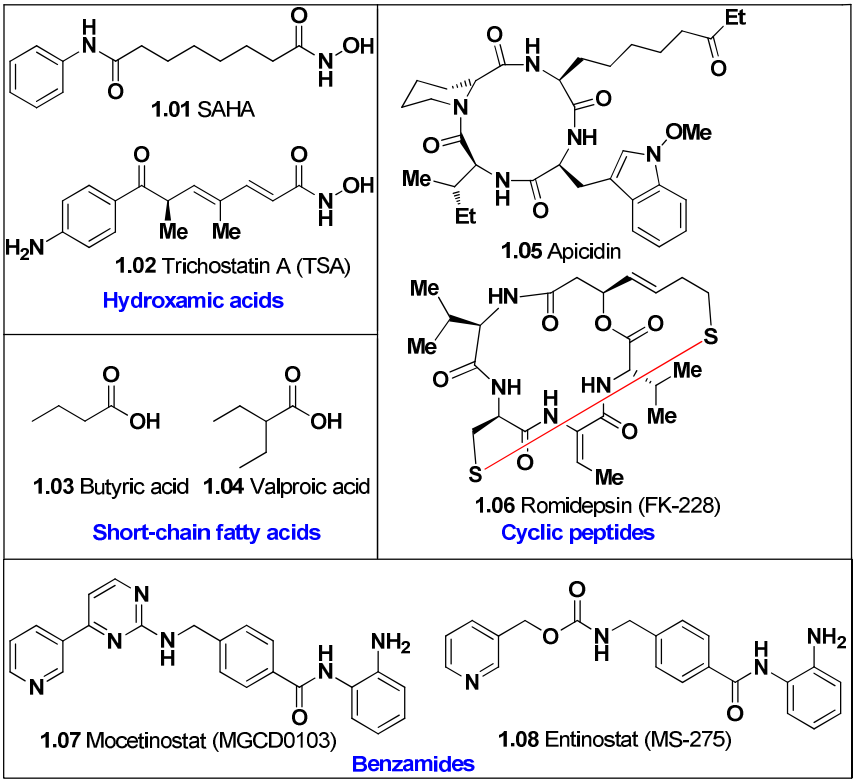

Figure 1-4. Classification of HDAC inhibitors.

The first HDAC inhibitor to be approved by the FDA for clinical treatment was suberoylanilide hydroxamic acid (SAHA, **1.01**). SAHA (Trade name: Zolinza) was approved for the treatment of cutaneous T-cell lymphoma (CTCL) in 2006. The structure was inspired by the observation that dimethylsulfoxide (DMSO) inhibited murine-virus-infected erythroleukemia cells (MELC).[80] This discovery led to the development of compounds bearing two polar groups, which were separated by a methylene chain. One of these structures was hexamethylenebisacetamide (HMBA).

Further studies established that substituting the acetamide functionalities in HMBA with hydroxamic acids increased potency.[81] In order to probe if two polar groups were necessary for activity and to evaluate the incorporation of a hydrophobic group, one of the hydroxamic acid functionalities was substituted to an anilide.[82] These modifications resulted in SAHA. The biological mechanism responsible for the promising anti-cancer effect of SAHA was not clear and the molecular target was first identified two years later by Breslow and coworkers.[83] They realized the similarity in chemical structure between trichostatin A (TSA, **1.02**), a known HDAC inhibitor, and SAHA. Indeed, they found that SAHA was able to inhibit all class I and II HDACs. After this discovery, SAHA was characterized intensively and commenced phase I clinical trials in 2003.[84]

In 2009, the cyclic peptide romidepsin (Trade name: Istodax, **1.06**) was the second HDAC inhibitors to be approved for treatment of CTCL. Several HDAC inhibitors are currently in clinical trials for treating various cancers (Table 1-3).[74]

Table 1-3. Selection of HDAC inhibitors and their clinical indications.[74]

Inhibitor	Clinical phase (positive response against)
SAHA	I-III (Refractory solid tumours and leukaemias)
FK-228	I/II (T-cell cutaneous or peripheral lymphoma and solid tumours)
MS-275	I/II (none observed)
Valproic acid	I/II (Leukaemias and myelodysplasia)

The chemical structures of the compounds shown in figure 1-3, do not appear to be structurally related, but they share a common pharmacophore, which is found in many HDAC inhibitors

Figure 1-5). From the pharmacophore model it can be hypothesized that the inhibitors mimic the substrate for HDACs (**1.10**). In the substrate, the acetylated amine functionality of lysine, which coordinates to the zinc atom, is separated from the rest of the bulky protein by an alkyl linker. The inhibitors, exemplified by trapoxin B (**1.09**) in Figure 1-5, show the same structural arrangement, where the zinc-coordinating functionality is separated from the rest of the molecule by an alkyl linker.

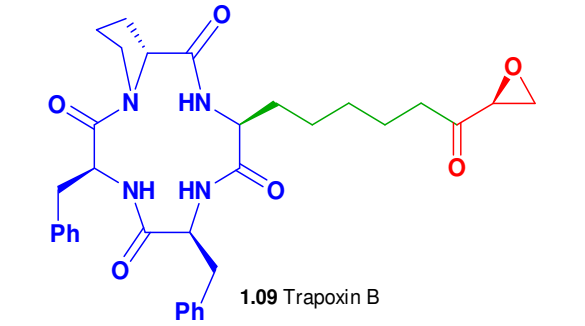

1.09 Trapoxin B

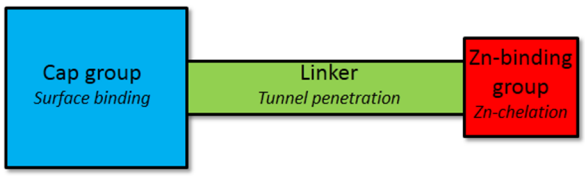

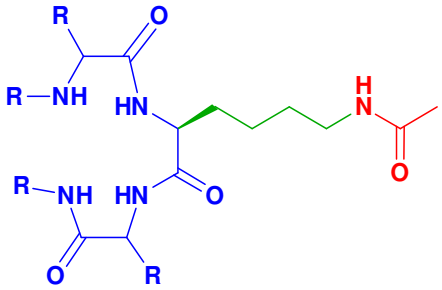

1.10 Lysine substrate

Figure 1-5. The pharmacophore model proposed for HDAC inhibitors. The cap group is shown in blue, the linker in green, and the zinc-binding functionality in red.

The pharmacophore model has been confirmed by X-ray structures and modeling experiments of different HDAC inhibitors in histone deacetylase-like protein (HDLP), HDAC4, HDAC7, and HDAC8.[85, 86, 87, 88, 89, 90] Furthermore, X-ray structures without co-crystalized inhibitors have been reported on HDAC1 and HDAC3.[91, 92] Four different hydroxamic acid inhibitors were co-crystallized with HDAC8 in 2008 by Tari and co-workers.[90] The SAHA–HDAC8 co-crystal structure is shown in Figure 1-6.

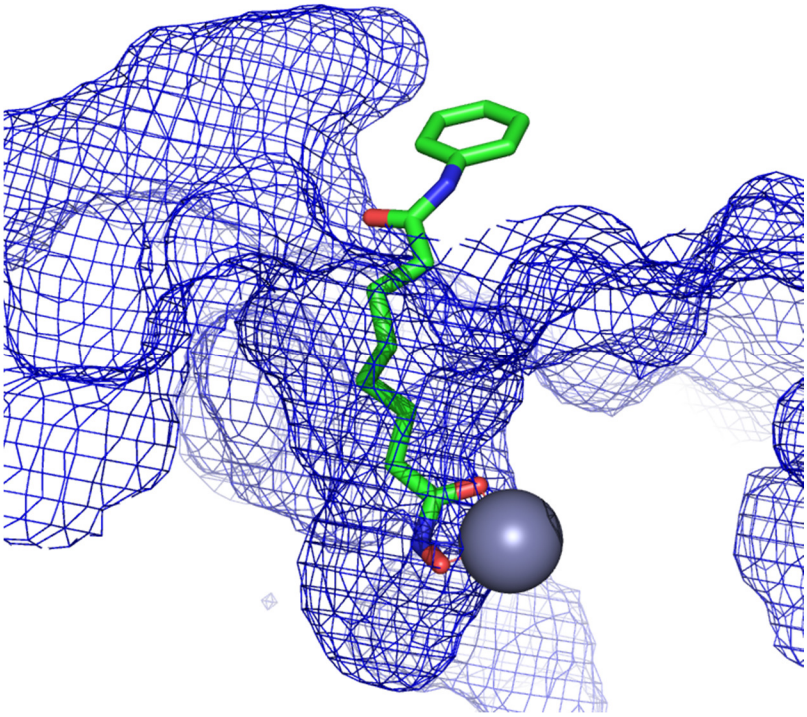

Figure 1-6. Crystal structure of SAHA (sticks) bound to HDAC8 (surface mesh). The zinc atom is shown as a sphere. (PDB: 1T69)

From this structure several general features can be highlighted. In Figure 1-6, the hydrophobic cap group of SAHA is positioned on the surface of the protein. In SAHA the cap group is an aniline moiety, which can participate in favorable interactions with hydrophobic regions near the entrance to the 11 Å channel, leading to the internal cavity. In trapoxin B the cap group is the cyclic tetrapeptide core (Figure 1-5). The linker connects the cap group of SAHA to the zinc-binding group. The linker is found inside the 11 Å channel and the length is important for activity.[93] The linker can have favorable hydrophobic interactions with the residues that forms the channel (see section 1.4.2).[70] The function of the zinc-binding group is to chelate the Zn^{2+} in the internal cavity (see section 1.4.3) .[70] Several mechanism have been proposed for the zinc-catalyzed deacetylation of lysine side chains. Based on DFT calculations on HDLP, Geerlings and co-workers proposed a mechanism where a zinc-bound hydroxide ion, which also makes a hydrogen bond to Tyr297, attacks the amide carbon to create a tetrahedral transition state (Figure 1-7).[94]

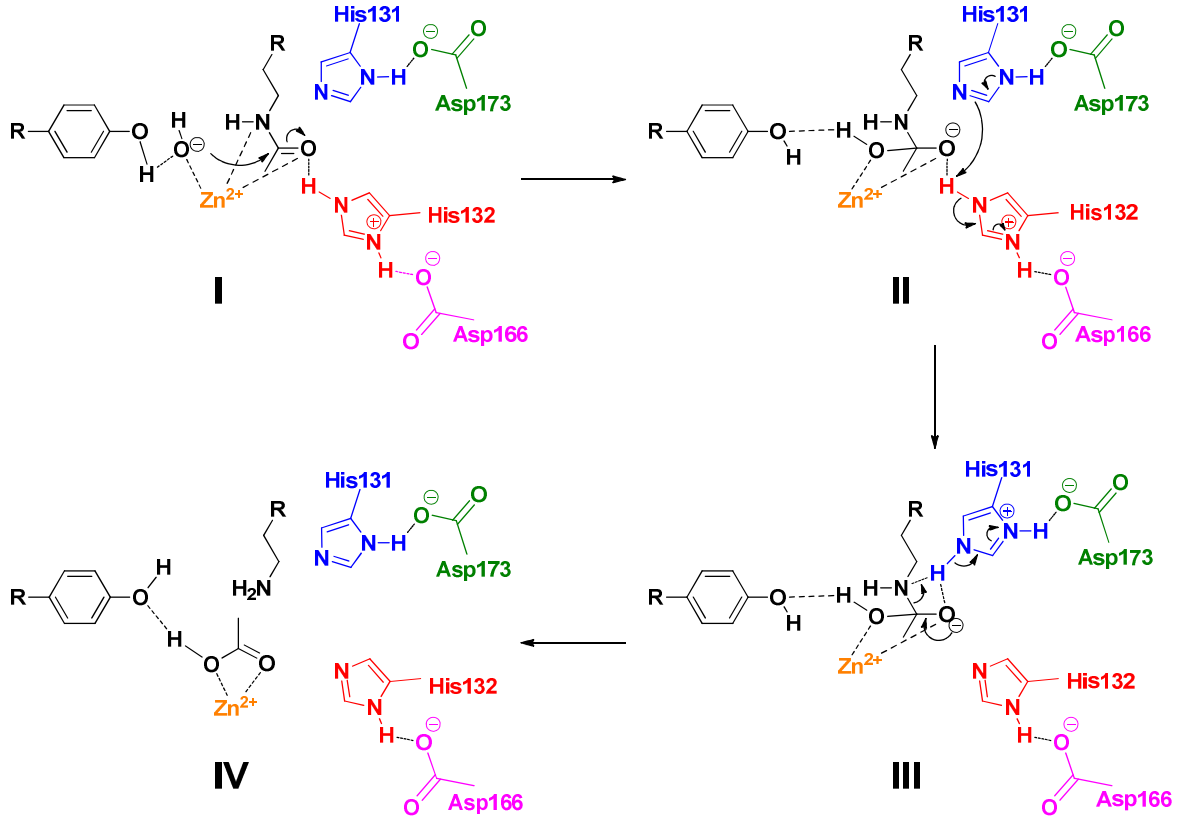

Figure 1-7. Proposed mechanism for the HDAC catalyzed deacetylation of lysine side chains. Amino acid numbering correspond to HDLP residues. (Adapted from Geerlings and co-workers).[94]

The amide carbon is activated by coordination to the zinc atom and hydrogen bonding to His131 (**I**). According to calculations, the tetrahedral transition will place an excess of negative charge between the nitrogen of His132 and the amide nitrogen. This state is energetically unfavorable and a proton transfer from His131 to His132 will produce a state that is lower in energy (**III**). The tetrahedral intermediate is now setup to break the amide bond, which produces the free amine of the lysine and acetic acid (**IV**). His132 is converted back to the neutral form and a proton transfer from acetic acid to the free amine gives the acetate byproduct. To complete the catalytic cycle a water molecule may bind to the Zn^{+} and re-protonate His131. A broad variety of functional groups have been used to mimic the natural amide substrate. As previously discussed, hydroxamic acids are excellent zinc-chelators, but also carboxylic acids, thiols, and ortho anilines have been used. Mechanistic considerations, as shown in Figure 1-7, have inspired the development of zinc-binding groups, which mimic the different intermediates found in the catalytic cycle. Boronic acid derivatives mimic the initial step in the catalytic cycle where the boron atom is attacked by a water molecule, which creates a stable tetrahedral boronic acid complex.[95] Also sulfones, sulfoxides[96], and trifluoromethyl ketones[97] have been prepared to mimic the tetrahedral intermediate (see section 1.4.3).

The different HDAC inhibitors display different binding mechanisms. The majority of the compounds shown in Figure 1-4 display a fast on/fast off inhibitory mechanism, but the benzamides are an exception. Gottesfeld and co-workers showed that SAHA-inspired benzamide inhibitor (**1.11**, Figure 1-8) was a slow tight-binding inhibitor of HDAC1–3.[98]

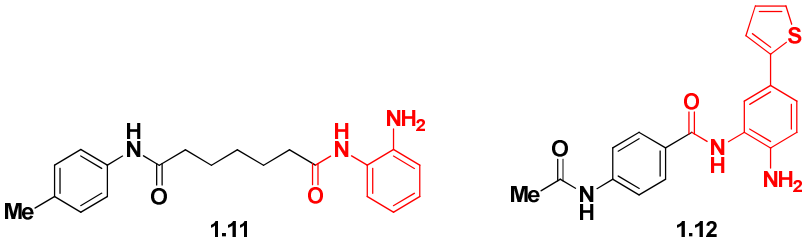

Figure 1-8. Benzamide HDAC inhibitors displaying a slow on/slow off binding mechanism.

In contrast to SAHA, which is a fast on/fast off inhibitor, compound **1.11** showed a time-dependent inhibitory profile. Even after 2 hours the IC_{50} for compound **1.11** was still decreasing, whereas SAHA reached its maximum inhibitory effect within 15 minutes. On HDAC3 a 15-fold decrease in IC_{50} was observed when pre-incubating the inhibitor for 3 hours compared to no pre-incubation. Steiner and co-workers reported similar results for the benzamide inhibitor **1.12**. They elaborated on the impact of binding kinetics on gene transcription and cell death.[99] As expected hyperacetylation was delayed with compound **1.12** compared to SAHA and this delay was transferred to gene expression. Interestingly, compound **1.12** and SAHA was co-crystalized with HDAC2 with 1.6 and 1.9 Å resolution, respectively. Analysis of these co-crystal structures showed that the two inhibitors chelate the zinc-atom in a similar fashion and the difference in kinetics could be caused by a rearrangement in the protein structure. In order to fit the amino-benzamide–thiophene moiety into the foot pocket of the binding cavity, Leu-144 has to move and considerable rearrangement of the protein is necessary. Furthermore, a stabilizing intramolecular hydrogen bond in compound **1.12**, between one of the amine hydrogens and the carbonyl oxygen from the neighboring amide, has to be broken in order to achieve zinc-binding and inhibitor–protein hydrogen bonds. The combination of protein rearrangement and breaking of a stabilizing intramolecular hydrogen bond in the inhibitor, could explain the "slow on" aspect and the formation favorable inhibitor–protein hydrogen bonds can explain the "slow off" aspect.[99]

1.4.1 Isoform selectivity obtained from cap group modifications

In terms of selectivity, the general trend observed when moving from simple phenyl derived cap groups (**1.01** and **1.08**) to more complex cyclic peptide cap groups, is an increase in isoform selectivity. The selectivity is explained by an increase in favorable interactions between the cap group and the regions surrounding the entrance to the channel.[100, 93, 52, 101] An excellent example is tubacin (**1.13**), which is derived from SAHA (Figure 1-9).

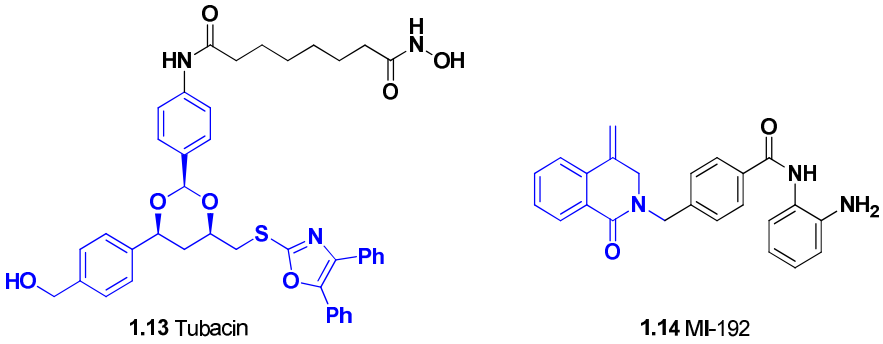

Figure 1-9. Structure of Tubacin and MI-192. The cap groups are shown in blue.

The introduction of a bulky and hydrophobic substituent in the para-position of the aromatic ring in SAHA induced a 7-fold increase in the selectivity towards HDAC6 compared to HDAC1. Molecular dynamics

calculations have shown an important hydrophobic interaction between the 2,3-diphenyl oxazole moiety of tubacin and Phe181 and Phe182 in HDAC6. This interaction is not possible in HDAC1 and could explain the observed selectivity.[102] If the cap group is further elaborated to cyclic peptide or depsipeptide scaffolds, the selectivity towards class I isoforms generally increases. Trapoxin B displays more than 3000-fold selectivity towards HDAC1 over HDAC6.[93] However, selectivity within class I is difficult to achieve, even with large and complex cap groups. A recent breakthrough by Cockerill and co-workers showed how modifications in the cap moiety of mocetinostat (**1.07**) resulted in the selective inhibitor MI-192 (**1.14**, Figure 1-9).[103] MI-192 displays 160-fold selectivity towards HDAC2 (IC_{50}= 30 nM) and 300-fold selectivity towards HDAC3 (IC_{50}= 16 nM), compared to HDAC1 (IC_{50}= 4.8 μM). Within class I, this is by far the most isoform selective HDAC inhibitor ever reported and this discovery indicates that the synthesis of selective inhibitors within this class is challenging, but not impossible. Unfortunately, the structural features responsible for the selectivity was not addressed in this work, but hopefully such studies will contribute to the overall structure pharmacophore of HDAC inhibitors.

1.4.2 Isoform selectivity obtained from linker modifications

Modifications to the linker part of known HDAC inhibitors have revealed class I-selective inhibitors. Most work has been done on hydroxamic acid derivatives. Incorporation of an amide and a phenyl ring in the linker part of TSA (**1.02**) resulted in compound SK-7041 (**1.15**, Figure 1-10). Unlike TSA, compound **1.15** was selective for HDAC1 and 2 compared to HDAC3, 4, 5, and 6.[104] Analyses of the crystal structures of HDLP, FB188 HDAH, and HDAC8 revealed the presence of two Phe residues (Phe152 and Phe208) in the 11 Å channel. The two aromatic rings from these residues are oriented in a way where favorable π–π interactions with the aromatic group in the linker is possible. [85] Insertion of phenyl rings and indole motifs in the linker section has resulted in the development of HDAC8 selective inhibitors. Compound **1.17** demonstrated more than 290-fold selectivity towards HDAC8 over HDAC1–3, 6, and 10. The isoform selectivity is attributed to a hydrophobic sub-pocket found only in HDAC8. This pocket forms when Phe152 is moved away from its normal position (Figure 1-11).[90, 105]

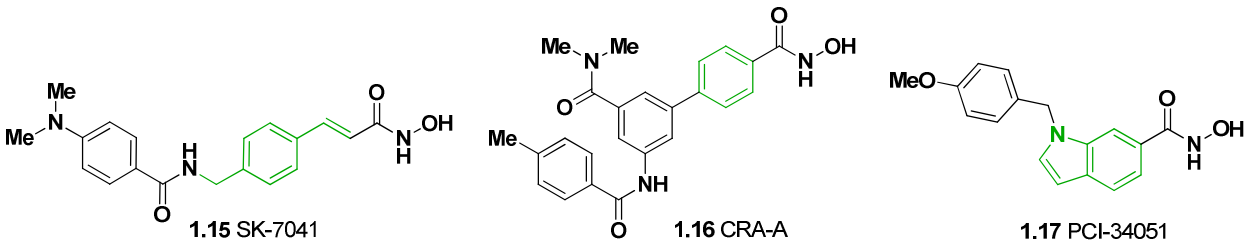

Figure 1-10. Selective HDAC inhibitors with modified linkers. The linker modification is shown in green.

This sub-pocket has only been observed with compound **1.16** (CRAA-A, Figure 1-10), but it is likely that the HDAC8 selectivity observed with other aromatic linkers could be explained by this unique pocket.

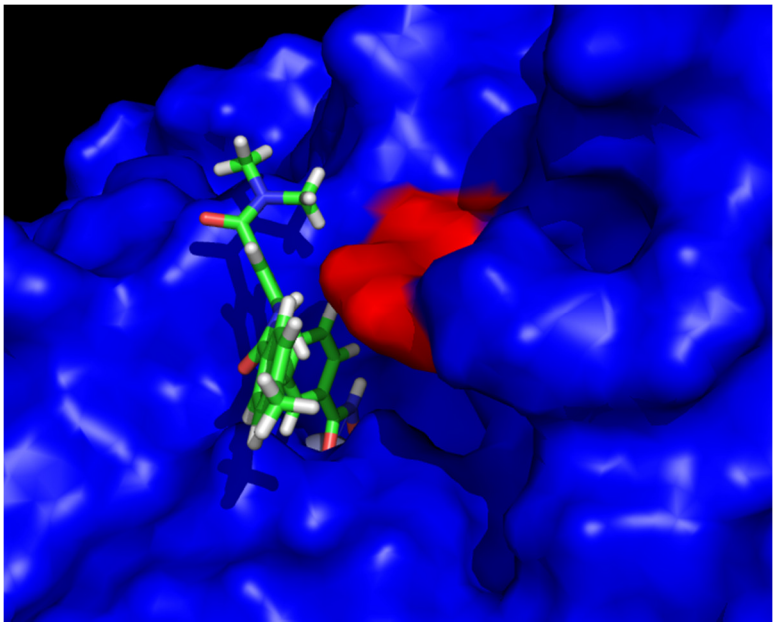

Figure 1-11. Crystal structure of HDAC8 (blue) bound to CRA-a (**1.16**, sticks). Phe152 is marked in red and the sub-pocket is found below F152 (PDB: 1VKG).

1.4.3 Isoform selectivity obtained from zinc-binding group modifications

Selectivity has also been obtained by exploring an 14 Å cavity found deep within the internal cavity of HDLP, FB188 HDAH, and HDAC8. This cavity seems to be reserved for class I HDACs.[70] The cavity may facilitate removal of the acetate byproduct after deacetylation. By introducing a thienyl substituent (compound **1.18**, in Figure 1-12) in the 5-position of the benzamide zinc-binding group of MS-275 (**1.08,** Figure 1-4), a 5-fold selectivity for HDAC1 over HDAC2 was observed compared with the parent compound.[106] Even higher selectivity was observed with a similar compound, where the cap group of compound **1.08** was modified to obtain the 2-aminophenyl benzamide derivative (**1.19**).

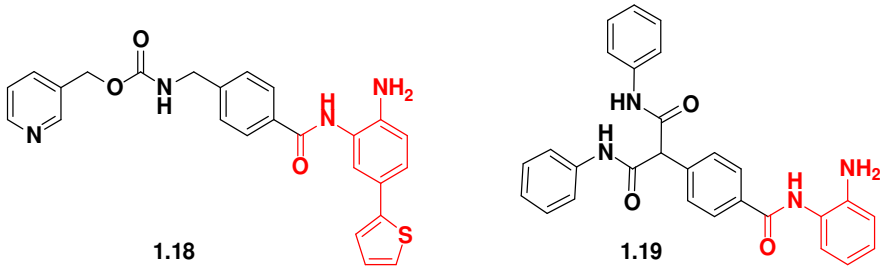

Figure 1-12. Isoform selective inhibitors within class I.

Compound **1.19** shows a 10-fold and 20-fold selectivity towards HDAC1 compared to HDAC2 and HDAC3, respectively.[107] This result implies that the combination of cap group and zinc-binding group modifications could result in isoform selective HDAC inhibitors.

Trifluoromethylketones (TFMK) have emerged as interesting zinc-binding groups (Figure 1-13). Davidsen and co-workers synthesized a series of SAHA-inspired TFMKs (**1.21**, Figure 1-13), which demonstrated low μM activity against a mixture of HDAC1 and 2.[108] Furthermore, these compounds displayed anti-proliferative activity. The discovery of TFMKs as HDAC inhibitors was further investigated by Steinkühler and co-workers.[109] They reported class II enzyme activity against an "unnatural" trifluoroacetamide substrate (**1.20**, Figure 1-13). Class II enzymes demonstrate low deacetylase activity against standard acetylated HDAC

substrates, which has made it difficult to develop screening assays against this class. The discovery of **1.20** provided a useful substrate for developing class II screening assays.

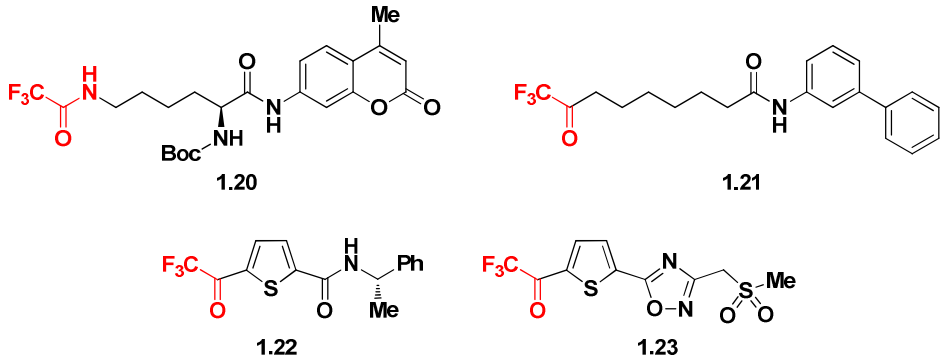

Figure 1-13. Compounds with trifluoromethylketones as zinc-binding groups.

Compound **1.21** showed preferential inhibition of HDAC4 with 42-fold and 4-fold selectivity compared to HDAC1 and HDAC3, respectively. Improved HDAC4 selectivity was reported with the 5-(trifluoroacetyl)thiophene-2-carboxamide **1.22**, which exhibited 31-fold selectivity over HDAC1 and 55-fold selectivity over HDAC3.[97] In the same study, a derivate of **1.22** was crystalized in HDAC4 and this structure showed that the trifuoromethylketones chelate the zinc atom in its hydrated form. The hydrated form is a result of a nucleophilic attack of water on the carbonyl and subsequent protonation. Furthermore, the co-crystal structure revealed a small pocket in the bottom of the active site, which accommodates the trifluoromethyl group. Altering the carboxyamide part of **1.22** to an 1,2,4-oxadiazole moiety (**1.23**) increased the HDAC4/HDAC1 selectivity to over 100-fold.[110]

1.5 Cyclic peptide inhibitors

1.5.1 Macrocyclic peptides

Macrocyclic peptide HDAC inhibitors are often natural products or natural product analogs. This family includes apicidins (Figure 1-15), azumamides (Table 1-4), chlamydocin (Figure 1-14), trapoxin (Figure 1-14), microsporins (Figure 1-14), and HC-toxins (Figure 1-14). These inhibitors are characterized by having a ring size between 12–14 atoms and being constructed of either four α-amino acids or one β-amino acid in combination with three α-amino acids.

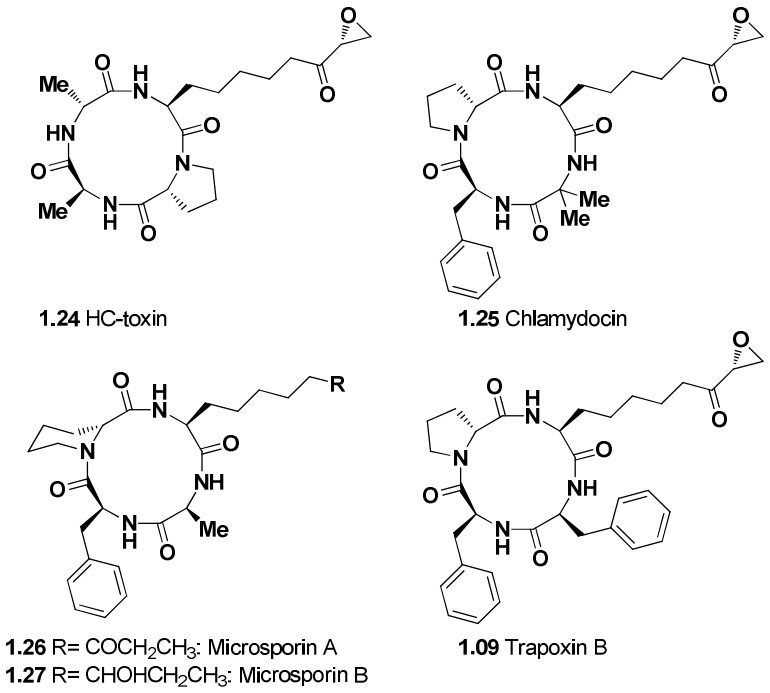

Figure 1-14. HDAC inhibitors with a macrocyclic peptide scaffold.

A common feature of these compounds is the presence of a terminal zinc-coordinating functionality (α,β-epoxyketone, ethyl ketone, carboxyamide or carboxylic acid) in one of the unusual amino acid side chains.

Ethyl ketone containing cyclic peptides: Apicidins and microsporins

The apicidin family include apicidin (**1.05**)[111] and apicidin A–F (**1.28**–**1.35**, Figure 1-15).[112, 113]

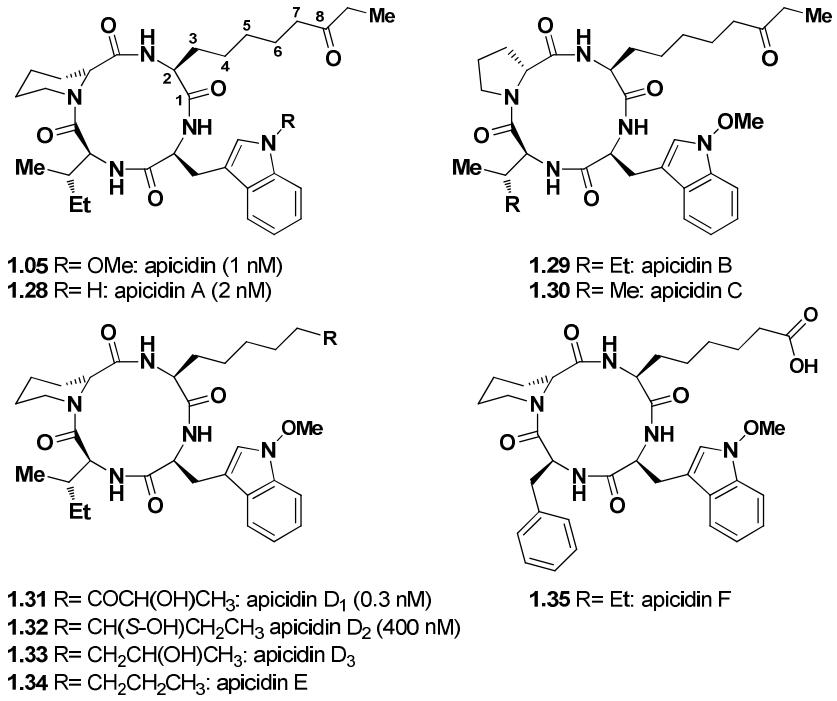

Figure 1-15. The apicidin family. The biological data is obtained from inhibition assays on partially purified HDAC from human Hela extracts.[114]

Apicidin (**1.05**) was first isolated in 1996 from *Fusarium pallidoroserum*[111] and the structure was elucidated in the same paper. The compound displayed broad spectrum antiprotozoal activity and the molecular target was recognized to be the apicomplexan histone deacetylase.[115] Following the discovery of apicidin, isolation of structurally related compounds provided the rest of the current family, with apicidin F (**1.35**) being discovered in 2013.[113] The first total synthesis of apicidin was reported by Singh and Mou in 2001.[116] All nine apicidins contain three standard α-amino acids and an unusual α-amino acid residue, which is believed to mimic the lysine substrate for HDAC. The presence of a zinc-binding group is important for obtaining high potency. For instance, apicidin E (**1.34**), which has an aliphatic side chain, is inactive. Apicidin D_2 (**1.32**) and apicidin D_3 (**1.33**) contain a weak zinc-binding functionality (hydroxyl group) in the side chain at C-8 and C-9, respectively. Apicidin D_2 is 400-fold less active than apicidin (**1.05**) and this difference reflects the weaker zinc-binding properties of a hydroxyl group *vs* a ketone. Apicidin D_3, where the hydroxyl group is shifted to C-9, is inactive and oxidizing the C-9 hydroxyl to the ketone did not restore the activity. These results show that the C-8 ketone is critical for activity. The α-hydroxy keto containing compound (**1.31**) is the most potent HDAC inhibitor in the family and the activity is independent of the stereochemistry at C-9. The superior activity of this compound can be attributed to improved zinc-binding properties of a α-hydroxy ketone *vs* a ketone. Furthermore, the presence of an aromatic amino acid residue next to the extended amino acid is required for high activity.[114] Interestingly, apicidin is found in three different conformations in DMSO.[117] These three conformations are found in an 80:15:5 ratio and the major conformation is the all *trans* conformation (t-t-t-t) and the second-most-populated conformation is the *cis–trans–trans–trans* (c-t-t-t). The *cis*-amide bond was found to be located between the pipecolic acid residue and isoleucine. Rich and co-workers had proposed that the bioactive conformation of the related cyclic tetrapeptides (HC-toxin, **1.24** and chlamydocin, **1.25**) was the less populated (c-t-t-t) conformation.[118] This trend was confirmed to include apicidin in 2009.[119] Ghadiri and co-workers designed apicidin analogs, where the pipecolic acid residue was substituted with a 1,4-disubstituted 1,2,3-triazole or a 1,5-disubstituted 1,2,3-triazole to lock the amide bond in the *trans* and *cis* conformation, respectively. The NMR solution structures of the triazole analogs were compared to the known (t-t-t-t) and (c-t-t-t) conformations of apicidin to validate if the analogs provided a faithful mimic of these conformations. The overlays revealed a significant overlap in the cyclic peptide backbone and the C_α–C_β vectors were found to be similar. The biological testing showed that the 1,5-disubstituted 1,2,3-triazole analog with a (c-t-t-t) conformation was 2–3-fold more active against HDAC1 and 3 compared to the all *trans* compound. This work presents strong evidence that the conformations observed in NMR solution structures of cyclic tetrapeptides, not necessarily reflect the bioactive conformations.

Microsporin A (**1.26**) and B (**1.27**) were isolated in 2007 by Silverman and co-workers (Figure 1-14).[120] The two compounds were isolated from the marine sponge *Microsporum* cf. *gypseum* and in the same paper the total synthesis of microsporin A was reported. Microsporin A is a potent HDAC inhibitor and display promising anticancer activity against human colon adenocarcinoma (HCT-116). Microsporin B (**1.27**), which differ from microsporin A (**1.26**) by having a hydroxyl group at C-8 instead of carbonyl group, was more than 10-fold less potent against HCT-116. This result confirms the importance of the C-8 carbonyl in these type of compounds.

α,β-epoxyketone containing cyclic peptides: HC-toxin, chlamodycin, and trapoxin

HC-toxin (**1.24**, Figure 1-14) is the only compound in the family, which do not contain an aromatic amino acid. The structure of HC-toxin was correctly assigned by Walton and co-workers[121] in 1983 by using NMR spectroscopy and the first total synthesis was achieved by Kawai and Rich.[122] The *α,β*-epoxyketone moiety, which is also found in chlamydocin (**1.25**) and trapoxin B (**1.09**), is essential to activity. It is hypothesized that a nucleophilic residue in the catalytic site of the HDAC enzyme attacks the epoxide, leading to a covalent bond between the enzyme and cyclic peptide.[123] Related structures have been isolated and these compounds

were denominated, HC-toxin II (substitution of the alanine adjacent to the α,β-epoxyketone residue to a glycine) and HC-toxin III (substitution of proline to 3-hydroxyproline).[124]

Chlamydocin (**1.25**) is similar to Trapoxin B (**1.08**) in overall structure, but a aminoisobutyric acid (Aib) residue has replaced one of the phenylalanine residues in peptide backbone. It was isolated in 1974[125] and a crystal structure for the dihydro-analog was reported in 1976.[126] This crystal structure established the stereochemistry of the C-9 stereocenter to be the (*S*)-configuration. The stereochemistry have been found to be important for activity as compound **1.36**, which has the (*R*)-configuration in the 9-position, showed a decrease in activity. Furthermore, substituting the Aib residue to an aromatic residue (compound **1.37**) increased activity.[127]

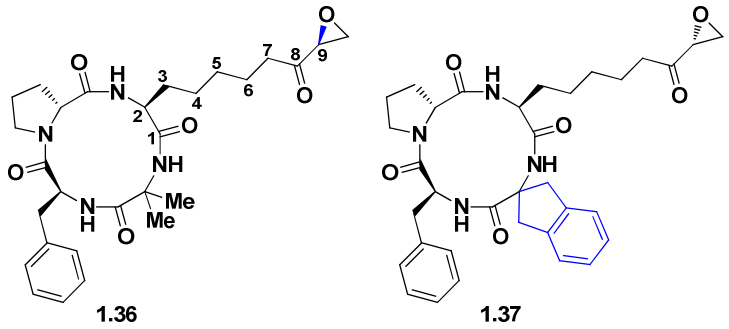

Figure 1-16. Chlamydocin analogs. Modifications are shown in blue.

Trapoxin A and B (**1.09**, Figure 1-14) were isolated in 1990 and the crystal structure of Trapoxin A, which contains an (*R*)-pipecolic acid residue instead of an (*R*)-proline residue, was reported in the year after.[128, 129]. Both compounds were cytotoxic towards cancer cells. The molecular target was identified to be HDACs and it was shown that these potent inhibitors bind irreversible to the enzymes.[123] Actually, the irreversible binding abilities of trapoxin B was used to isolate the first mammalian HDAC by construction of a trapoxin B-based affinity matrix. [18, 123]

Expanding the macrocyclic ring

The cyclic tetrapeptide architecture was systematically investigated by Ghadiri and coworkers.[130] They designed a series of cyclic tetrapeptide frameworks, which were inspired by natural products. In this work, one or two β-amino acid residues was inserted in the macrocyclic ring (Figure 1-17).

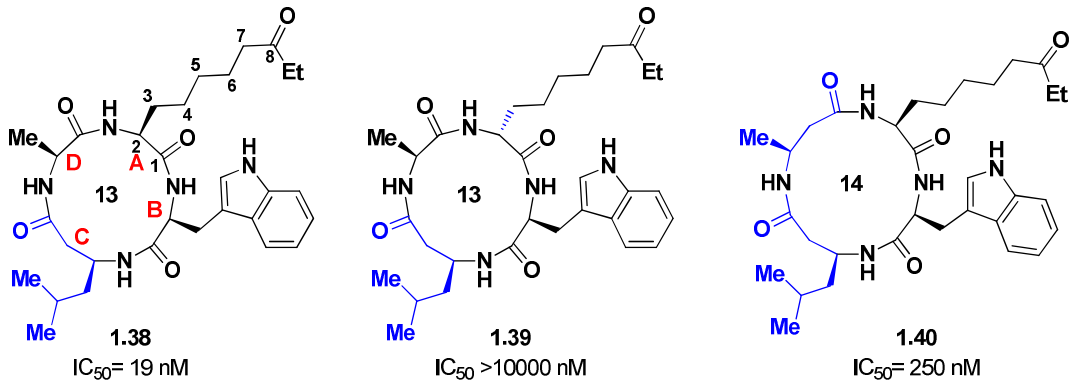

Figure 1-17. Cyclic tetrapeptides with one or two β-amino acids. Modifications are shown in blue. The HDAC inhibition assays were performed on Hela nuclear extracts.

The incorporation of a single β-amino acid in position C (**1.38**) was well tolerated and produced a compound with HDAC activity comparable to apicidin. Incorporation of β-amino acids in position B and D resulted in compounds with a 22–53-fold decrease in activity. The compounds containing two β-amino acids were generally found to be less potent than apicidin (**1.40**). The biological data was combined with high-resolution NMR solution structures to provide interesting information about the structural requirements necessary for high potency. In general, the chirality of the unnatural (*S*)-2-amino-8-oxodecanoic acid (*S*-Aoda, **1.39**), as well as the presence of an aromatic amino acid in position B, was found to be highly important in terms of potency. Furthermore, small changes in the orientation of the C_2–C_3 vector (see Figure 1-17) in Aoda mediated a significant loss in potency. Finally, optimal distances between the C_2 of tryptophan to C_2 in Aoda and C_2 in leucine were determined to be 5.0–5.3 Å and 5.1–5.3 Å, respectively (Figure 1-18).

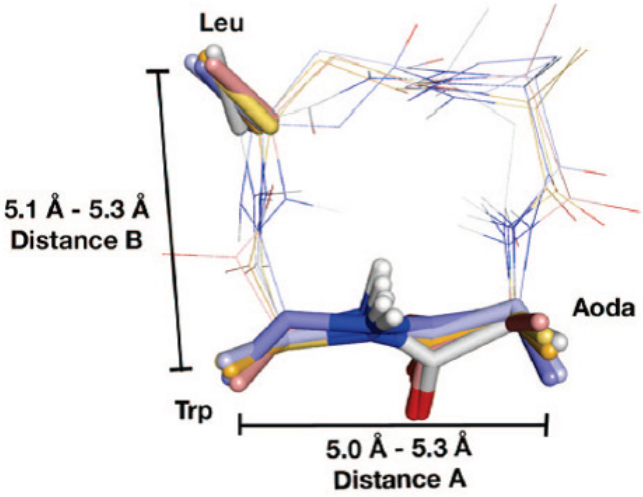

Figure 1-18. Optimal distances found in potent cyclic tetra peptides. (Adapted from Ghadiri and co-workers)[130]

Hybrid structures

Hybrid structures have been prepared, where the structural features of different HDAC inhibitors have been combined. An excellent example is the preparation of cyclic hydroxamic acid-containing peptides (CHAPs) by Horinouchi and co-workers.[93] The cyclic peptide scaffold from epoxyketone containing compounds (e.g. trapoxin B (**1.09**) and chlamodycin (**1.25**)) was combined with other zinc-binding groups, e.g. hydroxamic acid moiety from TSA (**1.02**). A selection of the resulting potent hybrid structures is shown in Figure 1-19.

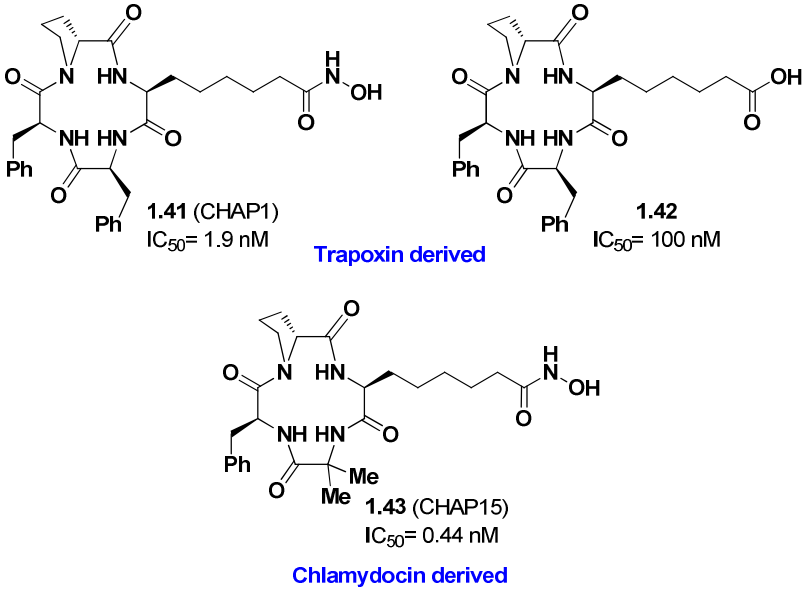

Figure 1-19. Cyclic hydroxamic acid-containing peptides developed by Horinouchi and co-workers.[93]

Trapoxins have been found to bind irreversibly to the HDAC enzymes with the exception of HDAC6. Irreversible inhibition is probably mediated by alkylating key residues in the active site.[131] Introduction of a hydroxamic acid moiety on a trapoxin peptide produced a highly potent compound (**1.41**), which displayed reversible inhibition of HDAC1. This suggest that the epoxyketone functionality is responsible for the irreversible binding. The length of the aliphatic chain in the side chain was also explored. CHAPs with 4-, 5-, and 6-carbon chains were synthesized and the optimal length was found to be the 5-carbon chain. The 5-carbon chain creates a length between the cyclic tetrapeptide core and the hydroxamic acid, which corresponds to the length between the peptide backbone and the acetylated nitrogen of a lysine (Figure 1-5).

1.5.2 Macrocyclic depsipeptides

A family of macrocyclic HDAC inhibitors, which is closely related to the cyclic tetrapeptides, is the depsipeptides. Spiruchostatin, (**1.44**), Largazole (**1.45**), and FK-228 (**1.06**, Figure 1-4) are examples of compounds from this family (Figure 1-20).[132]

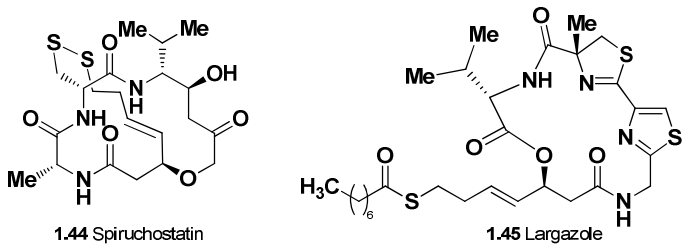

Figure 1-20. Macrocyclic depsipeptide HDAC inhibitors.

A common feature shared by the depsipeptide HDAC inhibitors is the requirement for pre-activation in order to release a free thiol, which acts as a potent zinc-binding group. In the case of spiruchostatin (**1.44**) and FK-228 (**1.06**) the zinc-binding free thiols are produced by reduction of the disulfide bridge.[133, 52] Largazole (**1.45**) needs activation by enzymatic hydrolysis of the thioester to give the free thiol.[134] In 2011, a co-crystal structure of an HDAC8–largazole complex was reported with a 2.14 Å resolution (Figure 1-21).[89] This structure confirms the overall binding mode of macrocyclic HDAC inhibitors and illustrates how the macrocyclic ring

accommodates on the surface of the protein. Furthermore, this work emphasis the importance of the thiolate-zinc coordination geometry, which in this X-ray structure is very close to optimal.

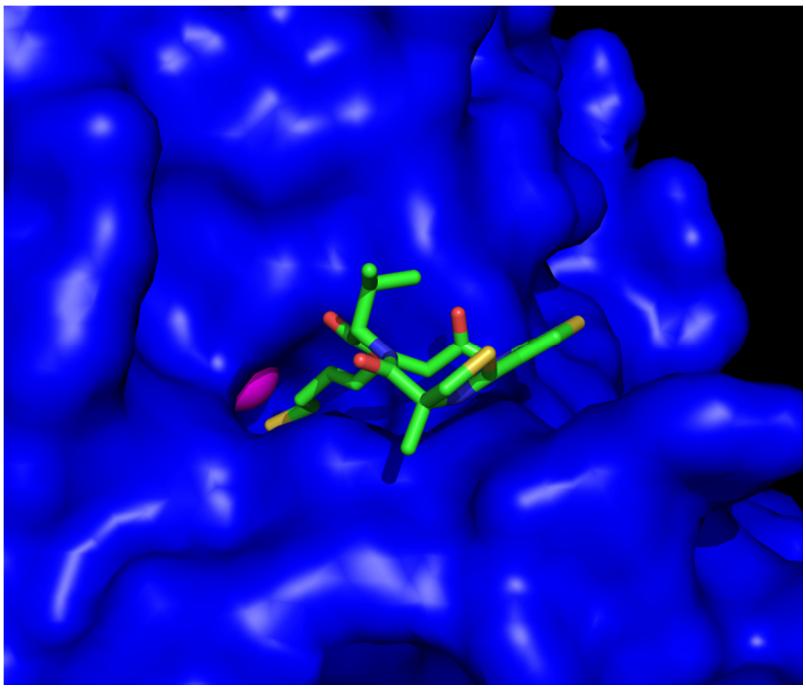

Figure 1-21. Crystal structure of largazole (**1.45**, sticks) in HDAC8 (blue, surface). The zinc atom is shown in magneta. (PDB: 2RQD)

1.5.3 The azumamides

An interesting class of cyclic petide HDAC inhibitors is the azumamides. The azumamides are natural products, which were isolated from the marine sponge *Mycale izuensis* by Fusetani and coworkers in 2006 (Table 1-4).[135] These compounds are cyclic tetrapeptides with a unique di-substituted β-amino acid and an unusual all retro-reverso configuration compared to the compounds in Figure 1-14.

Table 1-4. The structure and IC_{50}-values of azumamide A–E. [a] The IC_{50}-values were determined on a lysate from K562 human leukemia cells.[135] The numbering shown in the β-amino acid will be used throughout this thesis.

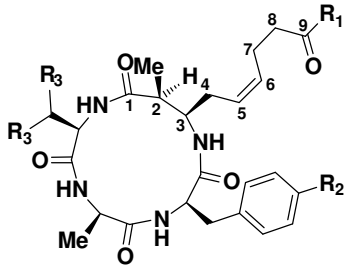

Azumamide	R_1	R_2	R_3	IC_{50}[a] (nM)
A (AzuA)	NH_2	H	Me	45
B (AzuB)	NH_2	OH	Me	110
C (AzuC)	OH	OH	Me	110
D (AzuD)	NH_2	H	H	1300
E (AzuE)	OH	H	Me	64

In spite of their weak zinc-binding groups (carboxylic acid or carboxyamide) the azumamides are still relatively potent HDAC inhibitors and they exhibit ~100-fold selectivity towards class I HDACs compared to class II.[136] Currently, three total syntheses of azumamide E have been reported and azumamide A has been prepared as well. However, Azumamide B–D has not yet been synthesized. The three total syntheses are presented below.

De Riccardis route

The first synthesis was reported by De Riccardis and coworkers in 2006.[137] The β-amino acid building block was prepared in 14 steps and an overall yield of 19% from 3-(benzyloxy)propanol (Scheme 1-2). The chiral centers were constructed by a highly diastereo- and enantioselective crotylation reaction using a chiral borane. Reductive ozonolysis of the terminal alkene followed by protection group manipulations afforded the alcohol **1.48**. Mesylation of the alcohol followed by an S_N2 reaction with sodium azide afforded the correct stereochemistry at the β^3-position. Subsequent reduction of the azide and Boc-protection of the resulting amine provided compound **1.50**. The benzylether protecting group was removed and the alcohol oxidized to the aldehyde (**1.51**). The (*Z*)-double bond was installed with a Wittig reaction and followed by deprotection of the silylprotected alcohol and oxidation to the acid to give the desired β-amino acid building block (**1.53**).

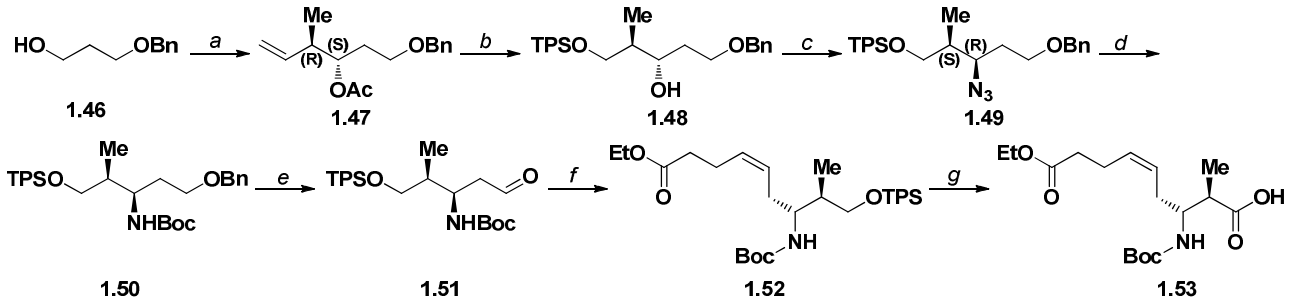

Scheme 1-2. Reagents and conditions: (a) $(COCl)_2$, DMSO, Et_3N, CH_2Cl_2, 98%; *i*) (+)-Ipc_2BOMe, (*E*)-2-butene, ^{t}BuOK, nBuLi, $BF_3{\cdot}Et_2O$, THF, –78° C; *ii*) Ac_2O, pyridine, CH_2Cl_2, 80%; (b) O_3, CH_2Cl_2, then PPh_3; *i*) $NaBH_4$, EtOH; *ii*) K_2CO_3, MeOH; *iii*) TPSCl, DMAP, pyridine, CH_2Cl_2, 57%, over 4 steps; (c) MsCl, Et_3N, THF; *i*) NaN_3, DMF, 60° C , 89% over two steps; (d) H_2, Pt_2O, EtOAc; *i*) Boc_2O, Et_3N, CH_2Cl_2, 92% over two steps; (e) H_2, Pd/C, EtOH; *i*) $(COCl)_2$, DMSO, Et_3N, CH_2Cl_2, 93% over two steps; (f) KHMDS, $Ph_3PBr(CH_2)_3COOEt$, aldehyde **1.51** THF, –78° C to RT, 76%; (g) HF/pyridine, pyridine; *i*) TEMPO, phosphate buffer, $NaClO_2$, NaClO, MeCN, 75% over two steps.

The β-amino acid was coupled to the tripeptide H_2N-(D)-Val-(D)-Ala-(D)-Phe-O^{t}Bu in solution followed by removal of the ^{t}Bu-protecting group and the resulting tetrapeptide was cyclized, by preparing the active ester with pentafluorophenyl diphenylphosphinate (FDPP). The cyclization proceeded in 37% yield and three days were needed to achieve complete conversion. Hydrolysis of the ethyl ester gave azumamide E (5%) and subsequent amidation with diphenylphosphoryl azide (DPPA) afforded azumamide A (2%).

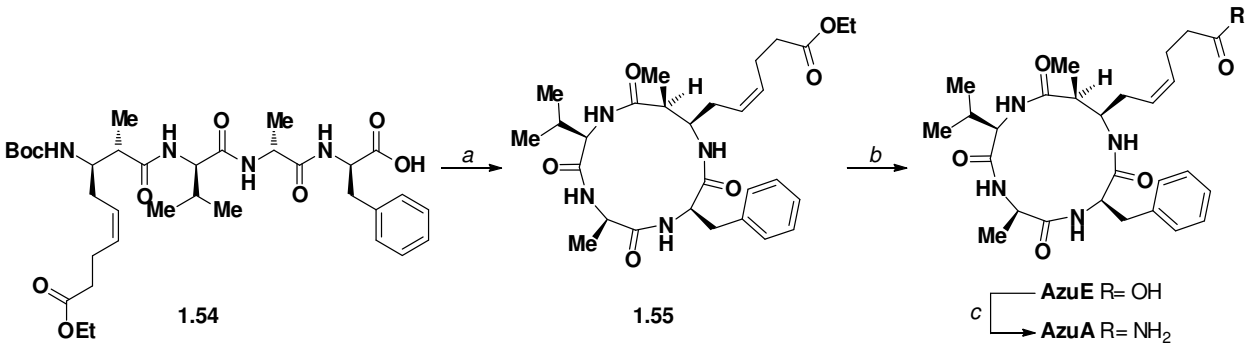

Scheme 1-3. Reagents and conditions: (a) FDPP, *i*Pr$_2$NEt, DMF, 3 days, 37%; (b) LiOH, H$_2$O/THF, 0° C, 75%; (c) DPPA, NH$_4$Cl, Et$_3$N, DMF, 54%.

In another study by De Riccardis and coworkers, the DMSO solution-state structure of azumamide E was docked in histone deacetylase-like protein (HDLP). The docking model proposed important hydrophobic interactions between the surface of the protein and the macrocyclic core, since the hydrophobic side chain of D-phenylalanine was found to accommodate a hydrophobic pocket near the entrance to the 11 Å channel.[136]

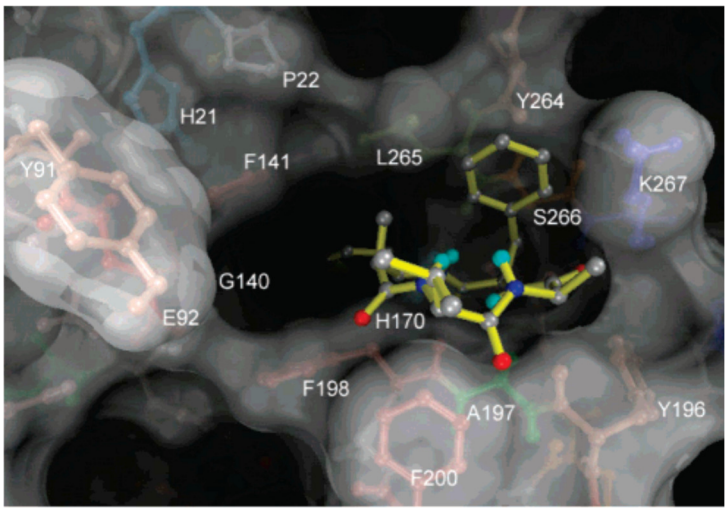

Figure 1-22. Docking of azumamide E in HDLP. Azumamide E is represented with a sticks (yellow) and balls (by atom type). HDLP is illustrated as both a molecular surface and sticks and balls. (Adapted from De Riccardis and co-workers)[136]

Ganesan route

The second total synthesis was reported by Ganesan and coworkers.[138] In this work, both β-amino acid stereocenters were constructed in one step by a diastereoselective Mannich reaction (Scheme 1-4). The chiral sulfinyl imine (**1.58**) was prepared in six steps from pent-4-ynoic acid (**1.56**). Protection of the acid, as the 1,2,3-trichloroethyl ester (Tce), followed by allylation and dihydroxylation of the terminal alkene provided the diol **1.57**. Reduction of the alkyne moiety with Lindlar catalyst and oxidative cleavage of the vicinal diols resulted in a fragile aldehyde, which was condensed with Ellmans chiral sulfinyl amine (*R*)-2-methylpropane-2-sulfinamide). The key step in this route is the Mannich reaction between the titanium enolate of PMB-propionate and the chiral sulfinyl imine (**1.58**). This reaction nicely provided the β-amino ester with the desired stereochemistry. However, low yields were reported for the last two steps. This was attributed to the low stability of the sulfinyl imine (**1.58**) and the aldehyde precursor. Removal of the PMB-group gave the β-amino acid building block (**1.59**) in 16% over 8 steps.

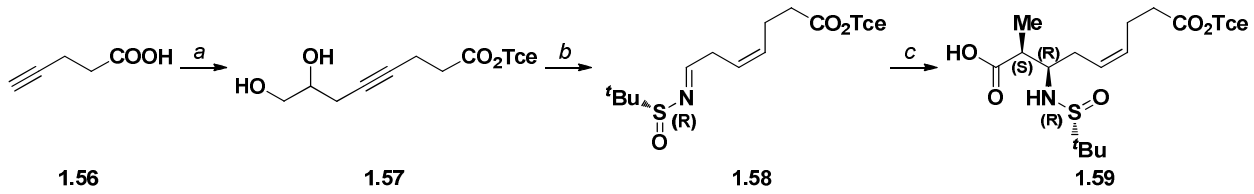

Scheme 1-4. Reagents and conditions: (a) 2,2,2-trichloroethanol, DIC, DMAP, CH_2Cl_2; *i*) Allylbromide, , K_2CO_3, CuCl, DMF: *ii*) OsO_4, NMO, aq. THF, 78% over three steps; (b) H_2, Lindlar cat., EtOAc; *i*) $NaIO_4$, aq., CH_2Cl_2; *ii*) H_2NSO^tBu, $CuSO_4$, CH_2Cl_2, 53% over three steps; (c) $CH_3CH_2CO_2PMB$, LDA, $TiCl(O\text{-}^iPr)_3$, THF; *i*) TFA, anisole, 37%, over two steps.

Building block **1.59** was elaborated to the linear tetrapeptide by coupling to the dipeptide H_2N-(D)-Val-(D)-Ala-OAll in solution, followed by deallylation and coupling to Boc-(D)-Phe-OH (Scheme 1-5).

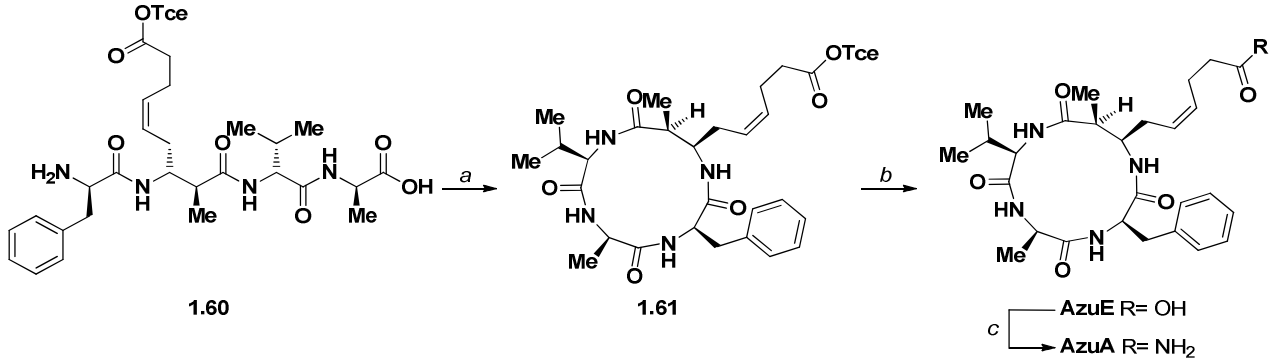

Scheme 1-5. Reagents and conditions: (a) HATU, iPr$_2$NEt, DMF/CH_2Cl_2, 85% (including deprotection); (b) Zn, AcOH, 94%; (c) EDC, HOBt, NH_3, 92%.

After removal of the *N*- and *C*-terminal protection groups, the linear peptide (**1.60**) was cyclized using a slow addition protocol.[138] In this protocol a solution of the linear peptide in DMF–CH_2Cl_2 (1:10) was added slowly to a solution of HATU and base in CH_2Cl_2. Overall yields between 52–85% were observed for the deprotection and cyclization steps. The trichloroethyl ester was reductively removed with zinc to give azumamide E. Azumamide E was subsequent amidated with EDC/HOBt and ammonia to afford azumamide A in good yield.

Bhadra route

The latest report on total synthesis of azumamide E was published by Bhadra and coworkers.[139] They obtained the β-amino ester (**1.67**) in impressive 29% yield over 10 steps (Scheme 1-6).

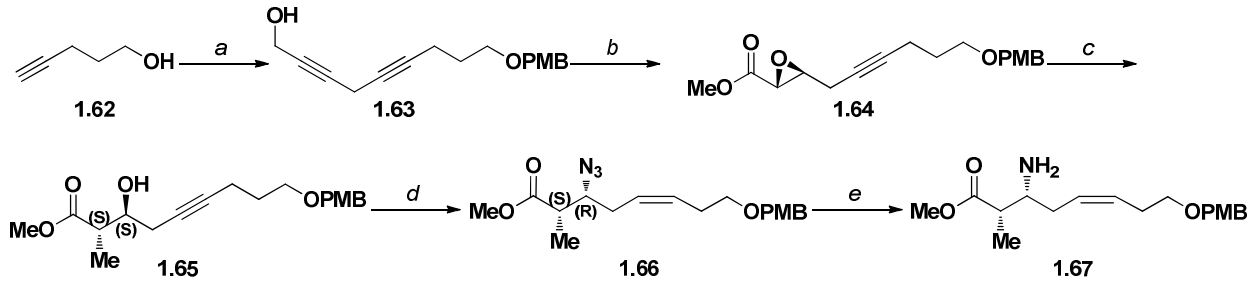

Scheme 1-6. Reagents and conditions: (a) PMBCl, NaH, THF, $(Bu)_4NI$; *i*) CuI, NaI, K_2CO_3, $HOCH_2CCCH_2Cl$, DMF, 82% over two steps; (b) $LiAlH_4$, Et_2O, 74%; *i*) (+)-diethyl tartrate, $Ti(O\text{-}^iPr)_4$, TBHP, CH_2Cl_2, 97%; *ii*) IBX; *iii*) $NaClO_2$, NaH_2PO_4, 2-metyl-2-butene; *iv*), CH_2N_2, 74% over three steps; (c) $(CH_2)_2CuLi$, Et_2O, 78%; (d) $Pd/CuCO_3$, quinoline, benzene, 99%; *i*) PPh_3, DIAD, DPPA, THF, 86%; (e) PPh_3, THF/H_2O.

4-pentyne-1-ol was PMB-protected and coupled to 4-chlorobutyne-1-ol to give the bis(acetylene) **1.63**. Selective reduction of the triple bond of the propargylic moiety gave the *E*-alkene, which was subjected to Sharpless asymmetric epoxidation to give the epoxide (**1.64**). The alcohol functionality was transformed to the corresponding methyl ester in a three-step procedure. Regioselective opening of the epoxide with lithium dimethyl cuprate afforded the correct stereochemistry in the 2-position (**1.65**). Hydrogenation of the alkyne followed by conversion of the alcohol to the azide under Mitzunobu conditions, established the correct stereochemistry in the 3-position. Finally, reduction of the azide with a Staudinger reaction afforded the free amine (**1.67**), which was coupled to the tripeptide Boc-(D)-Val-(D)-Ala-(D)-Phe-OH (Scheme 1-7).

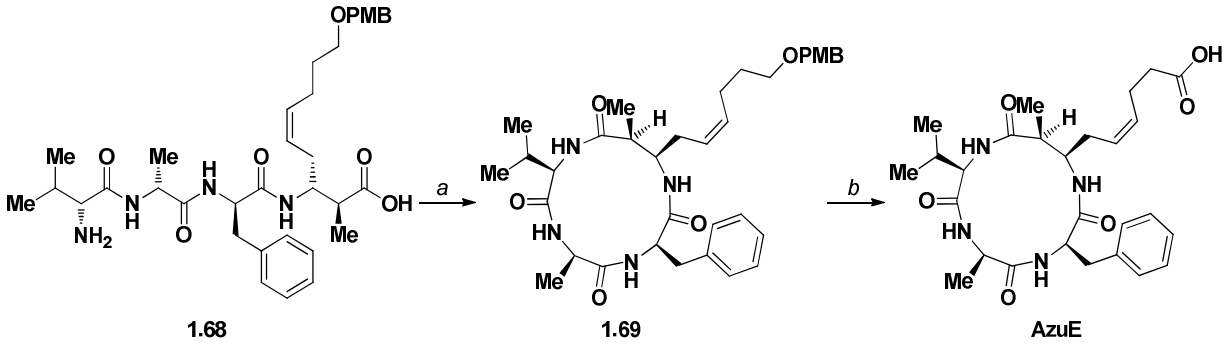

Scheme 1-7. Reagents and conditions: (a) EDCI, HOBt, CH_2Cl_2, 79%; (b) DDQ, CH_2Cl_2/H_2O, 95%; *i*) BAIB, TEMPO, $MeCN/H_2O$, 85%.

After removal of the *N*- and *C*-terminal protecting groups the linear tetrapeptide (**1.68**) was cyclized using EDC/HOBt, to afford the cyclic peptide (**1.69**) in 77% yield. Oxidative removal of the PMB group, followed by TEMPO-mediated oxidation of the alcohol to the acid, provided azumamide E in good yield. The three routes are compared in Table 1-5.

Table 1-5. Comparison of reported total synthesis for azumamide E.[a] The yield is calculated from the longest linear sequence.

Group	steps, β-aa	yield, β-aa (%)	total steps	total yield[a] (%)
De Riccardis	14	19	18	5
Ganesan	8	16	15	6
Bhadra	10	29	16	11

If the three synthetic routes are compared, in terms of obtaining the β-amino acid building block, it is clear that Ganesan has the shortest route, but also the lowest yield. The short synthesis can be attributed to the diastereoselective Mannich reaction, where both stereocenters are constructed in the same step. In the two other routes, the desired stereochemistry in the 2-position is prepared first, while at the same time obtaining the undesired chirality in the 3-position. Full inversion of the stereochemistry in the 3-position is then achieved by transformation of the hydroxyl group into a leaving group and subsequent addition of a nucleophile. Bhadra´s route is superior in terms of yield, and is only one step longer than Ganesan´s.

1.5.4 Azumamide analogs

The importance of the zinc-binding moiety in the azumamides was investigated by Ganesan and coworkers.[138] They exchanged the zinc-binding group in azumamide E to a hydroxamic acid (**1.70**, Figure 1-23). This resulted in a 15-fold increase in activity.[138] The increase in activity is attributed to the increased zinc-chelation abilities of the hydroxamic acid compared to the carboxylic acid.[140] However, the strong coordination properties of the hydroxamic acid functionality could cause problems in relation to unwanted binding to other metal

centers found in non-target proteins. Promiscuous binding to other metal proteins could lead to problems with toxicity. Several azumamide analogs, beside the hydroxamic acid compound, have been prepared (Figure 1-23).

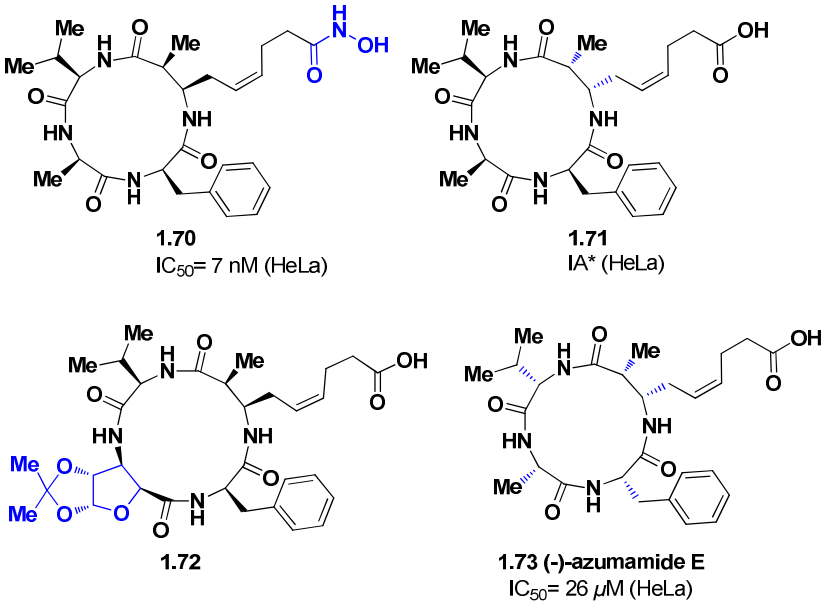

Figure 1-23. Reported azumamide analogs and their HDAC activity. Modifications are shown in blue.* Inactive up to 50 μM. [139, 136, 138]

The $\beta^{2,3}$-epimerized analog (**1.71**) was inactive and the enantiomer of azumamide E (**1.73**) showed a significant reduction in potency.[136] The lack of activity observed with the $\beta^{2,3}$-epimer **1.71**, can be explained by the altered C_3–C_4-vector of the β-amino acid. Inversion of the stereochemistry in the 3-position, will direct the zinc-binding side chain away from the 11 Å tunnel. However, the stereochemistry in the 2-position is also inverted. Therefore, the effects of the individual stereocenters cannot be evaluated from compound **1.71.** The sugar amino acid-containing analog (**1.72**) showed increased potency (96% inhibition at 20 μM) compared to azumamide E (71% at 20 μM) against HeLa extract.[139]

1.6 Specific aim of the project

Azumamide E is the only azumamide which has been subjected to HDAC profiling (HDAC1–9).[138, 137, 139] However, in vitro profiling against recombinant HDACs has improved significantly since azumamide E data was published. Especially, data on class IIa enzymes should be reevaluated as later studies have proven that the observed activity can be attributed to the presence of endogenous co-purified class I HDACs. [141, 34] In order to explore the HDAC profile of the azumamides, and elucidate any selectivities, we decided to synthesize the complete selection of natural products and screen the compounds against HDAC1–11. Furthermore, the total syntheses of azumamide B–D have not been reported and this study would allow validation of the proposed structures.[135] Based on the principles of diverted total synthesis (DTS), described by Danishefsky[142], the synthetic route should also allow access to structurally edited analogs by subtle changes in the synthetic route.

1.7 Background for synthesis of azumamides and epimeric analogs

We envisioned two major challenges in the synthesis of the azumamides. Firstly, the preparation of the $\beta^{2,3}$-amino acid building block could be challenging as two stereocenters have to be prepared. Secondly, the

cyclization of small peptides in known to be difficult. The next section will present a brief overview over different methods for β-amino acid synthesis.

1.8 β-amino acids

There has been developed a broad variety of methods for preparing β-amino acids. The β-amino acids that will be discussed here have been divided into four groups based on their substitution pattern; β^2-amino acids, β^3-amino acids, $\beta^{2,3}$-amino acids, and $\beta^{2,2,3}$ -amino acids (Figure 1-24).

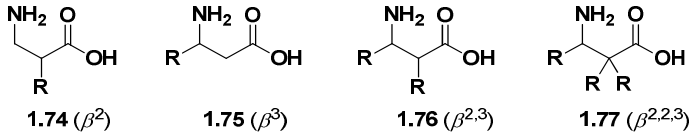

Figure 1-24. General structure of β-amino acids.

A $\beta^{2,3}$-amino acid needs to be prepared for the synthesis of the azumamides. In the interest of developing azumamide analogs with modifications in the β-amino acids, this section will also include a short discussion of some of the relevant protocols developed for synthesis of β^2-amino acids, β^3-amino acids, and $\beta^{2,2,3}$ -amino acids. Focus will be directed to methodologies, which will produce scaffolds relevant to this project.

1.9 Methods for the preparation of β^2-amino acids

Several methods have been developed for the synthesis of β^2-amino acids. Seebach has successfully employed a modified version of Evans auxillary to direct the stereochemistry in a diastereoselective aminomethylation (Scheme 1-8).[143] By this method both enantiomers of the β^2-amino acid can be accessed from the enantiomerically pure oxazolidinones.

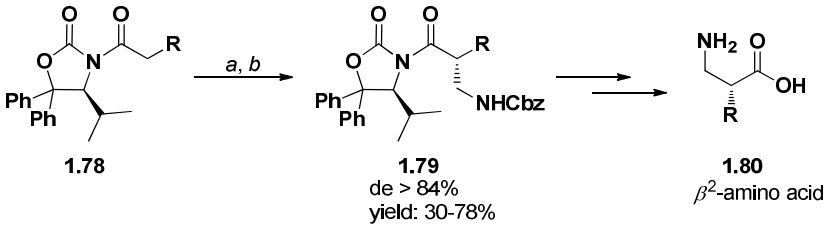

Scheme 1-8. Seebachs β^2-amino acid synthesis using 4-isopropyl-5,5-diphenyloxazolidin-2-one. Reagents and conditions: (a) $TiCl_4$, Et_3N or iPr_2NEt; (b) $TiCl_4$, $CbzNCH_2OMe$, CH_2Cl_2, 0 °C.

A different approach was reported by Goodman and coworkers.[144] In their work, pseudoephedrine was used as chiral auxillary for the diastereoselective alkylation of β-alanine (Scheme 1-9).

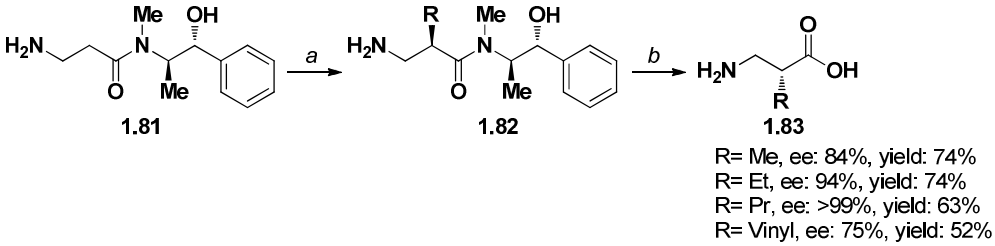

Scheme 1-9. Reagents and conditions: (a) RX, LiHMDS, LiCl, THF, –5 → 0 °C; (b) H_2O, heat. The yield is calculated from 1.81.

Compared to the ozazolidinone used by Seebach, pseudoephedrine is cheaper and commercially available. Only a couple of methods have been discussed here, but several others have been developed. Protocols using chiral isoxazolidinones[145], chiral pyrimidinone[146], C–H activation[147], and Oppolzer's sultam[148] have been reported.

1.10 Methods for the preparation of β^3-amino acids

1.10.1 Homologation and the use of α-amino acids.

A classical approach for preparing β^3-amino acids is by Arndt–Eistert homologation of α-amino acids. This procedure has been reported by Liberek and coworkers (Scheme 1-10, *top*).[149] The *N*-protected α-amino acids were converted to the corresponding diazoketones (**1.85**) and subsequent treatment with silver(I) oxide and water provided the β^3-amino acids with retention of configuration.

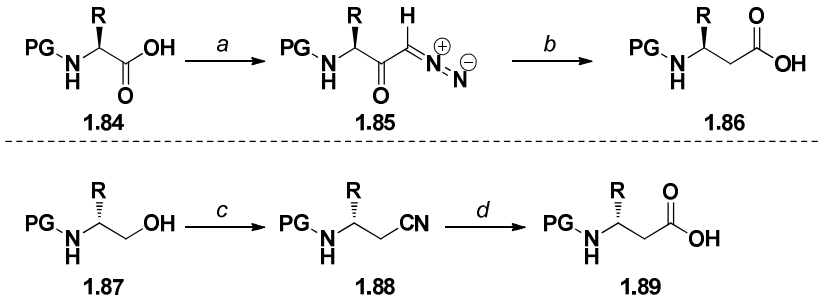

Scheme 1-10. *Top:* Reagents and conditions: (a) ^{i}BuOCOCl; *i*) CH_2N_2; (b) Ag_2O; *i*) H_2O. *Bottom:* Reagents and conditions: (c) TsCl; *i*) NaCN; (d) NaOH.

Starting from α-amino alcohols another homologation strategy has been described by Kibayashi and co-workers (Scheme 1-10, *bottom*).[150] First, the hydroxyl group is tosylated and displaced with cyanide. The resulting nitrile (**1.88**) is then hydrolyzed to afford the β^3-amino acids. Furthermore, aspartic acid and aspargine are obvious starting materials for preparing β^3-amino acids. For aspartic acid, the side chain carboxylic acid can be protected and the free acid transformed into a good leaving group by selective reduction to the alcohol. Subsequent tosylation of the alcohol and substitution to the iodide allows alkylation and thus incorporation of a β^3-side chain.[151]

1.10.2 β^3-amino acids obtained from acrylates via Michael additions and hydrogenations

Michael addition of amines to β-substituted acrylates creates a new stereocenter. To control the stereochemistry of the product, a chiral input from either the amine or the acrylate is required.

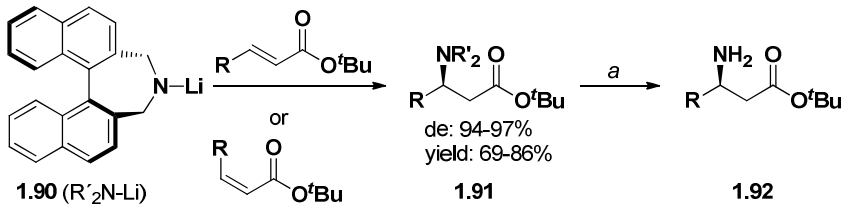

Scheme 1-11. Reagents and conditions: (a) $Pd(OH)_2/C$, ammonium formate. (Adapted from Hawkins and Lewis.)[152]

Scheme 1-11 shows the Michael addition of a chiral lithium amide (**1.90**) to different *tert*-butyl acrylates.[152] With (*E*)-alkyl esters high diastereoselectivity was observed. Hydrogenolysis of the benzylic C–N bonds was performed with Pearlman`s catalyst to give the β^3-amino esters (**1.92**).

The first reported asymmetric hydrogenation of β-amino acrylates was published by Noyori and co-workers in 1991.[153] Noyori used a ruthenium catalyzed protocol with (*R*)-BINAP as ligand and obtained >85% ee for most (*E*)-enamine esters. However, low enantioselectivity was observed with (*Z*)-enamine esters and protection of the amine was required. In 2004, these problems were overcome by Malan and co-workers, who developed a protocol using rhodium and ferrocenophosphine ligands (**1.94**, Scheme 1-12).[154] High yields and high ee were observed for unprotected (*Z*)-enamine methyl esters.

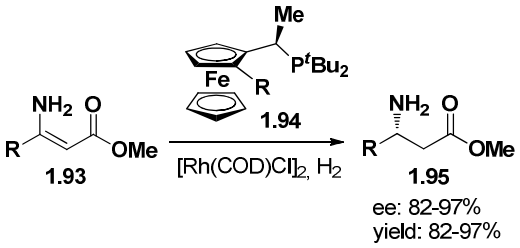

Scheme 1-12. Rhodium-catalyzed hydrogenation of β-amino acrylates reported by Hsiao and co-workers.[154]

The major drawbacks of metal-catalyzed asymmetric hydrogenations are the use of expensive transition state metals and the strict regulations concerning heavy metals in drug intermediates.[155]

1.10.3 Mannich reactions

One of the most well studied reactions, for preparing β-amino acids by C–C bond formation, is the Mannich reaction. The Mannich reaction was first described and characterized by Carl Mannich in 1912. [156] He reported the condensation reaction between formaldehyde, ammonia, and antipyrin to yield a tertiary amine. Since this discovery, the Mannich reaction has been modified and explored extensively. This has lead to more advanced and practically useful variants.[157] Mannich reactions are especially valuable in the synthesis of therapeutical agents (e.g. morphine)[158] and complex natural products containing nitrogen atoms (e.g. strychnine).[159]

A wide variety of asymmetric Mannich reactions has been developed. The addition of nucleophiles to imines is a direct and fast method for obtaining β-amino acid derivatives. The chiral input can originate from a chiral auxillary or from asymmetric catalysis. Utilizing chiral auxiliaries, the strategy can be divided into two categories, having the stereodetermining moiety placed in either the imine-part or in the nucleophilic part. The catalytic approach can be subdivided into metal -and organo-catalyzed reactions.

1.10.4 Organocatalytic Mannich reactions

For organocatalytic asymmetric synthesis of β^3-amino acids, the addition of nucleophiles to *N*-functionalized aldimines has been studied extensively (Scheme 1-13).[160] Jacobsen was the first to report an organocatalytic asymmetric Mukaiyama-Mannich-type reaction between a silyl ketene acetal (**1.96**) and *N*-Boc aryl imines (Scheme 1-13).[161] Jacobsen designed a thiourea catalyst (**1.98**), which provided high ee and high yields. The reaction was sensitive to modifications in both the silyl and alkoxy moieties of the nucleophile. Smith and co-workers prepared a catalyst (**1.99**) for the same system, which displayed superior catalytic properties.[162]

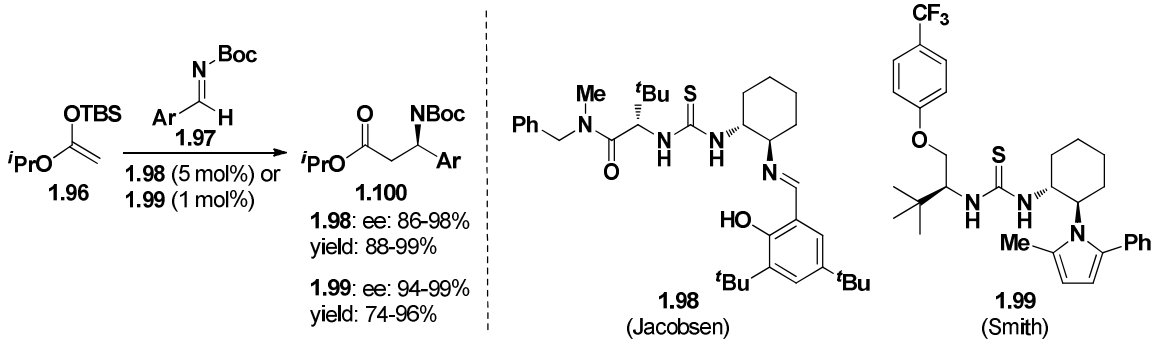

Scheme 1-13. *Left:* Mukaiyama-Mannich reactions reported by Jacobsen[161] and Smith[162]. *Right:* Developed catalysts.

Acetaldehyde can also be utilized in the enantioselective addition to *N*-Boc imines.[163] The enantioselectivity is induced by adding 20 mol% of (*S*)-proline. The β-amino aldehydes (**1.103**) obtained in this reaction can be oxidized to the Boc-protected β^3-amino acids (**1.104**) under Pinnik oxidation conditions in excellent yields (Scheme 1-14).

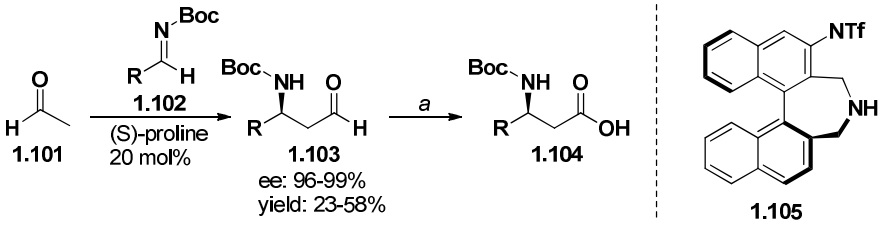

Scheme 1-14. *Left:* Mannich reactions between aldehydes and *N*-Boc imines. Reagents and conditions: (a) $NaClO_2$. *Right:* Amino sulfonamide catalyst developed by Maruoka and co-workers.

Excellent enantioselectivity was observed, but the reported yields were only low to moderate. The low yields were attributed to the high nucleophilicity of the enamine intermediate, which facilitated side reactions. This system was optimized by Maruoka and co-workers, who developed an axially chiral bifunctional amino sulfonamide catalyst (**1.105**), which increased both yield (70–92%) and the ee (98–99%).[164] The catalyst was designed to reduce the nucleophilicity of the intermediate enamine by incorporation of a dibenzylic secondary amine moiety. Interestingly, aliphatic imines worked well in both studies.

1.10.5 Mannich reactions with chiral auxillaries

The use of a chiral oxazolidinone enolate, for the preparation of β^3-amino acids, has been reported by Wang and co-workers.[165] High selectivities and good yields were observed for the addition of (*S*)-4-benzyl-2-oxazolidinone acetamide enolate (**1.106**) to *N*-tosyl arylaldehyde imines (Scheme 1-15). The scope of this study was limited to aryl-substituted imines, yet it nicely demonstrates the use of chiral nucleophiles for asymmetric preparation of β-aryl β-amino acid derivatives.

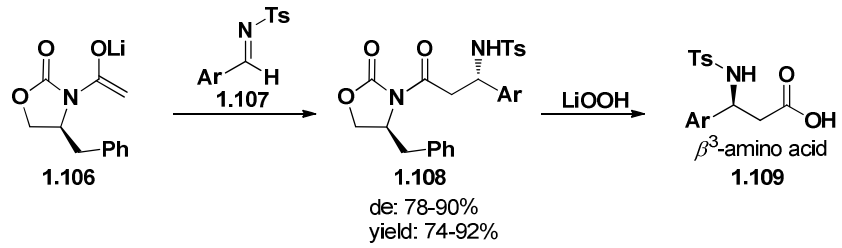

Scheme 1-15. Addition of a chiral lithium enolate to *N*-tosyl arylaldehyde imines. (Adapted from Wang and co-workers)[165]

Ellman and co-workers reported a highly diastereoselective Mannich type reaction between methyl acetate enolates and chiral sulfinyl imines (Scheme 1-16).[166] Transmetalation of the lithium enolate to the titanium enolate improved selectivity and dr > 90% was achieved with two equivalents of $ClTi(O\text{-}iPr)_3$.

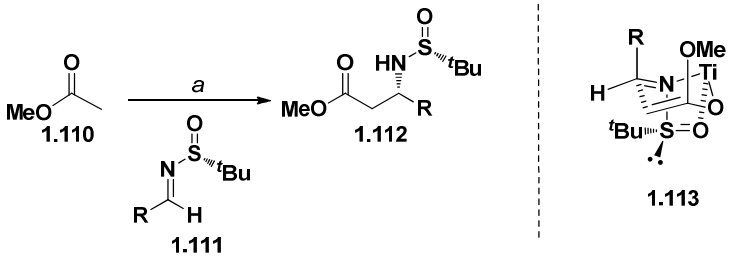

Scheme 1-16. *Left:* Reagents and conditions: (a) LDA (2.1 equiv), THF, –78 °C, 30 min; then $Ti(O\text{-}iPr)_3Cl$ (2.0 equiv), THF, –78 °C, 30 min; then imine (1.111), –78 °C. *Right:* Proposed six-membered Zimmerman–Traxler transition state. [166]

Different sulfinyl imines were investigated in the reaction shown above. The results are presented in Table 1-6.

Table 1-6. Screening of different imines in the Mannich reaction shown in Scheme 1-16.

entry	R	dr	yield, %
1	Me	99:1	94
2	*i*-Pr	98:2	85
3	*i*-Bu	98:2	80
4	Ph	98:2	90
5	3-pyridine	95:5	70

Both the nature of metal ion and solvent affected the selectivity. The six-membered Zimmerman–Traxler-type transition state (**1.113**), facilitating the diastereoselectivity observed by Ellman, has been well validated by other groups.[166, 167, 168] The transition state was first proposed by Davis and coworkers. They investigated the diastereoselective asymmetric synthesis of *cis*-N-(p-toluenesulfinyl)-2-carbomethoxyaziridines via a Darzens-type reaction of the lithium enolate of methyl bromoacetate with sulfinyl imines.[168] The The transition state is obtained by attack of the enolate from the least hindered side of the sulfinyl imine (Scheme 1-16, *right*). Coordination of the sulfinyl oxygen to titanium stabilizes the transition state.

This approach is attractive for the preparation of β^3-amino acids, as the free amine or the free carboxylic acid can be obtained in one step by treatment with acid or base, respectively. As shown in Table 1-6, both aliphatic and aromatic sulfinyl imines work well in this reaction.

1.11 Methods for the preparation of $\beta^{2,3}$-amino acids

Many of the methods introduced for the synthesis of β^3-amino acids (section 1.10) can be elaborated to produce $\beta^{2,3}$-amino acids.

1.11.1 Michael addition of chiral lithium amides to α,β-disubstituted acrylates

Parallel to the methodology showed in Scheme 1-11, Davies and co-workers reported the diastereoselective 1,4-addition of a chiral lithium amide (**1.115**) to (*E*)-*tert*-butyl 2-methylcinnamate (**1.118a,** Scheme 1-17).[169] After *in situ* protonation of the intermediate enolate with a hindered acid, the β-amino ester (**1.114**) was isolated. Removal of the protection groups provided (2*S*,3*S*)-α-methyl-β-phenylalanine in 69% yield over two steps. Performing the reaction with *tert*-butyl cinnamate (**1.118b**), followed by methylation of the isolated β-amino esters, via the lithium enolate, nicely provided the (2*R*,3*S*)-adduct (**1.117**).

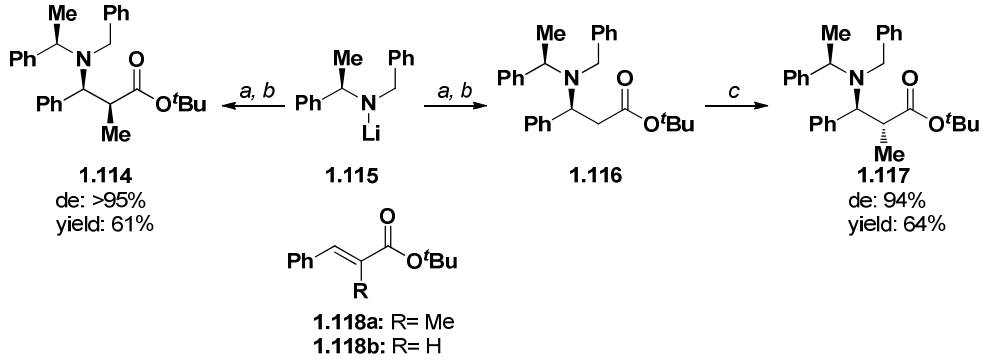

Scheme 1-17. Reagents and conditions: (a) **1.118a** or **1.118b**, toluene; (b) 2,6-di-tertbutylphenol, THF; (c) LDA, THF; then MeI.

This specific reaction was only explored with a phenyl group in the β-position and the general scope of this methodology was not elaborated. However, Lewis and Hawkins reported a similar protocol. They reported the addition of the chiral amide (**1.90**, Scheme 1-11) to *tert*-butyl crotonate, and subsequent trapping of the enolate with methyl iodide, provided the *anti*-product (de: 86%, yield: 71%).[170] The *syn*-product was prepared by the addition of **1.90** to (*E*)-tert-butyl 2-methylbut-2-enoate and protonation with ammonium chloride (de: 67%, yield: 63%).

1.11.2 Organocatalytic Mannich reactions

Addition of acetaldehyde to *N*-boc imines, as shown in Scheme 1-14, has been extended to other aldehydes.[171] This methodology effectively and selectively produced the *syn*-Mannich products shown below.

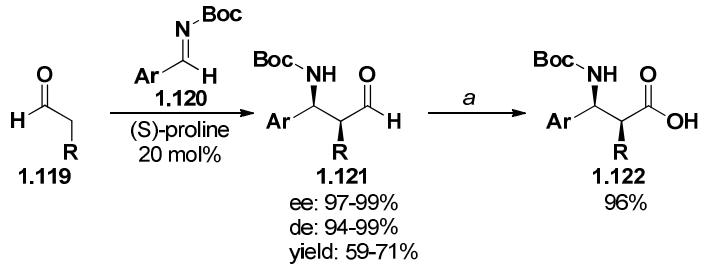

Scheme 1-18. Proline catalyzed addition of aldehydes to *N*-Boc imines. Reagents and conditions: (a) NaH_2PO_4, 2-methyl-2-butene, $NaClO_2$. R= *n*Bu, *i*Pr, Me.[171]

Excellent ee and de was observed with aromatic imines, but aliphatic imines did not produce the desired product. The aldehyde functionality was efficiently oxidized to the free carboxylic acid with sodium chlorite. The proposed mechanism for the diastereoselective Mannich reaction is shown below (Scheme 1-19).

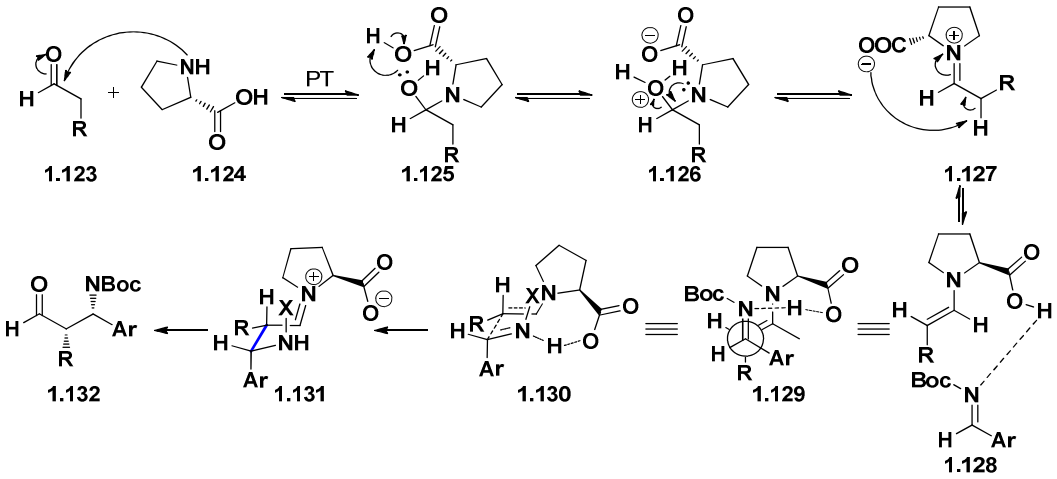

Scheme 1-19. Mechanism for the diastereoselective (*S*)-proline-catalyzed Mannich reaction between aldehydes and *N*-Boc imines.[172] X= Boc, PT= proton-transfer.

Condensation of the aldehyde and proline produces an iminium ion (**1.127**), which is in equilibrium with the energetically favored (*E*)-enamine (**1.128**). The enamine attacks the *N*-Boc protected imine from the si-face. This selectivity is mediated by the proton-transfer interaction between the carboxylic acid and the imine nitrogen (**1.129**). Furthermore, the R-group is positioned antiperiplanar to the imine group to minimize steric strain. As a result, C–C bond formation occurs on the re-face of the enamine and this selectivity is also controlled by the proton-transfer. The proton-transfer also enhances the electrophilicity of the imine.[172] Finally, the iminium specie (**1.131**) is hydrolysed to regenerate the catalyst and produce the β-amino aldehydes (**1.132**).

1.11.3 Metal catalyzed Mannich reactions

Recently, efficient metal-catalyzed asymmetric Mannich reactions have been developed. An excellent example was published by Shibasaki and co-workers in 2007.[173] Shibasaki developed a catalytic system composed of lithium aryloxide and a lanthanum aryloxide–pybox complex (Scheme 1-20). This system catalyzed the highly enantioselective Mannich reaction between 2-thiophenesulfonyl imines (**1.134**) and 1,1,1-trichlorobutan-2-one (Scheme 1-20). Both aryl, heteroaryl, alkenyl, and aliphatic imines worked well under these conditions and the Mannich products could effectively be elaborated to the *N*-boc protected β-amino esters.

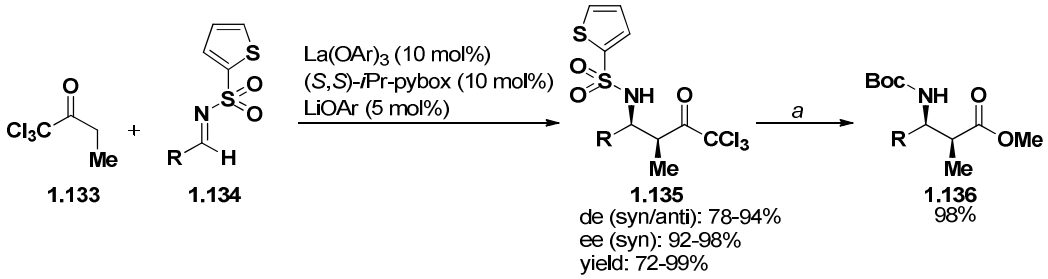

Scheme 1-20. Lanthium catalyzed Mannich reactions developed by Shibaski and co-workers.[173] Reagents and conditions: (a) NaOMe, MeOH, *i*) Boc_2O, DMAP.

1.11.4 Mannich reactions with chiral auxillaries

The Mannich reaction between acetate enolates and chiral sulfinyl imines, shown in Scheme 1-16, has been further developed to include propionate enolates.[166] This reaction allowed access to α-methylated β-amino esters (**1.139**).

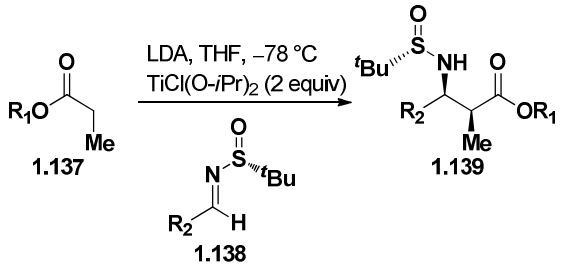

Scheme 1-21. Diastereoselective Mannich reaction. (Adapted from Ellman and co-workers)[166]

Different propionate esters and sulfinylimines were tested to explore the scope of this reaction (Table 1-7). Good selectivities were observed in all cases, except for entry 3. The reduction in selectivity reported for entry 3 could be explained by the increase in bulk, when moving from methyl- and PMB-esters to *tert*-butyl esters. 2-benzyl- and 2-(4-methoxy benzyl) propionate esters also worked well for the introduction of benzyl substituents in the α-position.[166]

Table 1-7. Screening of different imines and propionate esters in the Mannich reaction shown in Scheme 1-21.

entry	R_1	R_2	d.r.[b]	yield, %
1	Me	Me	92:7:1:0	96
2	Me	*i*-Bu	95:3:2:0	81
3	CMe_3	*i*-Bu	59:19:17:5	87
4	4-MeOBn	*i*-Bu	88:12:0:0	85
5	Me	Ph	96:4:0:0	85

1.12 Methods for the preparation of $\beta^{2,2,3}$-amino acids

1.12.1 Alkylation at the α-position

The most obvious approach to prepare $\beta^{2,2,3}$-amino acids, where the two α-substituents are identical, is to perform a simple double α-alkylation of the β^3-amino esters or to perform a mono alkylation of $\beta^{2,3}$-amino esters.[174,175]

1.12.2 Metal catalyzed Mannich reactions

Metal catalyzed enantioselective Mannich reactions between a silyl ketene acetal (**1.140**) and an imine (**1.141**) have been reported by Kobayashi[176] and Yamashita[177] to produce the enantiomeric α-dimethylated β-amino esters (**1.142** and **1.143**) in good yields and with high enantioselectivities (Scheme 1-22).

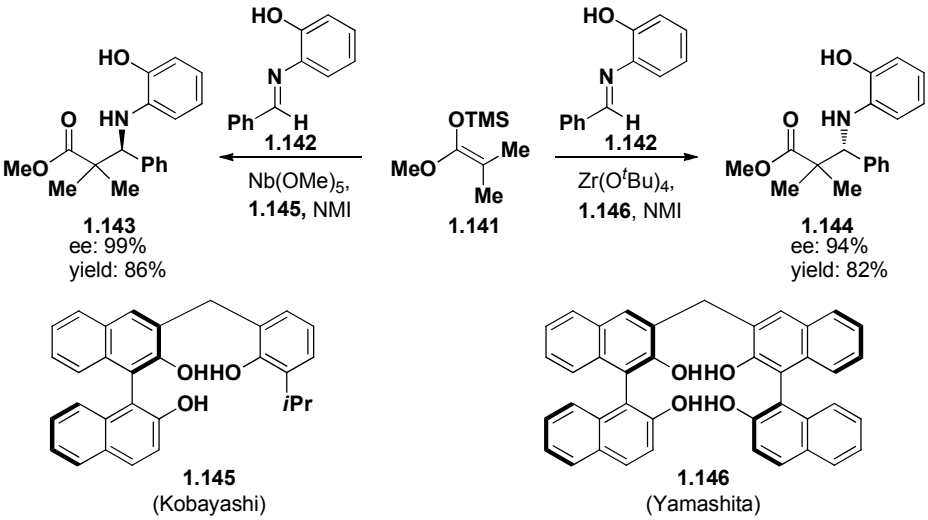

Scheme 1-22. Metal catalyzed Mannich reactions producing $\beta^{2,2,3}$-amino acids. NMI= *N*-methyl imidazole.

Noteworthy, the two protocols produce enantiomers with the exact same substrates and differ only in the choice of metal center and ligands. A quaternary stereocenter at the α-position can also be prepared by metal catalysis. Shibasaki and co-workers prepared α-tetrasubstituted anti-α,β-diamino esters in high yields (67–96%) and good diastereomeric ratios (86:14–>97:3) using nickel catalyzed addition of α-nitro esters to *N*-Boc imines.[178] Both aromatic, hetereoaromatic, and aliphatic imines were found to work well under these conditions.

1.12.3 Organocatalytic Mannich reactions

Formation of a quaternary stereocenter at the α-position can also be achieved with organocatalysis. Equivivalent to the diastereoselective preparation of $\beta^{2,3}$-amino acids from aldehydes and *N*-Boc imines, shown in Scheme 1-18 , Barbas and coworkers investigated the diastereoselective Mannich reaction between α,α-disubstituted aldehydes (**1.147**) and *N*-paramethoxyphenyl (PMP) protected imines (**1.148**) to yield $\beta^{2,2,3}$-amino aldehydes (**1.149**, Table 1-8).[179]

Table 1-8. Mannich reactions catalyzed by (*S*)-proline.

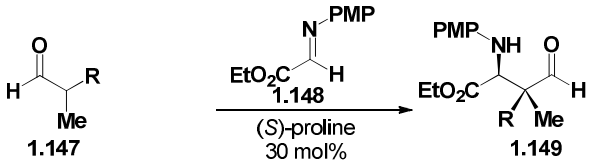

entry	R	syn:anti	ee (syn)	yield, %
1	Phe	85:15	86	66
2	thiophene	83:17	92	80
3	4-methylPh	75:25	88	82
4	(4-*i*Pr)Bn	61:39	96	80
5	(4-*tert*-Bu)Bn	60:40	99	80
6	3,4-dioxolBn	70:30	88	91

The selectivities presented in Table 1-8 are lower than the selectivities obtained from linear aldehydes (Scheme 1-18). The decreased selectivity can be explained by the difference in the energetic barriers between the intermediate *cis*- and *trans*-enamines produced from linear aldehydes and from α,α-disubstituted aldehydes. The *cis*-*trans* energy barrier for the enamines of α,α-disubstituted aldehydes is often significantly lower than for the corresponding linear aldehydes.[179] The geometry of the enamine is important for the stereochemistry in the 2-position and a mixture of *cis*- and *trans*-enamines will reduce the selectivity. The Mannich products can be oxidized to the *N*-PMP $\beta^{2,2,3}$-amino acids in good yields.[179]

1.12.4 Mannich reactions with chiral auxillaries

Ellman and coworkers have investigated the Mannich reaction between methyl isobutyrate and different (*R*)-sulfinyl imines (**1.151**, Scheme 1-23). Excellent diastereoselectivity (99:1) was observed for these reactions.[166] This protocol works well with aliphatic and aromatic imines and provides the β-amino esters (**1.152**) in good yields.

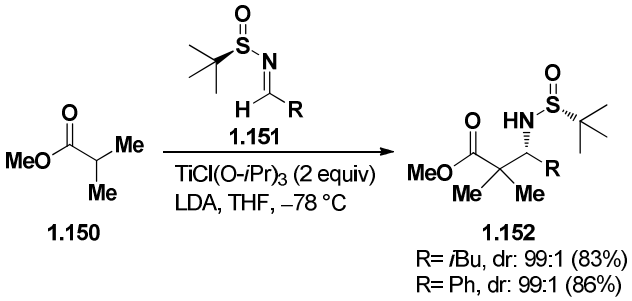

Scheme 1-23. Diastereoselective Mannich reactions between methyl isobutyrate ester enolates and chiral sulfinyl imines. Yields are shown in parentheses. (Adapted from Ellman and co-workers)[166]

2 Synthesis of azumamides and epimeric analogs

2.1 Retrosynthesis of the azumamides

Retrosynthetic analysis reveales two major challenges in obtaining the azumamides. First, the macrolactamization step is particular difficult for small cyclic peptides.[180, 181] This general observation is confirmed by previous work done on the azumamides, where the yields of the macrolactamization step is ranging from 0 to 85%. It seems that both the cyclization point and the choice of coupling reagent play critical roles in this step.[139, 136, 138, 135] We initially found it attractive to assemble the tripeptide fragment (**2.02**) on resin using standard solid-phase peptide synthesis (SPPS) and prepare the β-amino acid fragment in solution and couple this building block as the last residue (Scheme 2-1). This convergent route would result in a cyclization point between the β-amino acid and the aromatic amino acid residue.

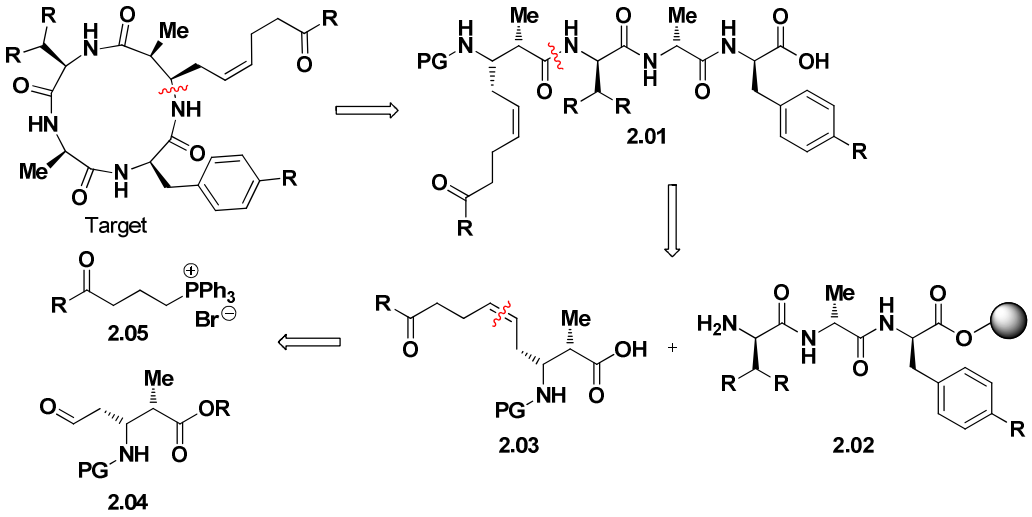

Scheme 2-1. Retrosynthetic analysis of the azumamides.

The second challenge is the synthesis of the $\beta^{2,3}$-amino acid fragment (**2.03**). Especially, preparation of the two adjacent stereocenters could be challenging, however as accounted for in the previous chapter several potential options are available. A Wittig reaction was chosen to install the *cis*-double bond in the side chain. This reaction could be utilized to introduce different functionalities in the side chain by using different Wittig reagents. The aldehyde (**2.04**) could be obtained by oxidation of the corresponding alcohol. The arguments for choosing our specific route is presented below.

2.2 Choice of route for preparation of the β-amino acid present in the azumamides

The synthetic route was designed with the intention to develop a short, efficient, and flexible protocol for obtaining the desired $\beta^{2,3}$-amino acid. To shorten down the route, the two stereocenters should be prepared in one step and the substrates should be readily available. To avoid the use of expensive metal catalysts, the focus was set on using chiral auxillaries. A common drawback of many of the methods presented in section 1.11 is the requirement of aromatic imines. An aliphatic β^3-side chain is required in the target β-amino acid and the protocols that were limited to aromatic imines, were discarded. Ellman´s Mannich reaction-approach (1.11.4) fulfill all the requirements listed above and this methodology has been used by Ganesan in the synthesis of azumamides. Using Ellman´s chiral *tert*-butylsulfinyl auxiliary we expected to be able to direct the stereochemistry in the Mannich reaction. The *tert*-butylsulfinyl group thus serves both as a chiral auxillary and an amine protection group. Furthermore, these Mannich reactions produce β-amino esters,

which easily can be hydrolyzed to give the free acids. By performing the Mannich reaction with different α-substituted esters, this methodology also provides an elegant way to incorporate different substituents in the 2-position of the β-amino acid.

Ganesan reported problems with the stability of the sulfinyl imine (**1.58**, Scheme 1-4) and the aldehyde required to prepare the imine (Scheme 1-4). The instability resulted in low yields in the final steps of the β-amino acid synthesis.[138] For this reason we chose to perform the Mannich reaction at an earlier stage in our synthetic route (Scheme 2-2) and prepare sulfinyl imine **2.07** insted.

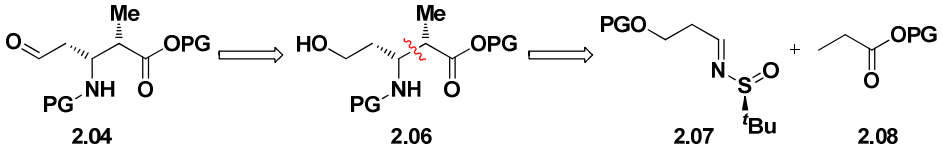

Scheme 2-2. Retrosynthesis of key intermediate (**2.04**).

We envisioned that the key imine intermediate (**2.07**) could be obtained from an appropriately protected 1,3-propanediol and the commercially available (*R)-tert*-butylsulfinamide (**2.09**). A silylether was chosen for the protection of the alcohol functionality as this group can be cleaved under mild conditions with fluoride.

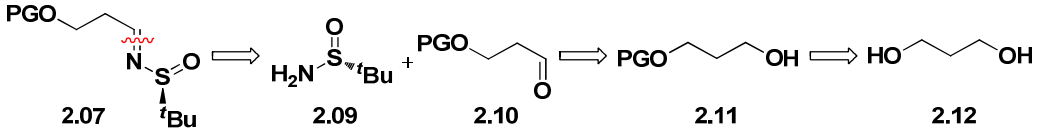

Scheme 2-3. Retrosynthesis of key sulfinylimine (**2.07**).

2.3 Synthesis of β-amino acids

2.3.1 Synthesis of chiral sulfinyl imine **2.14**

Monoprotection of 1,3-propanediol with NaH and triisopropylsilylchloride provided alcohol **2.13**, which was oxidized to the corresponding aldehyde under Swern conditions (Scheme 2-4).[182] Copper(II)sulfate mediated condensation of the aldehyde with (*R)-tert*-butyl sulfinamide provided the desired chiral sulfinyl imine (**2.14**) in 54% yield over three steps. Sulfinyl imine **2.14** is stable and can be stored in the freezer for years and only the (*E*)-imine was observed in the NMR spectra.

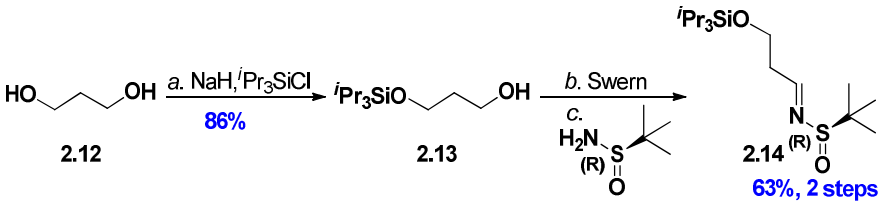

Scheme 2-4. Reagents and conditions: (a) NaH (1.0 equiv), dry THF, 30 min; then triisopropyl chloride (1.1 equiv) in dry THF, 20 h. (b) DMSO (3.2 equiv), $(COCl)_2$ (1.6 equiv), CH_2Cl_2, –78 °C, 25 min; then alcohol (**2.13**), 30 min; then Et_3N (5.2 equiv), –78° C, 40 min. (c) (*R*)-tert-butyl sulfinamide (0.95 equiv), $CuSO_4$ (2.6 equiv), dry CH_2Cl_2, 16 h, then $CuSO_4$ (0.6 equiv), 25 h.

2.3.2 Screening of propionate esters for the diastereoselective Mannich reaction

Based on Ellman´s and Ganesan´s results, an optimization study was performed, where various propionate esters were screened in the Mannich reaction with sulfinylimine **2.14** (Table 2-1).

Table 2-1. Mannich reaction screen. Reagents and conditions: 2.92 (2.0 equiv), LDA (2.1 equiv), THF, –78° C, 30 min, then Ti(O-*i*Pr)$_3$Cl (4.2 equiv), 30 min, –78° C, then imine (**2.14**).

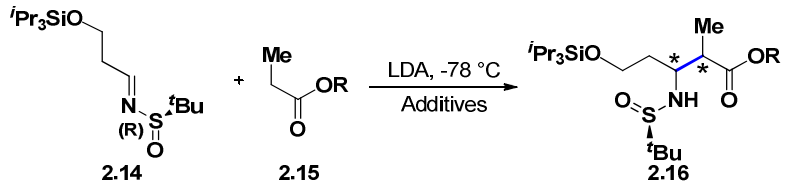

entry	R[1]	additive	enolate[a]	d.r.[b]	major isomer
1	Me	TiCl(O-*i*Pr)$_3$	*E*	47:39:10:4	ND[c]
2	Et	TiCl(O-*i*Pr)$_3$	*E*	49:29:11:11	ND
3	Allyl	TiCl(O-*i*Pr)$_3$	*E*	46:34:10:10	ND
4	PMB	TiCl(O-*i*Pr)$_3$	*E*	46:33:11:10	ND
5	^{t}Bu	TiCl(O-*i*Pr)$_3$	*E*	60:26:8:6	(*2S,3S*)[d]
6	^{t}Bu	HMPA	*E*	71:15:14:0	(*2S,3S*)[e]

[a]Major configuration of the enolate as determined by NMR and by trapping with ^{t}BuMe$_2$SiCl. [b]Diastereomeric ratio determined by ^{1}H NMR. [c]ND = not determined. [d]Determined by X-ray crystallography on its desilylated homologue. [e]Determined by comparison of spectroscopic data with the compound from entry 5.

In disagreement with the previously reported experiments, poor diastereoselectivities were observed with methyl, ethyl, allyl, and PMB propionates.[166, 138] This could indicate the presence of an alternative transition state. The best selectivity was observed with *tert*-butyl propionate (entry 5). However, the major product was not the expected (2*S*,3*R*)-diastereomer, as would be expected from the transition state mode proposed by Ellman, but the (2*S*,3*S*) diastereoisomer (Figure 2-1).This observation confirms the possibility of an alternative transition state

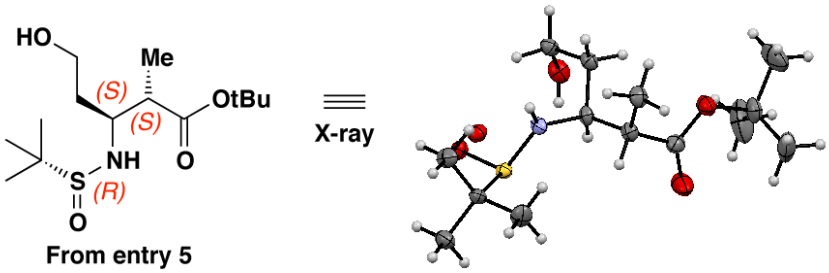

Figure 2-1. X-ray structure of the desilylated product from Table 2-1 , entry 5.

To investigate this observation, we conducted the Mannich reaction with addition of HMPA (3.0 equiv), which should break up the six-membered transition state by coordinating the metal ion. This resulted in the same major diastereoisomer as Table 2-1, entry 5 (Figure 2-2), further supporting the hypothesis of an alternative transition state.

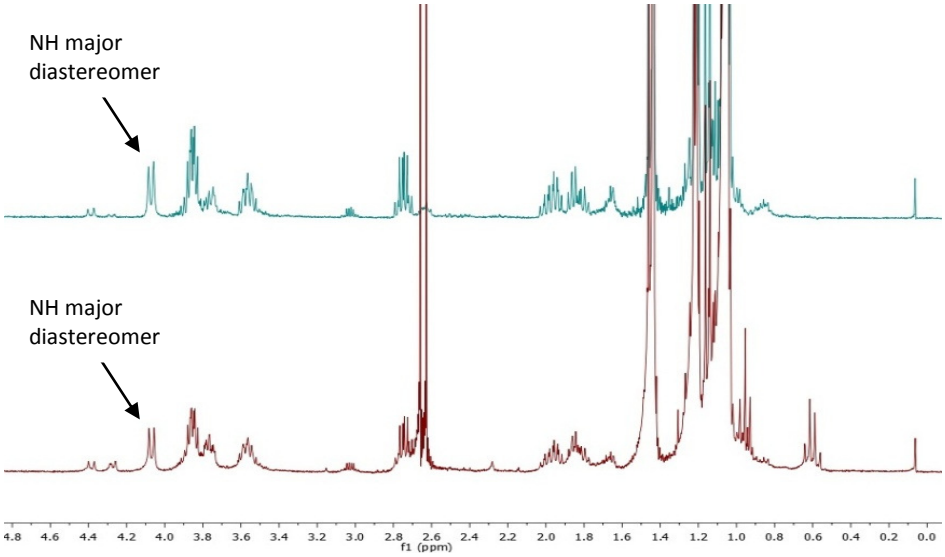

Figure 2-2. Overlay of crude ^{1}H NMR of the products obtained from Table 2-1, entry 5 (blue) and Table 2-1, entry 6 (red).

The HMPA experiment could suggest the absence of a metal coordinated six-membered transition state in the Mannich reaction. Others have reported similar "anti-Ellman" selectivities and the possibility of a nonchelated open transition state has been rationalized.[183, 184, 185, 186] Aitken and co-workers proposed an open transition state for the formation of the major diastereoisomer (**2.19**) in the Mannich reaction shown in Scheme 2-5.[183]

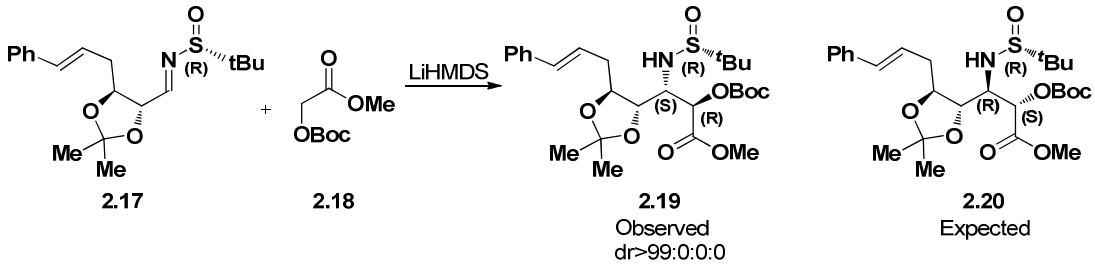

Scheme 2-5. Key Mannich reaction reported in the synthesis of the β-amino acid constituents of Microslerodermins C, D and E.

In Scheme 2-5 the diastereoselectivity was highly sensitive towards substituent changes in the enolate. The selectivity decreased to (78:22:0:0) if the methyl ester was changed to an allyl ester. Furthermore, a 2-O-trityl-protected methyl ester resulted in decomposition of the starting material.

The imine **2.14** is believed to adopt its lowest energy conformation in the open transition state. The conformation of *tert*-butanesulfinimines has been studied by several groups through computational calculations.[187, 188] Exploring the rotation around the N–S bond, two conformations (C1 and C2) can be drawn (Figure 2-3).

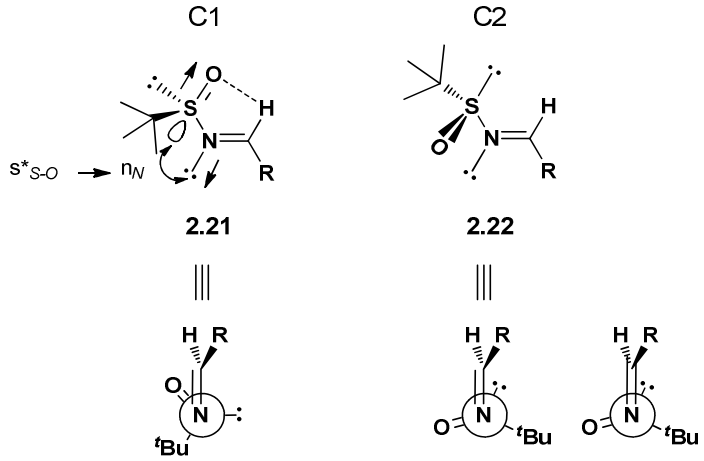

Figure 2-3. Conformations of chiral sulfinyl imines. (Adapted from Chemla and co-workers)[187]

The conformation in C1 is favored by three stabilizing features. First, the oxygen atom can participate in an intermolecular electrostatic interaction between the aldimine C–H and O. This interaction is not possible in C2. The second feature is the antiperiplaner geometry found between the S–O bond and the lone pair on the nitrogen atom. This orientation minimizes electronic repulsion between the lone pairs on oxygen and nitrogen. Finally, the antibinding σ* S–O orbital can participate in a negative hyperconjugative interaction with the lone pair on the nitrogen (n_N). If the R-group is (E)-allylbenzene the energy difference between the two conformations is 24.34 kJ/mol.[187] In the open transition state, one face of the imine is shielded by the *tert*-butyl group and the enolate attacks from the opposite face (re-face). By flipping the enolate, two reaction pathways can be hypothesized, which leads to C2-epimers (Figure 2-4, A and B).

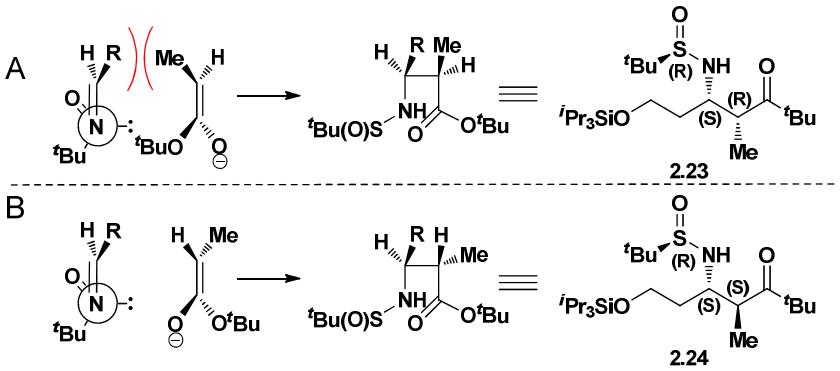

Figure 2-4. Open transition state of the Mannich reaction and the expected products. All enolates are in the *E*-configuration and the sulfur has the *R*-stereochemistry. (R= $CH_2CH_2OSi(^iPr)_3$).

In Figure 2-4, transition state B looks favored compared to A, as the sterical clash between the methyl group and the R-group is removed in transition state B. Newman projections of the transition states reveal another important interaction (Figure 2-5).

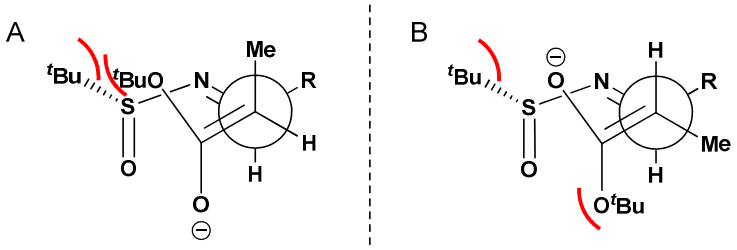

Figure 2-5. Newman projections of the two possible transition states (A and B) for the Mannich reaction.

In TS A the two bulky *tert*-butyl groups come closer together, compared to TS B. This unfavorable sterical clash also favors TS B. The (2*S*,3*S*)-stereochemistry (**2.24**) predicted by transition state B is in agreement with the major isomer observed in Table 2-1 (entry 5 and 6). The descreased selectivity observed in Table 2-1, entry 5, compared to entry 6, could be attributed to a small amount of the sulfinylimine reacting through the expected six-membered transition state in the presence of titanium.

2.3.3 Exploring the alcohol protection group

To address whether disruption of the six-membered transition state was a consequence of the bulky triisopropylsilyl ether, the less bulky benzyl (**2.30**), para-methoxybenzyl (**2.28**), and triethylsilyl (**2.27**) ether protected sulfinylimines were prepared (Scheme 2-6.). The low yield observed in the preparation of the triethylsilyl protected imine (**2.27**) was attributed to the instability of both imine (**2.27**) and alcohol (**2.25**) during purification. The imines in Scheme 2-6 were subjected to the Mannich conditions using *tert*-butyl propionate (Table 2-2).

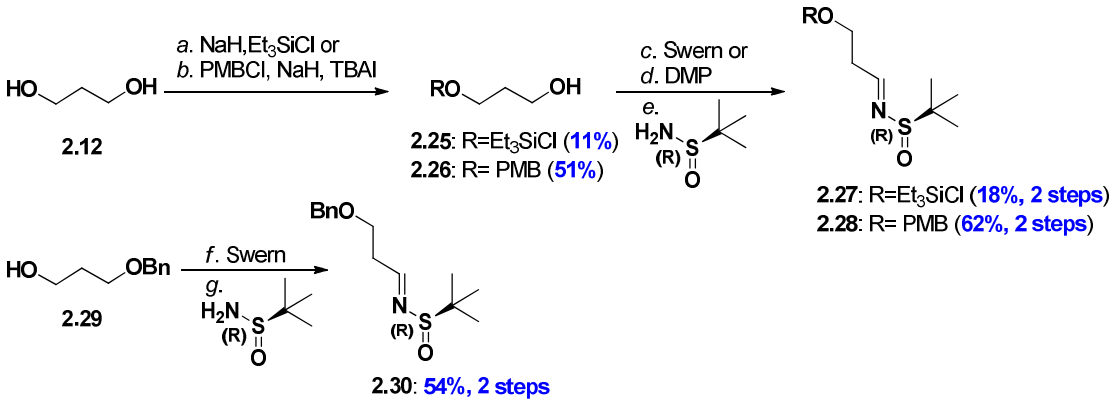

Scheme 2-6. Reagents and conditions: (a) NaH (1.0 equiv), dry THF, 35 min; then Et_3SiCl (1.0 equiv) in dry THF, 16 h. (b) NaH (0.95 equiv), TBAI (0.05 equiv), PMBCl (1.0 equiv), 17 h; (c) $(COCl)_2$ (2.2 equiv), DMSO (4.8 equiv), –78° C, 30 min, then alcohol **2.26**, –78° C, 30 min, then Et_3N (7.3 equiv), –78° C→ rt, 30 min; (d) DMP (1.1 equiv), CH_2Cl_2, 45 min; (e) (*R*)-*tert*-butyl sulfinamide (1.0 equiv), $CuSO_4$ (4–6.4 equiv), dry CH_2Cl_2, 16–20 h; (f) $(CO)_2Cl_2$ (1.1 equiv), DMSO (2.2 equiv), –78° C, 20 min, then alcohol **2.29**, –78° C, 20 min, then Et_3N (5.0 equiv), –78° C→ rt, 30 min; (g) (*R*)-*tert*-butyl sulfinylamide (1.0 equiv), $CuSO_4$ (2.2 equiv), dry CH_2Cl_2, then crude aldehyde from step f (1.1 equiv), 22 h.

The major product was still found to be the (2*S*,3*S*) diastereoisomer and the selectivities were slightly increased for the PMB- and triethyslilyl-protected imines. Even though higher selectivities were obtained with these protection groups, the isolated yield of the major diastereoisomer was lower compared to entry 5 and 6 in Table 2-1. The lower isolated yield was associated with problems in the chromatographic separation of the diastereomers.

Table 2-2. Screening of different alcohol protecting groups.

entry	auxiliary	R	additive	enolate[a]	d.r.[b]	major isomer
1	*R*	*O*Bn	$TiCl(O\text{-}iPr)_3$	*E*	70:18:12:0	ND[c]
2	*R*	*O*PMB	$TiCl(O\text{-}iPr)_3$	*E*	77:13:10:0	(*2S,3S*)[d]
3	*R*	*O*Si(Et)$_3$	$TiCl(O\text{-}iPr)_3$	*E*	75:21:4:0	(*2S,3S*)[e]

[a]Major configuration of the enolate as determined by NMR and by trapping with ^{t}BuMe$_2$SiCl. [b]Diastereomeric ratio determined by ^{1}H NMR. [c]ND = not determined. [d]Determined by comparison of spectroscopic data with the compound from entry 5. [e]Determined by X-ray crystallography on its desilylated homologue.

The (2*S*,3*S*)-stereochemistry, obtained from the Mannich reaction, is somewhat unexpected, but this β-amino scaffold could be elaborated to the interesting β^3-epimeric azumamides via building block **2.31** (Scheme 2-7). This β^3-azumamide epimer will give useful information about the specific stereochemical requirements in the 3-position in the β-amino acid. The synthesis of **2.31** is presented in the experimental section (Figure S1).

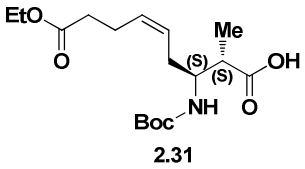

2.31

Scheme 2-7. β-amino acid building block required for the synthesis of β^3-epimeric azumamides.

Changing the chirality of the sulfur from *R* to *S*, in the Mannich reaction shown in Table 2-1, provided the enantiomeric (2*R*,3*R*) β-amino ester (**2.37**, Scheme 2-9). The stereochemistry of this compound is interesting, as it can be elaborated to provide a building block (**2.41**, Scheme 2-9), which will allow the synthesis of β^2-epimeric azumamides. These novel epimeric azumamides have not been reported previously and they will provide information about the stereochemical requirements in the 2-position and 3-postion of the β-amino acid.

2.3.4 Synthesis of β^2-and β^3-epi-building blocks

Silylether **2.32** was desilylated using TBAF and the *Z*-double bond was introduced by Dess Martin oxidation to the aldehyde followed by a Wittig reaction with 3-(ethoxycarbonyl)propyl] triphenylphosphonium bromide (Scheme 2-9). Initially, yields between 44% and 65% were observed for the desilylation step. Besides the desired alcohol, a byproduct was observed. NMR and LC-MS analyses indicated formation of lactone **2.34** (Scheme 2-8).

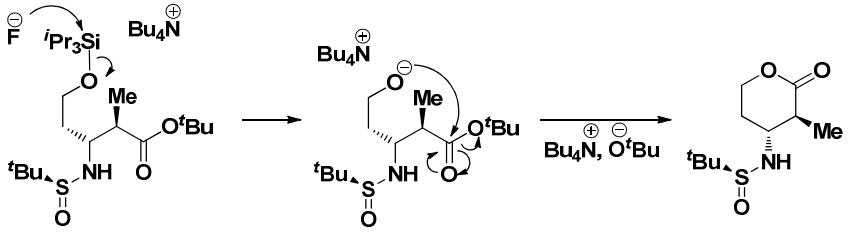

2.32 **2.33** **2.34**

Scheme 2-8. Proposed mechanism for the synthesis of lactone byproduct.

This lactone could be the result of an intramolecular reaction, where the forming alkoxide attacks the *tert*-butyl ester. This results in a stable six-membered lactone. Similar reactions have been reported for methylesters.[189] The problem was solved by adding one equivivalent of acetic acid, which protonates the

forming alkoxide, rendering it a much poorer nucleophile. The addition of acetic acid increased the yield to 76–92%. The two step alkene formation also required optimization. Oxidation under Swern conditions, provided the aldehyde (**2.39**) in low yields (<30%). Switching to a milder Dess Martin periodinane oxidation gave higher crude yields (75–90%). Controlling reaction temperature and reaction time was found to be critical for obtaining the fragile aldehydes. Thorough drying of the Wittig reagent was crucial in order to achieve complete conversion of the aldehyde in the Wittig reaction. In a model study the aldehyde (**2.39**) was replaced with benzaldehyde. This reaction provided the desired alkene in quantitative yield, indicating that aldehydes of the type shown in Scheme 2-9, could be unstable under the conditions used. However, the desired *Z*-olefin (**2.40**) was obtained in 59% yield, over two steps, by addition of the crude aldehyde to an unstabilized phosphonium ylide. Removal of the *tert*-butyl ester and the sulfinyl group under acidic conditions, followed by reprotection of the amine with *tert*-butoxy anhydride, afforded β-amino acid **2.41**. This β-amino acid could then serve as a building block in the synthesis of β^2-epi-azumamides. The Boc-group was introduced on the nitrogen as the selective removal of the *tert*-butyl group with TFA was sluggish and resulted in cleavage of the sulfinyl group. Using the same chemical transformations as in Scheme 2-9, the β-amino ester obtained fromTable 2-1, entry 5, was used to synthesize the (2*S*,3*S*) β-amino acid building block (**2.31**).

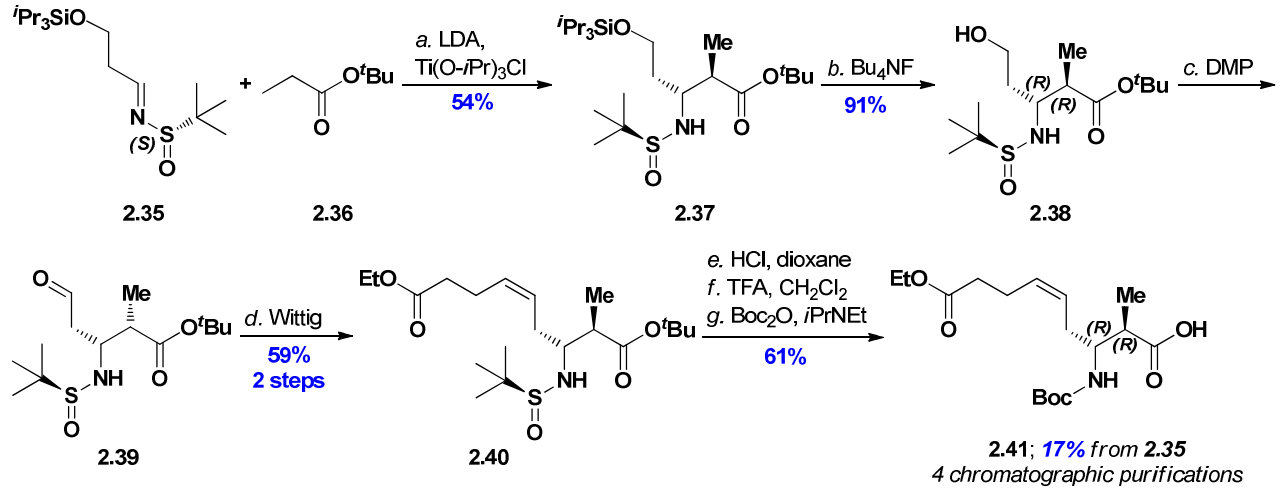

Scheme 2-9. Reagents and conditions: (a) LDA (2.6 equiv), *tert*-butyl propionate (2.5 equiv), THF, –78 °C, 30 min; then Ti(O-*i*Pr)$_3$Cl (4.5 equiv), THF, –78 °C, 30 min; then imine (2.35), –78 °C, 30 min. (b) AcOH (1.0 equiv), Bu$_4$NF (1.2 equiv), THF, 0 °C, 10 min. (c) NaHCO$_3$ (1.4 equiv), Dess-Martin periodinane (1.4 equiv), dry CH_2Cl_2, 0 °C, 15 min; then NaHCO$_3$ (0.3 equiv), Dess-Martin periodinane (0.2 equiv), 25 min. (d) KHMDS (1.9 equiv), $Ph_3PBr(CH_2)_3COOEt$, (2.0 equiv), dry THF, –78 °C, 30 min.; then aldehyde **2.39** in dry THF, 1 h, –78 °C → rt (e) TFA–CH_2Cl_2 (1:1, 10 mL), rt, 1 h. (f) HCl (4.0 M in dioxane, 6.3 equiv), dioxane, 2.5 h. (g) *i*Pr$_2$NEt (1.4 equiv), Boc$_2$O (1.4 equiv), dry CH_2Cl_2, 16 h; then *i*Pr$_2$NEt (0.2 equiv), Boc$_2$O (0.2 equiv), 1 h.

2.3.5 Synthesis of building block for the natural products

With the building blocks for the two azumamide epimers in hand, we turned our attention to the building block required for the natural products. If the Mannich reaction proceeds through an open state transition state, as shown in Figure 2-4, it should be possible to modulate the stereochemistry in the 2-position by performing the reaction with the *Z*-enolate instead of the *E*-enolate. The expected transition states are shown in Figure 2-6.

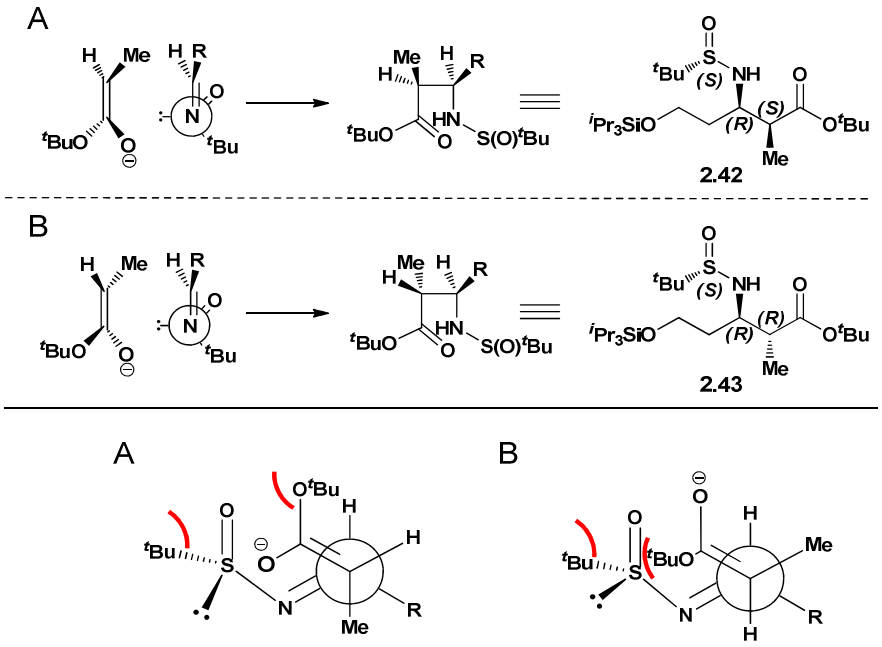

Figure 2-6. *Top:* Transition states for the Mannich reaction using the *Z*-enolate and the (*S*)-imine. *Bottom:* Newman projection of the two transition states.

In TS A the steric clash between the two *tert*-butyl groups is minimized, but the methyl group from the enolate and the R group will clash. In TS B the reverse is the case and the two *tert*-butyl groups will clash, whereas the methyl–R-group interaction will be avoided. The major diastereoisomer observed from the experiment is the desired (2*S*,3*R*), which can be explained from transition state A. This selectivity indicates that the *tert*-butyl–*tert*-butyl steric interaction is more important than the methyl–R-group interaction in determining the stereochemistry. This rationale is also in agreement with the selectivity observed for compounds **2.24** and **2.43**.

Where the *E*-enolate is formed by deptrotonating in THF, the *Z*-enolate can be prepared by deprotonating the *tert*-butyl ester with LDA in HMPA–THF (23:77, v/v).[190, 191, 192] The observed selectivity can be explained by the transition states shown in Figure 2-7. In THF, which is a relative weak coordinating solvent, the lithium ion will coordinate strongly to the carbonyl oxygen resulting in an increase in bulk at this face (Figure 2-7, **2.44**). Therefore the methyl group will be oriented away from this face. In the presence of HMPA, a strong coordinator of lithium, the interaction with the carbonyl oxygen will be reduced significantly. This resulting reduction in bulk at this face, will favor the positioning of the methyl group away from the steric interactions with the *tert*-butyl group (**2.45**).

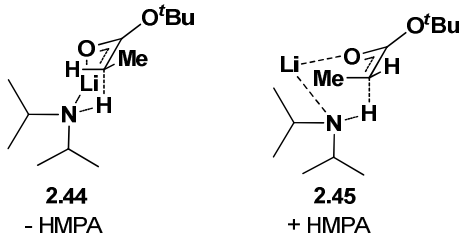

Figure 2-7. Transition states showing the enolate formation in absence (**2.44**) and presence (**2.45**) of HMPA.

To determine the *E*:*Z* selectivity, the enolates were trapped as the *tert*-butyldimethyl silylenol ethers and the *E*:*Z* ratio was determined by ^{1}H NMR. For the HMPA–THF (23:77, v/v) and THF conditions the *E*:*Z* ratio was 18:82 and 94:6, respectively (Scheme 2-10). Attempts to improve the *E*:*Z* selectivity, by deprotonating with the more sterically hindered base lithium tetramethylpiperidide (LTMP)[193] proved unsuccessful.

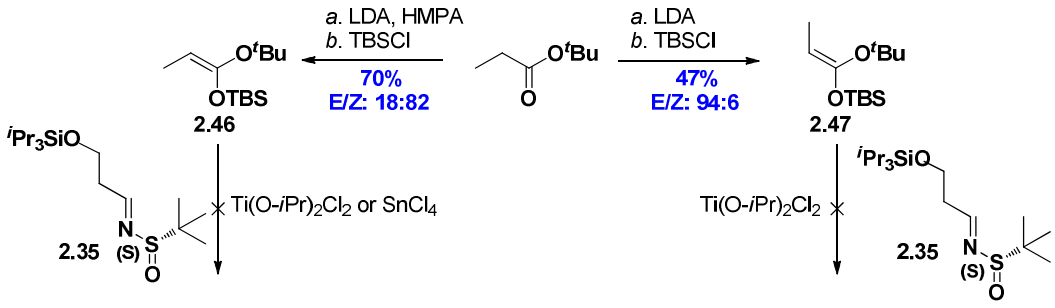

Scheme 2-10. Preparation of *E*/*Z*-silylenol ethers from *tert*-butyl propionate and attempted Mannich-Mukayama-type reactions.

With the silylenol ethers (**2.46** and **2.47**) in hand, the Mannich-Mukayama-type reactions, catalyzed by Lewis acids, were investigated. This approach would provide a simpler Mannich reaction protocol where *in situ* preparation of the enolate is avoided. Disappointingly, no conversion of the imine (**2.35**) was observed with either titanium di-isopropoxydichloride or stannic tetrachloride (Scheme 2-10).

The *Z*-enolate worked well in the Mannich reaction and nicely provided the desired (2*S*,3*R*)-β-amino ester (**2.42**). This compound was elaborated to the β-amino acid building block **2.51** (Scheme 2-11). The Fmoc group was chosen as the amine protecting group, as this allows introduction of the β-amino acid in all positions of the liniar tetrapeptide. As a result, cyclization can be performed at different positions. The stereochemistry of the building block was confirmed by comparison of spectroscopic data from the Boc protected homolog (**2.52**) to the data previously reported for this compound.[136, 194]

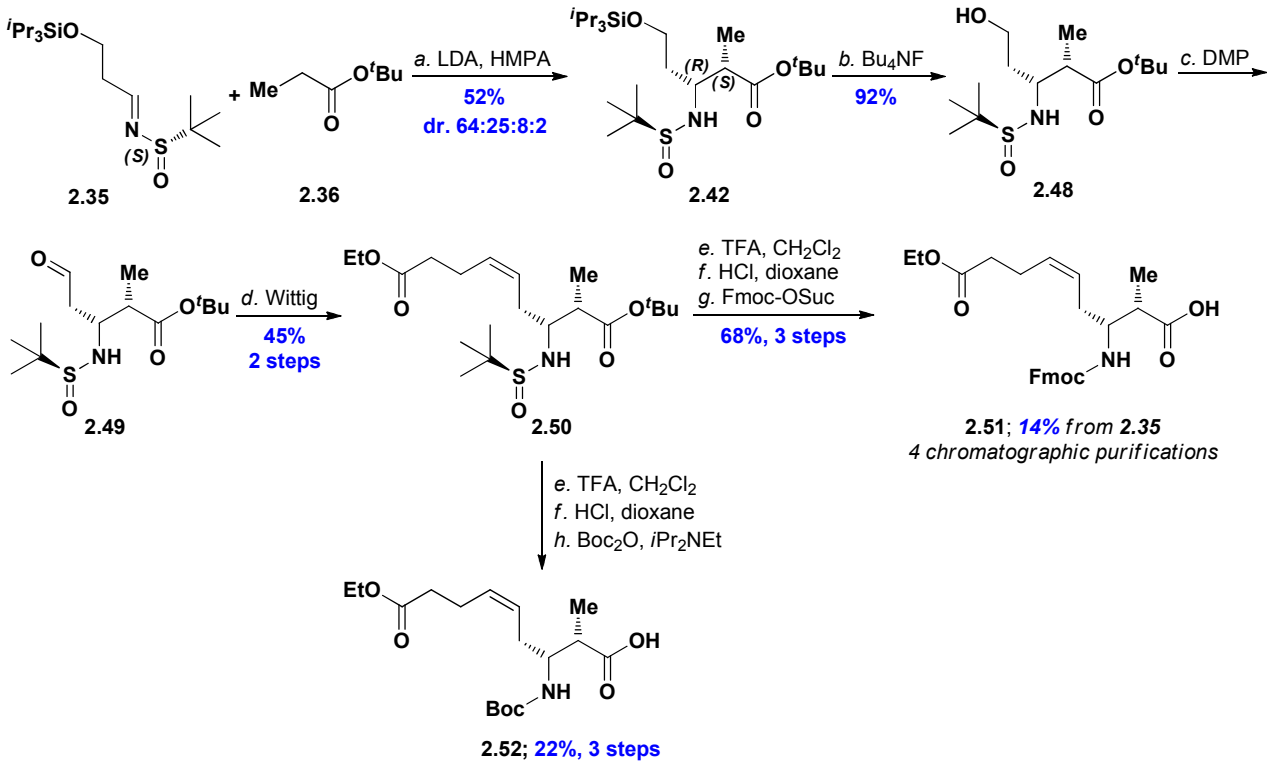

Scheme 2-11. Reagents and conditions: HMPA (6.4 equiv), LDA (2.6 equiv), *tert*-butyl propionate (2.5 equiv), THF, –78 °C, 30 min; then imine (2.35), –78 °C, 30 min. (b) AcOH (1.0 equiv), Bu_4NF (2.0 equiv), THF, 0 °C → rt, 1.5 h. (c) $NaHCO_3$ (1.5 equiv), Dess-Martin periodinane (1.4 equiv), dry CH_2Cl_2, 0 °C → rt, 1.5 h. (d) KHMDS (1.9 equiv), $Ph_3PBr(CH_2)_3COOEt$, (2.0 equiv), THF, –78 °C; then aldehyde **2.49** in dry THF → rt, 18 h. (e) TFA–CH_2Cl_2 (1:1, 10 mL, 80 equiv), 0 °C → rt, 3 h. (f) HCl (4.0 M in dioxane, 3.0 equiv), dioxane, 3 h. (g) Na_2CO_3 (4.0 equiv), Fmoc-OSuc (1.2 equiv), dioxane–H_2O, 0 °C → rt, 2 h; (h) iPr_2NEt (3.0 equiv), Boc_2O (2.1 equiv), CH_2Cl_2, 3 h, then iPr_2NEt (3.0 equiv), 18 h.

The reduction in diastereoselectivity observed with the *Z*-enolate compared to the selectivity from Table 2-1, entry 6, can be explained by the difference in *E*:*Z* ratio shown in scheme 2-24. Having 18% of the *E*-isomer present, compared to only 6% *Z*-isomer in the reverse case, will lower the selectivity. The mismatch between the two steric interactions, proposed for the reaction mechanism involving the *Z*-enolate in Figure 2-6 A, could also induce a reduction in selectivity.

2.3.6 Concluding remarks

Through the optimized Mannich conditions developed in this project, it is possible to access all four diastereomers of the $\beta^{2,3}$-amino acid building block (Scheme 2-12). The (2*R*,3*S*)-diastereoisomer (**2.53**) was not prepared as $\beta^{2,3}$-epi-azumamide E, which contains the (2*R*,3*S*)-stereochemistry, has been reported by DeRiccardis and co-workers.[136] The scope of this reaction is discussed further in chapter 3.8.

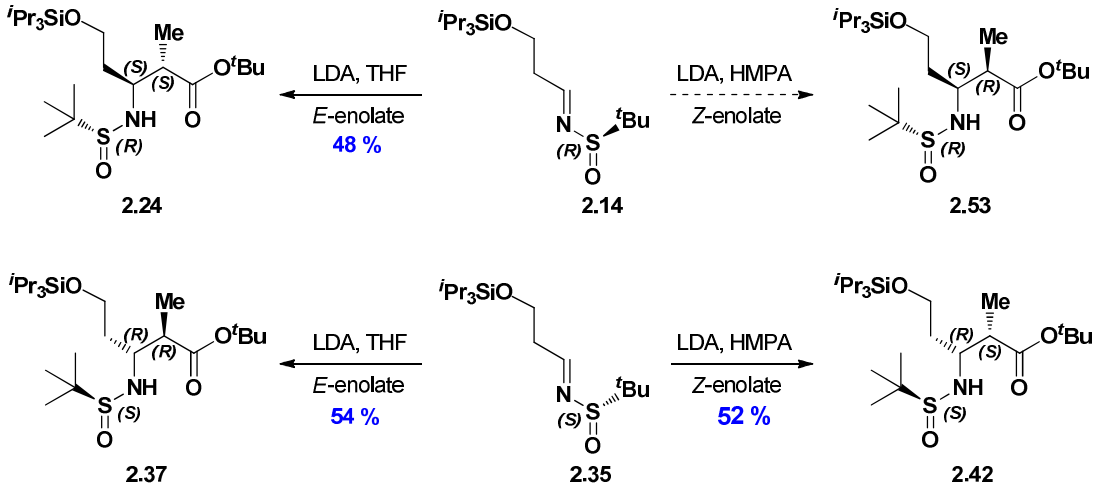

Scheme 2-12. The diastereoselective Mannich reactions between chiral sulfinyl imines and *tert*-butyl propionate enolates.

2.4 Peptide synthesis

2.4.1 Synthesis of β^2-epi-azumamide E and β^3-epi-azumamide E

The linear tetrapeptides **2.54** and **2.57** were prepared on solid support (polystyrene 2-chlorotrityl resin) using commercially available Fmoc-D-amino acids and the β-amino acids **2.31** and **2.41**, respectively. Couplings were performed using HATU and 2,6-lutidine in DMF. Treatment of the resin with TFA cleaved the peptide from the solid support and removed the Boc-group, rendering the peptide ready for cyclization. Cyclization under dilute conditions (< 1mM) using HATU, followed by hydrolysis of the side chain ethyl ester, provided the epimeric azumamide E analogs (**2.56** and **2.57**, Scheme 2-13).

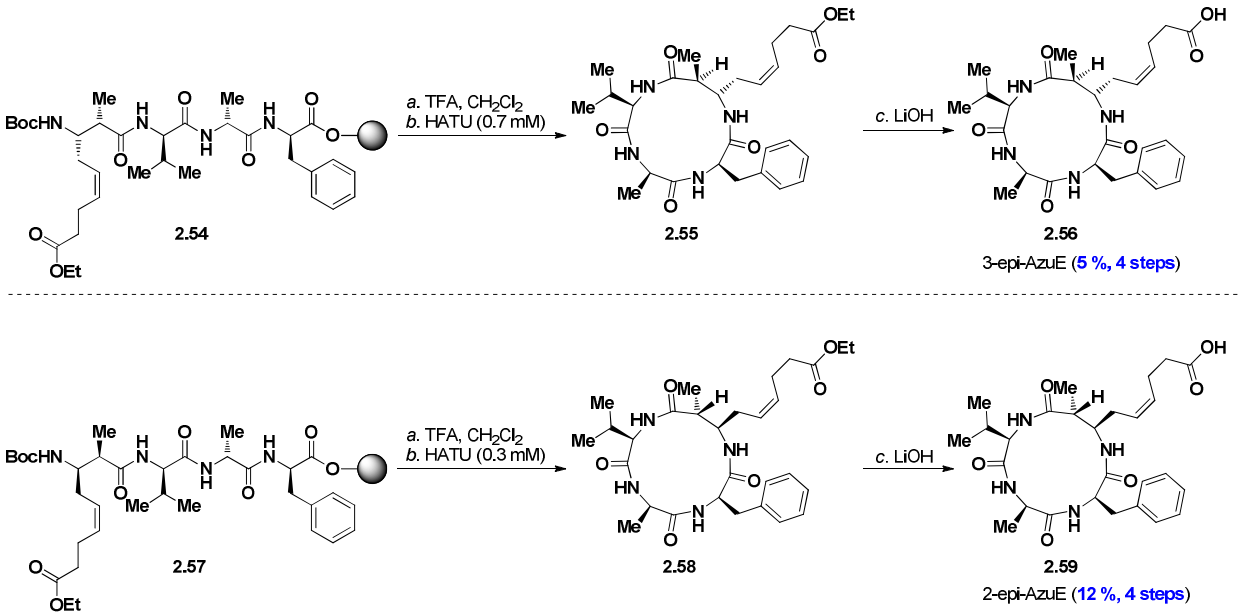

Scheme 2-13. Reagents and conditions: (a) TFA–CH_2Cl_2 (1:1), 2 × 30 min; (b) HATU, *i*Pr_2NEt (8.0 equiv), DMF (0.3–0.7 mM peptide concentration), 17–21 h; (c) LiOH, THF–H_2O (1:1), 16 h.

The low overall yield observed with the synthesis of these cyclic peptides can be attributed to two major obstacles; the cyclization step and solubility/purification issues. As mentioned in the retrosynthetic section,

cyclization of small peptides is challenging. The cyclization step will be discussed further in section 2.4.2. All the final macrocyclic peptides were purified using preparative HPLC. These macrocyclic peptides are poorly soluble in water and the risk of precipitation on the column is present, when purifying compounds with low water solubility by means of preparative HPLC. Purification of the same compounds by vacuum liquid column chromatography (VLC), resulted in higher yields (up to 25%), but the purity was unfortunately not high enough for biological testing (residual iPr$_2$NEt could be detected in the NMR spectrum). This observation indicates that some material is lost during HPLC purification. In the HPLC purification the eluent is made slightly acidic by adding TFA. In retrospect it could have been interesting to purify with a slightly basic eluent instead, as the some of the azumamides contain a free carboxylic acid. A basic eluent might increase the water solubility of these compounds.

2.4.2 Synthesis of azumamide A–E

The same overall synthetic strategy, used to obtain the epi-analogs, was applied for synthesis of the natural products. The linear tetrapeptides were obtained in good yields and good purities after cleavage from the resin and precipitation with ether. Several cyclization positions and conditions were tested to increase the yield of the cyclization step. Besides the HATU-mediated cyclization using dilute conditions, the slow addition protocol developed by Ganesan was also tested.[138] The cyclization results are summarized in Table 2-3.

Table 2-3. Cyclization experiments. N.D = Not determined.

entry	peptide sequence	conditions	yield (from linear peptide)	dimer (LC-MS)
1	H$_2$N-β-aa-(D)Val-(D)Ala-(D)Phe-OH	Dilute	23% (VLC)	Observed
2	H$_2$N-(D)Ala-(D)Phe-β-aa-(D)Ala-OH	Dilute	19% (VLC)	Not observed
3	H$_2$N-(D)Phe-β-aa-(D)Val-(D)Ala-OH	Slow addition	25% (VLC)	Observed
4	H$_2$N-(D)Val-(D)Ala-(D)Tyr-β-aa-OH	Dilute	11% (HPLC)	Observed
5	H$_2$N-β-aa-(D)Val-(D)Ala-(D)Phe-OH	Slow addition	N.D	Not observed

For all reactions we observed full conversion of the linear peptide and the only byproducts observed were varying amounts of dimer and trace amounts of epimeric cyclic peptide (Figure 2-8).

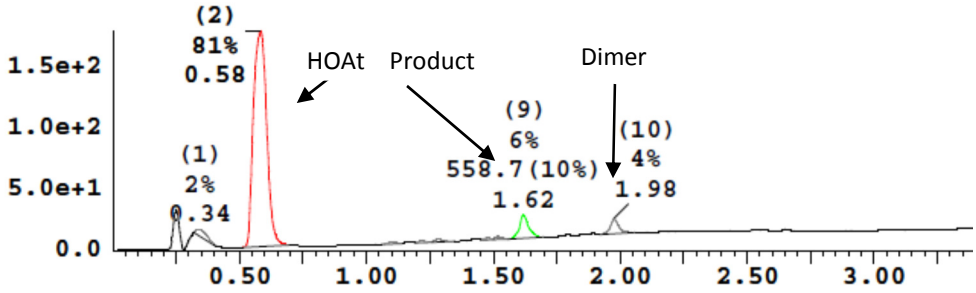

Figure 2-8. Chromatogram showing the crude reaction mixture from Table 2-3, entry 5.

In our hands, neither the peptide sequence nor the cyclization conditions seemed to alter the yields dramatically. The synthesis of azumamide C and B is presented in Scheme 2-14.

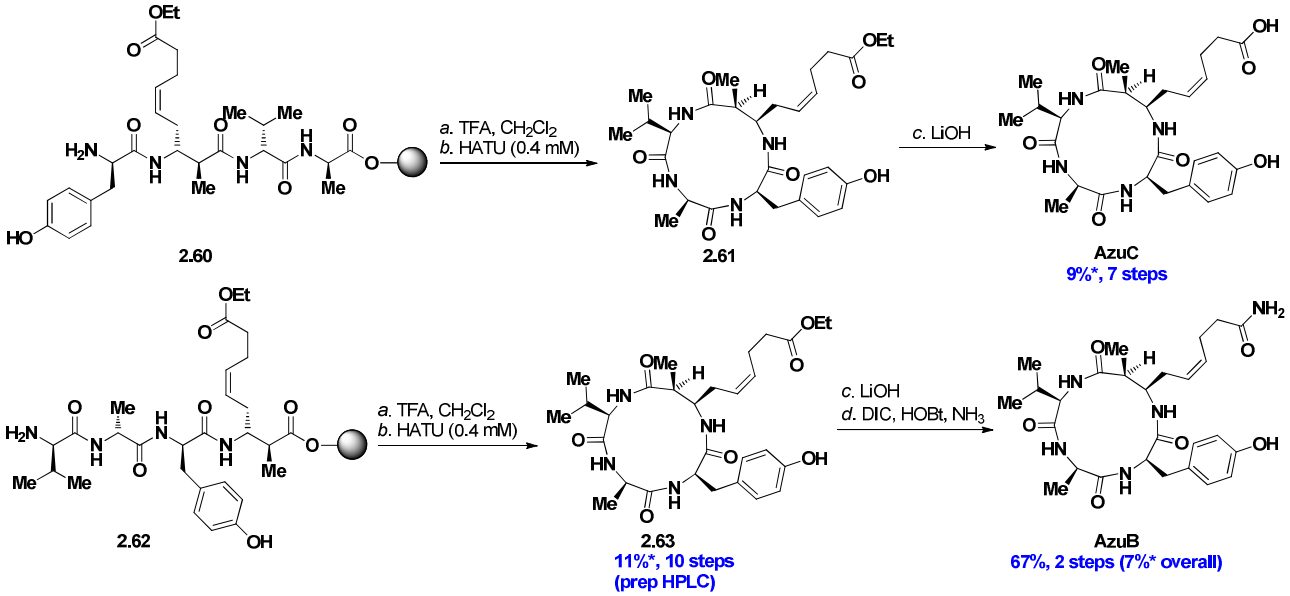

Scheme 2-14. Reagents and conditions: (*a*) TFA–CH_2Cl_2 (1:1), 2 × 30 min; (*b*) HATU, *i*Pr_2NEt (8–10 equiv), DMF (0.3–0.4 mM peptide concentration), 3–18 h; (*c*) LiOH, THF–H_2O (1:1); (*d*) DIC (11 equiv), HOBt (3.0 equiv), *i*Pr_2NEt (4.0 equiv), NH_3–dioxane (25 equiv), DMF–CH_2Cl_2 (2:1), 5 d. *Yields are based on resin loadings.

Azumamide C was prepared from the tetrapeptide **2.60**, without any purification after the cyclization step. The hydrolysis of the ethyl ester goes “peak to peak” in the LC-MS and this step does not seem to cause any problems.

Azumamide B was cyclized between the sterically demanding valine and the β-amino acid residue and the reaction mixture was purified by preparative HPLC (Table 2-3, entry 4). A cyclization study performed on a simplified model peptide had shown this cyclization site to be favorable. However, judging by LC-MS and the purified yields (cyclic petide 11%; dimer 5%) this cyclization site resulted in dimer formation (Figure 2-9). In the peptide used to perform the model study, the β^2-methyl group had been removed, which decrease the bulk around the C-terminal. This could explain the difference in the cyclization yields. This result indicates that the cyclization reaction is extremely sensitive, even to small modifications in the linear peptide. The increase in dimer formation observed with the Val to β-aa cyclization compared to β-aa to Phe (Table 2-3, entry 1) can be explained by a sterically induced reduction in cylization rate. When the cyclization reaction is slowed down, there will be more time for the peptide to form dimers. However, Bhadra and coworkers have reported 79% yield for the EDCI/HOBt mediated cyclization of the H_2N-(D)Val-(D)Ala-(D)Phe-β-aa-OH sequence, having a PMB protected alcohol in β-amino acid side chain. In their study no observation of dimer was reported.[139]

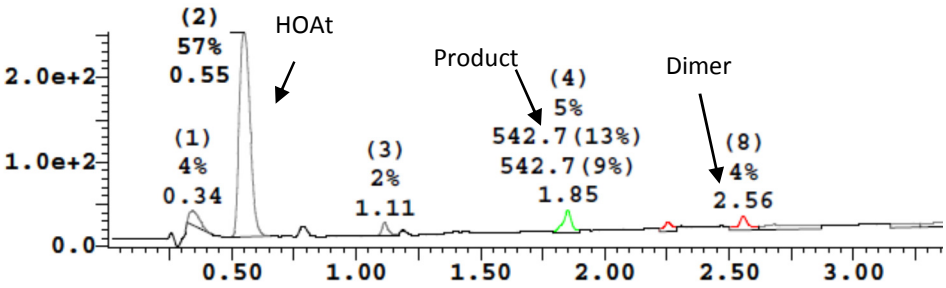

Figure 2-9. Chromatogram showing the crude reaction from Table 2-3, entry 4 to afford **2.63**.

The purified ethyl ester (**2.63**, Scheme 2-14) was converted to the corresponding carboxylic acid with LiOH and activated by a combination of DIC and HOBt. Addition of ammonia afforded azumamide B in good yield (over two steps), albeit prolonged reaction time was needed. The good yield observed for the hydrolysis and amidation step, indicates that the critical step is indeed the cyclization. The spectral overlay of the ^{1}H NMR of the originally isolated azumamide B and our synthetic sample is shown below (Figure 2-10).

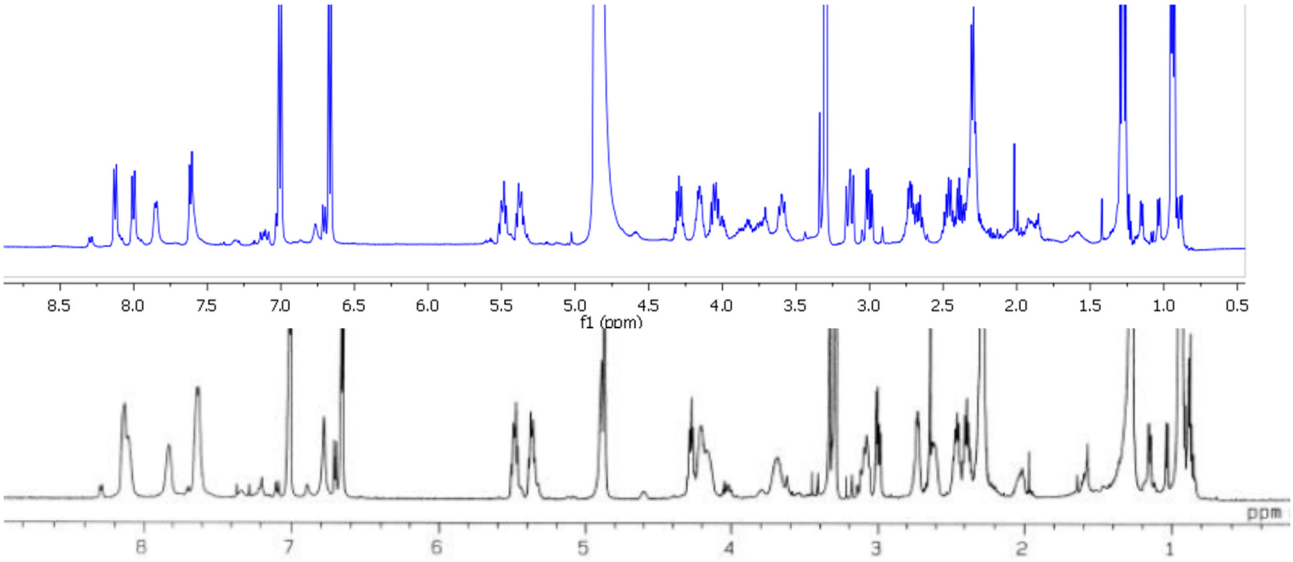

Figure 2-10. Overlay of synthetic azumamide B (blue) and natural azumamide B (black).[135]

Azumamide D is structurally different from the other azumamides in the cyclic peptide backbone. In azumamide D the valine residue is substituted for an alanine. This feature allows an alanine to alanine cyclization, which could be favorable in the terms of reducing sterical hindrance in the cyclization reaction (Scheme 2-15).[181]

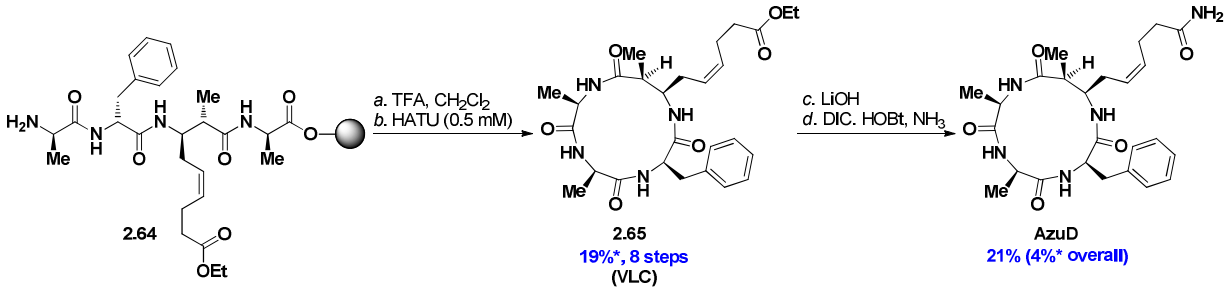

Scheme 2-15. Reagents and conditions: (a) TFA–CH_2Cl_2 (1:1), 2 × 30 min; (b) HATU (1.1 equiv), *i*Pr_2NEt (8.0 equiv), DMF (0.5 mM peptide concentration), 19 h; (c) LiOH (50 equiv), THF–H_2O (1:1), 4 h; DIC (6.0 equiv), HOBt (3.0 equiv), *i*Pr_2NEt (4.0 equiv), NH_3–dioxane and NH_3–MeOH (30 equiv), CH_2Cl_2–DMF (2:1), 13 d. *Yields are based on resin loadings.

However, the yield was slightly lower using the alanine to alanine cyclization (Table Table2-3, entry 2) compared to Table 2-3, entry 1 and 3. This result could illustrate that the structural geometry of the linear precursor outweighs the importance of sterics and peptide sequence in this case.[195, 196] The low overall isolated yield of azumamide D can be attributed to difficulties in the amidation reaction. Complete conversion was not achieved even after several days and excessive addition of coupling reagents and ammonia. Diphenylphosporylazide (DPPA) mediated amidation using triethylamine and ammoniumchloride did not produce the desired amide.[137]

To avoid dimer formation, as observed for azuamide B, azumamide A was cyclized between phenylalanine and alanine, using the slow addition protocol reported by Ganesan (Scheme 1-5).[138] LC-MS anaylsis showed no dimer and the cyclized product was purified using VLC. This procedure also resulted in a poor yield compared to the literature. Amide formation was achieved with HATU as the activating agent. Changing coupling reagent from DIC/HOBt to HATU resulted in a significant reduction in reaction time (6 hours vs 5 days) and an acceptable yield (Scheme 2-16).

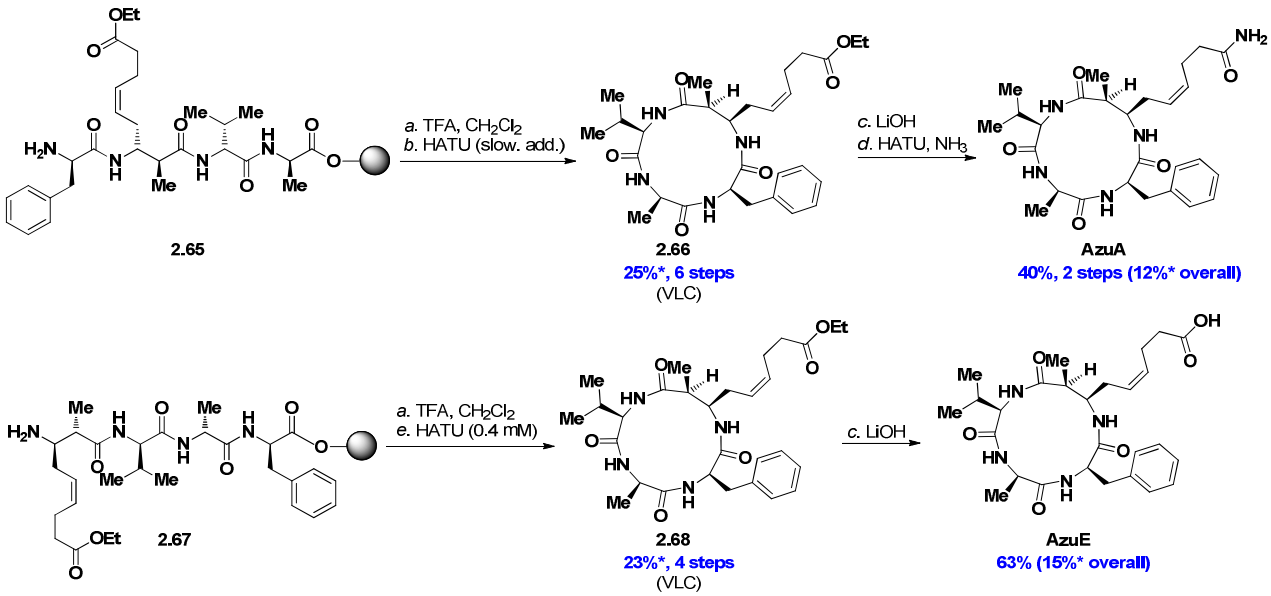

Scheme 2-16. Reagents and conditions: (a) TFA–CH_2Cl_2 (1:1), 2 × 30 min; (b) HATU (2.0 equiv), *i*Pr_2NEt (4.5 equiv), CH_2Cl_2; then linear peptide in DMF–CH_2Cl_2 (1:10) over 3.5 h; then HATU (1.0 equiv and *i*Pr_2NEt (2.3 equiv), 14 h; (c) LiOH, THF–H_2O (1:1); (d) HATU (5.0 equiv), *i*Pr_2NEt (5.5 equiv), NH_3–dioxane (25 equiv), 6 h; (e) HATU (1.1 equiv), *i*Pr_2NEt (8.0 equiv), DMF (0.4 mM peptide concentration), 22 h; then HATU (0.5 equiv), *i*Pr_2NEt (4.0 equiv), 3 h.*Yields are based on resin loadings.

Azumamide E was obtained in 15% overall yield with cyclization between the β-amino acid and phenylalanine. These results indicate that cyclization between phenylalanine and alanine is slightly more favorable than cyclization between the β-amino acid and phenylalanine. However, the two cyclizations were performed under different conditions, making a direct comparison difficult.

When comparing the cyclization yields in this study with the previously reported total syntheses, it is clear that the yields are lower. From LC-MS analyses the reactions appear to go completion and most cyclization sites only produced a small amount of dimer. One possible explanation could be the use of VLC for purification. VLC uses silica with a smaller particle size than regular flash chromatography. The smaller particle size could be a problem when purifying large macrocyclic peptides, as the compounds might be trapped on the column. This aspect, combined with the low solubility of these compounds, could explain the low quantities isolated after VLC. Furthermore, the column is sucked dry after each fraction, which will lead to precipitation of the compound on the column. If the cyclic peptides have poor solubility in the eluent, it will be hard to re-dissolve the peptide and recover the material from the column. However, these explanations do not explain the poor overall yield obtained when all the material is taken through the synthesis without purification, as it is the case for azumamide C. A second problem, which is also associated to the solubility problems observed with these compounds, is the risk of losing material into the aqueous phase when doing aqueous work up. To remove HOAt after the cyclizations, a mild acidic work up was performed. A large excess of organic solvent (8-15 times) was used and the aqueous phase was analyzed for residual product. LC-MS analyses of the aqueous phases implied that the desired product had been extracted to the organic phase, implying that the aqueous work up is not a problem.

2.4.3 Concluding remarks

In summary, all five azumamides were synthesized using a combination of solution and solid phase chemistry. This is the first reported total syntheses of azumamide B–D and this work confirms the structures originally proposed by Fusetani and coworkers.[135] The exploration of a diastereoselective Mannich reaction allowed access to two site-specifically edited azumamide analogs, which can aid in understanding the stereochemical requirements in the unique β-amino acid moiety.

2.5 Methods for biochemical profiling

2.5.1 Fluorogenic HDAC assays

The five azumamides and the two epimeric analogs were tested on HDAC1–9 by utilization of a protocol reported by Bradner et al.[35] The profiling of HDAC10 and 11 were conducted using protocols and substrates developed in our group.[197, 198] The principles of the fluorogenic assay are presented in Scheme 2-17.

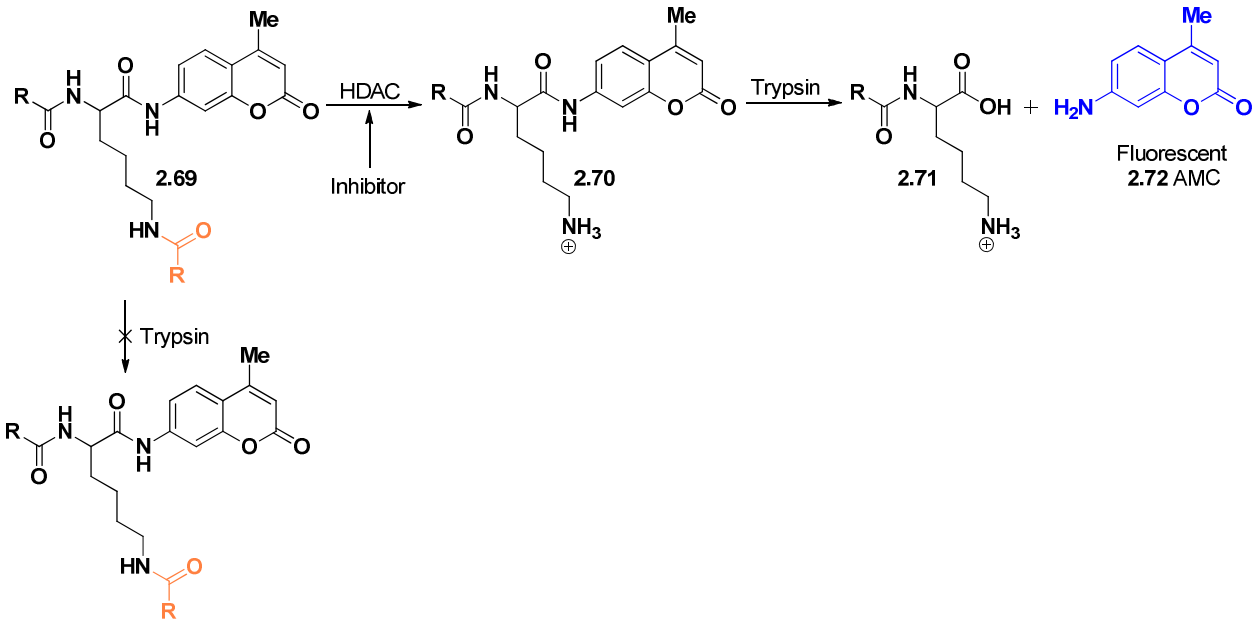

Scheme 2-17. Schematic showing the principles of the HDAC assays.

The HDAC of interest is incubated with a known peptide substrate (**2.69**) containing an *ε*-amino acetylated lysine and a fluorophore. The fluorophore, 7-amino-4-methyl coumarin (**2.72**, AMC), is attached directly to the acetylated lysine at the C-terminal of the peptide sequence. The fluorescence of AMC is quenched when the molecule is coupled to the peptide sequence. The rest of the peptide sequence (R, in Scheme 2-17) depends on the HDAC isoform under investigation (see section 2.5.2). After incubation trypsin is added as a developer. Trypsin cleaves amide bonds *C*-terminal to positively charged residues. In this case the positive charge is found in the deacylated lysine side chain. The resulting cleavage produces the highly fluorescent AMC molecule, which can be detected on a plate reader at very low concentrations (<250 nM). If the acyl group is still present on the *ε*-amino group, trypsin is unable to cleave the amide bond between AMC and lysine and no fluorescence will be detected. Thus, potential HDAC inhibitors can be evaluated by adding them during the incubation and measuring the fluorescence after addition of trypsin.

2.5.2 Substrates for HDAC screening

The tripeptide **2.73**(Scheme 2-18) is a good substrate for HDAC1–3, 6, and 11, however the class II enzymes display low activity on this substrate. Therefore, the more labile trifluoroacetylated substrate (**2.74**) was used for all class II isoforms, with the exception of HDAC10.[197] The peptide sequence in **2.73** and **2.74** was originates from the *N*-terminal tail of HDAC4.[198] HDAC10 was used in combination with tetrapeptide **2.75**, which originally was marketed as a HDAC8 substrate. The peptide sequence in **2.75**, which is based on a peptide fragment from p53.[198] This sequence has been reported to produce good results for HDAC10.[197]

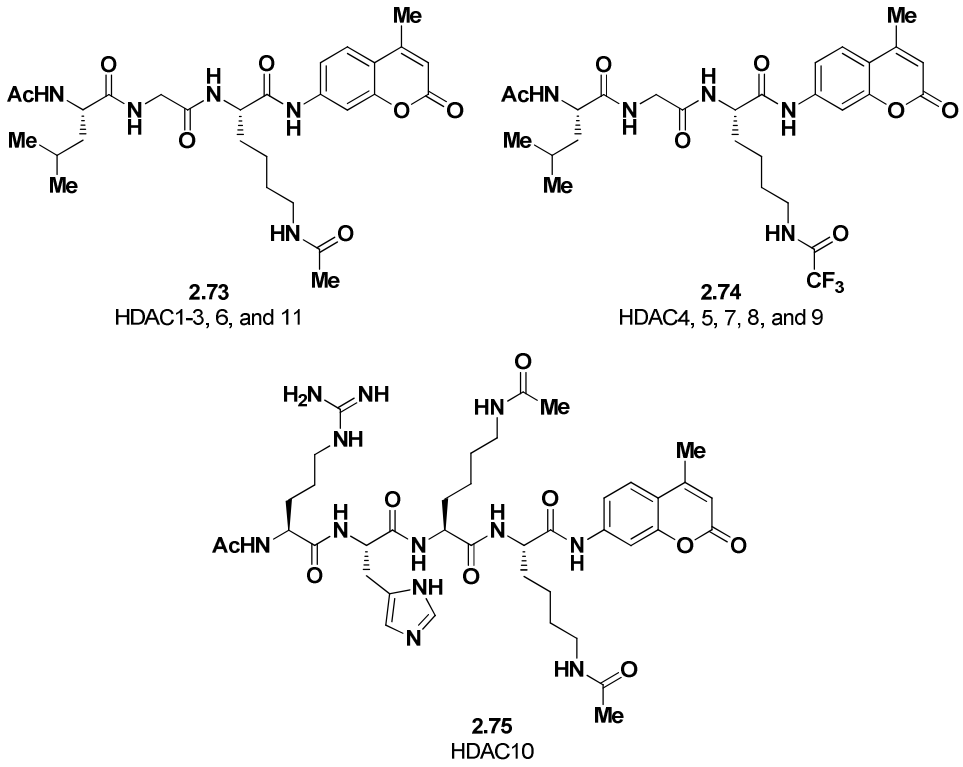

Scheme 2-18. Peptide substrates used in the HDAC assays.

HDAC8 is placed in class I, but has different substrate preferences compared to HDAC1–3. HDAC8 was therefore profiled with the trifluoroacetylated substrate (**2.74**) used on class II enzymes.

2.6 Biochemical profiling of azumamides and epimeric analogs

2.6.1 Two concentration screening

All five natural products, as well as the two epi-analogs, were screened against the 11 recombinant human HDAC isoforms by a colleague in our group (Helle Esbjørn Kristensen). Initially, the compounds were tested at 50 μM and 5 μM concentrations to get a quick overview of the activities. Compounds which did not show a minimum of 50% inhibition at 50 μM were regarded as inactive.

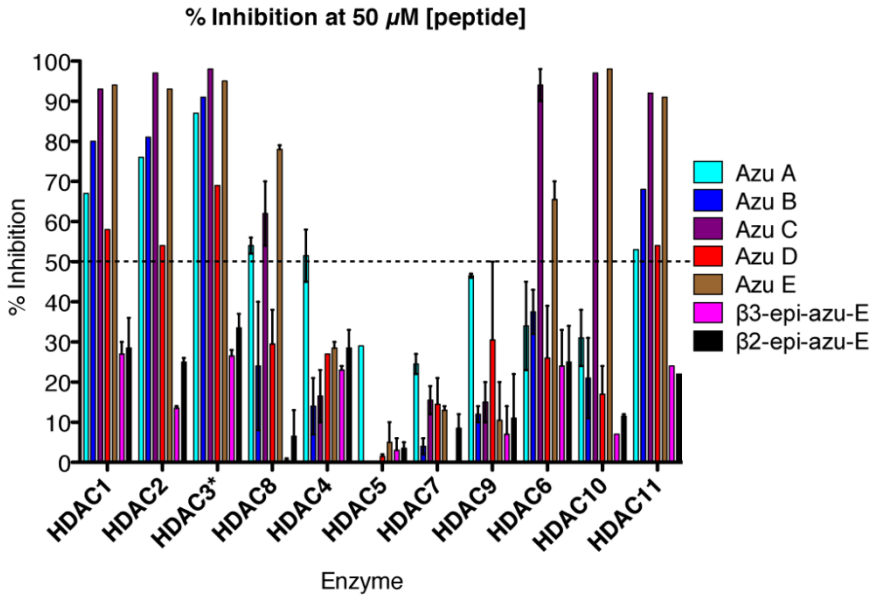

Figure 2-11. Screening of compounds at 50 μM concentration. (Azumamide A shows 52% inhibition at 50 μM). (adapted from Olsen and co-workers)[194]

Figure 2-11 shows that azumamides A–E are poor inhibitors of class IIa HDACs. These data are not in agreement with the previous data on azumamide E, where IC_{50}-values between 9.7 and >50 μM have been reported on class IIa enzymes.[136] The modest class IIa inhibitory activity observed by De Riccardis and coworkers is most likely an artefact, which can be attributed to the presence of co-purified class I HDACs in the class IIa enzyme stocks.[141, 34] The decreased activity towards class IIa enzymes, could be explained by key structural features found in the class IIa enzymes. Ficner and coworkers have studied the crystal structure of a bacterial homologue to class IIa HDACs, called FB188 HDAH.[199] They reported the presence of two loops near the entrance to the 11 Å channel. These loops are absent in class I HDACs and represent a major structural difference in the protein surface topology. It has been hypothesized that the two loops prevent binding of sterically-demanding macrocyclic peptide inhibitors to class IIa HDACs.[101] Our results support this hypothesis and univocally establish the azumamides as poor class IIa inhibitors.

Both epimerized analogs were inactive at 50 μM against the entire selection of enzymes. The observed loss of activity observed, when inverting the stereochemistry of the zinc-binding side chain (β^3-epi-azumamide E, **2.56**), can be explained by the change in side chain orientation relative to the cyclic peptide backbone. This change in overall topology prevents the side chain from accessing the 11 Å channel and reach the zinc ion, while the macrolactam ring still retains its favorable interactions with the surface of the protein. [136, 130] Ghadiri and co-workers reported a similar observation when they inverted the stereochemistry of the zinc-binding side chain of another cyclic peptide (**1.39**, Figure 1-17). Alternatively, the cyclic peptide could adopt an inactive conformation, when the stereochemistry is modulated. The complete absence of activity observed for the β^2-epimerized analog (**2.59**) is somewhat surprising. One possibility could be that the β^2-methyl group has a hydrophobic interaction with the protein, which is removed when flipping the stereochemistry. However, docking studies of azumamide E in histone deacteylase-like protein (HDLP) does not indicate any hydrophobic interactions between the β^2-methyl group and the protein.[136] Instead, the answer might be found in conformational changes in the cyclic peptide backbone. Ghadiri and coworkers have explored this phenomenon and reported radical changes in the conformation of cyclic tetrapeptides, when inverting the stereochemistry in a single amino acid residue. Especially, the *cis-trans* geometry of the amide bonds is

sensitive to changes in the stereochemistry.[119] Conformational changes can affect both the important C_3–C_4 vector in the β-amino acid, as well as the interactions of the macrolactam with the surface of the proteins. The methyl group may also serve as a guide for the orientation of the zinc-binding side chain. The rotation around the C_4–C_5 bond is limited by the methyl group, and it is possible that flipping the methyl group, will make the zinc-binding side chain able to adapt an unfavorable orientation. Finally, there might be a steric clash with the surface of protein and the inverted methyl group. From the docking of azumamide E in HDLP (Figure 1-22) it is difficult to see if the methyl group will clash with F198, but the distance between C_2 of the β-amino acid and the C_β of F198 is reported to be 3.8 Å.[136] If the bond length of a typical C–C bond (1.54 Å) and a C–H bond (1.1 Å) is considered, it seems likely that the inverted methyl group will come dangerously close to F198.

The initial screen also indicated that the carboxylic acid containing compounds are more potent inhibitors than their carboxyamide homologs. This was confirmed by the dose-response experiments performed on HDAC1–3, 8, 6, 10, and 11.

2.6.2 Dose-response characterization of azumamides

Dose-response experiments were performed on class I, IIb, and IV HDACs and the results are shown in Table 2-4.

Table 2-4. Potencies of the azumamides against the Zn^{2+}-Dependent HDACs given as K_i Values (nM)[a]

	class I				class IIb		class IV
compound	HDAC1	HDAC2	HDAC3	HDAC8	HDAC6	HDAC10	HDAC11
(azuA)	>5,000	>5,000	3,200	>5,000	IA	IA	>5,000
(azuB)	5,000	3,000	3,000	IA[b]	IA	IA	>5,000
(azuC)	32±1	40±20	14±1	>5,000	2,000	10±4	35±3
(azuD)	>5,000	>5,000	3,700	IA	IA	IA	>5,000
(azuE)	67±7	50±30	25±5	4,400	>5,000	20±12	60±16
2.56: (β^3-epi-azuE)	IA	IA	IA	IA	IA	IA	IA
2.59: (β^2-epi-azuE)	IA	IA	IA	IA	IA	IA	IA

[a] IC_{50} values were determined from at least two individual dose–response experiments performed in duplicate and the K_i values were calculated using the Cheng-Prusoff equation. [b] IA = inactive (<50% inhibition at 50 μM [inhibitor]).

The initial biochemical evaluations of the azumamides, reported that the carboxyamides were equipotent or more potent than their carboxylic acid variants, when tested on cell extract.[135] Our data show up to a 120-fold decrease in potency (HDAC3), when substituting from a carboxylic acid to a carboxyamide. This is in accordance with the observations reported by Ganesan and coworkers, where azumamide E is was found to be 53-fold more potent than azumamide A on HeLa cell extracts.[138] Interestingly, azumamide C was found to be slightly more active than azumamide E on HDAC1–3, 6, 10, and 11, indicating that a Phe to Tyr substitution is favorable. This result also contradicts the initial results obtained on cell extracts. It is possible that the hydroxyl group from tyrosine can participate in hydrogen bonding on the surface on the enzyme, thus favoring binding. The only HDAC isoform which prefers a phenylalanine residue instead of a tyrosine residue, is HDAC8.

The azumamides display class selectivity towards class I, class IIb and class IV over class IIa. Regarding isoform selectivity within class I, azumamide C and E are 120–350-fold and 60–170-fold more potent toward HDAC1–3 compared to HDAC8, respectively. In comparison, apicidin is only 8–42 times more potent towards HDAC1–3 compared to HDAC8.[130] Isoform selectivity was also observed in class IIb. Here, >200-fold selectivity for

HDAC10 over HDAC6 was observed for azumamide C and E. A similar selectivity profile has been reported for the cyclic peptide apicidin and a series of analogs.[130]

2.6.3 Concluding remarks

This work reports the first total syntheses of azumamide B–D and verify the originally proposed structures. The developed flexible synthetic route, with a diastereoselective Mannich reaction as the key step, allowed preparation of two site-specifically edited epimeric analogs. These two analogs contributed to the overall structure-activity relationships for the azumamides and show that the β-amino acid is highly sensitive to modifications in the stereochemistry. Azumamide A–E were profiled against the entire panel of HDAC enzymes. In contrast to previous findings, azumamide C was found to be ~2-fold more potent than azumamide E against the majority of enzymes. Furthermore, the azumamides were poor inhibitors of class IIb (IC_{50} < 50 μM) in our hands, which is in disagreement with the results reported by DeRiccardis and co-workers (IC_{50} values between 9.7 and >50 μM).[136] In terms of isoform selectivity, azumamide C and E were more potent towards HDAC1–3 compared to HDAC8 (60–350-fold). Finally, isoform selectivity was observed in class IIb, where azumamide C and E displayed >200-fold selectivity for HDAC10 over HDAC6. Further investigation of the cytotoxic properties of the azumamides is ongoing and docking studies on HDAC3 will be performed.

3 Synthesis of β^2-modified azumamide analogs

3.1 Introduction

The poor HDAC inhibitory activity of the β^2, β^3 and $\beta^{2,3}$-epimers of azumamide E underline the importance of the stereochemistry of the β-amino acid. However, no efforts have been made to evaluate the importance of the substituent in the 2-position of the β-amino acid in the azumamide scaffold. In the $\alpha_3\beta$-tetrapeptides, shown in Figure 1-17, there is no substituent in the 2-position of the β-amino acid. With this in mind, it would be interesting to investigate β^2-desmethyl azumamide analogs, where the β^2-methyl group has been removed (**3.01**–**3.03**, Scheme 3-1, *left*). Furthermore, it would be interesting to insert an extra methyl group in the β^2-position and obtain β^2-dimethylated analogs. The introduction of β^2-dimethyl β-amino acid residues in linear peptides induces conformational changes, but whether this effect can be transferred to cyclic peptides is not clear.[200] To explore these modification, a series of dimethylated analogs were prepared (**3.04**–**3.06**, Scheme 3-1, *right*).

As previously mentioned, the nature of the aromatic amino acid is important for activity. Tryptophan is found in apicidin, but not in the azumamides. Therefore, tryptophan analogs were prepared in order to investigate this substitution.

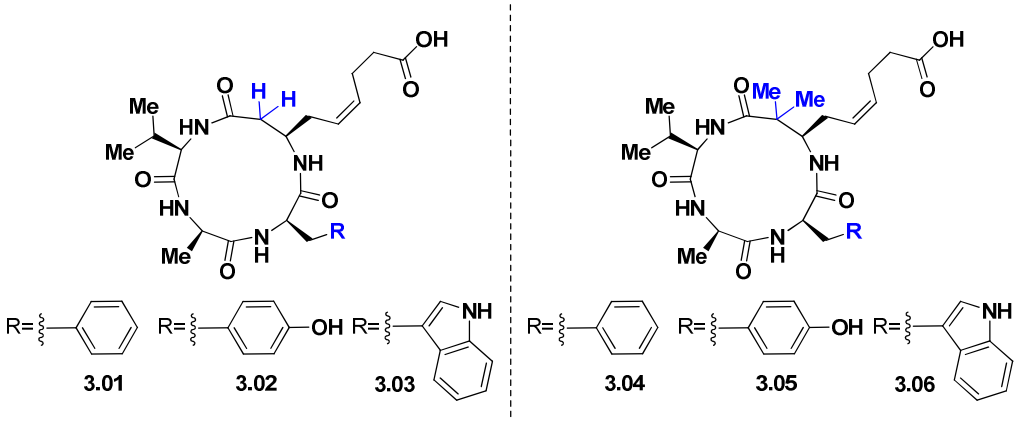

Scheme 3-1. *Left:* Target compounds for β^2-desmetylated azumamide analogs. *Right:* Target compounds for β^2-dimetylated azumamide analogs.

Having developed the diastereoselective Mannich reaction for the synthesis of the natural products, we envisioned that this methodology could also be used to set the stereocenters in the β-amino acids needed for the β^2-edited analogs. Here, only one stereocenter is generated and the challenge with *E* and *Z*-enolates is avoided.

3.2 Retrosynthesis

The same retrosynthetic strategy, which was used for the synthesis of the natural products, was applied for the synthesis of the β^2-modified analogs. This strategy reduces the synthetic challenge to the synthesis of β-amino acids **3.07** and **3.08** (Scheme 3-2).

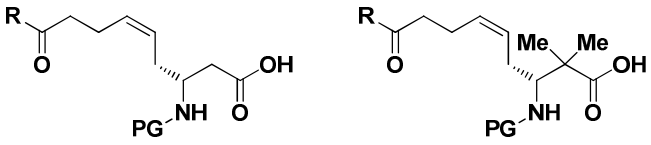

3.07 Desmethyl building block **3.08** Dimethyl building block

Scheme 3-2. Key building blocks for synthesis of β^2-edited azumamide analogs.

3.3 Synthesis of β^2-dimethyl building block

Having observed unexpected results with the propionate esters (as described in chapter 2), a screening study was performed with the isobutyrate esters. Different sulfinyl imines were screened against various isobutyrate esters, to identify the combination producing the correct stereochemistry, the best selectivity, and the highest yield. Different protection groups were introduced on the alcohol functionality in order to explore the importance of sterics at this position. The results are summarized in Table 3-1.

Table 3-1. Screening results from the Mannich reaction shown below.

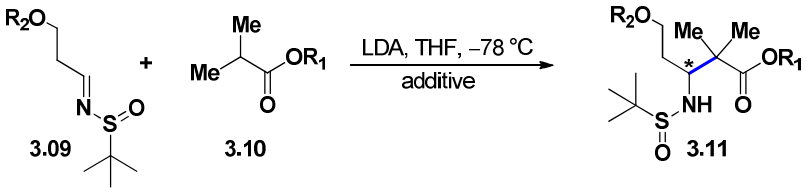

entry	auxiliary*	R^1	R^2	additive	d.r.[b]	major isomer (yield, %)
1	*R*	PMB	Si(*i*Pr)$_3$	TiCl(O-*i*Pr)$_3$	65:35	ND (47)
2	*R*	Et	Si(*i*Pr)$_3$	TiCl(O-*i*Pr)$_3$	64:36	ND (29)
3	*R*	^{t}Bu	Si(*i*Pr)$_3$	TiCl(O-*i*Pr)$_3$	ND	*3S* (36[a])
4	*S*	^{t}Bu	Si(*i*Pr)$_3$	TiCl(O-*i*Pr)$_3$	84:16	*3R*[c] (58)
5	*R*	Et	Bn	TiCl(O-*i*Pr)$_3$	53:47	ND (78[b])
6	*R*	^{t}Bu	PMB	TiCl(O-*i*Pr)$_3$	83:17	*3S*[d] (70[b])
7	*R*	Et	PMB	TiCl(O-*i*Pr)$_3$	66:33	ND (77[b])

[a]Full conversion of the imine was not observed. [b]Seperation not possible. The reported yield is for both diastereomers. [c]Determined by X-ray crystallography on its desilylated homologue. [d]Determined by comparison of spectroscopic data from its desilylated derivate and the desilylated homologue from entry 4.

The best selectivities were observed with *tert*-butyl isobutyrate in combination with either the triisopropylsilyl- or the PMB-protected imine (entry 4 and 6, respectively). The (*S*)-sulfinyl imine was again required to obtain the desired stereochemistry, which indicates the involvement of a nonchelated open transition state, as described in section 2.3.2. The results in Table 3-1 is in accordance with the results obtained for the propionate esters in section 2.3.2, but in disagreement with Ellman`s findings.[166]

Difficulties with separation of the diastereomers from entry 6, made the triisopropylsilyl-protected β-amino ester (entry 4, **3.12**) more attractive for further elaboration. Alcohol deprotection with TBAF afforded a crystalline compound (**3.13**) and X-ray analysis showed the desired (*R*)-configuration in the 3-position (Scheme 3-3). The alcohol (**3.13**) was elaborated to the desired β-amino acid building block (**3.16**) by the same chemical modifications used previously (Scheme 2-9).

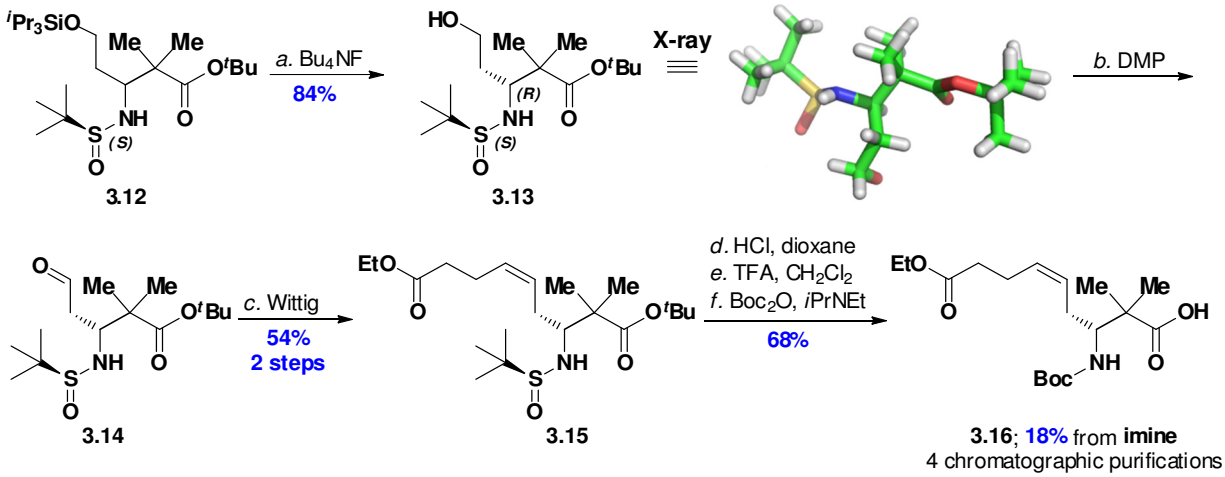

Scheme 3-3. Reagents and conditions: (a) AcOH (1.0 equiv), Bu_4NF (2.0 equiv), THF, 0 °C → rt, 30 min, then Bu_4NF (0.2 equiv), 15 min; (b) $NaHCO_3$ (1.5 equiv), Dess-Martin periodinane (1.5 equiv), dry CH_2Cl_2, 0 °C, 20 min; then 40 min, 0 °C → rt. (c) KHMDS (1.9 equiv), $Ph_3PBr(CH_2)_3COOEt$, (2.0 equiv), dry THF, –78 °C, 30 min; then aldehyde **3.14** in dry THF, 16 h, –78 °C → rt. (d) TFA–CH_2Cl_2 (1:1, 10 mL), 0 °C → rt, 2 h. (e) HCl (4.0 M in dioxane, 1.5 equiv), dioxane, 2 h, then HCl (4.0 M in dioxane, 0.4 equiv), 30 min. (f) *i*Pr_2NEt (2.1 equiv), Boc_2O (2.0 equiv), dry CH_2Cl_2, 20 h.

3.4 Synthesis of β²-desmethyl building block

3.4.1 Ester screening

In pursuit of the desmethylated β-amino acid building block, required for preparation of desmethylated azumamide analogs, we conducted our own Mannich reaction screening experiments. Different acetate esters were screened together with the (*R*)-sulfinyl imine (**2.14**). The results are presented below.

Table 3-2. Addition of acetate enolates to chiral the sulfinyl imine **2.14**.

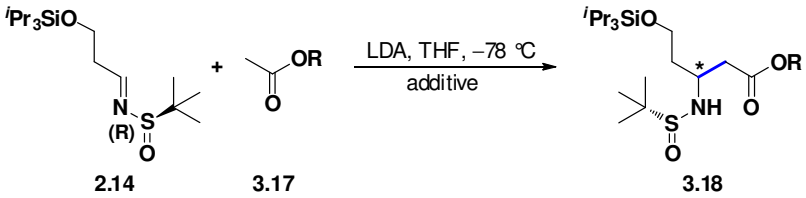

entry	R^1	additive	d.r.[b]	major isomer, yield (%)
1	Et	$TiCl(O^iPr)_3$	>99:1	*3R*[a] (94)[c]
2	^{t}Bu	$TiCl(O^iPr)_3$	74:26	*3R*[b] (68)[d]
3	^{t}Bu	HMPA	28:72	*3S*[b] (19), (42[d])
4	PMB	$TiCl(O^iPr)_3$	82:18	ND

[a]Determined by X-ray crystallography from the desilylated and re-esterified *tert*-butyl ester. [b]Determined spectroscopically by comparison with the crystallized alcohol from entry 1. [c]Crude yield. [d]Diastereomers could not be separated. The total yield is reported.

In entry 1, only one diastereoisomer was observed and re-esterification to the *tert*-butyl ester, followed by removal of the triisopropylsilylether provided the alcohol **3.27** as a crystalline solid (Scheme 3-4). The X-ray structure shows the desired 3*R*-stereochemistry. This observation is in contrast to our previous results, where propionate and isobutyrate enolates required the (*S*)-sulfinyl imine to produce the correct stereochemistry in the 3-position and indicates that ethyl acetate can participate in the six-membered Zimmerman–Traxler transition state. Increasing the bulk of the acetate enolate (entry 2) reduced the selectivity, but still provided

the desired stereochemistry. This indicates that the six-membered transition becomes too sterically crowded (**3.19**, Figure 3-1) when the bulk of the ester is increased. Therefore, approximately one fourth of the reaction takes place through an open transition state. Attempts to remove the alcohol protection group in the crude PMB-protected *β*-amino ester, obtained in entry 4, resulted in decomposition and lactone formation and the PMB protecting group was not explored further.

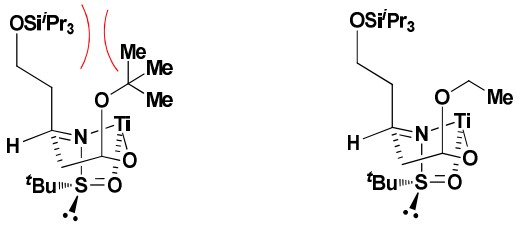

Figure 3-1. *Left:* The steric clash between the *tert*-butyl group of the ester enolate and the bulky silyl group or the isopropoxide ligands on the metal. *Right:* The same transition state performed with the less bulky ethyl ester.

To validate the hypothesis of the open *vs* cyclic transition state, a control experiment was performed. Here, HMPA was added instead of TiCl(O-*i*Pr)$_3$ (Table 3-2, entry 3). In Figure 3-2 is shown an overlay of the ^{1}H NMR of the major products from Table 3-2, entry 2 and 3 as well as the *tert*-butyl ester obtained from re-esterfication of the ethyl ester from entry 1.

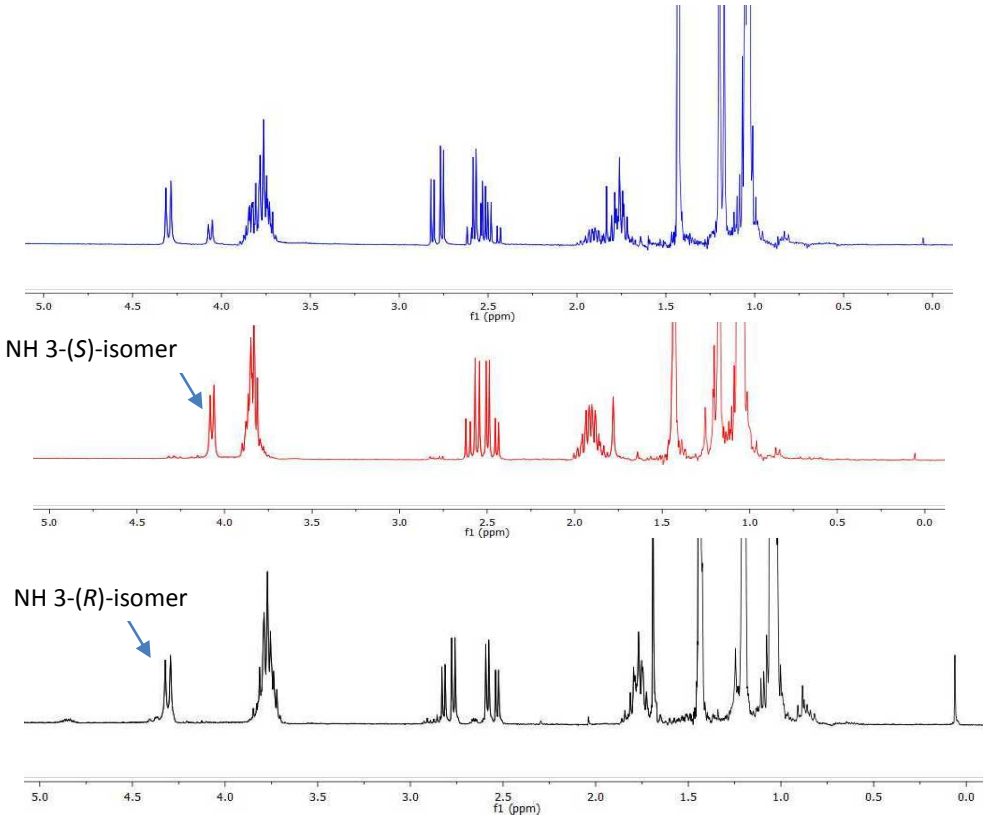

Figure 3-2. Overlay of ^{1}H NMR spectra of the *tert*-butyl esters obtained from Table 3-2 entry 1 (EtOAc, TiCl(O-*i*Pr)$_3$, black), entry 2 (*tert*-butyl acetate, TiCl(O-*i*Pr)$_3$, blue), and entry 3 (*tert*-butyl acetate, HMPA, red).

3.4.2 Shimizu´s results

Shimizu and coworkers reported similar results, when investigating the addition of *tert*-butyl acetate enolates to chiral *p*-tolylsulfinyl imines.[184] Different metal enolates were prepared and added to chiral sulfinyl imine **3.21** and the effects of solvents and different additives were explored (Table 3-3).

Table 3-3. Addition of *tert*-butyl acetate enolates to the chiral sulfinylimine **3.21**.[a] (Adapted from Shimizu and co-workers)[184]

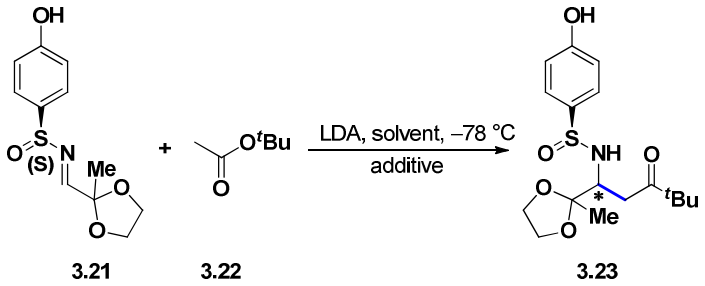

3.21 **3.22** **3.23**

entry	metal	additive (equiv)	solvent	3*R*:3*S*	yield (%)[b]
1	Li	-	THF	14:86	65
2	Li	HMPA (3.0)	THF	2:98	68
3	Li	HMPA (4.5)	THF	4:96	71
4	Li	-	Et_2O	82:18	75
5	Ti	$TiCl(O\text{-}iPr)_3$	THF	96:4	89
6	Al	$AlEt_2$	THF	84:16	39
7	Al	AlEtCl	THF	77:23	79
8	K	18-Crown-6 (3.0)	THF	6:94	51

[a] Reactions were performed with 3.0 equiv. of enolate in respect to the imine at –78 °C.[b] Isolated yield of major diastereomer.

Table 3-3 shows a switchover in diastereoselectivity when moving from the lithium enolate in the presence of HMPA, to the titanium enolate in the absence of HMPA (entry 3 and 5, respectively). This observation is consistent with a change in transition state. The six-membered transition state, initially proposed by Davis and co-workers,[168] can explain the stereochemical outcome of the reaction in the presence of titanium and the open state transition state can explain the major diastereoisomer from entries 2 and 3.

3.4.3 Building block synthesis

The ethyl ester from Table 3-2, entry 1 was hydrolyzed and the *tert*-butyl ester was prepared with *tert*-butanol in the presence of Boc_2O and DMAP (Scheme 3-4). Re-esterification was carried out in part because of the need for an orthogonal protection group, but also because the *tert*-butyl *β*-amino alcohols had proven to be crystalline. Upon desilylation, the alcohol (**3.27**) crystallized and the structure was elucidated by X-ray crystallography (Scheme 3-4). The alcohol was elaborated to the Fmoc- and Boc-protected *β*-amino acids using the standard chemical transformations.

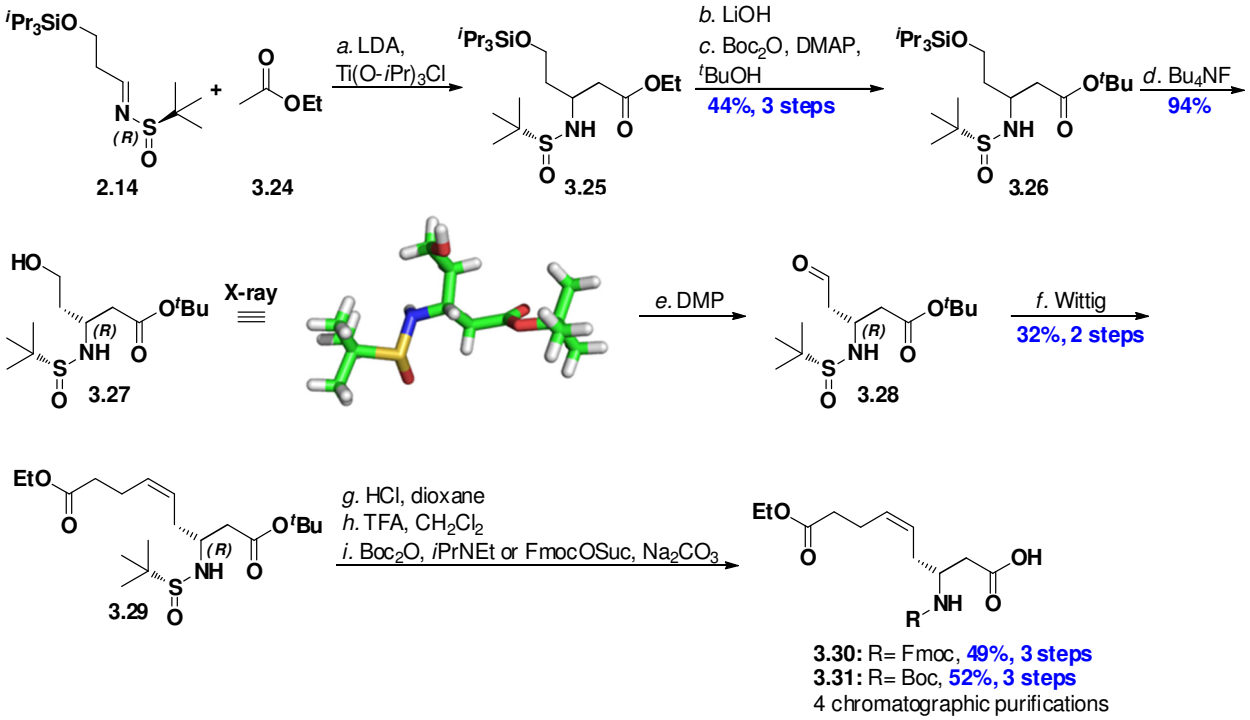

Scheme 3-4. Reagents and conditions: : (a) LDA (2.1 equiv), EtOAc (2.0 equiv), THF, –78 °C, 30 min, then $(Ti(O\text{-}iPr)_3Cl$ (4.2 equiv), 30 min, then imine 2.14; (b) LiOH (1.5 equiv), 1h, rt, then LiOH (3.0 equiv), 16 h; (c) Boc_2O (1.4 equiv), DMAP (0.3 equiv), *tert*-BuOH, 16h, then Boc_2O (0.3 equiv), 1.5h; (d) AcOH (1.0 equiv), Bu_4NF (2.0 equiv), THF, 0 °C → rt, 15 min, then 1h, rt; (e) $NaHCO_3$ (1.5 equiv), Dess-Martin periodinane (1.5 equiv), dry CH_2Cl_2, 0 °C, 40 min; (f) KHMDS (1.9 equiv), $Ph_3PBr(CH_2)_3COOEt$, (2.0 equiv), dry THF, –78 °C, 30 min; then aldehyde **3.28** in THF, 30 min, –78 °C; (g) TFA–CH_2Cl_2 (1:1, 10 mL), 0 °C → rt, 2 h, then rt, 1h; (h) HCl (4.0 M in dioxane, 1.8 equiv), dioxane, 1 h, rt; (*i*) iPr_2NEt (3.0 equiv), Boc_2O (2.0 equiv), dry CH_2Cl_2, 6 h, then Boc_2O (1.0 equiv), 16 h or Na_2CO_3 (4.0 equiv), FmocOSu (1.2 equiv), 0 °C, 45 min.

3.4.4 Comments on transition states

In the Mannich reaction between chiral sulfinyl imines and acetate, propionate and isobutyrate ester enolates, we have observed a connection between the overall bulk of the reactants and the preferred transition state. The only enolates which seem to react through the predicted six-membered transition state, with the imines investigated in this work, are acetate enolates. When increasing the bulk of the enolate, by addition of a methyl group in the α-position, the cyclic transition state seemingly becomes disrupted. This resulted in Mannich products where the observed stereochemistry can be explained by an open transition state (Figure 2-6). The same is the case for the even bulkier isobutyrate enolates. In Figure 3-3 the cyclic Zimmerman–Traxler transition state is drawn.

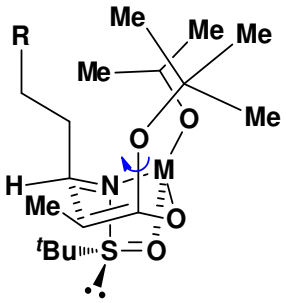

Figure 3-3. The cyclic Zimmerman–Traxler transition state.

The titanium ion coordinates to the alkoxy oxygen, the imine nitrogen, and the oxygen from the sulfinyl group. This leaves one isopropoxide ligand still present on the metal. The tetrahedral shape of titanium(IV)-complexes will place the rather bulky isopropoxy group on the same face of the six-membered ring as the imine side chain.[201] In the case of the bulky *tert*-butyl esters, the isopropoxy group will at the same time be positioned close to the *tert*-butyl group of the incoming enolate. This scenario creates a sterically crowded environment at the top face of the six-membered ring. Rotation around the =C–O^{t}Bu bond in the enolate (as shown in Figure 3-3), will minimize the steric clash between the *tert*-butyl group and the isopropoxy group (Figure 3-4, right).

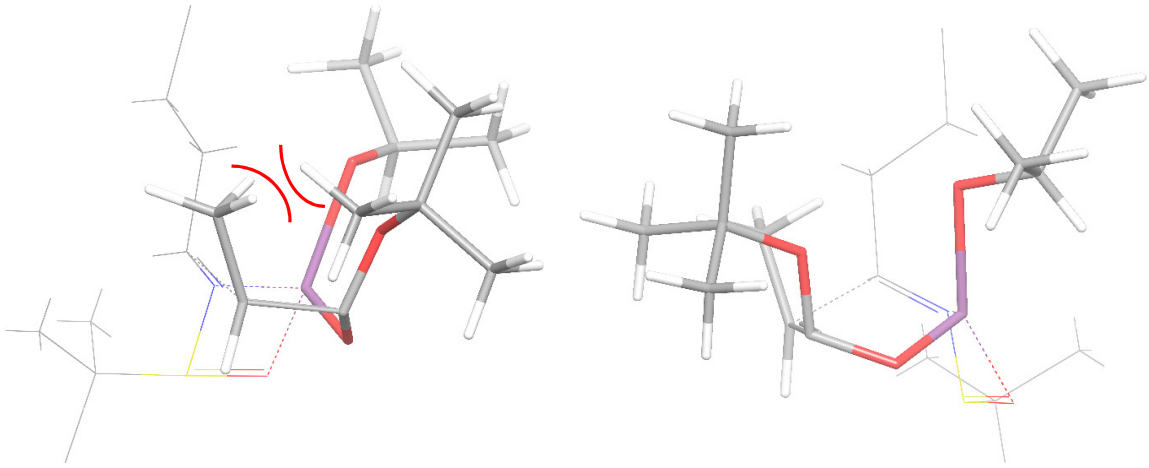

Figure 3-4. Zimmerman-Traxler TS with tert-butyl propionate, viewed from two different positions. Red: oxygen, blue: nitrogen, Purple: titanium, yellow: sulfur. The terminal part of the imine side chain has been omitted for clarity.

At the same time this rotation allows the isopropoxy group to move further away from the imine side chain. In the (*E*)-*tert*-butyl propionate enolate, the degree of rotation is limited by the presence of the *cis*-methyl group. If the *tert*-butyl group is rotated, to be located as far away from the isopropoxy group as possible, the *tert*-butyl group will clash with the methyl group (Figure 3-4, left). The methyl group probably forces the bulky *tert*-butyl group to flip towards the isopropoxy group and this steric interaction disrupts the six-membered transition state.

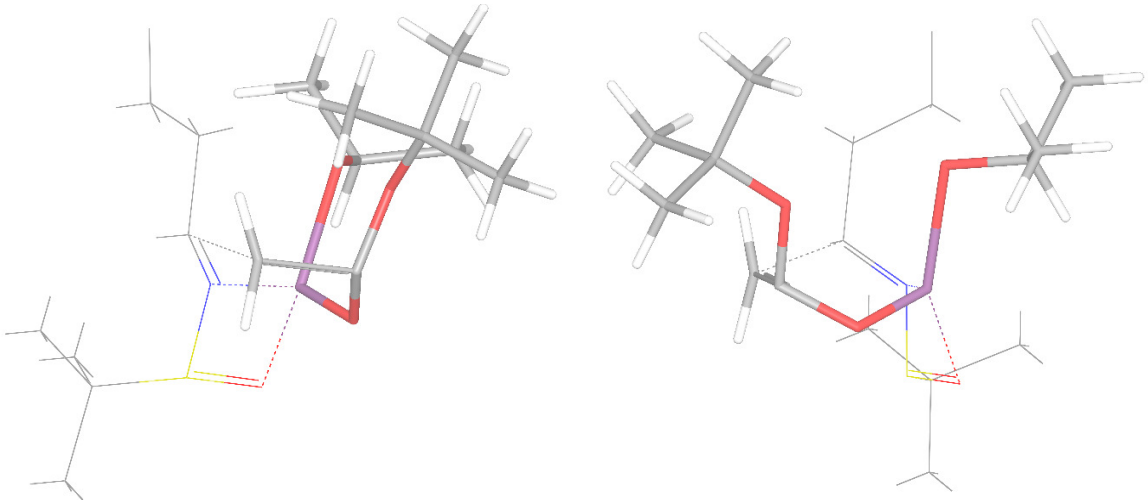

Figure 3-5. Zimmerman-Traxler TS with tert-butyl acetate, viewed from two different positions. Red: oxygen, blue: nitrogen, Purple: titanium, yellow: sulfur. The terminal part of the imine side chain has been omitted for clarity.

The same scenario is the case for *tert*-butyl isobutyrate enolate. However, in *tert*-butyl acetate, the methyl group is substituted to a less bulky hydrogen atom. This decrease in bulk at the *α*-position of the incoming enolate, allows the molecule to adapt a conformation where the *tert*-butyl group can accommodate an orientation, which is favorable in respect of reducing the steric clash with the isopropoxy group (Figure 3-5, right). This difference in the positioning of the *tert*-butyl group of the enolates, could explain why the *tert*-butyl acetate enolate is able to react through the Zimmerman–Traxler transition state, whereas the *tert*-butyl-(*E*)-propionate and isobutyrate enolates are not. Yet, this explanation does not account for the low selectivities observed with the less bulky methyl, ethyl, allyl, and PMB-esters. These enolates should be able to adopt a conformation where the six-membered transition state is favored. The observation that the less bulky propionate and isobutyrate enolates produce lower selectivities is in accordance with the open transition state. If the bulk of the ester is reduced, the steric interaction between the *tert*-butyl group on the sulfinylimine and the alkoxy group of the enolate will become reduced. It is this steric interaction which discriminates TS A from TS B (Figure 2-6) and therefore a lower selectivity would be expected.

The only experimental difference between Ellman`s experiments and the experiments performed in this work, is the preparation of LDA. Ellman prepares the LDA *in situ* from diisopropylamine with butyllithium. We use a commercially available LDA solution in THF/heptane/ethylbenzene. To the best of our knowledge there is no literature describing any effects of different LDA preparation methods.

3.5 Synthesis of β²-desmethyl azumamide analogs

The building blocks **3.30** and **3.31** were elaborated to the linear tetrapeptides by coupling to three different tripeptides on resin (Scheme 3-5). For the tryptophan-containing peptide the cleavage was performed under mild conditions (trifluoroethanol–AcOH–CH_2Cl_2, 6:2:2 (v/v/v)) to keep the Boc-group on the indole-nitrogen.

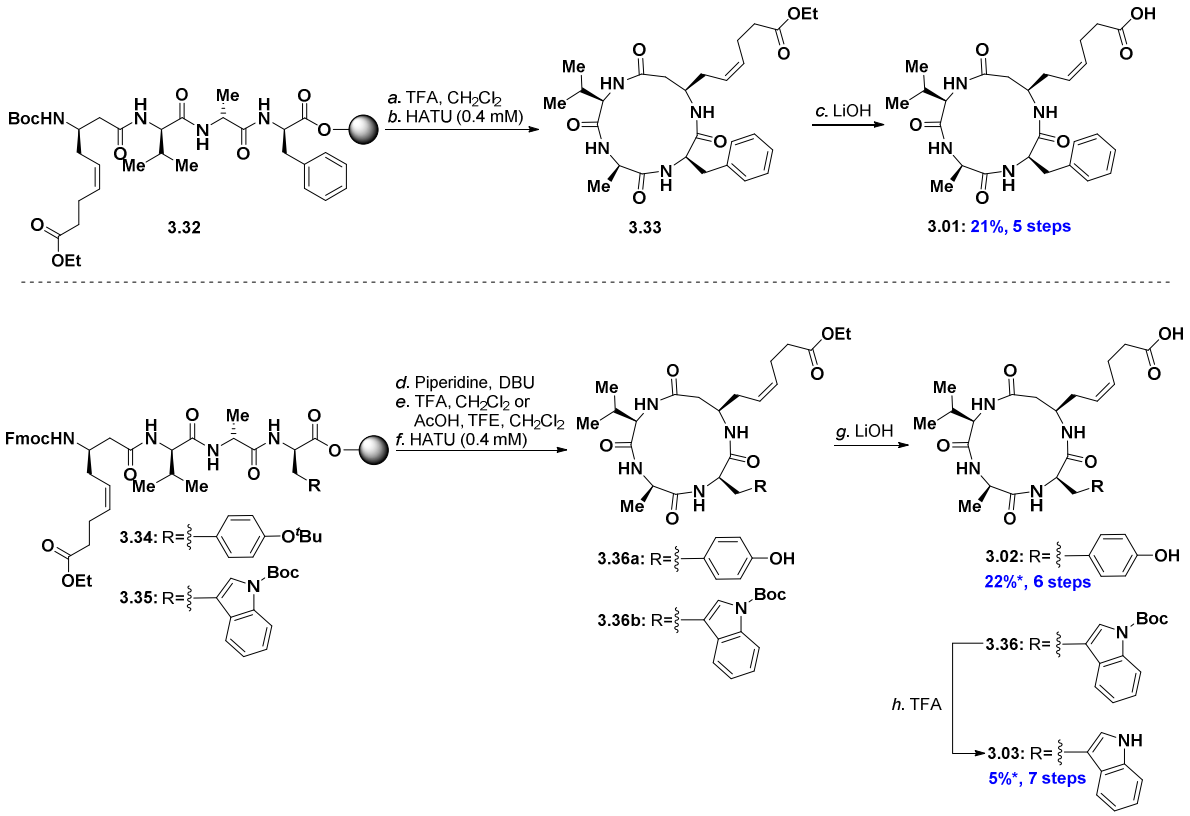

Scheme 3-5. Reagents and conditions: (a) TFA–CH_2Cl_2 (1:1), 2 × 30 min; (b) HATU (2.2 equiv), *i*Pr_2NEt (10 equiv), DMF, 16 h; (c) LiOH (36 equiv), THF–H_2O (1:1), 16 h; (d) Piperidine–DMF (1:4), 2 × 30 min, then piperidine–DBU–DMF

(2:2:96), 30 min. (e) TFA–CH_2Cl_2 (1:1), 2 × 45 min or trifluoroethanol–AcOH–CH_2Cl_2 (2:2:6), 2 × 2 h; (f) HATU (1.5 equiv), *i*Pr_2NEt (8–10 equiv), 16h; (g) LiOH (50 equiv), THF–H_2O (1:1), 17 (h) TFA–CH_2Cl_2 (1:1), 1h. *Yields are based on resin loadings.

The linear peptides were cyclized with HATU and subsequent cleavage of the ethyl esters with LiOH afforded β^2-desmethyl azumamides E (**3.01**) and C (**3.02**). The isolated yields are slightly higher compared to the synthesis of azumamide E, which was cyclized at the same position and under the same conditions. The removal of the methyl group at the β^2-position decreases the sterical hindrance in the cyclization reaction and this can explain the increase in yield. In the case of the tryptophan-analog, the Boc-group was removed with TFA to give the final product (**3.03**).

Parallel to the synthesis of the compounds in Scheme 3-5, a series of related desmethyl analogs (**3.04**–**3.06**) were prepared by a fellow PhD-student, Alex Maolanon (Scheme 3-6). These compounds were included in the study to obtain better and more elaborated structure-activity relationships (SAR).

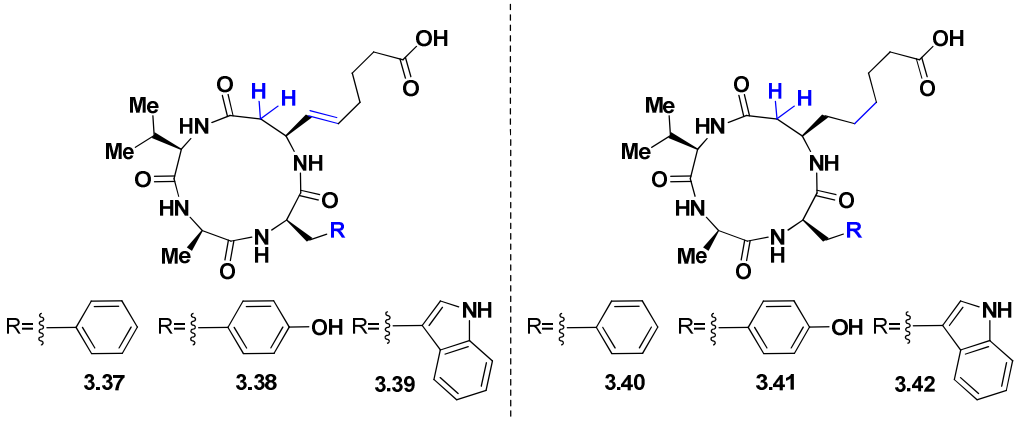

Scheme 3-6. Azumamide analogs with a modified β-amino acid side chain. Sites with modifications are marked with blue.

These compounds were designed to explore the importance of the *cis*-double bond in the β-amino acid side chain. The first series was inspired by romidepsin (**1.06**, Figure 1-4), and the double bond was moved one position closer to the macrolactam ring and changed to a *trans*-double bond (**3.37**–**3.39**). The compounds in the second series have a saturated β^3-amino acid side chain linker (**3.40**–**3.42**). Saturated side chain linkers are found in other macrocyclic peptide HDAC inhibitors such as apicidin, HC-toxin, chlamydocin and microsporins (Figure 1-14 and Figure 1-15). To simplify the β-amino acid building block synthesis, a route was developed where the chirality was obtained from the chiral pool and the β^2-methyl group was removed. Starting from *N*-Boc- and *tert*-butyl protected aspartic acid (**3.43**), an efficient, robust, and scalable synthetic route was developed (Scheme 3-7).

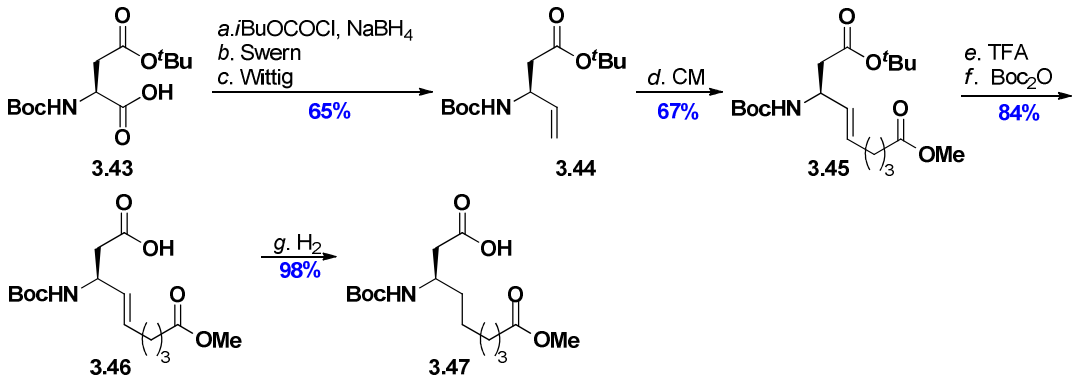

Scheme 3-7. (a) *N*-methylmorpholine (1.0 equiv), isobutyl chloroformate (1.0 equiv), $NaBH_4$ (3.0 equiv), MeOH, THF; (b) $(COCl)_2$ (1.7 equiv), DMSO (3.3 equiv), Et_3N (5.0 equiv.), CH_2Cl_2; (c) PPh_3CH_3Br (2.2 equiv), KHMDS (0.5 M in toluene) (2.1 equiv), THF; (d) methyl 5-hexenoate (3 equiv), Hoveyda Grubbs 2nd gen. catalyst (0.1 equiv), CH_2Cl_2; (e) TFA–CH_2Cl_2 (1:3); (f) Boc_2O (1.3 equiv.), *i*Pr_2NEt (2.6 equiv.), CH_2Cl_2; (g) H_2, 1 wt.% Pd/C, THF.

Building blocks **3.46** and **3.47** were elaborated to the cyclic peptides by preparation of the linear tetrapeptides on resin, followed by cleavage and cyclization in solution. Compounds **2.37–3.41** were cyclized with the β-amino acid as the *N*-terminal residue. The isolated yields were between 3–10%. Compound **3.42** was cyclized with the β-amino acid as the C-terminal residue and was isolated in 58% yield over 12 steps. This result emphasizes the importance of the cyclization site. Unfortunately, the compounds shown in Scheme 3-5 were prepared prior to this result and the overall yield might have been improved if the cyclization had been performed with the β-amino acid as the *C*-terminal residue.

3.6 Synthesis of β²-dimethyl azumamide analogs.

The synthesis of the β²-dimethylated analogs was obtained by coupling the Boc-protected β-amino acid (**3.16**) to the tripeptides on resin. After cleavage with TFA the linear peptides were cyclized under dilute conditions with HATU. Subsequent hydrolysis of the ethyl ester with LiOH provided the target compounds after preparative HPLC (Scheme 3-8).

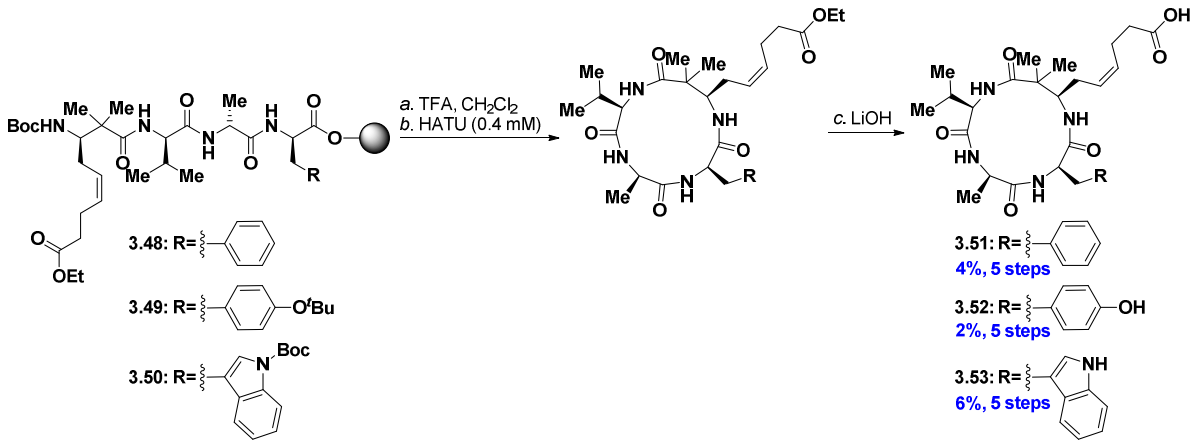

Scheme 3-8. Reagents and conditions: (a) TFA–CH_2Cl_2 (1:1), 2 × 30–60 min; (b) HATU (1.5–2.0 equiv), *i*Pr_2NEt (5–10 equiv), DMF, 16–17 h; (c) LiOH (35–50 equiv), THF–H_2O (1:1) 16–18 h. Yields are based on resin loadings.

The isolated yields for the Phe and Tyr containing cyclic peptides were lower than for the desmethylated analogs. The geminal α-methyl groups create a bulk in the β-amino acid, close to the *C*-terminal of the peptide and this could explain the low yields in the cyclization reactions. The conformation of the linear peptide may also be affected by the two methyl groups. In the synthesis of the Trp-containing analog the compound was

purified by VLC after cyclization. Here, the dimer was isolated in 24% yield and the cyclized product in 34% yield. The formation of dimer indicates that the linear peptide adapts a conformation where the *N*-and *C*-terminal have problems reaching each other. This conformation could be induced by the geminal methyl groups.

3.7 Biochemical profiling of des-and dimethylated analogs

The des- and dimethylated analogs were profiled against relevant HDAC isoforms. The nine desmethylated analogs (divided into three series) were characterized with dose–response experiments against class I, class IIb, and class IV HDAC isoforms. Single dose–response experiments data on HDAC4 and HDAC7 agreed with the trend observed for the natural products, as no activity could be observed towards these class IIa enzymes with concentrations up to 100 μM. On this background no further testing was performed on class IIa enzymes. Table 3-4 shows the K_i values obtained from the biochemical profiling of the nine desmethylated analogs.

Table 3-4. Biochemical profiling of desmethylated analogs. The potencies are given as K_i values (nM)[a].

	class I				class IIb		class IV
Compound	HDAC1	HDAC2	HDAC3	HDAC8	HDAC6	HDAC10	HDAC11
3.37: Phe, trans	700±180	900±20	800±160	4,300±1,800	>20,000	>20,000	1,800±300
3.38: Tyr, trans	400±130	300±140	300±130	>20,000	1,300±480	150±2	700±210
3.39: Trp, trans	300±40	200±150	300±220	1,700±1,030	2,200±180	130±2	600±300
3.40: Phe, sat.	500±200	400±60	400±120	6,400±2900	>20,000	260±80	1200±640
3.41: Tyr, sat.	400±340	200±100	100±80	>20,000	2000±1,120	80±40	500±410
3.42: Trp, sat.	600±70	800±190	1,200±460	6,100±390	>20,000	190±30	1,600±900
3.01: Phe, cis	300±130	500±70	500±80	6,700±870	>20,000	140±20	900±130
3.02: Tyr, cis	200±120	100±40	200±140	>20,000	3,500±360	80±3	400±200
3.03: Trp, cis	100±65	100±7	300±80	3000±350	>20,000	70±20	500±360

[a] IC_{50} values were determined from at least two individual dose–response experiments performed in duplicate, and the K_i values were calculated using the Cheng-Prusoff equation.

3.7.1 Analogs *vs* natural products – Importance of the β^2-methyl group

To investigate the direct effect of the β^2-methyl group, compounds **3.01** and **3.02** can be compared to azumamides E and C, respectively. The desmethylated analogs show decreased activity towards HDAC1–3 compared to the natural products. The level of reduction varies from 3–18-fold across the different isoforms. The greatest difference is observed on HDAC3, where desmethyl azumamide E (**3.01**) shows an 18–fold reduction in activity, whereas desmethyl azumamide C (**3.02**) only exhibits a 3-fold reduction in activity on HDAC2. A 7–8-fold decrease in activity was observed on HDAC10 and for HDAC11 a 13–14-fold reduction in activity was observed. Interestingly, all nine desmethylated analogs are more active than azumamide A, B, and D against the entire panel of enzymes. Azumamide A, B, and D contain a carboxyamide as their zinc-binding group, whereas the desmethylated analogs have a carboxylic acid. The carboxyamide is a weaker zinc-chelator than the carboxylic acid and this can explain superior activity of desmethylated compounds.

The methyl group is less important with regards to HDAC6 and HDAC8. A 1.5-fold reduction in activity is observed for desmethyl azumamide E (**3.01**) on HDAC8 and a 1.8-fold reduction is observed for desmethyl azumamide C (**3.02**) on HDAC 6. Instead, the inhibition of these two HDAC isoforms is dependent on the nature of the aromatic amino acids found in these analogs (see section 3.7.2).

The decrease in activity, observed on HDAC1–3, HDAC10, and HDAC 11, is interesting. Several structural or steric features could be responsible for the loss of activity. One possibility could be that the methyl group has an important hydrophobic interaction with the protein. However, as mentioned in section 2.6.1, the docking model in HDLP does not imply such an interaction. Instead the reduction in activity could be explained by alterations in the conformation of the cyclic peptide backbone. As previously mentioned, changes in the conformation of the cyclic peptide can affect the C_3–C_4 vector in the β-amino acid, as well as disrupt the interactions of the macrolactam with the surface of the protein.

Removal of the methyl group can also influence the flexibility of the β^3-side chain. The zinc-binding side chain can rotate more freely around the C_4–C_5 bond, when there is no methyl group in the α-position. The increase in rotational freedom decreases the possibility to find the side chain in the optimal orientation. In other words, the β^2-methyl group might assist in directing the zinc-binding side chain in a favorable direction.

To get insight into the possible structural changes induced by removal of the β^2-methyl group an NMR-study was performed. The study was done by our colleagues in the NMR group (Charlotte H. Gotfredsen and Casper Hoeck). The solution state NMR structures of **3.02** and azumamide A in DMSO were elucidated using NOESY experiments and molecular modelling. The NMR structure of azumamide A was found to be similar to the reported structure of azumamide E.[136] An overlay of azumamide A and **3.02** is shown in Figure 3-6.

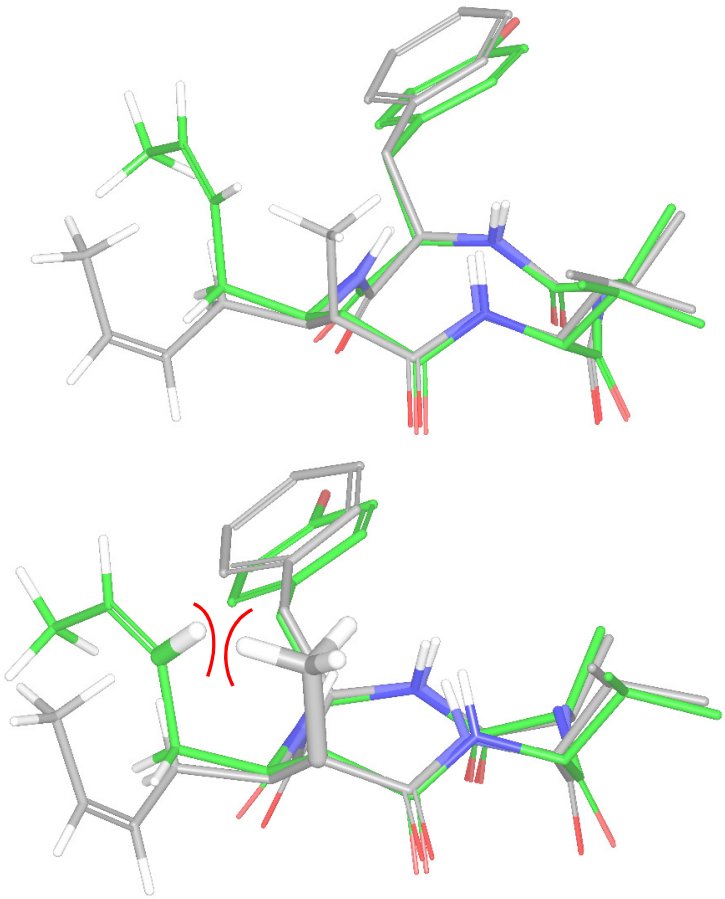

Figure 3-6. *Top:* Overlay of NMR solution structures of compound **3.02** (carbon: green, hydrogen: white, oxygen: red, nitrogen: blue) and azumamide A (carbon: grey, hydrogen: white, oxygen: red, nitrogen: blue). The β^3-side chain beyond C_6 have been omitted for clarity. The superimposition was made on all the atoms in the cyclic peptide backbone. *Bottom:* Highlighting the clash between the β^2- methyl ground and the C_5-proton of the desmethylated analog.

The two NMR structures overlay well and there is no significant changes in the conformation of the cyclic peptide backbones. The C_3–C_4 vector in the desmethylated β-amino acid (**3.02**) is slightly different from the vector observed in azumamide A. The β^3-side chain in azumamide A is projected closer to the plane of the peptide backbone compared to desmethylated analog. Whether this small difference is enough to explain the reduction in activity is difficult to investigate. In spite of the C_3–C_4 vectors being similar, the rest of the β^3-side chain occupy different positions (Figure 3-6, *Top*). The side chain of azumamide A is occupying the space in the plane of the peptide backbone, whereas the side chain in **3.02** is found above the ring. This difference could be explained by the presence of the methyl group in the 2-position. If the side chain of azumamide A was to adopt the same position as the desmethylated analog, the C_5-alkene proton would clash with the β^2-methyl group (Figure 3-6, *bottom*). This steric interaction directs the side chain away from the methyl group and down into the plane of the macrocycle. When the methyl group is removed, the β^3-side chain will be more free to move around and based on the NMR structure the side chain will be found above the plane of the ring. The biological data suggest that the side chain position, found in the natural products is more favorable than the side chain position found in the desmethylated analogs. Docking of azumamide E in HDLP (Figure 1-22) indicates that the entrance to the 11 Å channel is found in the plane or slightly below the plane of the cyclic peptide backbone. The zinc-binding side chain in the natural products has a preference for being directed down towards the 11 Å channel by the neighboring methyl group. This "directing feature" is not found in the desmethylated analogs and the side chain will not be pointing towards the 11 Å channel. The difference in the positioning of the zinc-binding side chains in the natural products and the desmethylated analogs could potentially explain the different activities. However, it should be mentioned that due to increased rotational freedom the uncertainty associated with the NMR structures increase, when you move away from the conformational restricted macrolactam rings. Thus, the positioning of the β^3-side chain may not be as well defined as shown in Figure 3-6.

3.7.2 Importance of the aromatic amino acid residue

The aromatic amino acid in cyclic tetrapeptide HDAC inhibitors has been shown to participate in hydrophobic interactions with the surface of the proteins.[136] In our study, the tyrosine and tryptophan-containing compounds were 2–5-fold more active against HDAC1–3, HDAC10, and HDAC 11 compared to the corresponding phenylalanine compounds. In contrast to Tyr and Trp, the side chain of Phe is unable to form hydrogen bonds. It is possible that the ability of Tyr and Trp to establish favorable hydrogen bonds on the surface of the protein can induce binding of these compounds. An exception to this trend is compound **3.42**, which displayed lower activity than the phenyalanine homolog.

Interestingly, compounds **3.37**, **3.39**, and **3.03** were more active against HDAC8 than the natural products. In the *cis* and *trans* series, incorporation of Trp promotes binding to HDAC8 compared to Phe. In contrast, tyrosine has a negative impact on the activity against HDAC8 in all three series. This tendency was also observed for the natural products, were azumamide C was more potent than azumamide E against all isoforms, except HDAC8.[194] In HDAC6, the Phe-containing compounds were inactive up to 20 μM and only **3.39** showed activity amongst the Trp-containing analogs. However, the three compounds containing tyrosine were active.

3.7.3 Importance of the *cis*-double bond

The effect of the β^3-side chain modifications cannot be related directly to the azumamides, as the removal of the β^2-methyl group clearly plays a significant role. It is not known whether the modifications are additive or subtractive. In general, a 1.5–3-fold reduction in activity towards HDAC1–3, 10, and 11 was observed for the compounds where the double bond is shifted one position closer to the macrolactam ring, and transformed from a *cis* to a *trans* double bond. This subtle decrease in activity could be a consequence of the side chain

being directed in a less favored orientation by the shifted *trans* double bond compared to the *cis* double bond. However, the activities on HDAC3 were comparable to the *cis* series and on HDAC6 and 8 the *trans* compounds were more active. Substituting to a saturated side chain did not display any clear trend for the activity of the Phe and Tyr analogs. A 2-fold reduction in activity was observed on HDAC1 and 2, whereas the saturated compounds were more active on HDAC3. For the tryptophan analog, a 2–8-fold reduction was observed against all isoforms. A saturated side chain would be expected to be more flexible than the unsaturated *cis* and *trans* versions. The flexibility can be an advantage if the C_3–C_4 vector, in the β-amino acid, is slightly off. The increased flexibility will then enable the side chain to adapt an orientation, where it still fits into the 11 Å channel. On the other hand, there will be more degrees of freedom in a saturated side chain and the possibility to find the side chain in the optimal conformation is lower compared to a more rigid unsaturated side chain.

3.7.4 Dimethylated analogs

Preliminary results indicated low activity of the three dimethylated analogs against class I, class IIb, and class IV. With this in mind, these analogs were only tested at two concentrations against HDAC1–3, HDAC6, HDAC8, HDAC10, and HDAC11 (Table 3-5)

Table 3-5. HDAC profiling of dimethylated analogs. Values represent %-inhibition.

	3.51: Phe, cis		**3.52: Tyr, cis**		**3.53: Trp, cis**	
	20 μM	10 μM	20 μM	10 μM	20 μM	10 μM
HDAC1	16±9	10±8	15±16	11±6	65±16	54±8
HDAC2	8±4	4±2	11±3	8±2	68±9	53±25
HDAC3	8±8	5±1	8±1	7±1	62±7	47±21
HDAC6	IA	IA	IA	IA	40±33	17±23
HDAC8	IA	IA	IA	IA	14±6	6±1
HDAC10	IA	IA	IA	IA	7±7	IA
HDAC11	IA	IA	IA	IA	26±9	22±20

The %-values were determined from at least two individual experiments performed in duplicate. IA= inactive at 20 μM.

Low activity was observed for the Phe and Tyr-containing analogs (**3.51** and **3.52**, respectively) against HDAC1–3 and no inhibition at 20 μM was observed on HDAC6, HDAC8, HDAC10, and HDAC11. However, the tryptophan-containing compound displayed activity against HDAC1–3, with ~50% inhibition at 10 μM. HDAC6, HDAC8, HDAC10, and HDAC11 were inhibited by **3.53**, albeit none of these isoforms were inhibited more than 50% at 20 μM. The positive effect of tryptophan indicates that this aromatic amino acid is superior to Phe and Tyr in establishing favorable interactions with the surface of the HDAC enzymes. Overall, the dimethylated analogs displayed low activity compared to the natural products. These results confirm that the β^2-position is extremely sensitive to modifications. The NMR solution structures of the dimethylated analogs have not been elucidated, which makes predictions about the positioning of the zinc binding side chain difficult. However, if it is assumed that the overall conformation of the dimethylated cyclic peptides is similar to the conformation observed for the natural products, the reduction in activity could be an effect of the extra methyl group. The extra methyl group will be located below the ring and occupy the same space as the methyl group in the β^2-epimerized compound (**2.59**). As discussed in section 2.6.1 the β^2-methyl group found in **2.59** might class with the surface of the protein. It is possible that the extra methyl group in the dimethylated compounds will have a similar clash with the protein and this can explain the loss of activity.

Analogous to the desmethylated analogs, the reduction in activity can be explained by a change in the conformation of the cyclic peptides. There is also a possibility of a steric clash between the second methyl group and the protein (see section 2.6.1).

3.8 Development of an azumamide C analog lacking a zinc-binding group

In 2012, Ghadiri and co-workers reported the synthesis of $\alpha_3\beta$-tetrapeptide HDAC inhibitors lacking a Zn^{2+}-binding functional group (Figure 3-7).[51] Compound **3.54** and **3.55**, bearing a propyl side chain, showed IC_{50} values around 1 μM for HDAC1–3.

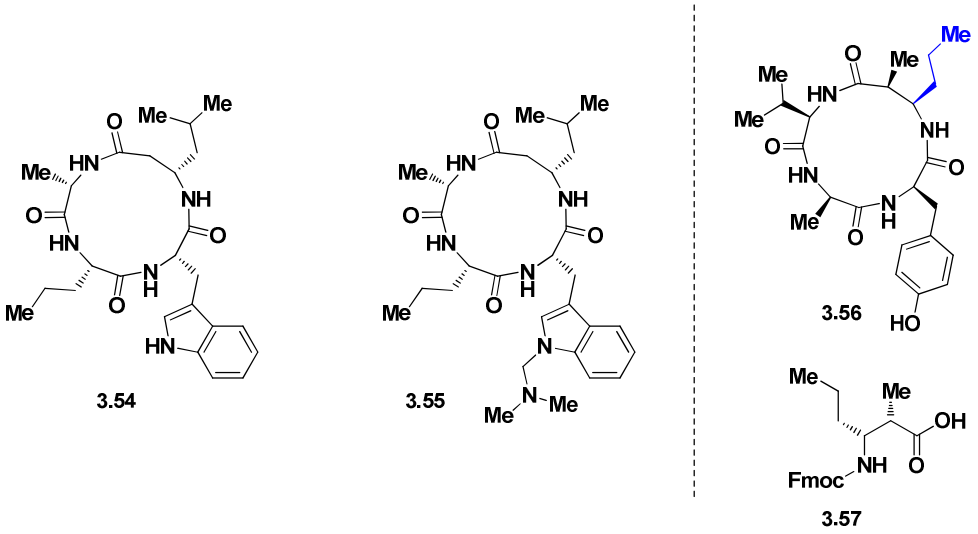

Figure 3-7. *Left:* Structures of the tetrapeptide HDAC inhibitors, lacking a zinc-binding group, reported by Ghadiri and co-workers.[51] *Right:* β^2-propyl azumamide C and the β-amino acid required for the synthesis. The modification is shown in blue.

Inspired by these results, we designed a β^2-propyl analog of azumamide C (**3.56**). To test the scope and utility of the developed Mannich reaction, the required β-amino acid (**3.57**) was prepared from the butanal derived (*S*)-imine (**3.59**) and the *Z*-enolate of *tert*-butyl propionate (Scheme 3-9). The β-amino acid (**3.57**) is also interesting from a broader perspective as this scaffold is found in various natural products.[202,203]

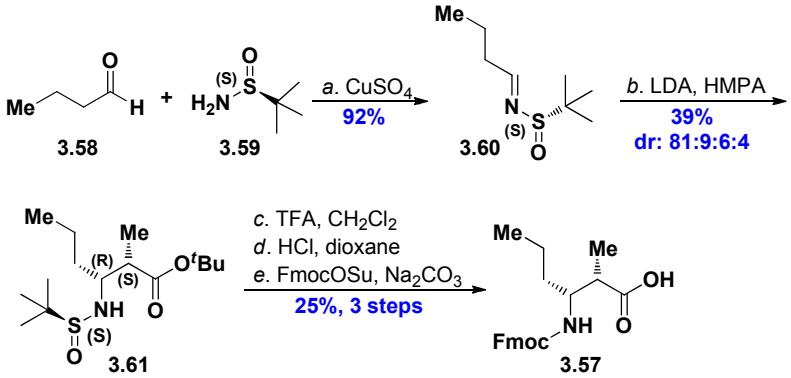

Scheme 3-9. Reagents and conditions: (a) $CuSO_4$ (5.0 equiv), dry CH_2Cl_2, 20 h; (b) *tert*-butyl propionate (2.5 equiv), LDA (2.6 equiv), HMPA (5.7 equiv, 23 vol%), THF, –78 °C, 30 min; then imine **3.60**; (c) TFA–CH_2Cl_2 (1:1), rt, 5 h; (d) HCl (4.0 M in dioxane, 3.0 equiv), dioxane, 1.5 h; (e) Na_2CO_3 (4.0 equiv), Fmoc-OSu (1.2 equiv), DMF–H_2O, 0 °C, 3 h.

The dr of the key Mannich reaction is slightly higher than the dr observed for imine **2.35** used to prepare the natural products. However, separation of the diastereoisomers produced from the above reaction, proved

more difficult than for the diastereoisomers in Scheme 2-9. This explains the low isolated yield from the Mannich reaction. The *N*-Fmoc protected *β*-amino acid (**3.57**) was prepared by standard three step protocol (Scheme 3-9). The stereochemistry of the *β*-amino ester (**3.61**) was solved by elaborating the Mannich product to the *N*-(benzyloxy) methyl ester (**3.67**), which has previously been prepared by MacMillan and co-workers (Scheme 3-10).[204]

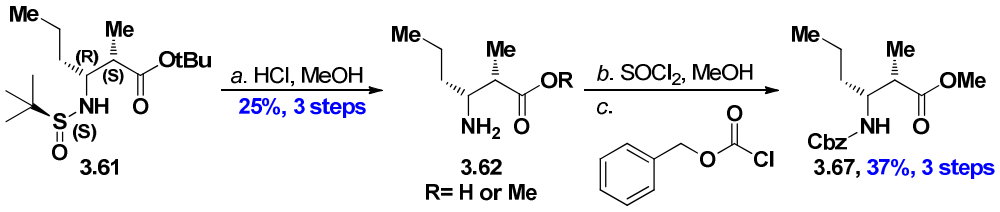

Scheme 3-10. Reagents and conditions: (a) HCl (4M, dioxane, 30 equiv), MeOH, 22 h; (b) thionyl chloride (3.0 equiv), MeOH, 0 °C, then reflux, 23 h, then thionyl chloride (1.5 equiv), MeOH, 0 °C→ rt, 22 h; (c) $NaHCO_3$–ethyl acetate (1:1), benzylchloroformate, 18 h.

The Mannich product was fully deprotected with hydrochloric acid in methanol, which produced a mixture of the free acid and the methyl ester (**3.62**). To ensure full conversion to the methyl ester, the mixture was added thionyl chloride in the presence of excess methanol. Finally, the amine was protected as the benzyloxy carbamate (**3.67**). The optical rotation and spectral data was in agreement with the previously reported data. The linear tetra peptide was obtained by HATU-mediated coupling of the *β*-amino acid to the tripeptide H_2N-(D)Val-(D)Ala-(D)Tyr on resin (Scheme 3-11).

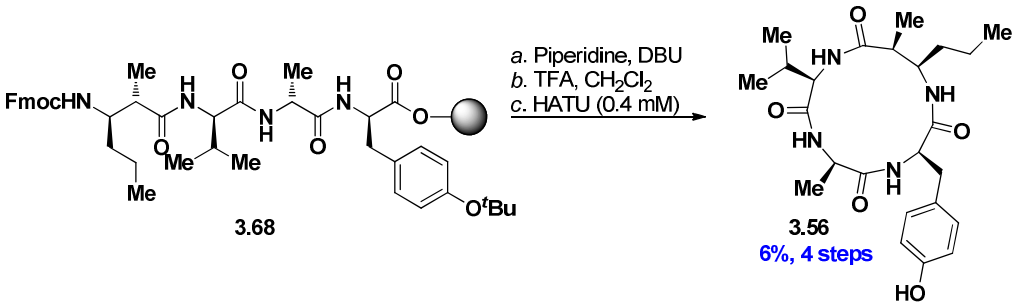

Scheme 3-11. Reagents and conditions: (a) Piperidine–DMF (1:4, 2 × 30 min, DBU–piperidine–DMF (2:2:96, 20 min); (b) TFA–CH_2Cl_2 (1:1, 2 × 30 min); (c) HATU (1.5 equiv), *i*Pr_2NEt (5 equiv), DMF (0.4 mM peptide concentration), 19 h.

The Fmoc-group was removed with piperidine and the tetrapeptide cleaved from the resin with TFA. The crude linear tetrapeptide was cyclized under dilute conditions with HATU and purified by preparative HPLC to afford the target compound (**3.56**).

Compound **3.56** was screened against HDAC3 and displayed inhibitory activity with an IC_{50} value of 2.9 μM (Figure 3-8).

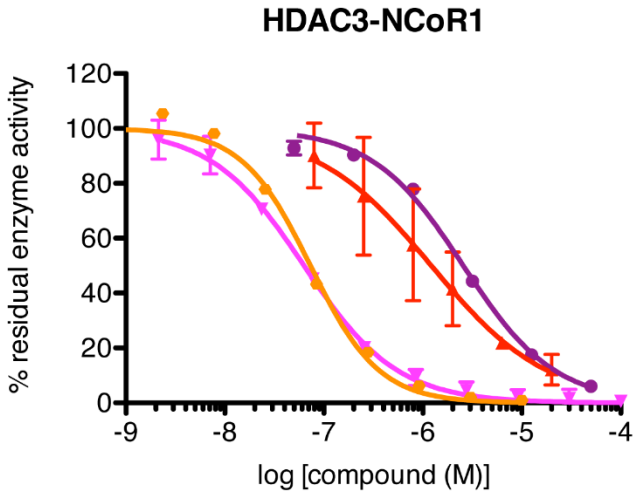

Figure 3-8. Dose–response data on **3.56** (purple), **3.02** (desmethyl azuC, red), azumamide C (pink), and **1.01** (SAHA, orange). Experiments were performed in duplicate for **3.56**, **3.02**, and azumamide C, whereas SAHA data is based on a single experiment.

This result confirms Ghadiri`s work and emphasizes that the cap group of macrocyclic peptides can inhibit HDAC enzymes without contribution from a zinc-binding group.[51] Interestingly, the propyl analog is more potent than azumamide A, B, and D on HDAC3, which could question the zinc-binding properties of the amide functionality in the side chain of the natural products. The straightforward synthesis of β-amino acid **3.57** is an excellent example on the broad perspective of the developed Mannich reaction. Compound **3.56** is interesting from a medicinal chemistry perspective. Azumamide C and E carry a carboxylic acid functionality, which will be deprotonated at physiological pH. The resulting negative charge could impair the membrane penetrating abilities of the natural products. In contrast, the neutral propyl analog may penetrate the membrane more efficiently and therefore be more active *in vivo*. Compound **3.56** will be tested in cell assays within the nearest future.

3.9 Future azumamide analogs and perspectives

With the conditions developed in this work it is possible to access all four diastereomers of a $\beta^{2,3}$-amino acid scaffold. The chirality of the sulfur auxillary directs the chirality in the 3-position and the configuration of the enolate dictates the stereochemistry in the 2-position (Scheme 3-12).

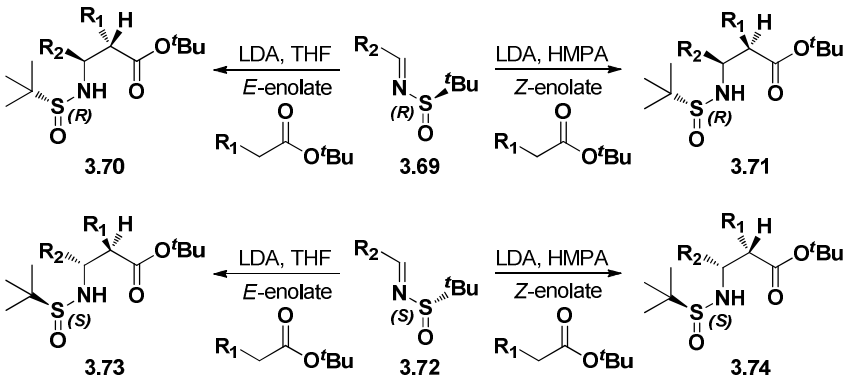

Scheme 3-12. Diversity of the developed Mannich reaction protocol.

In the case of the azumamides, this methodology will allow the design and synthesis of a broad variety of analogs, were the stereochemistry and structure of the β-amino acid side chains can be modulated. The

Introduction of a desired side chain in the β^2-position can be achieved by utilization of different *tert*-butyl esters (**3.75**) in the diastereoselctive Mannich reaction (Scheme 3-13, *top*). It could be interesting to explore the steric requirements in this position and the insertion of an ethyl or isopropyl substituent could easily be achieved by performing the reaction with *tert*-butyl butyrate and *tert*-butyl 3-methyl butanoate, respectively.

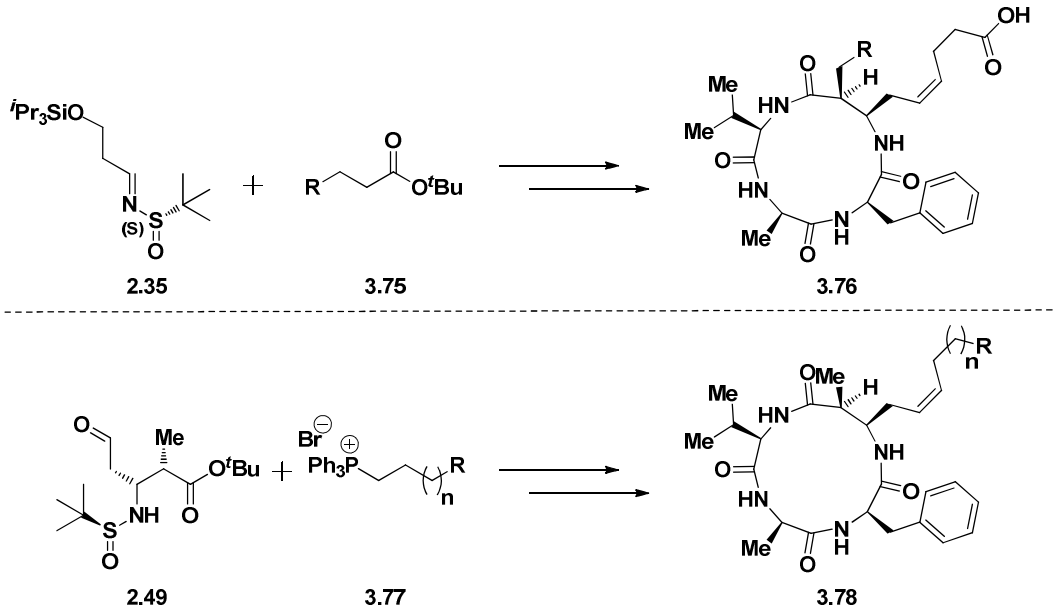

Scheme 3-13. Possible azumamide analogs. *Top:* Modifications in the β^2-position. *Bottom:* Modifications of the zinc-binding moiety.

A large variety of Wittig reagents are commercially available. These reagents could be utilized to incorporate different functionalities in the terminal part of the zinc-binding side chain of the β-amino acid by reaction with aldehyde **2.49**. This could provide a convenient strategy for screening different zinc-binding moieties.

The developed Mannich methodology could also be useful in structure elucidation of natural products where a $\beta^{2,3}$-amino acid scaffold, with unknown stereochemistry, is present. Furthermore, the $\beta^{2,3}$-amino acid scaffold is found in various known biologically active natural products and this strategy could provide a fast and efficient synthesis of epimeric analogs, as well as analogs with different substituents in the β-amino acid moeity.[205, 206,207, 208] The cyclic pentapeptides, motupurin (**3.79**) and nodularin (**3.80**), are potent protein phosphatase type 1 inhibitors and motuporin has shown a promising cytotoxic profile (Scheme 3-14, *left*).[209] Both structures contain $\beta^{2,3}$-amino acid scaffolds and our Mannich protocol could deliver the full selection of epimers. The ulongamides (**3.81–3.83**) are cyclic depsipeptides with the same $\beta^{2,3}$-amino acid scaffold prepared in section 3.8.[210] The stereochemistry of the $\beta^{2,3}$-amino acid scaffold found in the ulongamides could be prepared from imine **3.60** (Scheme 3-9) and the *E*-enolate from *tert*-butyl propionate. Again, the epimers of the ulongamides are easy accessible with our methodology.

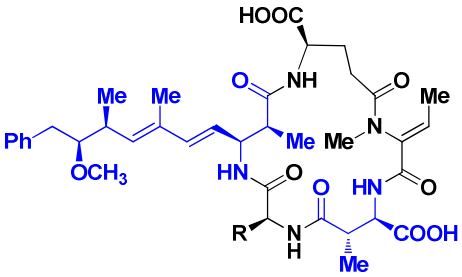

3.79: Motuporin: R=CH(CH$_3$)$_2$
3.80: Nodularin: R= (CH$_2$)$_3$NHC(=NH)NH$_2$

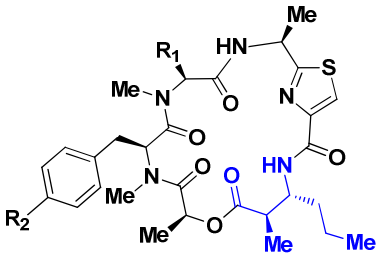

Ulongamides A–C
3.81: R$_1$=*i*-Pr, R$_2$= H
3.82: R$_1$=*i*-Pr, R$_2$= OH
3.83: R$_1$=Bn, R$_2$= OH

Scheme 3-14. Examples of bioactive natural products, which contain a $\beta^{2,3}$-amino acid scaffold (shown in blue).

Synthesizing epimers and substituted analogs of bioactive natural products could provide interesting structure activity relationships and guide optimization of these structures.

3.10 Concluding remarks

Two synthetic routes have been developed, providing β^2-des- and dimethylated azumamide analogs. The synthesis of these analogs provided information about the structural requirements of the β-amino acid scaffold found in the azumamides. The dimethylated analogs were poor HDAC inhibitors with high IC$_{50}$ values (> 10 μM). The desmethylated analogs showed a 3–18-fold reduction in activity compared to the natural products and NMR studies suggested that these analogs have the same peptide backbone conformations as the natural products. To explain the reduction in activity, we hypothesize that the β^2-methyl group, directs the zinc-binding side chain towards the entrance of the 11 Å channel. When the β^2-methyl group is removed, the zinc-binding side chain will not be directed towards the 11 Å channel and this could result in weaker binding.

Disappointingly, the modified azumamide scaffold did not induce isoform selectivity. Actually, the selectivity observed for azumamide C and E on HDAC1–3 and HDAC10 compared to HDAC8 and 6, respectively, was reduced for desmethylated anaolgs.

Furthermore, the scope of the diastereoselective Mannich reaction protocol was elaborated with the synthesis of a $\beta^{2,3}$-amino acid building block required for the preparation of an β^3-propyl azumamide analog. Even though this analog lacks a zinc-binding functionality it was able to inhibit HDAC3 with an IC$_{50}$ of 3 μM.

The analogs presented in this chapter will be tested for cytotoxicity in different cancer and healthy cell lines. Furthermore, docking studies on the azumamides and the desmethylated analogs are currently being conducted and hopefully these data can assist in identifying the important inhibitor–protein interactions.

4 Towards a thiol-sensitive linker for antibody-drug conjugates (ADC`s)

This work was performed in the group of Professor Fernando Albericio at the Institute for Research in Biomedicine, Barcelona, during a three months stay abroad.

4.1 Introduction to antibody-drug conjugates (ADC`s)

Antibody-drug conjugates (ADC`s) are macromolecules, which show great potential as pharmaceuticals.[211, 212] The field of antibody-drug conjugates is relatively new and the first ADC (brentuximab vedotin, **4.01**, Figure 4-1) was approved by the FDA in 2011, for treatment of Hodgkin's lymphoma and systemic anaplastic large cell lymphoma.[213] The general ADC is built up of three fragments; antibody, linker, and drug (Figure 4-1).

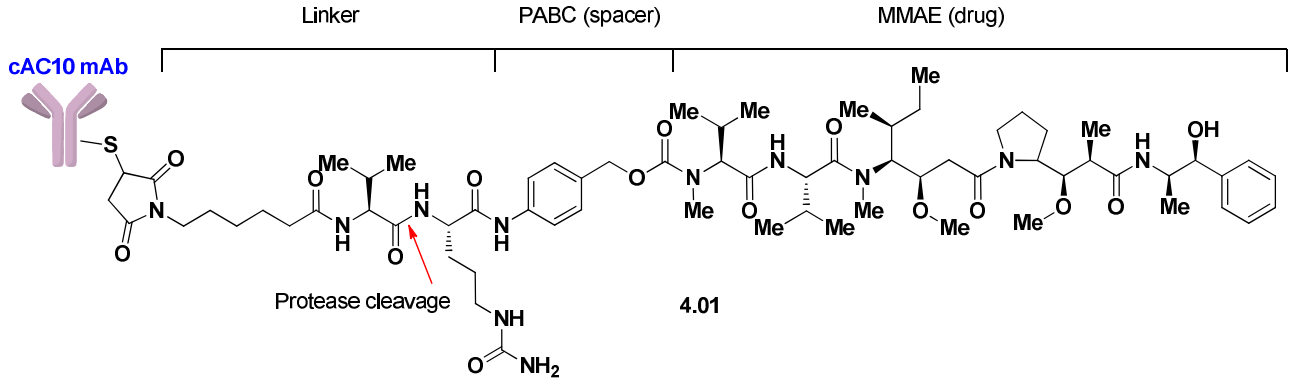

Figure 4-1. Brentuximab vedotin structure. (Adapted from Sievers and Senter)[213]

The antibody directs the conjugate to its target, making this approach highly specific. Receptor-mediated endocytosis transports the ADC into the cell, where the drug is released by a carefully chosen mechanism. To prevent premature release of the drug, the linker should be stable in the bloodstream. On the other hand, the drug should be efficiently released, when the conjugate reaches its target inside the cell. In the case of brentuximab vedotin, a protease cleavable linker was developed. The proteases found in lysosomes of the cell, cleave the amide bond between valine and citrulline and release the unmodified drug after decomposition of the PABC-spacer (Figure 4-1).

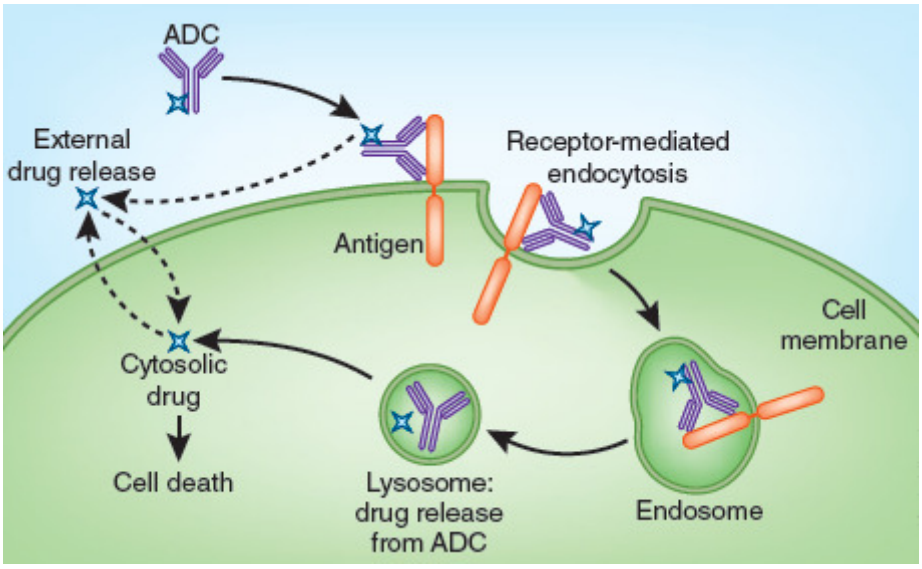

Figure 4-2. General mechanism of ADCs. (Adapted from Sievers and Senter)[213]

Development of good linkers for ADC systems is essential for the preparation of successful therapeutic agents. The target of interest is often located inside the cell and for this project, the concept is to take advantage of the different environments found in the bloodstream and inside the cell. The concentration of low molecular weight thiols is relatively low in the bloodstream. [214] The two most abundant thiol species are glutathione (GSH, ~5 μM) and cysteine (~7 μM).[215] The remaining free thiols in human plasma are primarily found as sulphydryl groups in albumin. However, the protein bound thiols are not expected to react with macrostructures such as ADCs. The cytosolic concentration of GSH is estimated to be in the range 0.1–10 mM.[216, 217] This concentration is 20–2.000-fold higher than in the bloodstream. If a linker scaffold could be designed where the cleavage is mediated by nucleophilic attack of GSH, the drug will be selectively released inside the cells.

4.2 Linker design and the Bsmoc group

The linker design is inspired from the Bsmoc protection group, which has been used as an amine protection group.[218] The Bsmoc group is constructed of a 1,1-dioxobenzothiophene scaffold, which is coupled to the amine through a carbamate linkage (Scheme 4-1).

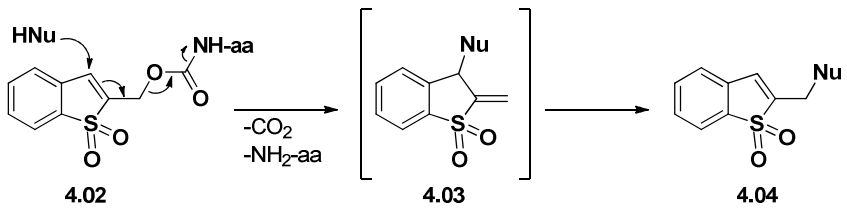

Scheme 4-1. The Bsmoc group and the deprotection mechanism. aa = amino acid.

The deprotection step involves addition of an external nucleophile, which attacks in the 3-position (Michael position) and produces the free amine, carbon dioxide, and an intermediate alkene. This alkene by-product rearranges to the aromatic compound **4.04**. The Bsmoc-scaffold can be utilized to construct a linker scaffold if an antibody is attached to the phenyl ring via the functionality (Y) and the drug molecule contains an amine functionality that allows preparation of the carbamate (**4.05**, Scheme 4-2). The addition of a nucleophile (low molecular weight thiol) will then release the drug and create carbon dioxide and an antibody–linker adduct

(Scheme 4-2). Interestingly, Ashley and co-workers have reported that the cleavage rate of similar system can be controlled by modulating the R-group in Scheme 4-2.[219] Incorporation of electron-donating R-groups will decrease the reactivity of the 3-position, whereas electron-withdrawing groups will increase the electrophilicity of the 3-position. Hopefully, tuning of the cleavage rate in this system can be achieved by modulating the R-group. The oxidation state of the benzothiophene sulfur can also affect the reactivity in the 3-position. Sulfoxides are expected to less reactive than their corresponding sulfones.

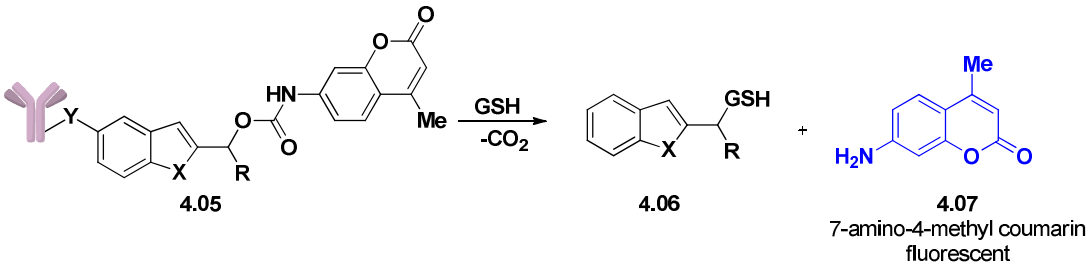

Scheme 4-2. Model system for preparation of a thiol-sensitive Bsmoc-linker.

To explore this strategy a model system was set up using the fluorophore, 7-amino-4-methyl coumarin (AMC), as the model drug and benzothiophene as the linker scaffold (Scheme 4-2). The use of a fluorophore allows quantitative detection of the cleavage reaction at low concentrations. Six target compounds were chosen to evaluate the model system (Scheme 4-3). An electron-donating (**4.08**) and an electron-withdrawing group (**4.10**) was introduced in the scaffolds. The unsubstituted analog **4.09** was prepared as well. Furthermore, both the sulfoxide and the sulfone-versions should be prepared for all the three compounds in Scheme 4-3.

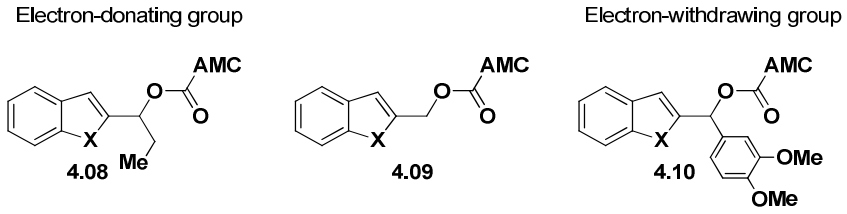

Scheme 4-3. Target compounds for evaluation of linker-model system. X= SO and SO_2.

4.3 Synthesis of linker scaffold and stability studies

Our retrosynthetic analyses was based on coupling AMC to the Bsmoc scaffold in the last step. This can be done by coupling AMC to the chloroformates of 2-hydroxybenzothiophenesulfone derivatives. The benzothiophene alcohols **4.13–4.15** were obtained in good to excellent yields by deprotonating benzothiophene with butyllithium and subsequent addition of the respective aldehydes (Scheme 4-4). Oxidation of the sulfur with magnesium monoperoxyphtalate (MMPP) provided the sulfones **4.16–4.18** in moderate to good yields.[218]

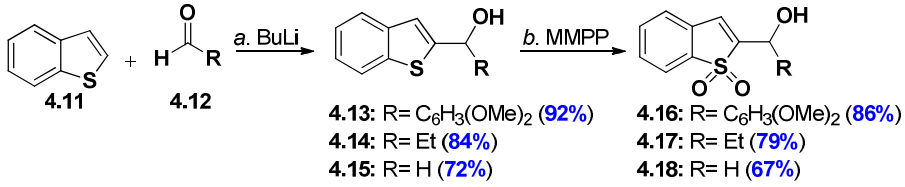

Scheme 4-4. Synthesis of benzothiophenesulfone alcohols. Reagents and conditions: (a) BuLi (1.3 equiv), 30–50 min, then aldehyde in dry THF, 2–15 h; (b) MMPP (1.3–1.4 equiv), MeOH, 2–16 h.

Attempts to oxidize the benzothiophene alcohols, to the desired sulfoxides, with mCPBA or TFA/H_2O_2 proved unsuccessful. It was envisioned that the carbamates could be accessed by preparing the chloroformates i*n situ*, with triphosgene or phosgene, and then adding AMC as the nucleophile. This approach did not provide the target compounds. Instead, products were isolated were the AMC attacks in the Michael position or performs a substitution reaction on the R-substituted carbon (Scheme 4-5, compound **4.21**). To lower the reactivity of the system the carbonyl imidazolyl compounds **4.19** and **4.20** were prepared from the benzothiophene alcohols with carbonyldiimidazole (CDI).[220] These compounds can be isolated and stored for months in the fridge. In the presence of DMAP, the coupling between compound **4.20** and benzylamine as a test substrate, gave the carbamate **4.22** in 62% yield. Disappointingly, using AMC in the same reaction failed to produce the desired carbamate. Increasing temperature and attempting a microwave induced coupling did not afford the carbamate. At high temperatures the substitution product **4.21** was isolated in 30 % yield.

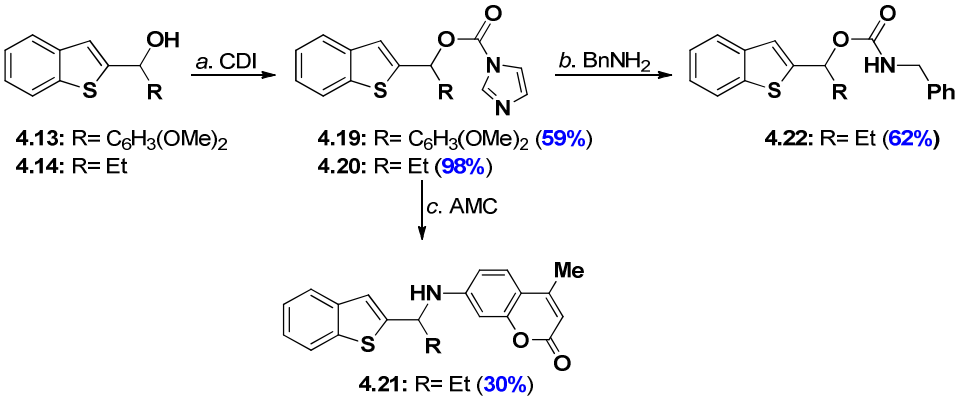

Scheme 4-5. Reagents and conditions: (a) CDI (1.4 equiv), CH_2Cl_2, 1.5–2 h; benzyl amine (1.2 equiv), Et_3N (1.2 equiv), CH_2Cl, 15 h, then DMAP (6 mol%) and benzyl amine (1.0 equiv), 35 °C, 20 h; (c) AMC (2.0 equiv), DMF, 100 °C, 16 h.

From these results we hypothesized that the low nucleophilicity of the coumarin, compared to benzyl amine, was responsible for the difference in reactivity. To circumvent this problem, the chlorocarbamate **4.23** was prepared *in situ* by the addition of triphosgene and base to AMC. The benzothiophene sulfone alcohols (**4.16** or **4.17**) were then added as nucleophiles. This reverse strategy has been used in the synthesis of a thiocarbamate from 7-amino-4-methyl coumarin.[221] In this work the ethane thiol nucleophile was added to the chlorocarbamate (**4.23**) and provided the thiocarbamate in 73% yield. As shown in scheme 54, this approach afforded the two desired benzothiophene sulfone carbamates (**4.24** and **4.25**), albeit in low yields. The primary alcohol **4.18** also seemed to work in this reaction, but purification by flash chromatography did not provide the pure carbamate.

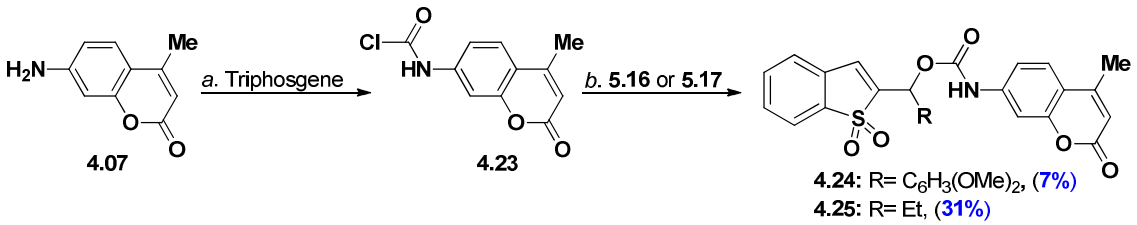

Scheme 4-6. Reagents and conditions: (a) Et_3N (10 equiv), triphosgene (1.5 equiv) in THF was added over 30 min, CH_2Cl_2, 0 °C, then 1 h; (b) **4.16** (1.5 equiv) or **4.17** (1.5 equiv), 2–19 h.

The same strategy was probed to obtain the benzothiophene sulfoxide carbamates. The benzothiophene alcohol **4.14** was added to the chlorocarbamate **4.23** to afford the carbamate **4.26** in 31% yield. The last step is oxidation of the sulfur to the sulfoxide. Several methods have been reported for the oxidation of sulfurs to the sulfoxides.[222, 223, 224] An oxidation screen was performed to develop a protocol that would provide the sulfoxide (Table 4-1). The best result was observed with triflic anhydride in the presence of hydrogen peroxide (entry 4). However, in the interest of time, the focus of the project was switched to the evaluation of the sulfone series.

Table 4-1. Screening of oxidation protocols for synthesis of sulfoxides.

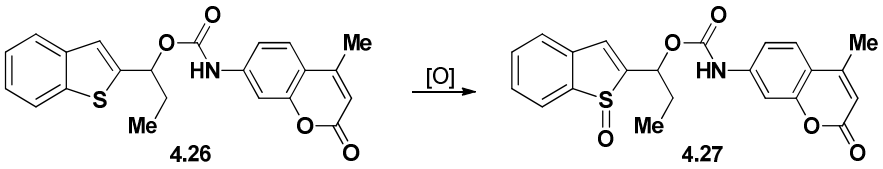

entry	reagent	solvent	observations
1	TFA/H_2O_2	TFA	Decomposition
2	$mCPBA/BF_3OEt_2$	CH_2Cl_2	Decomposition, trace of product
3	$NaIO_4$	THF/H_2O	No reaction
4	Tf_2O/H_2O_2	THF	Incomplete conversion, peak with correct mass
5	DMP	CH_2Cl_2	No reaction

4.4 Stability studies on the sulfone series

To test the stability of the linker scaffold in an aqueous media, compound **4.24** (c= 100 μM) and compound **4.25** (c= 150 μM) were dissolved in aqueous phosphate buffer (pH= 7.4) and the fluorescence measured after 2 hours, 24 hours, and 48 hours (Figure 4-3).

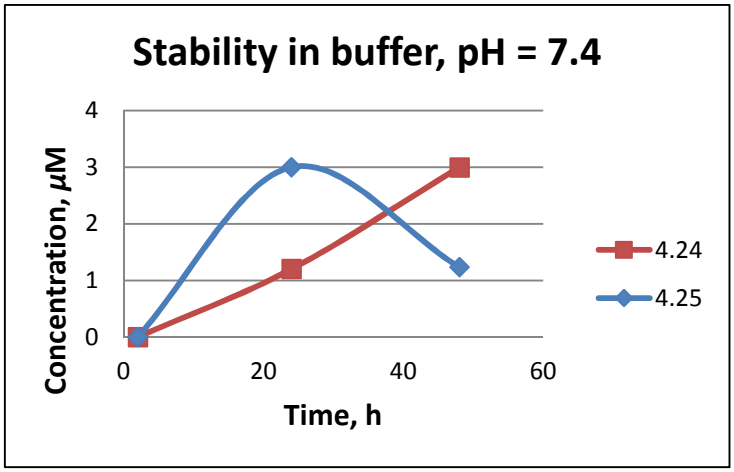

Figure 4-3. Stability study of compound **4.24** (red) and **4.25** (blue) over 48 hours. The concentrations were calculated from an AMC standard curve.

Figure 4-3 shows a slight increase in fluorescence over 48 hours, which indicates that a small amount of AMC is released. However, the measured concentrations correspond only to 2% cleavage, if the fluorescence after 2 hours is considered as the background fluorescence. HPLC analysis indicated that the linker is stable in MeCN–H_2O for a couple of hours, but after 24 hours substantial degradation was observed. These preliminary data indicate that the benzothiophene sulfone scaffold is relatively stable in an aqueous media and the next step would be to evaluate stability in human plasma and test whether addition of GSH can release the AMC from the linker. These studies are ongoing in Barcelona.

4.5 Concluding remarks

In summary, this preliminary work established the Bsmoc-based scaffold to be a potential scaffold for the linker moiety in antibody-drug conjugates. A model system was designed, where incorporation of a fluorophore as the model drug allowed evaluation of the cleavage rates. The synthetic route provided the sulfone-series, but preparation of the sulfoxide series was unsuccessful. The sulfone scaffold was found to be relatively stable in aqueous buffer and further investigation into the release of the model drug, by addition of a nucleophile, will determine if the Bsmoc-based scaffold is suitable as a linker-scaffold.

5 Conclusion

In pursuit of completing the total synthesis of the azumamides and constructing analogs, we have developed a synthetic route, which enabled the construction of the full diastereomeric matrix for the $\beta^{2,3}$-amino acid scaffold. The key step in this route is a diastereoselective Mannich reaction. In our hands, the reaction is hypothesized to go through an open transition state, which is in disagreement with the results from other research groups. However, this methodology nicely provided two site-specifically edited epimeric azumamide analogs. These analogs were inactive against the full panel of HDAC enzymes and show that the β-amino acid scaffold is highly sensitive to modifications in the stereochemistry. This work also reports the total syntheses of azumamides A–E and presents first total syntheses of azumamide B–D. The natural products were subjected to full HDAC profiling and we found that the azumamides were poor inhibitors of class IIa HDACs, but potent inhibitors of HDAC1–3, 10, and 11 (IC_{50} values between 14 nM to 67 nM). Furthermore, the HDAC screening established azumamide C to be ~2-fold more potent than azumamide E against the majority of enzymes, which is in disagreement with previous results. In terms of selectivity, azumamide C and E were between 60–350-fold more potent towards HDAC1–3 over HDAC8. Furthermore, these two compounds displayed >200-fold selectivity for HDAC10 over HDAC6.

Our synthetic route also enabled the synthesis of β^2-des- and dimethylated azumamide analogs as well as a β^3-propyl analog. The incorporation of a methyl group in the 2-position resulted in poor HDAC inhibitors with IC_{50} values (>10 μM). The desmethylated compounds were more active, but still suffered a decrease in activity (IC_{50} values just below 1 μM). Based on NMR solution structures, we hypothesize that the β^2-methyl group found in the natural products may guide the β^3-side chain towards the active site. Judging from the biochemical data on the desmethylated series, this directing feature is important for activity. Ongoing docking studies will hopefully contribute to this hypothesis. The β^3-propyl azumamide C analog was found to be active against HDAC3 with an IC_{50} of 3 μM. The straightforward synthesis of the β-amino acid required for this analog emphasizes the effectiveness of the developed Mannich reaction.

Thus, this work has contributed to the structure–activity relationship for the azumamides and illustrated that these compounds are sensitive to modifications in the β-amino acid scaffold. The developed diastereoselective Mannich reaction have been shown to be a powerful tool for synthesizing β-amino acid scaffolds and this reaction will aid in the future production of azumamide analogs. However, obtaining potent and isoform selective compounds based on the azumamide scaffold seems challenging

6 Experimental
Experimental for chapter 2

Biochemical profiling

Assay Materials

HDAC1 (Purity >45% by SDS-PAGE according to the supplier), HDAC4 (Purity >90% by SDS-PAGE according to the supplier), and HDAC 7 (Purity >90% by SDS-PAGE according to the supplier) were purchased from Millipore (Temecula, CA 92590). HDAC2 used for dose–response experiments (Full length, purity ≥94% by SDS-PAGE according to the supplier) and HDAC 5 (Full length, purity ≥4% by SDS-PAGE according to the supplier) and HDAC8 used for dose-response experiments (Purity ≥90% by SDS-PAGE according to the supplier) were purchased from BPS Bioscience (San Diego, CA 92121). HDAC2 used for initial screening experiments (Full length, purity 50% by SDS-PAGE according to the supplier), HDAC3-NCoR1* complex (Purity 90% by SDS-PAGE according to supplier), HDAC6 (Purity >90% by SDS-PAGE according to the supplier), HDAC8 for initial screening experiments (Purity >50% by SDS-PAGE according to the supplier), HDAC10 (Purity >50% by SDS-PAGE according to the supplier), and HDAC11 (Purity >50% by SDS-PAGE according to the supplier) were purchased from Enzo Life Sciences (Postfach, Switzerland). HDAC9 (Full length, purity 12% by SDS-PAGE according to the supplier) was purchased from Abnova (Taipei, Taiwan). The HDAC assay buffer [50 mM tris/Cl, pH 8.0, 137 mM NaCl, 2.7 mM KCl, 1 mM $MgCl_2$, and bovine serum albumin (0.5 mg/mL)]. Trypsin (10,000 units/mg, TPCK treated from bovine pancreas) was from Sigma Aldrich (Steinheim, Germany). All peptides were purified to homogeneity (>95% purity by $HPLC_{230\ nm}$ using reversed-phase preparative HPLC), and the white fluffy materials obtained by lyophilization were kept at –20 °C. For assaying, peptide substrates were reconstituted in DMSO to give 5–10 mM stock solutions, the accurate concentrations of which were determined by co-injection on HPLC with a standard of known concentration.

In Vitro Histone Deacetylase Inhibition Assays

For inhibition of recombinant human HDACs the dose–response experiments with internal controls were performed in black low binding NUNC 96-well microtiter plates. Dilution series (3-fold dilution, 10 concentrations) were prepared in HDAC assay buffer from 5–10 mM DMSO stock solutions. The appropriate dilution of inhibitor (10 μL of 5 $\times$ the desired final concentration) was added to each well followed by HDAC assay buffer (25 μL) containing substrate [*Ac-Leu-Gly-Lys(Ac)-AMC* (40 μM) for HDAC1, 2, and 3; (80 μM) for HDAC6 and 11; *Ac-Leu-Gly-Lys(Tfa)-AMC* (40 μM) for HDAC4; (240 μM) for HDAC5; (80 μM) for HDAC7; (400 μM) for HDAC8; and (160 μM) for HDAC9; and *Ac-Arg-His-Lys(Ac)-Lys(Ac)-AMC* (100 μM) for HDAC10]. Finally, a solution of the appropriate HDAC (15 μL) was added and the plate was incubated at 37 °C for 30 min [HDAC1: 150 ng/well, HDAC2: 100 ng/well, HDAC3: 10 ng/well, HDAC4: 2 ng/well, HDAC5: 40 ng/well, HDAC6: 60 ng/well, HDAC7: 2 ng/well, HDAC8: 5 ng/well, HDAC9: 40 ng/well, HDAC10: 500 ng/well, HDAC11: 500 ng/well]. Then trypsin (50 μL, 0.4 mg/mL) was added and the assay development was allowed to proceed for 15–30 min at room temperature, before the plate was read using a Perkin Elmer Enspire plate reader with excitation at 360 nm and detecting emission at 460 nm. Each assay was performed in duplicate. The data were analyzed by non-linear regression using GraphPad Prism to afford IC_{50} values from the dose-response experiments, and K_i values were determined from the Cheng-Prusoff equation [$K_i = IC_{50}/(1+[S]/K_m)$] assuming a standard fast-on–fast-off mechanism of inhibition.

Dose-response curves and IC_{50} values for "active" inhibitors.

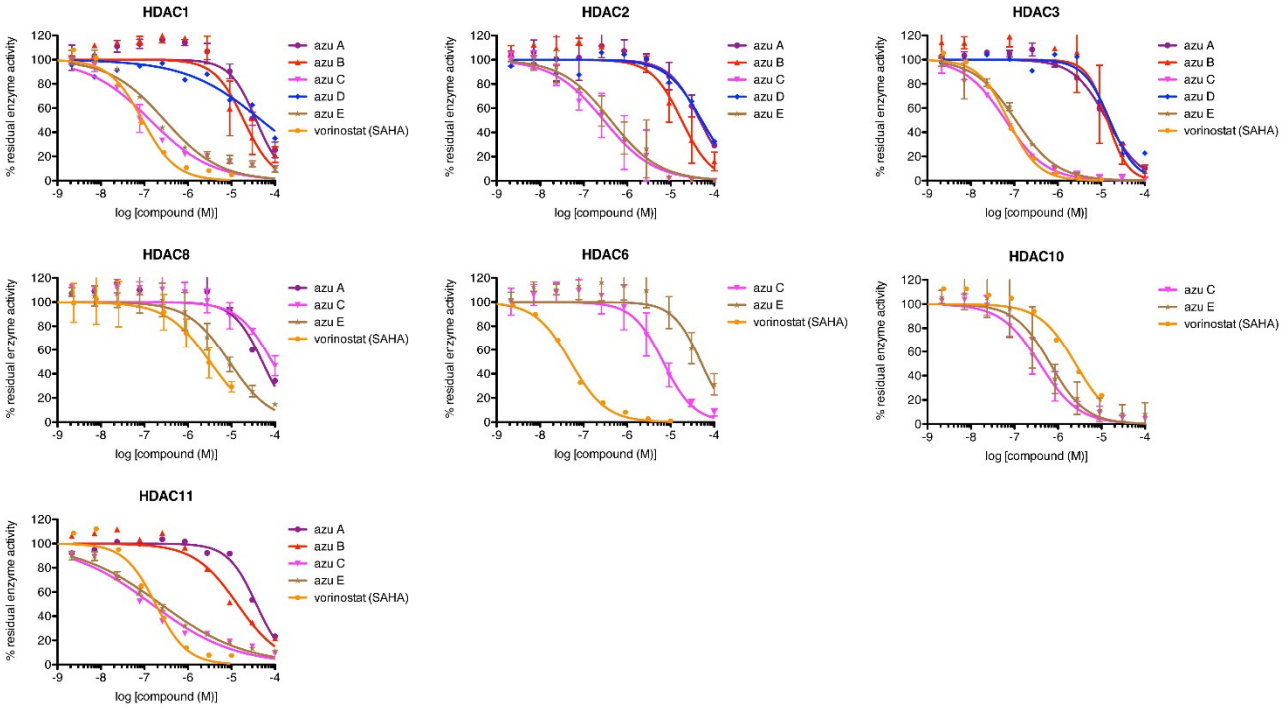

IC_{50} values ± standard deviation [μM], derived from the above dose–response experiments[a]

	class-I				class-IIa				class-IIb		class-IV
compound	HDAC1	HDAC2	HDAC3	HDAC8	HDAC4	HDAC5	HDAC7	HDAC9	HDAC6	HDAC10	HDAC11
azuA	>30	>30	14±0.7	>30	IA	IA	IA	IA	IA	IA	>30
azuB	21±13	20±13	14±9	IA[b]	IA	IA	IA	IA	IA	IA	13
azuC	0.14 ±0.004	0.27 ±0.15	0.06 ±0.004	>30	IA	IA	IA	IA	7±3.2	0.4	0.15 ±0.014
azuD	>30	>30	16	IA	IA	IA	IA	IA	IA	IA	IA
azuE	0.29 ±0.03	0.4 ±0.22	0.11 ±0.02	9±3.9	IA	IA	IA	IA	>30	0.8	0.24 ±0.07

[a]IC_{50} values determined from at least two individual dose–response experiments performed in duplicate using ten-point, three-fold dilution series of each compound (except for azuC and azuE against HDAC10, which were only performed in duplicate in a single assay). [b]IA = inactive (<50% inhibition at 50μM [inhibitor]).

Cheng–Prusoff K_i Calculations

Using the equation $K_i = IC_{50}/(1+[S]/K_m)$ by assuming a standard fast-on–fast-off mechanism of inhibition, the above IC_{50} values were converted to K_i values using the substrate concentrations outlined in the experimental section and the K_m values determined by Bradner *et al.*[35] for HDACs 1–9 and by Inks *et al.*[225] for HDAC11. For HDAC10, we derived a K_m value for the applied substrate (Ac-RHKacKac-AMC) from Michaelis-Menten experiments as previously described[197] (see figure below). AMC is the fluorophore (4-amino-7-methylcoumarin), which is attached to the C-terminal of the substrate molecules.

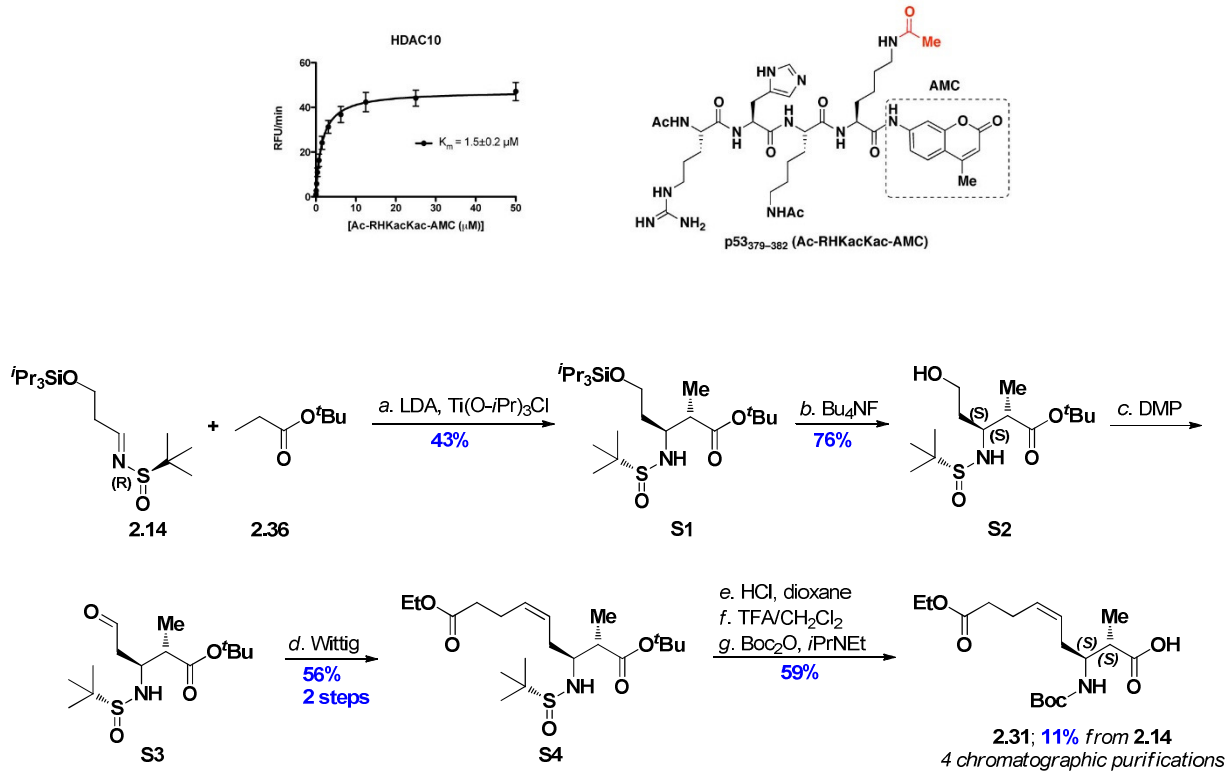

Figure S1. Synthesis of (2*S*,3*R*)-β-amino acid building block (**2.31**).

Material and Methods

General

All chemicals and solvents were analytical grade and used without further purification. Vacuum liquid chromatography (VLC) was performed on silica gel 60 (particle size 0.015−0.040 μm). UPLC−MS analyses were performed on a Waters Acquity ultra high-performance liquid chromatography system. A gradient with eluent I (0.1% HCOOH in water) and eluent II (0.1% HCOOH in acetonitrile) rising linearly from 0% to 95% of II during t = 0.00–2.50 min was applied at a flow rate of 1 mL/min (gradient A) or during t = 0.00–5.20 min (gradient B). Analytical HPLC was performed on a [150 mm × 4.6 mm, C_{18} Phenomenex Luna column (3 μm)] using an Agilent 1100 LC system equipped with a UV detector. A gradient, C, with eluent III (95:5:0.1, water−MeCN−TFA) and eluent IV (0.1% TFA in acetonitrile) rising linearly from 0% to 95% of IV during t = 2−20 min was applied at a flow rate of 1 mL/min. Preparative reversed-phase HPLC was performed on a [250 mm × 20 mm, C_{18} Phenomenex Luna column (5 μm, 100 Å)] using an Agilent 1260 LC system equipped with a diode array UV detector and an evaporative light scattering detector (ELSD). A gradient C with eluent III and eluent IV rising linearly from 0% to 95% of IV during t = 5−45 min was applied at a flow rate of 20 mL/min. 1D and 2D NMR spectra were recorded on a Varian Mercury 300 instrument or a Varian INOVA 500 MHz instrument. All spectra were recorded at 298 K. Correlation spectroscopy (COSY) spectra were recorded with a relaxation delay of 1.5 sec before each scan, a spectral width of 6k × 6k, collecting 8 FIDs and 1k × 512 data points. Heteronuclear single quantum coherence (HSQC) spectra were recorded with a relaxation delay of 1.5 sec before each scan, a spectral width of 6k × 25k, collecting 16 FIDs and 1k × 128 datapoints. Heteronuclear 2-bond correlation (H2BC) spectra were recorded with a relaxation delay of 1.5 sec before each scan, a spectral width of 4k × 35k, collecting 16 FIDs at 295 K and 1k × 256 datapoints. Heteronuclear

multiple-bond correlation (HMBC) spectra were recorded with a relaxation delay of 1.5 sec before each scan, a spectral width of 6k × 35 k, collecting 32 FIDs and 1k × 256 datapoints. Chemical shifts are reported in ppm relative to deuterated solvent peaks as internal standards (δH, DMSO-d_6 2.50 ppm; δC, DMSO-d_6 39.52 ppm, δH, CD_3OH 3.30 ppm, δH, $CDCl_3$ 7.26 ppm; δC, $CDCl_3$ 77.16 ppm). Coupling constants (*J*) are given in hertz (Hz). Multiplicities of ^{1}H NMR signals are reported as follows: s, singlet; d, doublet; t, triplet; q, quartet; m, multiplet.

3-((Triisopropylsilyl)oxy)propan-1-ol (2.13)

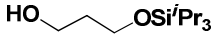

A solution of 1,3-propanediol (1.9 mL, 26.3 mmol) in dry THF (11 mL) was added dropwise to a stirred suspension of NaH (1.1 g, 26.3 mmol, l.0 equiv, 60 % in mineral oil) in dry THF (21 mL) under N_2. After 35 min triisopropyl chloride (5.5 mL, 25.7 mmol) in dry THF (11 mL) was added dropwise and the mixture stirred for 20 hours. After addition of sat. aq. $NaHCO_3$ (40 mL) the aqueous phase was extracted with EtOAc (80 mL) and ether (80 mL). The combined organic phases were dried with Na_2SO_4, filtered, and concentrated *in vacuo*. Purification by vacuum liquid chromatography (VLC) afforded **2.13** as a clear oil (4.54 g, 86%). ^{1}H NMR (300 MHz, $CDCl_3$) δ 3.92 (t, *J* = 5.6 Hz, 2H), 3.82 (t, *J* = 5.4 Hz, 2H), 2.77 (bs, 1H), 1.79 (pentet, *J* = 5.6 Hz, 2H), 1.09–1.04 (m, 21H); ^{13}C NMR (75 MHz, $CDCl_3$) δ 63.8, 62.9, 34.3, 18.1, 11.9.

(S_R)-(*E*)-2-Methyl-N-(3-((triisopropylsilyl)oxy)propylidene)propane-2-sulfinamide (2.14)

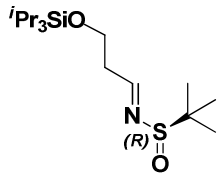

A solution of DMSO (2.1 mL, 28.9 mmol, 3.2 equiv) in dry CH_2Cl_2 (20 mL) was added dropwise via an addition funnel to a solution of oxalylchloride (1.3 mL, 14.5 mmol, 1.6 equiv) in dry CH_2Cl_2 (44 mL) at –78° C. After stirring for 25 min a solution of alcohol **2.13** (2.1 g, 9.0 mmol) in dry CH_2Cl_2 (20 mL) was added dropwise via an addition funnel. After 30 min Et_3N (6.5 ml, 46.6 mmol, 5.2 equiv) was added and after stirring for 40 min at –78 °C the cooling bath was removed and the mixture allowed to reach room temperature. EtOAc (130 mL) was added and the organic phase washed with sat. aq. NH_4Cl (60 mL) and brine (60 mL). The organic phase was concentrated *in vacuo* and the residue was pulled through a short plug of silica gel to afford the crude aldehyde as a clear oil (2.03 g, 99%), which was used directly without further purification. ^{1}H NMR (300 MHz, $CDCl_3$) δ 9.83 (t, *J* = 2.2 Hz, 1H), 4.07 (t, *J* = 6.1 Hz, 2H), 2.60 (td, *J* = 6.1, 2.2 Hz, 2H), 1.07–1.03 (m, 21H); ^{13}C NMR (75 MHz, $CDCl_3$) δ 202.4, 58.0, 46.9, 18.1, 12.0.

A solution of aldehyde (2.0 g, 8.7 mmol, 1.05 equiv) in dry CH_2Cl_2 (7 mL) was added dropwise to a solution of dried $CuSO_4$ (3.5 g, 21.9 mmol, 2.6 equiv) and (*R*)-(+)-2-methyl-2-propanesulfinamide (1.0 g, 8.3 mmol) in dry CH_2Cl_2 (45 mL). After stirring vigorously for 16 hours $CuSO_4$ (0.8 g, 5.0 mmol, 0.6 equiv) was added and after additionally 25 hours of stirring the mixture was poured into EtOAc (120 mL) and washed with water (120 mL). The aqueous phase was extracted with EtOAc (120 mL) and the combined organic phases were washed with water (120 mL) and concentrated *in vacuo*. Purification by VLC afforded *tert*-butanesulfinyl imine **2.14** as a clear oil (1.88 g, 63%, two steps).). $[\alpha]_D$: –157° (*c* = 0.8, CH_2Cl_2); ^{1}H NMR (300 MHz, $CDCl_3$) δ 8.11 (t, *J* = 4.8 Hz, 1H), 4.00 (t, *J* = 6.3 Hz, 2H), 2.74 (td, *J* = 6.2, 4.9 Hz, 2H), 1.18 (s, 9H), 1.03 (m, 21H); ^{13}C NMR (75 MHz, $CDCl_3$) δ 168.1, 60.1, 56.7, 39.8, 22.5, 18.1, 12.0. HRMS (ESI-TOF): *m/z* calcld. for $C_{16}H_{35}NO_2SSiH^+$: 334.2236; found: 334.2229 $[M+H]^+$.

General method for Mannich reactions

A solution of LDA (2.1 equiv) was added dropwise to a solution of the ester (2.0 equiv) in dry THF at –78 °C. After stirring for 30 min Ti(O-*i*Pr)$_3$Cl (4.2 equiv) in dry THF was added dropwise. The orange solution was

stirred for 30 min and the imine (1.0 equiv) in dry THF was added dropwise. The mixture was stirred for 3 h or until TLC showed full conversion of the imine. The mixture was quenched with sat. aq. NH_4Cl and allowed to reach room temperature. Water was added and the mixture decanted into a separatory funnel. The remaining Ti precipitate was added EtOAc–water (1:1) and stirred vigorously for 5 min before being added to the separatory funnel. The aqueous phase was extracted with EtOAc and the combined organic phases were washed again with water, dried ($MgSO_4$), filtered, and concentrated *in vacuo*.

(2*S*,3*S*)-*tert*-Butyl-3-((*R*)-1,1-dimethylethylsulfinamido)-2-methyl-5-((triisopropylsilyl)oxy)pentanoate (Table 2-1, entry 5, S1)

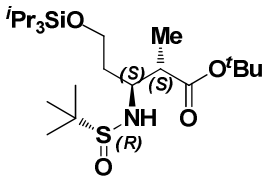

The general procedure was followed using imine **2.14** (0.86 g, 2.60 mmol), *tert*-butyl propionate (0.78 mL, 5.20 mmol), LDA (1.8 M, 3.0 mL, 5.40 mmol) and Ti(O-*i*Pr)$_3$Cl (2.80 mL, 11.1 mmol). Diastereoselectivity was determined by ^{1}H NMR integration of the crude reaction mixture (60:26:8:6). Purification by VLC afforded **S1** as a colorless oil (0.45 g, 38%) as well as a fraction containing a mixture of diasteromers (0.50 g, 43%). Characterization data for the (2*S*,3*S*) diastereomer. $[\alpha]_D$: –30.8° (*c* = 0.4, CH_2Cl_2); ^{1}H NMR (300 MHz, $CDCl_3$) δ 4.06 (d, *J* = 8.0 Hz, 1H), 3.85 (m, 2H), 3.56 (m, 1H), 2.74 (qd, *J* = 7.1, 4.9 Hz, 1H), 1.95 (m, 1H), 1.82 (m, 1H), 1.43 (s, 9H), 1.20 (s, 9H), 1.14 (d, *J* = 7.1 Hz, 3H), 1.05 (m, 21H). ^{13}C NMR (75 MHz, $CDCl_3$) δ 174.4, 80.8, 60.9, 57.4, 56.2, 44.4, 36.9, 28.2, 23.0, 18.2, 14.5, 12.0; HRMS (ESI-TOF): *m/z* calcld. for $C_{23}H_{49}NO_4SSiNa^+$: 486.3049; found: 486.3046 $[M+Na]^+$.

Ethyl 3-((*R*)-1,1-dimethylethylsulfinamido)-2-methyl-5-((triisopropylsilyl)oxy)pentanoate (Table 2-1, entry 2)

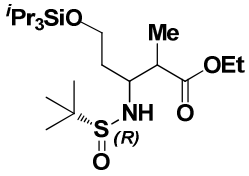

The general procedure was followed using imine **2.14** (179 mg, 0.54 mmol), ethyl propionate (155 μL, 1.34 mmol), LDA (1.2 M, 1.20 mL, 1.40 mmol) and Ti(O-*i*Pr)$_3$Cl (0.58 mL, 2.42 mmol). Diastereoselectivity was determined by ^{1}H NMR integration of the crude reaction mixture (49:29:11:11). The diastereomers could not be separated by VLC and the purification afforded a mixture of diastereomers as a pale yellow oil (0.12 g, 51%).

Methyl3-((*R*)-1,1-dimethylethylsulfinamido)-2-methyl-5-((triisopropylsilyl)oxy)pentanoate (Table 2-1, entry 1)

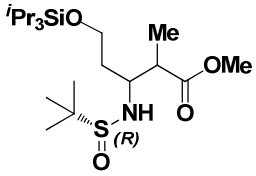

The general procedure was followed using imine **2.14** (137 mg, 0.41 mmol), methyl propionate (80 μL, 0.83 mmol), LDA (1.4 M, 0.62 mL, 0.86 mmol) and Ti(O-*i*Pr)$_3$Cl (0.41 mL, 1.72 mmol). Unreacted imine was removed by VLC to give a mixture of diastereomers [(47:39:10:4), 29 mg, 17%].

Allyl 3-((*R*)-1,1-dimethylethylsulfinamido)-2-methyl-5-((triisopropylsilyl)oxy)pentanoate (Table 2-1, entry 3)

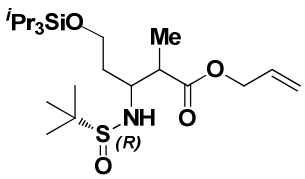

The general procedure was followed using imine **2.14** (144 mg, 0.43 mmol), allyl propionate (110 μL, 0.86 mmol), LDA (1.4 M, 0.65 mL, 0.91 mmol) and Ti(O-*i*Pr)$_3$Cl (0.43 mL, 1.81 mmol). Unreacted imine was removed by VLC to give a mixture of diastereomers [(46:34:10:10), 64 mg, 33%].

4-Methoxybenzyl-3-((*R*)-1,1-dimethylethylsulfinamido)-2-methyl-5-((triisopropylsilyl)oxy)pentanoate (Table 2-1, entry 4)

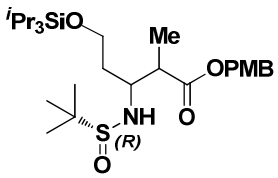

The general procedure was followed using imine **2.14** (165 mg, 0.50 mmol), 4-methoxybenzyl propionate (225 μL, 1.24 mmol), LDA (1.2 M, 1.10 mL, 1.29 mmol) and Ti(O-*i*Pr)$_3$Cl (0.56 mL, 2.23 mmol). Diastereoselectivity was determined by ^{1}H NMR integration of the crude reaction mixture (46:33:11:10). The diastereomers could not be separated by VLC and the purification afforded a mixture of diastereomers as a pale yellow oil (0.21 g, 81%).

(2*S*,3*S*)-*tert*-Butyl 3-((*R*)-1,1-dimethylethylsulfinamido)-2-methyl-5-((triisopropylsilyl)oxy)pentanoate (Table 2-1, entry 6, 2.37)

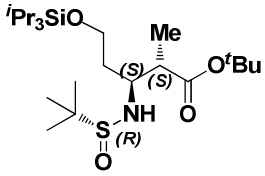

A solution of LDA (1.3 M in THF, 0.86 mL, 1.12 mmol, 2.6 equiv) was added dropwise over 5 min to *tert*-butyl propionate (163 μL, 1.08 mmol, 2.5 equiv) in dry THF (7.0 mL) at –78 °C. After stirring for 30 min HMPA (225 μL, 1.30 mmol, 3.0 equiv) was added dropwise and after additionally 10 min of stirring, imine **2.14** (144 mg, 0.43 mmol) in dry THF (1.5 mL) was added dropwise. After 1 hour the reaction was quenched with sat. aq. NH_4Cl and worked up according to the general procedure. Diastereoselectivity was determined by ^{1}H NMR integration of the crude reaction mixture (71:15:14:0). Purification by VLC afforded (89 mg, 45%) of the pure (*S,S*) diastereomer **2.37** as a clear oil. A fraction containing a mixture of diastereomers (77.0 mg, 39%) was obtained as well. Characterization data for the (2*S*,3*S*) diastereomer. $[\alpha]_D$: –24.0° (*c* = 8.3, CH_2Cl_2); ^{1}H NMR (300 MHz, $CDCl_3$) δ 4.07 (d, *J* = 8.0 Hz, 1H), 3.84 (m, 2H), 3.56 (m, 1H), 2.75 (qd, *J* = 7.1, 4.9 Hz, 1H), 1.96 (m, 1H), 1.83 (m, 1H), 1.43 (s, 9H), 1.21 (s, 9H), 1.15 (d, *J* = 7.1 Hz, 3H), 1.06 (m, 21H); ^{13}C NMR (75 MHz, $CDCl_3$) δ 174.4, 80.8, 60.9, 57.4, 56.2, 44.4, 36.9, 28.3, 23.0, 18.2, 14.5, 12.0; HRMS (ESI-TOF): *m/z* calcld. for $C_{23}H_{49}NO_4SSiNa^+$: 486.3049; found: 486.3046 $[M+Na]^+$.

3-(Benzyloxy)propanal (S5)

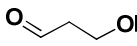

DMSO (3.13 mL, 44 mmol, 2.2 equiv) was added to a solution of oxalylchloride (1.91 mL, 22 mmol, 1.1 equiv) in dry CH_2Cl_2 (120 mL) at –78° C under nitrogen atmosphere. After stirring for 20 min a solution of 3-(benzyloxy)propanol (3.32 g, 22 mmol) in dry CH_2Cl_2 (7.5 mL) was added dropwise. After 20 min Et_3N (14 ml, 100 mmol, 5.0 equiv) was added and after stirring for 10 min at –78 °C, the cooling bath was removed and the mixture allowed to reach room temperature. After stirring for 30 min the reaction was quenched with sat. aq. NH_4Cl (15 mL). The aqueous phase was extracted with CH_2Cl_2 (2 × 30 mL) and the combined organic phases were washed with sat. aq. $NaHCO_3$ (2 × 20 mL), brine (20 mL), dried (Na_2SO_4), filtered, and concentrated *in vacuo*. Purification by VLC afforded the aldehyde crude **S5** as a clear oil (2.36 g, 72%). ^{1}H NMR (300 MHz, $CDCl_3$) δ 9.79 (d, *J* = 1.8 Hz, 1H), 7.53–7.01 (m, 5H), 4.53 (s, 2H), 3.81 (t, *J* = 6.1 Hz, 2H), 2.69 (td, *J* = 6.1, 1.8 Hz, 2H). ^{13}C NMR (75 MHz, $CDCl_3$) δ 201.2, 137.9, 128.5, 127.8, 127.8, 73.3, 63.9, 43.9.

(S_R)-(*E*)-*N*-(3-(Benzyloxy)propylidene)-2-methylpropane-2-sulfinamide (2.30)

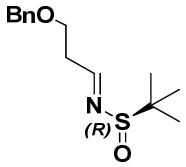

A solution of aldehyde **S5** (1.49 g, 9.08 mmol, 1.1 equiv) in dry CH_2Cl_2 (5 mL) was added dropwise to a solution of dry $CuSO_4$ (2.92 g, 18.2 mmol, 2.2 equiv) and (*R*)-(+)-2-methyl-2-propanesulfinamide (1.0 g, 8.25 mmol, 1.0 equiv) in dry CH_2Cl_2 (60 mL). After stirring vigorously for 22 hours the reaction mixture was filtered and the filtercake washed with CH_2Cl_2. The organic phase was washed with brine (2 × 30 mL), dried ($MgSO_4$), filtered, and concentrated *in vacuo*. Purification by VLC afforded *tert*-butanesulfinyl imine **2.30** as a clear oil (1.65 g, 75%). Spectral data were in accordance with those previously reported.[226] $[\alpha]_D$: –155° (*c* = 1.4, CH_2Cl_2); ^{1}H NMR (300 MHz, $CDCl_3$) δ 8.10 (t, *J* = 4.6 Hz, 1H), 7.42–7.20 (m, 5H), 4.51 (s, 2H), 3.77 (t, *J* = 6.2 Hz, 3H), 2.81 (td, *J* = 6.2 Hz and 4.6 Hz, 2H), 1.17 (s, 9H).^{13}C NMR (75 MHz, $CDCl_3$) δ 167.4, 137.9, 128.5, 127.7, 73.3, 66.2, 56.7, 36.6, 22.4.

***tert*-Butyl 5-(benzyloxy)-3-((*R*)-1,1-dimethylethylsulfinamido)-2- (Table 2-1, entry 1)**

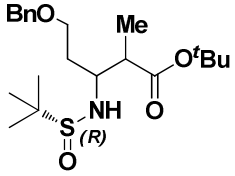

The general procedure was followed using imine **S5** (187 mg, 0.70 mmol), *tert*-butyl propionate (265 μL, 1.76 mmol), LDA (1.3 M, 1.40 mL, 1.82 mmol) and Ti(O-*i*Pr)$_3$Cl (0.75 mL, 3.15 mmol). Diastereoselectivity was determined by ^{1}H NMR integration of the crude reaction mixture (70:18:12:0). The diastereomers could not be separated by VLC and the purification afforded a mixture of diastereomers as a pale yellow oil (0.184 g, 66%).

3-((4-Methoxybenzyl)oxy)propan-1-ol (2.26)

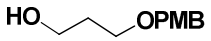

To a solution of 1,3-propanediol (3.20 mL, 44.3 mmol) in dry THF (50 mL) was added NaH (1.68 g, 42 mmol, 0.95 equiv, 60 % in mineral oil) in dry THF (21 mL) at 0 °C. The mixture was stirred under N_2 and after 15 min TBAI (0.82 g, 2.21 mmol, 0.05 equiv) was added followed by dropwise addition of *para*-methoxybenzyl chloride (6.0 mL, 44.3 mmol, 1.0 equiv). After 17 hours the mixture was concentrated to a small volume and added water (50 mL). The aqueous phase was extracted with EtOAc (150 mL + 75 mL) and the combined organic phases were dried with Na_2SO_4, filtered, and concentrated *in vacuo*. Purification by VLC afforded **2.26** as a yellow oil (4.19 g, 51%). Spectral data were in accordance with those previously reported in the literature.[227] ^{1}H NMR (300 MHz, $CDCl_3$) δ 7.25 (d, *J* = 8.4 Hz, 2H), 6.87 (*J* = 8.6 Hz, 2H), 4.44 (s, 2H), 3.79 (s, 3H), 3.75 (t, *J* = 8.6 Hz, 2H), 3.63 (t, *J* = 5.8 Hz, 2H), 2.42 (bs, 1H), 1.84 (pentet, *J* = 5.8 Hz, 2H).;^{13}C NMR (75 MHz, $CDCl_3$) δ 159.3, 130.2, 129.4, 113.9, 73.0, 69.2, 62.0, 55.4, 32.2.

(S_R)-(*E*)-*N*-(3-((4-Methoxybenzyl)oxy)propylidene)-2-methylpropane-2-sulfinamide (2.28)

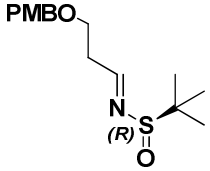

Oxalylchloride (1.02 mL, 22.4 mmol, 2.2 equiv) was added dropwise to a solution of DMSO (1.74 mL, 48.9 mmol, 4.8 equiv) in dry CH_2Cl_2 (25 mL) under argon at –78 °C. After stirring for 30 min a solution of alcohol **2.26** (2.0 g, 5.1 mmol) in dry CH_2Cl_2 (5 mL) was added dropwise. After 30 minutes, Et_3N (5.18 mL, 74.4 mmol, 7.3 equiv) was added and the mixture allowed to warm to room temperature. Water (50 mL) was added and the mixture extracted with CH_2Cl_2 (3 × 50 mL). The combined organics were washed with sat. aq. $NaHCO_3$ (3 × 50 mL), brine (50 mL), dried (Na_2SO_4), filtered, and concentrated *in vacuo* to yield the crude aldehyde (1.98 g), which was used without further purification. ^{1}H NMR (300 MHz, $CDCl_3$) δ 9.78 (t, *J* = 1.8 Hz, 1H), 7.25 (d, *J* = 8.2 Hz, 2H), 6.88 (d, *J* = 8.3 Hz, 2H), 4.46 (s, 3H), 3.80 (s, 3H), 3.77 (t, 2H), 2.68 (td, *J* = 6.1 Hz and 1.8 Hz, 2H).

A solution of aldehyde (0.99 g, 5.1 mmol) in dry CH_2Cl_2 (2 mL) was added dropwise to a solution of dry $CuSO_4$ (4.0 g, 20.4 mmol, 4.0 equiv) and (*R*)-(+)-2-methyl-2-propanesulfinamide (0.62 g, 5.1 mmol, 1.0 equiv) in dry CH_2Cl_2 (22 mL). After stirring vigorously for 16 hours, $CuSO_4$ (2.0 g, 12.5 mmol, 2.5 equiv) was added and after additionally 4 hours of stirring the mixture was filtered and the filtercake washed with CH_2Cl_2. The organic phase was washed with water (40 mL), brine (40 mL), dried (Na_2SO_4), filtered, and concentrated *in vacuo*. Purification by VLC afforded *tert*-butanesulfinyl imine **2.28** as a colorless oil (0.95 g, 62%, two steps). Spectral data were in accordance with those previously reported in the literature.[228] $[\alpha]_D$: –152° (*c* = 0.4, CH_2Cl_2); ^{1}H NMR (300 MHz, $CDCl_3$) δ 8.09 (t, *J* = 4.6 Hz, 1H), 7.23 (dt, *J* = 8.7 Hz and 2.0 Hz, 2H), 6.86 (dt, *J* = 8.7 Hz and 2.0 Hz, 2H), 4.44 (s, 2H), 3.79 (s, 3H), 3.74 (t, *J* = 6.3 Hz, 1H), 2.79 (td, *J* = 6.3, 4.6 Hz, 2H), 1.17 (s, 9H). ^{13}C NMR (75 MHz, $CDCl_3$) δ 167.5, 159.3, 130.1, 129.4, 113.9, 73.0, 66.0, 56.8, 55.4, 36.7, 22.4.

(2*S*,3*S*)-*tert*-Butyl 3-((*R*)-1,1-dimethylethylsulfinamido)-5-((4-methoxybenzyl)oxy)-2-methylpentanoate (Table 2-1, entry 2)

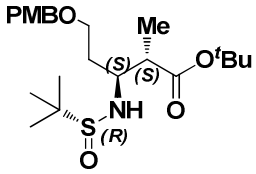

The general procedure was followed using imine **2.28** (166 mg, 0.56 mmol), *tert*-butyl propionate (210 μL, 1.40 mmol), LDA (1.3 M, 1.12 mL, 1.45 mmol) and Ti(O-*i*Pr)$_3$Cl (0.63 mL, 2.51 mmol). Diastereoselectivity was determined by ^{1}H NMR integration of the crude reaction mixture (77:13:10:0). Purification by silica gel chromatography afforded a mixture of two diastereomers [(88:12) 170 mg, 71%] and a small fraction containing a mixture of all three diastereomers (20 mg, 8%). NMR characterization of the major diastereomer: ^{1}H NMR (300 MHz, $CDCl_3$) δ 7.27 (dt, *J* = 8.7 Hz and 2.1 Hz, 2H), 6.86 (dt, *J* = 8.7 Hz and 2.1 Hz, 2H), 4.44 (s, 2H), 4.32 (d, *J* = 7.0 Hz, 1H), 3.79 (s, 3H), 3.73–3.39 (m, 3H), 2.64 (qd, *J* = 7.1, 5.2 Hz, 1H), 1.89 (q, *J* = 5.7 Hz, 1H), 1.42 (s, 6H), 1.15 (s, 6H), 1.11 (d, *J* = 7.1 Hz, 3H); ^{13}C NMR (75 MHz, $CDCl_3$) δ 174.1, 159.3, 130.4, 129.7, 113.8, 80.8, 72.9, 67.6, 57.1, 56.0, 55.4, 44.7, 33.1, 28.2, 23.0, 13.7.

(2*S*,3*S*)-*tert*-Butyl 3-((*R*)-1,1-dimethylethylsulfinamido)-5-hydroxy-2-methylpentanoate (S6)

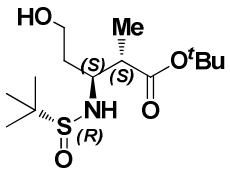

DDQ (49.0 mg, 0.21 mmol, 1.1 equiv) was added to a solution of the two PMB ethers obtained above [(88:12), (85 mg, 0.19 mmol)] in CH_2Cl_2 (5 mL) and water (0.25 mL). DDQ (5.0 mg, 0.02 mmol, 0.1 equiv) was added after 1 hour and the reaction quenched with sat. aq. $NaHCO_3$ (20 mL) after additionally 1 hour of stirring. The aqueous phase was extracted with CH_2Cl_2 (50 mL) and the organic phase washed with sat. aq. $NaHCO_3$ (20 mL), brine (20 mL), dried (Na_2SO_4), filtered and concentrated *in vacuo*. Purification by VLC afforded alcohol **S6** as a pure diastereomer (44 mg, 75%) as a colorless oil, which crystallized upon standing at room temperature. The spectral data were identical to the alcohol obtained from Table 9, entry 5 (**S2**). $[\alpha]_D$: –23.6° (*c* = 0.4, CH_2Cl_2).

3-((Triethylsilyl)oxy)propan-1-ol (2.25)

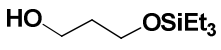

A solution of 1,3-propanediol (1.90 mL, 26.3 mmol, 1.05 equiv) in dry THF (10 mL) was added dropwise to a stirred suspension of NaH (1.0 g, 25.0 mmol, l.0 equiv, 60% in mineral oil) in dry THF (20 mL) under N_2. After 35 min triethylsilyl chloride (4.4 mL, 26.3 mmol, 1.05 equiv) in dry THF (8 mL) was added dropwise and the mixture stirred for 16 hours. After addition of sat. aq. $NaHCO_3$ (40 mL) the aqueous phase was extracted with EtOAc (70 mL) and ether (70 mL). The organic phases were washed with water (35 mL), dried with $MgSO_4$, filtered, and concentrated *in vacuo*. Purification by VLC afforded alcohol **2.25** as a colorless oil (0.51 g, 11%). Due to the poor stability of this compound in solution

at room temperature, it was used immediately after preparation. ^{1}H NMR (300 MHz, $CDCl_3$) δ 3.81 (m, 4H), 2.69 (bs, 1H), 1.77 (pentet, 5.8 Hz, 2H), 0.95 (t, *J* = 8.0 Hz, 9H), 0.61 (q, *J* = 8.0 Hz, 6H).

(S_R)-(*E*)-2-Methyl-N-(3-((triethylsilyl)oxy)propylidene)propane-2-sulfinamide (2.27)

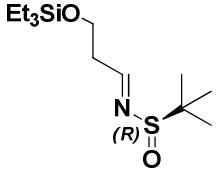

Dess-Martin periodinane reagent (1.28 g, 2.9 mmol, 1.1 equiv) was added to a stirred solution of alcohol **2.25** (0.51 g, 2.65 mmol) in dry CH_2Cl_2 (15 mL) under N_2. After 45 min the reaction was quenched with sat. aq. $Na_2S_2O_3$ (10 mL) and sat. aq. $NaHCO_3$ (10 mL). After stirring for 5 min the aqueous phase was extracted with CH_2Cl_2 (2 × 75 mL) and the combined organic layers were washed with sat. aq. $NaHCO_3$ (40 mL), brine (40 mL), dried ($MgSO_4$), filtered, and concentrated *in vacuo* to afford the crude aldehyde (465 mg, 93%) as a yellow oil, which was used without further purification. ^{1}H NMR (300 MHz, $CDCl_3$) δ 9.80 (t, *J* = 2.0 Hz, 1H), 3.97 (t, *J* = 6.1 Hz, 2H), 2.60 (td, *J* = 6.1 Hz and 2.0 Hz, 2H), 0.94 (t, *J* = 7.9 Hz, 9H), 0.59 (q, *J* = 7.9 Hz, 6H).

A solution of aldehyde (455 mg, 2.42 mmol) in dry CH_2Cl_2 (5 mL) was added dropwise to a solution of dry $CuSO_4$ (1.55 g, 9.68 mmol, 4.0 equiv) and (*R*)-(+)-2-methyl-2-propanesulfinamide (0.30 g, 2.42 mmol, 1 equiv) in dry CH_2Cl_2 (15 mL) under N_2. After stirring vigorously for 16 hours the mixture was added water (20 mL) and extracted with CH_2Cl_2 (2 × 40 mL). The combined organic phases were dried ($MgSO_4$), filtered, and concentrated *in vacuo*. VLC afforded *tert*-butanesulfinyl imine **2.27** as a clear oil (140 mg, 18%, two steps). ^{1}H NMR (300 MHz, $CDCl_3$) δ 8.08 (t, *J* = 4.8 Hz, 1H), 3.91 (t, *J* = 6.3 Hz, 2H), 2.72 (m, 2H), 1.17 (s, 9H), 0.93 (t, *J* = 8.0 Hz, 9H), 0.58 (q, *J* = 8.0 Hz, 6H). ^{13}C NMR (75 MHz, $CDCl_3$) δ 167.9, 59.3, 56.7, 39.6, 22.5, 6.9, 4.4.

(2*S*,3*S*)-*tert*-Butyl 3-((*R*)-1,1-dimethylethylsulfinamido)-2-methyl-5-((triethylsilyl)oxy)pentanoate (Table 2-2, entry 3, S7)

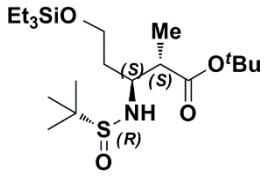

The general procedure was followed using imine **2.27** (140 mg, 0.48 mmol), *tert*-butyl propionate (181 μL, 1.20 mmol), LDA (1.3 M, 0.96 mL, 1.25 mmol) and Ti(O-*i*Pr)$_3$Cl (0.54 mL, 2.16 mmol). Diastereoselectivity was determined by ^{1}H NMR integration of the crude reaction mixture (75:21:4:0). Purification by VLC afforded **S7** as a pale yellow oil (83 mg, 41%) as well as a fraction containing a mixture of diasteromers (36 mg, 18%). Characterization data for the (2*S*,3*S*) diastereomer. ^{1}H NMR (300 MHz, $CDCl_3$) δ 4.26 (d, *J* = 6.9 Hz, 1H), 3.77 (m, 2H), 3.58 (pentet, *J* = 6.0 Hz, 1H), 2.71 (pentet, *J* = 6.6 Hz, 1H), 1.84 (m, 2H), 1.42 (s, 9H), 1.19 (s, 9H), 1.11 (d, *J* = 7.1 Hz, 3H), 0.94 (t, *J* = 7.9 Hz, 9H), 0.59 (q, *J* = 7.9 Hz, 6H). ^{13}C NMR (75 MHz, $CDCl_3$) δ 174.2, 80.7, 60.5, 57.11, 56.0, 44.4, 35.9, 28.2, 23.0, 13.8, 6.9, 4.4. HRMS (ESI-TOF): *m/z* calcld. for $C_{20}H_{43}NO_3SSiNa^+$: 444.2564; found: 444.2574 $[M+Na]^+$.

(2*S*,3*S*)-*tert*-Butyl 3-((*R*)-1,1-dimethylethylsulfinamido)-5-hydroxy-2-methylpentanoate (S2)

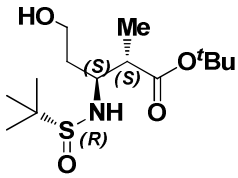

Acetic acid (10.7 μL, 0.19 mmol, 1.0 equiv) followed by TBAF (1.0 M, 0.38 mL, 0.38 mmol, 2.0 equiv) was added to a stirred solution of silyl ether **S7** (79.0 mg, 0.19 mmol) in dry THF (6.0 mL) at 0 °C under N_2. After stirring for 20 min the mixture was concentrated and purification by VLC afforded the alcohol (48 mg, 83%) as a clear oil, which can be crystallized from ethyl acetate and hexane. $[\alpha]_D$: –28.6° (*c* = 0.4, CH_2Cl_2); mp 62–64 °C. The spectral data were identical to those of the alcohol obtained from Table 9, entry 5 (**S2**).

(S_S)-(*E*)-2-Methyl-N-(3-((triisopropylsilyl)oxy)propylidene)propane-2-sulfinamide (2.35)

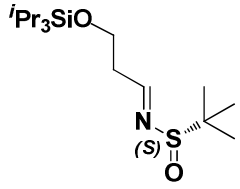

A solution of DMSO (1.0 mL, 14.1 mmol, 3.2 equiv) in dry CH_2Cl_2 (5 mL) was added dropwise to a solution of oxalylchloride (0.63 ml, 7.0 mmol, 1.6 equiv) in dry CH_2Cl_2 (25 mL) at –78 °C. After stirring for 30 min, a solution of alcohol **2.13** (1.0 g, 4.3 mmol) in dry CH_2Cl_2 (5.0 mL) was added dropwise. After 30 min Et_3N (3.1 mL, 22.4 mmol, 5.2 equiv) was added and after stirring for 10 min at –78 °C, the cooling was removed and the mixture allowed to warm to room temperature. EtOAc (75 mL) was added and the organic phase was washed with sat. aq. NH_4Cl (30 mL) and brine (30 mL). The organic phase was concentrated *in vacuo* and the residue was pulled through a short plug of silica gel to afford the crude aldehyde as a colorless oil (0.89 g, 90%), which was used without further purification.

A solution of aldehyde (0.89 g, 3.9 mmol) in dry CH_2Cl_2 (3.0 mL) was added dropwise to a solution of dried $CuSO_4$ (4.0 g, 18.6 mmol, 4.5 equiv) and (*S*)-(–)-2-methyl-2-propanesulfinamide (0.50 g, 4.1 mmol, 1.05 equiv) in dry CH_2Cl_2 (22 mL). After stirring vigorously for 22 hours $CuSO_4$ (1.0 g, 6.3 mmol, 1.6 equiv) was added and after additionally 2 hours of stirring the mixture was filtered and the solids washed with CH_2Cl_2 (250 mL). The filtrate was washed with water (40 mL), brine (40 mL), dried (Na_2SO_4), and concentrated *in vacuo*. Purification by VLC afforded *tert*-butanesulfinyl imine **2.35** as a colorless oil (0.95 g, 62%, two steps). $[\alpha]_D$: +155° (c = 0.5, CH_2Cl_2); ^{1}H NMR (300 MHz, $CDCl_3$) δ 8.11 (td, *J* = 4.8, 1.0 Hz, 1H), 4.00 (t, *J* = 6.3 Hz, 2H), 2.74 (q, *J* = 5.7 Hz, 2H), 1.18 (d, *J* = 1.1 Hz, 9H), 1.03 (m, 21H).^{13}C NMR (75 MHz, $CDCl_3$) δ 168.1, 60.1, 56.7, 39.8, 22.5, 18.1, 12.0. HRMS (ESI-TOF): *m/z* calcld. for $C_{16}H_{35}NO_2SSiH^+$: 334.2237; found: 334.2239 $[M+H]^+$.

(2*R*,3*R*)-*tert*-Butyl-3-((*S*)-1,1-dimethylethylsulfinamido)-2-methyl-5-((triisopropylsilyl)oxy)pentanoate (2.37)

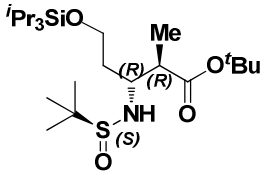

The general procedure was followed using imine **2.35** (0.47 g, 1.4 mmol), *tert*-butyl propionate (0.53 mL, 3.5 mmol), LDA (1.8 M, 2.8 mL, 3.6 mmol) and Ti(O-*i*Pr)$_3$Cl (1.6 mL, 6.3 mmol, 4.5 equiv). The diastereomeric ratio was determined by ^{1}H NMR integration of the crude reaction mixture (77:18:5:0). Purification by VLC afforded **2.37** as a colorless oil (0.35 g, 54%) as well as a fraction containing a mixture of diasteromers (0.26 g, 40%). Characterization data for the (2*R*,3*R*) diastereomer. $[\alpha]_D$: +33.4° (*c* = 0.6, CH_2Cl_2); ^{1}H NMR (300 MHz, $CDCl_3$) δ 4.06 (d, *J* = 8.0 Hz, 1H), 3.85 (m, 2H), 3.56 (pentet, *J* = 6.4 Hz, 1H), 2.74 (dd, *J* = 7.1 Hz and 5.0 Hz, 1H), 1.95 (m, 1H), 1.83 (m, 1H), 1.43 (s, 9H), 1.20 (s, 9H), 1.14 (d, *J* = 7.1 Hz, 3H), 1.05 (m, 21H). ^{13}C NMR (75 MHz, $CDCl_3$) δ 174.4, 80.8, 60.9, 57.4, 56.2, 44.4, 36.9, 28.2, 23.0, 18.2, 14.5, 12.0. HRMS (ESI-TOF): *m/z* calcld. for $C_{23}H_{49}NO_4SSiH^+$: 464.3231; found: 464.3255 $[M+H]^+$.

(*E*)-((1-(tert-butoxy)prop-1-en-1-yl)oxy)(tert-butyl)dimethylsilane (2.47)

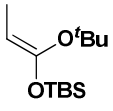

To a solution of LDA (36.7 mL, 55 mmol, 1.1 equiv) in dry THF (15 mL) was added *tert*-butyl propionate (7.5 mL, 55 mmol) over 10 min at –78 °C. After 5 min a solution of TBSCl (8.6 g, 55 mmol, 1.1 equiv) in THF–HMPA (1:1, 16 mL) was added over 5 min. After additional 5 min the cooling bath was removed and the mixture was stirred for 30 min. The reaction mixture was diluted with pentane (200 mL) and extracted with water (3 × 100 mL) and brine (100 mL). The organic phase was dried (Na_2SO_4), filtered, and concentrated *in vacuo* to afford the crude silyl ether. The (*E*:*Z*) ratio in the crude was determined by ^{1}H NMR to be (91:9). Purification by distillation afforded a mixture of the *E* and *Z*-silyl ethers (91:9, 5.7 g, 47%). Characterization of the major isomer: ^{1}H NMR (300 MHz, $CDCl_3$) δ 3.93 (q, *J* = 6.6 Hz, 1H),

1.49 (d, *J* = 6.6 Hz, 3H), 1.32 (s, 9H), 0.92 (s, 9H), 0.15 (s, 6H); ^{13}C NMR (75 MHz, $CDCl_3$) δ 152.4, 86.2, 78.5, 29.3, 25.7, 18.2, 11.1, –4.6.

(*Z*)-((1-(tert-butoxy)prop-1-en-1-yl)oxy)(tert-butyl)dimethylsilane (2.46)

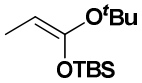

To a solution of LDA (37.0 mL, 55 mmol, 1.1 equiv) in a combination of dry THF (37 mL) and HMPA (23 mL, 23%) was added *tert*-butyl propionate (7.5 mL, 55 mmol) over 10 min at –78 °C. After 5 min a solution of TBSCl (8.6 g, 55 mmol, 1.1 equiv) in hexane (15 mL) was added over 5 min. After additional 5 min the cooling bath was removed and the mixture was stirred for 30 min. The reaction mixture was diluted with pentane (200 mL) and extracted with water (3 × 100 mL) and brine (100 mL). The organic phase was dried (Na_2SO_4), filtered and concentrated *in vacuo* to afford the crude silyl ether. Purification by distillation afforded a mixture of the *E* and *Z*-silyl ethers (18:82, 8.8 g, 70%). Characterization of the major isomer: ^{1}H NMR (300 MHz, $CDCl_3$) δ 3.97 (q, *J* = 6.7 Hz, 1H), 1.49 (d, *J* = 6.7 Hz, 3H), 1.28 (s, 9H), 0.95 (s, 9H), 0.16 (s, 6H); ^{13}C NMR (75 MHz, $CDCl_3$) δ 151.8, 87.2, 78.4, 29.3, 28.7, 18.2, 10.7, –4.0.

(2*S*,3*R*)-*tert*-Butyl-3-((*S*)-1,1-dimethylethylsulfinamido)-2-methyl-5-((triisopropylsilyl)oxy)pentanoate (2.42)

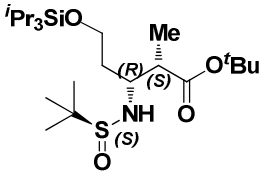

A solution of LDA (1.3 M in THF, 6.4 mL, 8.3 mmol, 2.8 equiv) was added over 10 minutes to a solution of HMPA (3.0 mL, 17.2 mmol, 5.7 equiv) in dry THF (10 mL) at –78 °C. After 10 minutes *tert*-butyl propionate (1.2 mL, 7.6 mmol, 2.5 equiv) was added dropwise. The resulting enolate solution was stirred for 45 minutes before adding the imine **2.35** (1.0 g, 3.0 mmol) in dry THF (2.0 mL) over 15 minutes. After 30 minutes TLC showed full conversion of the imine, and the mixture was quenched with sat. aq. NH_4Cl and allowed to warm up to room temperature. Water (30 mL) was added and the mixture extracted with EtOAc (2 × 100 mL). The combined organic phases were washed with 1 M HCl (50 mL) and the aqueous phase re-extracted with EtOAc (100 mL). The combined organic phases were washed with brine (75 mL), dried ($MgSO_4$), filtered, and concentrated *in vacuo*. Diastereoselectivity was determined by ^{1}H NMR integration of the crude reaction mixture (64:25:8:2). Purification by VLC afforded the pure (2*S*,3*R*) diastereomer **2.42** as a clear oil (0.74 g, 52%) as well as a fraction containing a mixture of diasteromers (0.23 g, 16%). Characterization data for the (2*S*,3*R*) diastereomer. $[\alpha]_D$: +42.2° (c = 0.8, CH_2Cl_2); ^{1}H NMR (300 MHz, $CDCl_3$) δ 3.91 (m, 1H), 3.83 (dt, *J* = 10.5 Hz and 5.3 Hz, 1H), 3.72 (m, 2H), 2.63 (dd, *J* = 7.0 Hz and 5.2 Hz, 1H), 1.86 (m, 2H), 1.43 (m, 9H), 1.18 (s, 9H), 1.11 (d, *J* = 7.0 Hz, 3H), 1.05 (m, 21H). ^{13}C NMR (75 MHz, $CDCl_3$) δ 173.9, 80.6, 60.6, 57.3, 56.1, 45.2, 36.5, 28.2, 23.0, 18.2, 12.8, 12.0. HRMS (ESI-TOF): *m/z* calcld. for $C_{23}H_{49}NO_4SSiH^+$: 464.3231; found: 464.3250 $[M+H]^+$.

(2*S*,3*S*)-*tert*-Butyl 3-((*R*)-1,1-dimethylethylsulfinamido)-5-hydroxy-2-methylpentanoate (S2)

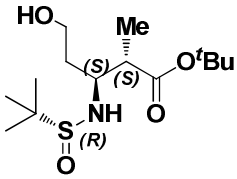

TBAF (1.0 M, 1.75 mL, 1.75 mmol, 1.2 equiv) was added over 10 min to a stirred solution of silyl ether **S1** (0.68 g, 1.46 mmol) in THF (20 mL) at 0 °C under N_2. After stirring for 10 min the mixture was concentrated and purification by VLC afforded alcohol **S2** (341 mg, 76%) as a clear oil, which can be crystallized from EtOAc and hexane. $[\alpha]_D$: –28.6° (c = 0.4 ,CH_2Cl_2); mp 62–64 °C; ^{1}H NMR (300 MHz, $CDCl_3$) δ 3.95 (d, *J* = 8.4 Hz, 1H), 3.88 (d, *J* = 6.5 Hz, 1H), 3.81 (m, 2H), 3.56 (tdd, *J* = 10.1 Hz, 6.8 Hz and, 3.9 Hz, 1H), 2.49 (qd, *J* = 7.1 Hz and 5.0 Hz, 1H), 1.94–1.62 (m, 3H), 1.44 (s, 9H), 1.24 (s, 9H), 1.15 (d, *J* = 7.1 Hz, 3H). ^{13}C NMR (75 MHz, $CDCl_3$) δ 173.9, 80.9, 59.8, 58.3, 56.4, 46.4, 36.4, 28.3, 23.0, 14.7; HRMS (ESI-TOF): *m/z* calcld. for $C_{14}H_{29}NO_4SH^+$: 308.1896; found: 308.1889 $[M+H]^+$.

(2*S*,3*S*)-*tert*-Butyl 3-((*R*)-1,1-dimethylethylsulfinamido)-2-methyl-5-oxopentanoate (S3)

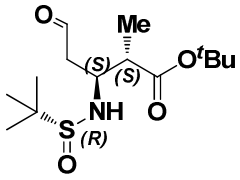

$NaHCO_3$ (86.5 mg, 1.0 mmol, 1.4 equiv) and Dess-Martin periodinane reagent (0.44 g, 1.0 mmol, 1.4 equiv) were added to a stirred solution of alcohol **S2** (221 mg, 0.72 mmol) in dry CH_2Cl_2 (8 mL) at 0 °C under N_2. Additional $NaHCO_3$ (18 mg, 0.2 mmol, 0.3 equiv) and Dess-Martin periodinane reagent (66 mg, 0.16 mmol, 0.2 equiv) were added after 15 min and after stirring for additionally 25 min, sat. aq. $Na_2S_2O_3$ (5 mL) and sat. aq. $NaHCO_3$ (10 mL) was added and the aqueous phase was extracted with CH_2Cl_2 (2 × 50 mL). The combined organic layers were washed with sat. aq. $NaHCO_3$ (35 mL) and brine (35 mL), dried (Na_2SO_4), filtered, and concentrated *in vacuo* to afford aldehyde **S3** (224 mg) as a clear oil, which was used without further purification. ^{1}H NMR (300 MHz, $CDCl_3$) δ 9.75 (t, *J* = 0.9 Hz, 1H), 4.20 (d, *J* = 10.0 Hz, 1H), 3.77 (m, 1H), 3.27–2.81 (m, 3H), 3.08 (ddd, *J* = 18.5 Hz, 5.1 Hz, and 1.1 Hz, 1 H) 2.72 (m, 1 H) 1.42 (s, 9H), 1.19 (s, 9H), 1.16 (d, *J* = 7.2 Hz, 3H). ^{13}C NMR (75 MHz, $CDCl_3$) δ 200.5, 174.0, 81.3, 56.6, 54.8, 48.5, 44.6, 28.2, 22.8, 15.4; HRMS (ESI-TOF): *m/z* calcld. for $C_{14}H_{27}NO_4SH^+$: 306.1740; found: 306.1734 $[M+H]^+$.

(7*S*,8*S*)-(*Z*)-9-*tert*-Butyl 1-ethyl 7-((*R*)-1,1-dimethylethylsulfinamido)-8-methylnon-4-enedioate (S4)

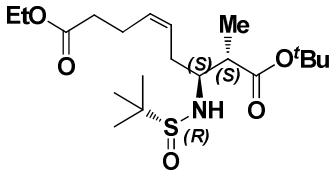

A flame dried round-bottomed flask was charged with (4-ethoxy-4-oxobutyl)triphenylphosphonium bromide (0.68 g, 1.5 mmol, 2.0 equiv) and the Wittig reagent was dried under high vacuum for 18 hours. The Wittig reagent was dissolved in dry THF (10 mL) under argon and cooled to –78 °C. KHMDS (0.5 M, 2.75 mL, 1.4 mmol) was added dropwise and the resulting orange solution was stirred for 30 min before the crude aldehyde **S3** (219 mg, 0.72 mmol) in dry THF (2.0 mL) was added dropwise. After 1 h at –78 °C the mixture was allowed to reach room temperature and water (30 mL) was added. The aqueous phase was extracted with EtOAc (2 × 60 mL). The combined organic layers were washed with brine (35 mL), dried ($MgSO_4$), filtered, and concentrated *in vacuo*. Purification by VLC afforded alkene **S4** as a clear oil (158 mg, 56%, 2 steps). $[\alpha]_D$: –32.8° (c = 0.4, CH_2Cl_2); ^{1}H NMR (300 MHz, $CDCl_3$) δ 5.55–5.35 (m, 2H), 4.10 (q, *J*= 7.2 Hz, 2H), 3.82 (d, *J* = 8.6 Hz, 1H), 3.34 (pentet, *J* = 6.12 Hz, 1H), 2.65–2.28 (m, 7H), 1.43 (s, 9H), 1.23 (t, *J* = 7.1 Hz, 3H), 1.20 (s, 9H), 1.14 (d, *J* = 7.2 Hz, 3H). ^{13}C NMR (75 MHz, $CDCl_3$) δ 174.1, 173.1, 131.3, 126.3, 81.0, 60.4, 59.4, 56.3, 43.7, 34.2, 32.5, 28.2, 23.0, 22.9, 14.8, 14.4; HRMS (ESI-TOF): *m/z* calcld. for $C_{20}H_{37}NO_5SH^+$: 404.2471; found: 404.2464 $[M+H]^+$.

(2*S*,3*S*)-(*Z*)-3-((*tert*-Butoxycarbonyl)amino)-9-ethoxy-2-methyl-9-oxonon-5-enoic acid (2.31)

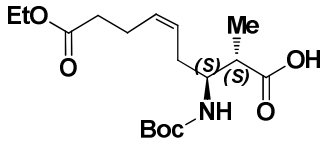

TFA (5 mL) was added to a solution of *tert*-butyl ester **S4** (153 mg, 0.38 mmol) in dry CH_2Cl_2 (5 mL) under argon. After stirring for 1 hour the mixture was concentrated and TFA was removed by co-evaporation with CH_2Cl_2–toluene (1:1, 3 × 10 mL) to afford a mixture of the *N*-sulfinyl protected β-amino acid and the β-amino acid containing the free amine (151 mg). To a solution of this crude mixture (151 mg, 0.38 mmol) in dioxane (5 mL) and water (0.10 mL) was added HCl (4.0 M in dioxane, 0.14 mL, 0.56 mmol, 1.5 equiv). Additional HCl was added after 50 min (4.0 M, 0.30 mL, 1.2 mmol, 3.2 equiv) and after 70 min (4.0 M, 0.15 mL, 0.6 mmol, 1.6 equiv). After stirring for 15 min after the last addition of HCl, TLC showed full conversion and the mixture was concentrated to afford the deprotected β-amino acid chloride salt (137 mg) as a yellow oil. The crude residue was dried under high vacuum for 16 hours. To a solution of the crude residue (106 mg, 0.38 mmol) in dry CH_2Cl_2 (6 mL) was added Boc_2O (118 mg, 0.54 mmol, 1.4 equiv) in dry CH_2Cl_2 (1.0 mL)

followed by *i*Pr_2NEt (90 μL, 0.52 mmol, 1.4 equiv) and the mixture was stirred under argon for 16 hours. To ensure complete protection af the amino group, additional Boc_2O (19 mg, 0.09 mmol, 0.2 equiv) and *i*Pr_2NEt (15 μL, 0.09 mmol, 0.2 equiv) were added, and after stirring for 1 h the reaction mixture was concentrated *in vacuo.* Purification by VLC (0.2% acetic acid in the eluent) afforded the β-amino acid **2.31** (79.4 mg, 61%, 3 steps) as a yellow oil after co-evaporation of residual acetic acid with CH_2Cl_2–toluene (1:1, × 3). $[\alpha]_D$: +12.3° (c = 1, CH_2Cl_2); ^{1}H NMR (300 MHz, $CDCl_3$) δ 5.41 (m, 2H), 5.27 (d, *J* = 9.6 Hz, 1H), 4.11 (q, *J* = 7.1 Hz, 2H), 3.78 (m, 1H), 2.74 (m, 1H), 2.19 (m, 6H), 1.42 (s, 9H) 1.24 (m, 6H). ^{13}C NMR (75 MHz, $CDCl_3$) δ 180.0, 173.5, 156.1, 130.5, 126.8, 79.4, 60.6, 52.6, 42.2, 34.1, 31.5, 28.5, 22.9, 14.7, 14.33; HRMS (ESI-TOF): *m/z* calcld. for $C_{17}H_{29}NO_6Na^+$: 366.1893; found: 366.1881 $[M+Na]^+$.

(2*R*,5*R*,8*S*,11*S*,12*S*)-(*Z*)-12-Amino-2-benzyl-8-isopropyl-5,11-dimethyl-4,7,10,18-tetraoxo-19-oxa-3,6,9-triazahenicos-14-en-1-oic acid (2.54)

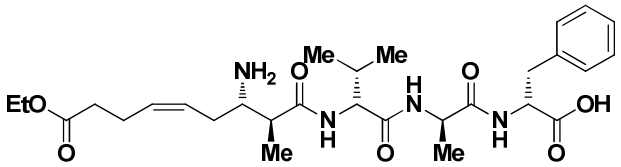

Polystyrene 2-chlorotrityl-bound Fmoc-(D)Val–(D)Ala–(D)Phe (246 mg, 0.081 mmol) was added to a fritted syringe and the Fmoc group was removed with piperidine–DMF (1:4, 4 mL, 2 × 25 min) and DBU–piperidine–DMF (2:2:96, 4 mL, 25 min). The resin was then washed with DMF (×3), MeOH (×3), CH_2Cl_2 (×3). β-Amino acid **2.31** (41.5 mg, 0.12 mmol, 1.5 equiv) in DMF (2.2 mL) was preincubated for 5 min with 2,6-lutidine (28 μL, 0.24 mmol, 3.0 equiv) and HATU (46.3 mg, 0.12 mmol, 1.5 equiv) before addition to the resin and the reaction was allowed to proceed on a rocking table for 16 hours. After washing [DMF (×3), MeOH (×3), CH_2Cl_2 (×3)] the resin was treated with TFA–CH_2Cl_2 (1:1, 4 mL) for 1 h followed by washing with CH_2Cl_2 (2 × 5 mL). A fresh portion of TFA–CH_2Cl_2 (1:1, 4 mL) was added to the resin and after additional 30 min the resin was drained and all the fractions were pooled and concentrated *in vacuo* to provide the linear peptide as an oily residue. Precipitation with diethyl ether afforded the TFA salt of the linear peptide **2.54** (52.3 mg, 96%) as a pale yellow solid.

^{1}H NMR (300 MHz, DMSO) δ 8.29 (d, *J* = 8.4 Hz, 1H), 8.14 (d, *J* = 7.9 Hz, 1H), 7.97 (d, *J* = 7.2 Hz, 1H), 7.75 (bs, 2H), 7.23 (m, 5H), 5.45 (m, 2H), 4.43 (m, 1H), 4.31 (t, *J* = 7.3 Hz, 1H), 4.19 (dd, *J* = 8.5, 6.2 Hz, 1H), 4.04 (q, *J* = 7.0 Hz, 2H), 3.18 (m, 1H), 3.02 (dd, *J* = 14.2, 5.0 Hz, 1H), 2.92 (dd, *J* = 14.2; 8.8 Hz, 1H), 2.86 (m, 1H), 2.42 (m, 1H), 2.38 (m, 1H), 2.24 (m, 1H), 1.97 (m, 1H), 1.16 (m, 9H), 0.83 (d, *J* = 7.4 Hz, 3H), 0.80 (d, *J* = 7.0 Hz, 3H). HRMS (ESI-TOF): *m/z* calcld. for $C_{29}H_{44}N_4O_7H^+$: 561.3283 found: 561.3286 $[M+H]^+$.

(*Z*)-Ethyl-6-((2*R*,5*R*,8*R*,11*S*,12*S*)-8-benzyl-2-isopropyl-5,12-dimethyl-3,6,9,13-tetraoxo-1,4,7,10-tetraazacyclotridecan-11-yl)hex-4-enoate (2.55)

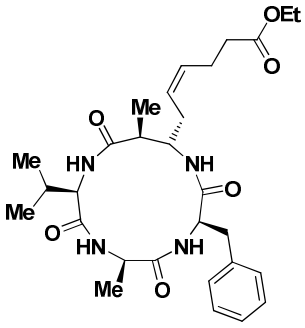

The linear peptide **2.54** (50.8 mg, 0.075 mmol) was dissolved in DMF (110 mL ≈ 0.7 mM) and *i*Pr_2NEt (131 μL, 0.75 mmol, 10 equiv) and HATU (43.7 mg, 0.11 mmol, 1.5 equiv) were added. The solution was stirred for 16 hours and the reaction mixture was concentrated to a small volume and transferred to a centrifugation tube, where precipitation with diethyl ether afforded the crude cyclic peptide **2.55** (66 mg) as a brown solid, which was used without further purification. HPLC gradient A, t_R = 1.69 min.

(*Z*)-6-((2*R*,5*R*,8*R*,11*S*,12*S*)-8-Benzyl-2-isopropyl-5,12-dimethyl-3,6,9,13-tetraoxo-1,4,7,10-tetraazacyclotridecan-11-yl)hex-4-enoic acid (2.56)

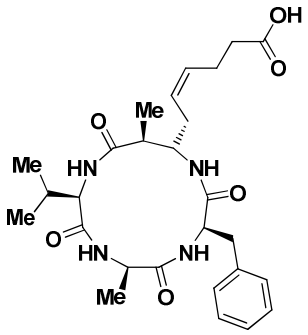

LiOH (40 mg, 1.67 mmol, 21 equiv) in water (5 mL) was added to the cyclic peptide **2.55** (44 mg, 0.081 mmol) in THF (5 mL) and the solution was stirred for 16 hours. The mixture was concentrated and aqueous HCl (1.0 M, 5 mL) was added, followed by extraction with EtOAc (200 mL + 50 mL). The combined organic phases were dried ($MgSO_4$), filtered, and concentrated. The crude residue was dissolved in DMF–MeCN (8:2, 1.0 mL) and purified by preparative HPLC to afford epi-β^3-azumamide E **2.56** (2.1 mg, 5%, 4 steps) as a white solid. $[\alpha]_D$: +60.0° (*c* = 0.1, MeOH); ^{1}H NMR (500 MHz, DMSO) δ 7.95 (bs, 2H), 7.59 (bs, 1H), 7.25 (m, 2H), 7.18 (m, 3H), 6.31 (bs, 1H), 5.35 (m, 1H), 5.26 (m, 1H), 4.45 (bs, 1H), 3.99 (bs, 1H), 3.88 (m, 2H), 3.38 (dd, *J* = 13.8, 3.9 Hz, 1H), 2.68 (dd, *J* = 13.8, 11.0 Hz, 1H), 2.53 (m, 1H), 2.21 (m, 6H), 2.10 (m, 1H), 1.12 (d, *J* = 7.2 Hz, 3H), 1.06 (d, *J* = 7.3 Hz, 3H), 0.93 (d, *J* = 6.4 Hz, 3H), 0.87 (d, *J* = 6.3 Hz, 3H); HRMS (ESI-TOF): *m/z* calcld. for $C_{27}H_{38}N_4O_6H^+$: 515.2870; found: 515.2882 $[M+H]^+$. HPLC gradient C, t_R = 12.34 min (>95%).

(2*R*,3*R*)-*tert*-Butyl 3-((*S*)-1,1-dimethylethylsulfinamido)-5-hydroxy-2-methylpentanoate (2.38)

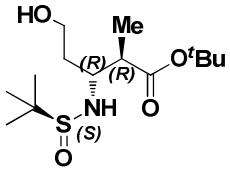

TBAF (1.0 M, 1.49 mL, 1.49 mmol, 2.0 equiv) was added over 10 min to a stirred solution of silyl ether **2.37** (0.35 g, 0.74 mmol) and AcOH (43 μL, 0.74 mmol, 1.0 equiv) in THF (20 mL) at 0 °C under N_2. After stirring for 30 min the cooling was removed and the mixture was stirred for 1 hour at room temperature before concentration and purification by VLC afforded alcohol **2.38** (208 mg, 91%) as clear oil, which can be crystallized from ethyl acetate and hexane to give needle shaped crystals. $[\alpha]_D$: +21.3° (*c* = 0.5, CH_2Cl_2); mp 66–67 °C; ^{1}H NMR (300 MHz, $CDCl_3$) δ 3.91 (d, *J* = 8.6 Hz, 1H), 3.83 (m, 2H), 3.56 (m, 1H), 2.49 (qd, *J* = 7.1 Hz and 5.1 Hz, 1H), 1.77 (m, 2H), 1.44 (s, 9H), 1.25 (s, 9H), 1.15 (d, *J* = 7.1 Hz, 3H). ^{13}C NMR (75 MHz, $CDCl_3$) δ 173.8, 80.8, 59.8, 58.3, 56.4, 46.3, 36.3, 28.2, 23.0, 14.6. HRMS (ESI-TOF): *m/z* calcld. for $C_{14}H_{29}NO_4SH^+$: 308.1896; found: 308.1893 $[M+H]^+$.

(7*R*,8*R*)-(*Z*)-9-*tert*-Butyl 1-ethyl 7-((*S*)-1,1-dimethylethylsulfinamido)-8-methylnon-4-enedioate (2.40)

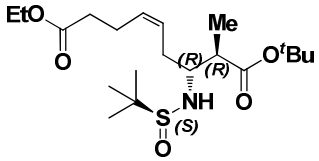

$NaHCO_3$ (84 mg, 1.0 mmol, 1.5 equiv) and Dess-Martin periodinane reagent (438 mg, 1.0 mmol, 1.5 equiv) were added to a stirred solution of alcohol **2.38** (205 mg, 0.67 mmol) in dry CH_2Cl_2 (8.0 mL) at 0 °C under N_2. After 30 min, the mixture was allowed to warm to room temperature and after stirring for 1 hour, sat. aq. $Na_2S_2O_3$ (10 mL) and sat. aq. $NaHCO_3$ (10 mL) were added and the aqueous phase was extracted with CH_2Cl_2 (2 × 35 mL). The combined organic layers were washed with sat. aq. $NaHCO_3$ (30 mL) and brine (30 mL), dried (Na_2SO_4), filtered, and concentrated *in vacuo* to afford aldehyde **2.39** (186 mg, 91%) as a pale yellow oil, which was used immediately without further purification.

A flame dried round-bottomed flask was charged with (4-ethoxy-4-oxobutyl)triphenylphosphonium bromide (0.64 g, 1.34 mmol, 2.0 equiv) and the Wittig reagent dried under high vacuum for 30 hours. The Wittig reagent was then dissolved in dry THF (10 mL) under argon and cooled to –78 °C. KHMDS (0.5 M, 2.5 mL, 1.3 mmol, 1.9 equiv) was added dropwise and the resulting orange solution was stirred for 30 min before crude aldehyde **2.39** (186 mg, 0.68 mmol) in dry THF (3.0 mL) was added dropwise. The mixture was allowed to warm to room temperature and after 16 hours, water (20 mL) was added. The aqueous phase was extracted

with EtOAc (2 × 60 mL) and the combined organic layers were washed with brine (35 mL), dried (Na_2SO_4), filtered, and concentrated *in vacuo*. Purification by VLC afforded alkene **2.40** as a pale yellow oil (158 mg, 59%, 2 steps). $[\alpha]_D$: +29.9° (*c* = 1, CH_2Cl_2); ^{1}H NMR (300 MHz, $CDCl_3$) δ 5.49 (m, 1H), 5.43 (m, 1H), 4.10 (q, *J* = 7.2 Hz, 2H), 3.82 (d, *J* = 8.6 Hz, 1H), 3.34 (pentet, *J* = 7.1 Hz, 1H), 2.60 (qd, *J* = 7.2 Hz and 5.0 Hz, 1H), 2.52–2.26 (m, 6H), 1.43 (s, 9H), 1.23 (t, *J* = 7.1 Hz, 1H), 1.20 (s, 9H), 1.15 (d, *J* = 7.2 Hz, 1H). ^{13}C NMR (75 MHz, CDCl3) δ 174.1, 173.1, 131.3, 126.3, 81.0, 60.5, 59.4, 56.3, 43.7, 34.2, 32.5, 28.2, 23.0, 22.9, 14.8, 14.4. HRMS (ESI-TOF): *m/z* calcld. for $C_{20}H_{37}NO_5SH^+$: 404.2471; found: 404.2497 $[M+H]^+$.

(2*R*,3*R*)-(*Z*)-3-((*tert*-Butoxycarbonyl)amino)-9-ethoxy-2-methyl-9-oxonon-5-enoic acid (2.41)

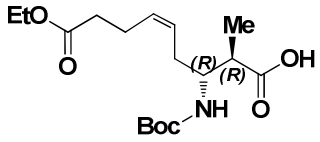

HCl in dioxane (4.0 M, 0.48 mL, 1.9 mmol, 5.0 equiv) was added to a solution of alkene **2.40** (155 mg, 0.38 mmol) and water (0.1 mL) in 1,4-dioxane (8.0 mL). After 55 minutes TFA (2.0 mL) was added and after stirring for 5 hours the mixture was concentrated and TFA/CH_2Cl_2 (1:1, 10 mL) and water (0.1 mL) was added. After stirring for 16 hours the solution was concentrated and TFA was removed by co-evaporation with toluene–hexane (1:1, 3 × 10 mL) to afford the crude β-amino acid (155 mg).

To a solution of the crude β-amino acid (155 mg) and *i*Pr_2NEt (0.21 mL, 1.2 mmol, 3.0 equiv) in dry CH_2Cl_2 (5.0 mL) was added Boc_2O (173 mg, 0.77 mmol, 2.0 equiv) in dry CH_2Cl_2 (1.0 mL) under argon. After 2.5 hours the reaction mixture was concentrated and *i*Pr_2NEt was removed by co-evaporation with toluene. Purification of the crude residue by VLC (0.2% acetic acid in the eluent) afforded β-amino acid **2.41** (80.2 mg, 61%, 3 steps) as a clear oil after co-evaporation of residual acetic acid with CH_2Cl_2–toluene (1:1, × 3). $[\alpha]_D$: –19.5° (*c* = 0.2, CH_2Cl_2); ^{1}H NMR (300 MHz, $CDCl_3$) ^{1}H NMR (300 MHz, $CDCl_3$) δ 5.59–5.32 (m, 1H), 5.25 (d, *J* = 9.5 Hz, 1H), 4.12 (q, *J* = 7.1 Hz, 1H), 3.78 (s, 1H), 2.84–2.60 (m, 1H), 2.49–2.12 (m, 3H), 1.42 (s, 5H), 1.30–1.16 (m, 3H). ^{13}C NMR (75 MHz, $CDCl_3$) δ 180.3, 173.5, 156.1, 130.6, 126.8, 79.4, 60.6, 52.6, 42.3, 34.1, 31.5, 28.5, 22.9, 14.7, 14.4. HRMS (ESI-TOF): *m/z* calcld. for $C_{17}H_{29}NO_6H^+$: 344.2070; found: 344.2080 $[M+H]^+$.

(2*R*,5*R*,8*S*,11*R*,12*R*)-(*Z*)-12-Amino-2-benzyl-8-isopropyl-5,11-dimethyl-4,7,10,18-tetraoxo-19-oxa-3,6,9-triazahenicos-14-en-1-oic acid (2.57)

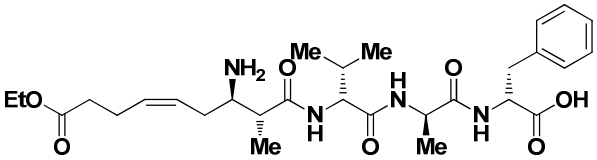

Polystyrene 2-chlorotrityl-bound Fmoc-(D)Val–(D)Ala–(D)Phe (201 mg, 0.10 mmol, 1.5 equiv) was added to a fritted syringe and swelled with CH_2Cl_2 before the Fmoc group was removed with piperidine–DMF (1:4, 4 mL, 2 × 25 min) and DBU–piperidine–DMF (2:2:96, 4 mL, 30 min). The resin was then washed with DMF (×3), MeOH (×3), CH_2Cl_2 (×3).

β-Amino acid **2.41** (22.8 mg, 0.067 mmol) in DMF (2.0 mL) was preincubated for 5 min with 2,6-lutidine (23.1 μL, 0.20 mmol, 3.0 equiv) and HATU (38 mg, 0.10 mmol, 1.5 equiv) and added to the resin. The reaction was allowed to proceed on a rocking table for 16 hours. After washing [DMF (×3), MeOH (×3), CH_2Cl_2 (×3)] the resin was treated with TFA–CH_2Cl_2 (1:1, 4 mL) for 30 min followed by washing with CH_2Cl_2 (5 mL). A fresh portion of TFA–CH_2Cl_2 (1:1, 4 mL) was added to the resin and after additional 30 min the resin was drained, washed with CH_2Cl_2 (5 mL) and all the fractions were pooled and concentrated *in vacuo* to provide the crude linear peptide **2.57** as an oily residue (56.4 mg), which was used without further purification. UPLC-MS gradient B, t_R = 1.46 min.

(*Z*)-Ethyl-6-((2*R*,5*R*,8*R*,11*R*,12*R*)-8-benzyl-2-isopropyl-5,12-dimethyl-3,6,9,13-tetraoxo-1,4,7,10-tetraazacyclotridecan-11-yl)hex-4-enoate (2.58)

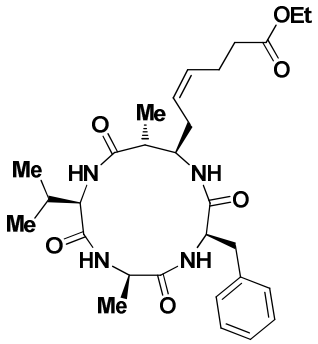

The crude linear peptide **2.57** (54.6 mg, 0.07 mmol) was dissolved in DMF (200 mL ≈ 0.33mM) and *i*Pr_2NEt (116 μL, 0.66 mmol, 10 equiv) and HATU (51 mg, 0.13 mmol, 2.0 equiv) were added. The solution was stirred for 16 hours and the reaction mixture was concentrated and added EtOAc (200 mL) which afforded a white precipitate (HOAt). The EtOAc was decanted off, washed with aq. HCl (1.0 M, 3 × 10 mL), and concentrated to afford the crude cyclic peptide **2.58** (95 mg) as a brown oil, which was used without further purification.

(*Z*)-6-((2*R*,5*R*,8*R*,11*R*,12*R*)-8-Benzyl-2-isopropyl-5,12-dimethyl-3,6,9,13-tetraoxo-1,4,7,10-tetraazacyclotridecan-11-yl)hex-4-enoic acid (2.59)

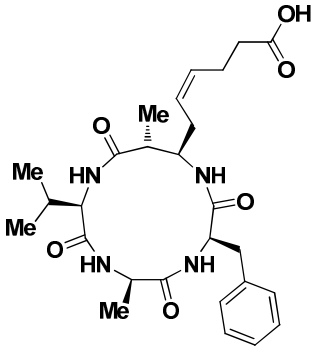

LiOH (56 mg, 2.32 mmol, 35 equiv) in water (5 mL) was added to the crude cyclic peptide **2.58** (95 mg) in THF (5 mL). The solution was stirred for 16 h and concentrated *in vacuo*. The resulting residue was dissolved in DMF (1.8 mL) by adding a few drops of TFA and then purification by preparative HPLC afforded β^2-epi-azumamide E **2.59** (4.2 mg, 12%, 4 steps) as a white solid. $[\alpha]_D$: +30° (*c* = 0.1, MeOH); ^{1}H NMR (500 MHz, DMSO) δ 7.88 (d, *J* = 8.0 Hz, 1H), 7.65 (bs, 1H), 7.40 (m, 1H), 7.31 (m, 1H), 7.27 (t, *J* = 7.1 Hz, 2H), 7.21 (m, 2H), 7.15 (d, *J* = 7.3 Hz, 2H), 5.50 (m, 1H), 5.36 (dd, *J* = 17.7 Hz and 7.8 Hz, 1H), 4.25 (m, 2H), 3.75 (m, 2H), 2.94 (dd, *J* = 13.9 Hz and 5.1 Hz, 1H), 2.76 (dd, *J* = 13.7 Hz and 10.0 Hz, 1H), 2.63 (m, 1H), 2.40 (d, *J* = 15.0 Hz, 1H), 2.25 (m, 5H), 1.95 (octet, *J* = 6.7 Hz, 1H), 1.14 (d, *J* = 7.3 Hz, 3H), 1.02 (d, *J* = 6.9 Hz, 3H), 0.94 (d, *J* = 6.7 Hz, 3H), 0.91 (d, *J* = 6.8 Hz, 3H). HRMS (ESI-TOF): *m/z* calcld. for $C_{27}H_{38}N_4O_6H^+$: 515.2870; found: 515.2864 $[M+H]^+$. HPLC gradient C, t_R = 12.22 min (>95%).

(2*S*,3*R*)-*tert*-Butyl 3-((*S*)-1,1-dimethylethylsulfinamido)-5-hydroxy-2-methylpentanoate (2.48)

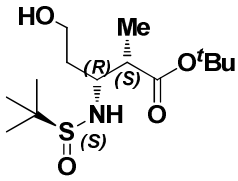

TBAF (1.0 M, 4.9 mL, 4.9 mmol, 2.0 equiv) was added over 10 min to a stirred solution of silyl ether **2.42** (1.14 g, 2.5 mmol) and AcOH (141 μL, 2.5 mmol, 1.0 equiv) in THF (20 mL) at 0 °C under argon. After stirring for 10 min the cooling bath was removed and the mixture was stirred for 2 hours at room temperature, before concentration and purification by VLC alcohol 2.48 (0.70 g, 92%) as clear oil. $[\alpha]_D$: +25.6° (*c* = 0.3, CH_2Cl_2); ^{1}H NMR (300 MHz, $CDCl_3$) δ 4.06 (s, 1H), 3.81 (d, *J* = 4.3 Hz, 3H), 3.72 (m, 2H), 2.42 (dd, *J* = 7.0, 5.1 Hz, 1H), 1.78 (m, 1H), 1.70 (m, 1H), 1.43 (s, 9H), 1.21 (s, 9H), 1.10 (d, *J* = 7.0 Hz, 3H). ^{13}C NMR (75 MHz, $CDCl_3$) δ 173.5, 80.9, 60.1, 58.4, 56.4 , 46.8, 36.2, 28.2, 22.9, 12.6. HRMS (ESI-TOF): *m/z* calcld. for $C_{14}H_{29}NO_4SH^+$: 308.1896; found: 308.1918 $[M+H]^+$.

(7*R*,8*S*)-(*Z*)-9-*tert*-Butyl 1-ethyl 7-((*S*)-1,1-dimethylethylsulfinamido)-8-methylnon-4-enedioate (2.50)

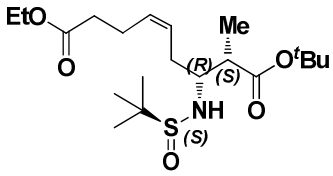

$NaHCO_3$ (175 mg, 2.1 mmol, 1.5 equiv) and Dess-Martin periodinane reagent (0.80 g, 1.8 mmol, 1.3 equiv) were added to a stirred solution of alcohol **2.48** (0.43 g, 1.4 mmol) in dry CH_2Cl_2 (10 mL) at 0 °C under N_2. After 30 min the mixture was raised from the cooling bath, allowing only cooling on the bottom of the flask. After 1 hour the mixture was allowed to warm to room temperature and added sat. aq. $Na_2S_2O_3$ (20 mL) and sat. aq. $NaHCO_3$ (20 mL). The aqueous phase was extracted with CH_2Cl_2 (2 × 100 mL). The combined organic layers were washed with sat. aq. $NaHCO_3$ (40 mL) and brine (50 mL), dried (Na_2SO_4), filtered, and concentrated *in vacuo* to afford aldehyde **2.49** (395 mg, 94%) as a pale yellow oil, which was used immediately without further purification. A flame dried round-bottomed flask was charged with (4-ethoxy-4-oxobutyl)triphenylphosphonium bromide (1.31 g, 2.8 mmol, 2.0 equiv) and the Wittig reagent dried under high vacuum for 24 hours. The Wittig reagent was the dissolved in dry THF (15 mL) under argon and cooled to –78 °C. KHMDS (0.5 M, 5.25 mL, 2.6 mmol, 1.9 equiv) was added dropwise and the resulting orange solution was stirred for 40 min before the crude aldehyde **2.49** (395 mg, 1.4 mmol) in dry THF (3.5 mL) was added dropwise. The mixture was allowed to warm to room temperature and after 16 hours the mixture was quenched with EtOAc (2 mL) and concentrated. Water (20 mL) was added and the aqueous phase was extracted with EtOAc (2 × 80 mL). The combined organic layers were washed with brine (40 mL), dried ($MgSO_4$), filtered, and concentrated *in vacuo*. Purification by VLC afforded alkene **2.50** as a pale yellow oil (250 mg, 45%, 2 steps). $[\alpha]_D$: +43.6° (*c* = 0.3, CH_2Cl_2); ^{1}H NMR (300 MHz, $CDCl_3$) δ 5.49 (m, 2H), 4.11 (q, *J* = 7.1 Hz, 2H), 3.63 (m, 1H), 3.27 (d, *J* = 7.9 Hz, 1H), 2.51 (qd, *J* = 7.1, 5.4 Hz, 1H), 2.43 (t, *J* = 6.5 Hz, 1H), 2.35 (m, 4H), 1.44 (s, 9H), 1.24 (t, *J* = 7.1 Hz, 3H), 1.19 (s, 9H), 1.11 (d, *J* = 7.1 Hz, 1H). ^{13}C NMR (75 MHz, $CDCl_3$) δ 173.8, 173.2, 131.6, 126.3, 80.9, 60.6, 58.6, 56.4, 44.8, 34.2, 32.3, 28.3, 23.1, 23.0, 14.5, 12.3. HRMS (ESI-TOF): *m/z* calcld. for $C_{20}H_{37}NO_5SH^+$: 404.2471; found: 404.2491 $[M+H]^+$.

(2*S*,3*R*)-(*Z*)-3-((((9H-Fluoren-9-yl)methoxy)carbonyl)amino)-9-ethoxy-2-methyl-9-oxonon-5-enoic acid (2.51)

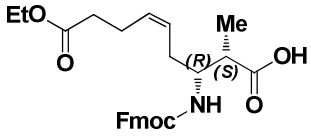

TFA (6.0 mL) was added to a solution of alkene **2.50** (0.33 g, 0.82 mmol) in dry CH_2Cl_2 (6.0 mL) at 0° C. After stirring for 1.5 hour at room temperature the mixture was concentrated and the TFA was removed by co-evaporation with toluene (×3) to afford the crude sulfinyl protected β-amino acid (0.36 g). HCl in dioxane (4.0 M, 0.41 mL, 1.6 mmol, 2.0 equiv) was added to a solution of the crude sulfinyl protected β-amino acid in 1,4-dioxane (8.0 mL). Additional HCl (0.1 mL, 0.40 mmol, 0.5 equiv) was added after 2 hours and 2.5 hours of stirring. After the last addition of HCl the mixture was stirred for 40 min and concentrated to afford the crude β-amino acid, which was used without further purification.

A solution of the crude β-amino acid in water (4.0 mL) was added Na_2CO_3 (0.35 g, 3.26 mmol, 4.0 equiv) and cooled to 0° C. Fmoc-O-succinimide (0.33 g, 0.98 mmol, 1.2 equiv) in 1,4-dioxane (4.0 mL) was added and the cooling removed. After 2 hours water (60 mL) was added and the mixture washed with ether (20 mL) and ethyl acetate (2 × 25 mL). The aqueous phase was cooled to 0° C and acidified with concentrated HCl until pH ≈ 2 and extracted with ethyl acetate (3 × 75 mL). The combined organic phases were washed with water (50 mL), brine (50 mL), dried (Na_2SO_4) and concentrated. Purification of the crude residue by VLC (0.2% acetic acid in the eluent) afforded β-amino acid **2.51** (257 mg, 68%, 3 steps) as a white solid after co-evaporation of residual acetic acid with CH_2Cl_2–toluene (1:1, 3 × 10 mL). $[\alpha]_D$ = –9.4 ° (*c* = 0.5, CH_2Cl_2); ^{1}H NMR (300 MHz, DMSO) δ 7.89 (d, *J* = 7.4 Hz, 2H), 7.68 (d, *J* = 7.3 Hz, 2H), 7.41 (t, *J* = 7.3 Hz, 2H), 7.32 (ddd, *J* = 7.4, 4.3, 1.2 Hz,

1H), 7.15 (d, *J* = 9.6 Hz, 1H), 5.33 (m, 2H), 4.26 (m, 3H), 4.02 (q, *J* = 7.1 Hz, 1H), 3.65 (m, 1H), 2.28 (m, 7H), 1.15 (t, *J* = 7.1 Hz, 3H), 1.00 (d, *J* = 7.0 Hz, 3H). ^{13}C NMR (75 MHz, $CDCl_3$) δ 179.6, 173.6, 156.4, 144.0, 141.4, 130.8, 127.8, 127.1, 126.8, 125.2, 120.1, 66.8, 60.7, 53.2, 47.3, 43.8, 33.9, 29.7, 22.8, 14.3, 13.5. HRMS (ESI-TOF): *m/z* calcld. for $C_{27}H_{31}NO_6H^+$: 466.2230; found: 466.2254 $[M+H]^+$.

(2*S*,3*R*)-(*Z*)-3-((*tert*-Butoxycarbonyl)amino)-9-ethoxy-2-methyl-9-oxonon-5-enoic acid (2.52)

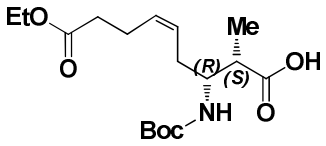

To a solution of the crude fully deprotected *β*-amino acid from above (**2.51**) (31 mg, 0.13 mmol) and *i*Pr_2NEt (67 *μ*L, 0.38 mmol, 3.0 equiv) in dry CH_2Cl_2 (3.0 mL) was added Boc_2O (59 mg, 0.27 mmol, 2.1 equiv) in dry CH_2Cl_2 (1.0 mL) under argon. After 3 hours *i*Pr_2NEt (67 *μ*L, 0.38 mmol, 3.0 equiv) was added and the reaction mixture stirred for 18 hours. After concentration the *i*Pr_2NEt was removed by co-evaporation with toluene. Purification of the crude residue by VLC (0.2% acetic acid in the eluent) afforded *β*-amino acid **2.52** (9.3 mg, 22%, 3 steps) as a clear oil after co-evaporation of residual acetic acid with CH_2Cl_2–toluene (1:1, × 3). Spectral data were in accordance with those previously reported (see figure S1).[S5] $[\alpha]_D$: –9.8° (*c* = 0.4, $CHCl_3$) Litt;[S5] $[\alpha]_D$: –9.5° (*c* = 1, $CHCl_3$); ^{1}H NMR (300 MHz, $CDCl_3$) ^{1}H NMR (300 MHz, $CDCl_3$) δ 5.43 (m, 2H), 4.91 (bs, 1H), 4.13 (q, *J* = 7.2 Hz, 1H), 3.89 (m, 1H), 2.67 (m, 1H), 2.44–2.21 (m, 6H), 1.42 (s, 9H), 1.25 (t, *J* = 7.2 Hz, 3H), 1.21 (d, *J* = 7.2 Hz, 3H). ^{13}C NMR (75 MHz, $CDCl_3$) δ 179.4, 173.5, 156.1, 130.4, 126.8, 79.6, 60.6, 52.6, 43.7, 34.1, 29.8, 28.5, 22.9, 14.4, 13.4.

(*R*)-2-((*S*)-2-((2*S*,3*R*)-(*Z*)-3-((*R*)-2-Amino-3-phenylpropanamido)-9-ethoxy-2-methyl-9-oxonon-5-enamido)-3-methylbutanamido)propanoic acid (2.65)

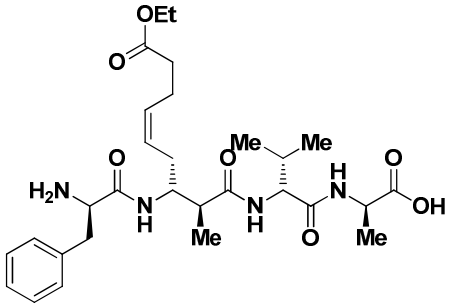

Polystyrene 2-chlorotrityl-bound Fmoc-(D)Val-(D)Ala (132 mg, 80 *μ*mol) was added to a fritted syringe and swelled with CH_2Cl_2 before the Fmoc group was removed with piperidine–DMF (1:4, 4 mL, 2 × 20 min) and DBU–piperidine–DMF (2:2:96, 4 mL, 20 min). The resin was then washed with DMF (×3), MeOH (×3), CH_2Cl_2 (×3).

β-Amino acid **2.51** (41 mg, 88 *μ*mol, 1.1 equiv) in DMF (2.0 mL) was preincubated for 5 min with 2,6-lutidine (30.5 *μ*L, 263 *μ*mol, 3.0 equiv) and HATU (43.3 mg, 114 *μ*mol, 1.3 equiv) before addition to the resin and the reaction was allowed to proceed on a rocking table for 2.5 hours. The resin was then washed with DMF (×3), MeOH (×3), CH_2Cl_2 (×3) and the Fmoc group was removed with piperidine–DMF (1:4, 4 mL, 2 × 25 min) and DBU–piperidine–DMF (2:2:96, 4 mL, 20 min). The resin was washed again with DMF (×3), MeOH (×3), CH_2Cl_2 (×3) before added a preincubated solution of Fmoc-(D)Phe-OH (93 mg, 239 *μ*mol, 3.0 equiv), 2,6-lutidine (55.4 *μ*L, 478 *μ*mol, 6.0 equiv) and HATU (89 mg, 235 *μ*mol, 2.95 equiv). The reaction was allowed to proceed on a rocking table for 16 hours. The resin was then washed with DMF (×3), MeOH (×3), CH_2Cl_2 (×3) and the Fmoc group was removed with piperidine–DMF (1:4, 4 mL, 2 × 25 min) and DBU–piperidine–DMF (2:2:96, 4 mL, 20 min). The resin was washed again with DMF (×3), MeOH (×3), CH_2Cl_2 (×3) and treated with TFA–CH_2Cl_2 (1:1, 4 mL) for 30 min followed by washing with CH_2Cl_2 (5 mL). A fresh portion of TFA–CH_2Cl_2 (1:1, 4 mL) was added to the resin and after additional 30 min the resin was drained, washed with CH_2Cl_2 (5 mL) and all the fractions were pooled in a tube. The solvent was removed under a stream of argon and precipitation with diethyl ether afforded the crude TFA salt of the linear peptide **2.65** (63 mg) as a pale yellow solid, which was used without further purification. UPLC-MS gradient A, t_R = 1.05 min.

(*Z*)-Ethyl-6-((2*R*,5*R*,8*R*,11*R*,12*S*)-8-benzyl-2-isopropyl-5,12-dimethyl-3,6,9,13-tetraoxo-1,4,7,10-tetraazacyclotridecan-11-yl)hex-4-enoate (2.66)

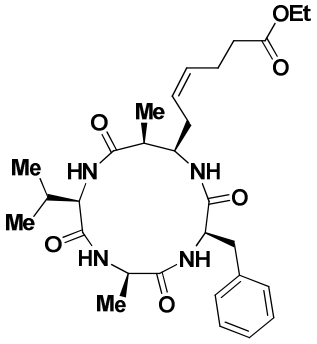

The crude linear peptide **2.65** (63 mg, 0.093 mmol) was dissolved in CH_2Cl_2–DMF (10:1, 24 mL) and added dropwise over 3.5 hours to a solution of HATU (71 mg, 0.19 mmol, 2.0 equiv) and *i*Pr_2NEt (73 μL, 0.42 mmol, 4.5 equiv) in CH_2Cl_2 (12 mL). After the addition additional HATU (36 mg, 0.095 mmol, 1.0 equiv) and *i*Pr_2NEt (37 μL, 0.21 mmol, 2.3 equiv) was added. The solution was stirred for 15 hours and concentrated. The brown residue was dissolved in CH_2Cl_2 (80 mL) and washed with aq. HCl (0.5 M, 10 mL and 1.0 M, 10 mL) and the combined aqueous phases were extracted with CH_2Cl_2 (2 × 50 mL). The combined organic phases were washed with brine (25 mL), dried (Na_2SO_4), filtered, and concentrated. Purification by VLC afforded a residue **2.66** (24.2 mg), which was found not to be sufficiently pure by ^{1}H NMR (residual *i*Pr_2NEt was observed; yield based on ^{1}H NMR, 25%). The residue was used without further purification. HPLC gradient B, t_R = 1.84 min.

Azumamide A [(*Z*)-6-((2*R*,5*R*,8*R*,11*R*,12*S*)-8-Benzyl-2-isopropyl-5,12-dimethyl-3,6,9,13-tetraoxo-1,4,7,10-tetraazacyclotridecan-11-yl)hex-4-enamide].

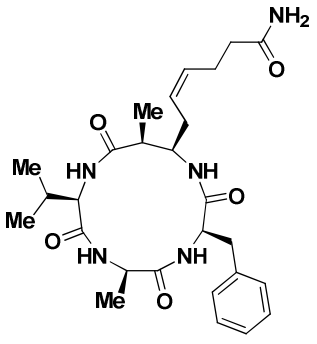

LiOH (89 mg, 3.72 mmol, 85 equiv) in water (4.0 mL) was added to a stirred solution of the impure cyclic peptide **2.66** (24.2 mg, approx. 0.045 mmol) in THF (4 mL). After 2.5 hours of stirring the organic solvent was removed *in vacuo*. The aqueous phase was acidified with 1 M HCl to pH 2 and extracted with EtOAc (4 × 30 mL) and CH_2Cl_2 (40 mL). The organic phases were dried (Na_2SO_4), filtered, and concentrated to afford crude azumamide E (102 mg), which was used without further purification. HPLC gradient A, t_R = 1.47 min. To a solution of the above crude azumamide E (102 mg, 0.045 mmol) in DMF (3.0 mL) was added HATU (34 mg, 0.09 mmol, 2 equiv), *i*Pr_2NEt (43 μL, 0.25 mmol, 5.5 equiv) and after 5 min, NH_3–dioxane (0.9 mL, 0.45 mmol, 10 equiv). After 1 h NH_3–dioxane (0.45 mL, 0.23 mmol, 5.0 equiv) was added. UPLC-MS analysis showed 50% conversion after 3 hours and HATU (34 mg, 0.09 mmol, 2.0 equiv) and NH_3–dioxane (0.45 mL, 0.23 mmol, 5.0 equiv) was added. After additionally 1 hour DMF (1.0 mL) followed by HATU (17 mg, 0.045 mmol, 1.0 equiv) and NH_3–dioxane (0.45 mL, 0.23 mmol, 5.0 equiv) was added and stirring continued for 1 hour before concentration in *vacuo*. The residue was dissolved in MeCN–H_2O and purified by preperative HPLC to give azumamide A (4.8 mg, 12%, 8 steps). $[\alpha]_D$: +56° (*c* = 0.2, MeOH) Litt;[229] $[\alpha]_D$: +33° (*c* = 0.1, MeOH); ^{1}H NMR (500 MHz, CD_3OH) δ 8.18 (d, *J* = 8.6 Hz, 1H), 8.16 (d, *J* = 9.0 Hz, 1H), 7.72 (d, *J* = 8.2 Hz, 1H), 7.59 (m, 2H), 7.20 (m, 5H), 6.74 (bs, 1H), 5.48 (m, 1H), 5.37 (m, 1H), 4.33 (dt, *J* = 9.0, 7.0 Hz, 1H), 4.24 (m, 2H), 3.81 (dd, *J* = 10.4Hz and 8.4 Hz, 1H), 3.10 (m, 2H), 2.72 (m, 1H), 2.57 (dt, *J* = 14.1 Hz and 6.9 Hz, 1H), 2.41 (m, 2H), 2.27 (m, 4H), 1.30 (d, *J* = 7.5 Hz, 3H), 1.23 (d, *J* = 7.3 Hz, 3H), 0.96 (d, *J* = 6.5 Hz, 3H), 0.94 (d, *J* = 6.7 Hz, 3H). HRMS (ESI-TOF): *m/z* calcld. for $C_{27}H_{38}N_4O_7H^+$: 514.3029; found: 514.3032 $[M+H]^+$. HPLC gradient C, t_R = 11.62 min (>95%).

(2*S*,3*R*)-(*Z*)-3-((*R*)-2-((*R*)-2-((*R*)-2-Amino-3-methylbutanamido)propanamido)-3-(4-hydroxyphenyl)propanamido)-9-ethoxy-2-methyl-9-oxonon-5-enoic acid (2.62)

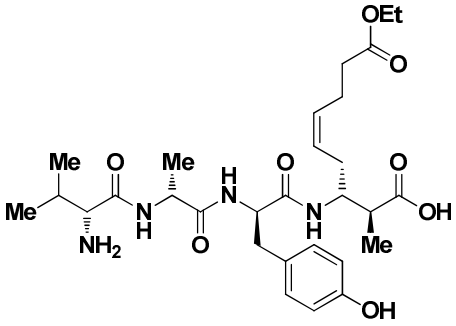

Polystyrene 2-chlorotritylchloride resin was added to a fritted syringe and swelled with dry CH_2Cl_2. A solution of β-amino acid **2.51** (47.5 mg. 0.10 mmol) and *i*Pr_2NEt (36 μL, 0.20 mmol, 2.0 equiv) in dry CH_2Cl_2 (2 mL) was added to the resin and the loading was allowed to proceed on a rocking table for 16 hours. After washing with CH_2Cl_2 (×3) the resin was capped with CH_2Cl_2–MeOH–*i*Pr_2NEt (7:2:1) for 30 min. The resin was then washed with DMF (×3), MeOH (×3), and CH_2Cl_2 (×3). The Fmoc group was removed with piperidine–DMF (1:4, 4 mL, 2 × 30 min) and DBU–piperidine–DMF (2:2:96, 4 mL, 30 min) and then washed as described above.

Fmoc-(D)Tyr(O^{t}Bu)-OH (188 mg, 0.41 mmol, 4.0 equiv) in DMF (2.0 mL) was preincubated for 5 min with 2,6-lutidine (95 μL, 0.82 mmol, 8.0 equiv) and HATU (153 mg, 0.40 mmol, 0.98 equiv) before addition to the resin and the reaction was allowed to proceed on a rocking table for 2 hours. After the washing procedure as outlined above the Fmoc group was removed with piperidine–DMF (1:4, 4 mL, 2 × 30 min) and DBU–piperidine–DMF (2:2:96, 4 mL, 30 min). The resin was then washed with DMF (×3), MeOH (×3), and CH_2Cl_2 (×3).

Fmoc-(D)Ala-OH (130 mg, 0.0.41 mmol, 4.0 equiv) in DMF (2.0 mL) was preincubated for 5 min with 2,6-lutidine (94.5 μL, 0.82 mmol, 8.0 equiv) and HATU (153 mg, 0.40 mmol, 0.98 equiv) before addition to the resin and the reaction was allowed to proceed on a rocking table for 2.5 hours. After the washing procedure as outlined above the Fmoc group was removed with piperidine–DMF (1:4, 4 mL, 2 × 30 min) and DBU–piperidine–DMF (2:2:96, 4 mL, 30 min). The resin was then washed with DMF (×3), MeOH (×3), CH_2Cl_2 (×3).

Fmoc-(D)Val-OH (139 mg, 0.41 mmol, 4.0 equiv) in DMF (2.0 mL) was preincubated for 5 min with 2,6-lutidine (94.5 μL, 0.82 mmol, 8.0 equiv) and HATU (153 mg, 0.40 mmol, 0.98 equiv) before addition to the resin and the reaction was allowed to proceed on a rocking table for 2 hours. After the washing procedure as outlined above the Fmoc group was removed with piperidine–DMF (1:4, 4 mL, 2 × 30 min) and DBU–piperidine–DMF (2:2:96, 4 mL, 30 min). The resin was then washed with DMF (×3), MeOH (×3), and CH_2Cl_2 (×3). The resin was treated with TFA–CH_2Cl_2 (1:1, 2 mL) for 30 min, followed by washing with CH_2Cl_2 (2 mL). A fresh portion of TFA–CH_2Cl_2 (1:1, 2 mL) was added to the resin and after additional 30 min the resin was drained, washed with CH_2Cl_2 (2 mL) and all the fractions were pooled in a tube and concentrated under a stream of argon. Precipitation with diethyl ether afforded the TFA salt of the linear peptide **2.62** (64 mg, 91%) as a pale yellow solid, which was used without further purification UPLC-MS gradient A, t_R = 1.03 min (>95%)

(*Z*)-Ethyl-6-((2*R*,5*R*,8*R*,11*R*,12*S*)-8-(4-hydroxybenzyl)-2-isopropyl-5,12-dimethyl-3,6,9,13-tetraoxo-1,4,7,10-tetraazacyclotridecan-11-yl)hex-4-enoate (2.63)

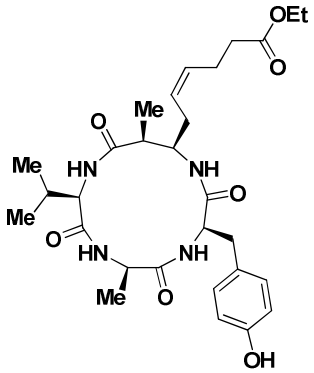

The TFA salt of the crude linear peptide **2.62** (64 mg, 0.09 mmol) was dissolved in DMF (240 mL ≈ 0.4 mM) and *i*Pr_2NEt (129 μL, 0.74 mmol, 8.0 equiv) and HATU (39 mg, 0.10 mmol, 1.1 equiv) were added. The solution was stirred for 17 hours and then added HATU (18 mg, 0.05 mmol, 0.6 equiv). After additionally 1 hour of stirring the reaction mixture was concentrated and purified by preparative HPLC to afford the ethylester of azumamide C **2.63** (6.1 mg, 11%, 10 steps) as a white solid. HRMS (ESI-TOF): *m/z* calcld. for $C_{29}H_{42}N_4O_7H^+$: 559.3131; found: 559.3123 $[M+H]^+$. UPLC-MS gradient A, t_R = 1.60 min (purity > 95%).

Azumamide B [(*Z*)-6-((2*R*,5*R*,8*R*,11*R*,12*S*)-8-(4-Hydroxybenzyl)-2-isopropyl-5,12-dimethyl-3,6,9,13-tetraoxo-1,4,7,10-tetraazacyclotridecan-11-yl)hex-4-enamide]

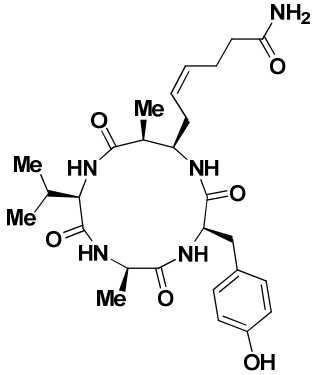

An aqueous solution of LiOH (0.5 M, 55 μL, 2.0 mmol, 2.5 equiv) was added to the cyclic peptide **2.63** (6.1 mg) in THF–H_2O ((1:1), 2 mL) at 0 °C. After 30 min the ice-bath was removed. Additional portions of LiOH solution (55 μL, 2.0 mmol, 2.5 equiv) were added after 2, 4, and 6 hours, and stirring was continued for additional 19 hours to ensure full conversion. Then water (0.5 mL) was added and the organic solvent removed *in vacuo*. The aqueous phase was acidified with 1 M HCl and extracted with EtOAc (5 × 20 mL). The organic phase was dried (Na_2SO_4), filtered and concentrated *in vacuo* to afford the crude azumamide C (20 mg), which was used without further purification.

To a solution of crude azumamide C (5.8 mg, 10.9 μmol) in DMF (2 mL) was added HOBt (4.4 mg, 33 μmol, 3.0 equiv), DIC (5.1 μL, 34 μmol, 3.0 equiv) and *i*Pr_2NEt (7.6 μL, 44 μmol, 4.0 equiv). After 10 minutes NH_3–dioxane (0.5 M, 0.11 mL, 55 μmol, 5.0 equiv) was added. After 1.5 hour DIC (5 μL, 34 μmol, 3.0 equiv) followed by NH_3–dioxane (0.5 M, 0.11 mL, 55 μmol, 5.0 equiv) were added. After stirring for 16 hours, additional DIC (2.0 equiv) and NH_3–dioxane (5.0 equiv) were added and this procedure was repeated once more after 18 hours. Finally, CH_2Cl_2 (1 mL) followed by DIC (3.0 equiv) and NH_3–dioxane (10 equiv) were added and after 2 days of stirring at room temperature, the reaction mixture was concentrated, dissolved in MeCN–H_2O (2:1), and purified by preparative HPLC to give azumamide B (3.6 mg, 62%, two steps) as a white solid. $[\alpha]_D$: +65° (*c* = 0.15, MeOH) Litt;[229] $[\alpha]_D$: +45° (*c* = 0.1, MeOH); ^{1}H NMR (500 MHz, CD_3OH) δ 8.13 (d, *J* = 7.9 Hz, 1H), 8.00 (d, *J* = 8.9 Hz, 1H), 7.85 (d, *J* = 7.2 Hz, 1H), 7.61 (d, *J* = 8.2 Hz, 1H), 7.01 (d, *J* = 8.4 Hz, 3H), 6.67 (d, *J* = 8.4 Hz, 3H), 5.49 (m, 1H), 5.37 (dd, *J* = 18.0 Hz and 7.3 Hz, 2H), 4.29 (pentet, *J* = 7.2 Hz, 1H), 4.15 (m, 1H), 4.05 (m, 1H), 3.60 (m, 1H), 3.13 (dd, *J* = 13.7, 10.1 Hz, 1H), 3.00 (dd, *J* = 13.8, 6.3 Hz, 1H), 2.70 (m, 2H), 2.36 (ddd, *J* = 22.3, 21.5, 7.1 Hz, 11H), 1.29 (d, *J* = 7.2 Hz, 3H), 1.27 (d, *J* = 7.4 Hz, 3H), 0.95 (d, *J* = 5.7 Hz, 3H), 0.93 (d, *J* = 6.0 Hz, 3H). HRMS (ESI-TOF): *m/z* calcld. for $C_{27}H_{39}N_5O_6H^+$: 530.2978; found: 530.2973 $[M+H]^+$. HPLC gradient C, t_R = 10.31 min (>95%).

(*R*)-2-((*S*)-2-((2*S*,3*R*)-(*Z*)-3-((*R*)-2-Amino-3-(4-hydroxyphenyl)propanamido)-9-ethoxy-2-methyl-9-oxonon-5-enamido)-3-methylbutanamido)propanoic acid (2.60)

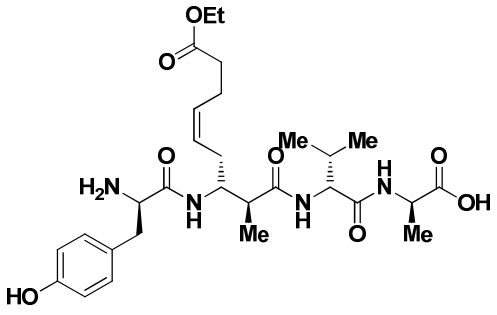

Polystyrene 2-chlorotrityl-bound Fmoc-(D)Val-(D)Ala (249 mg, 0.17 mmol) was added to a fritted syringe and swelled with CH_2Cl_2 before the Fmoc group was removed with piperidine–DMF (1:4, 4 mL, 2 × 30 min) and DBU–piperidine–DMF (2:2:96, 4 mL, 30 min). The resin was then washed with DMF (×3), MeOH (×3), CH_2Cl_2 (×3). β-Amino acid **2.51** (100 mg, 0.22 mmol, 1.3 equiv) in DMF (3.0 mL) was preincubated for 5 min with 2,6-lutidine (60 μL, 0.52 mmol, 3.0 equiv) and HATU (86 mg, 0.23 mmol, 1.3 equiv) before addition to the resin. The reaction was allowed to proceed on a rocking table for 16 hours. After the washing procedure as outlined above the resin was dried under high vacuum. The Fmoc group was removed with piperidine–DMF (1:4, 4 mL, 2 × 30 min) and DBU–piperidine–DMF (2:2:96, 4 mL, 30 min). The resin was then washed with DMF (×3), MeOH (×3), CH_2Cl_2 (×3).

Fmoc-(D)Tyr(O^{t}Bu)-OH (74 mg, 0.16 mmol, 3.6 equiv) in DMF (2.0 mL) was preincubated for 5 min with 2,6-lutidine (37 μL, 0.32 mmol, 7.1 equiv) and HATU (59 mg, 0.16 mmol, 3.6 equiv) before being added to polystyrene 2-chlorotrityl-bound H_2N-β-aa-(D)Val-(D)Ala (75 mg, 0.045 mmol) and the reaction was allowed to proceed on a rocking table for 16 hours. After the washing procedure as outlined above the Fmoc group was removed with piperidine–DMF (1:4, 4 mL, 2 × 30 min) and DBU–piperidine–DMF (2:2:96, 4 mL, 30 min). The resin was treated with TFA–CH_2Cl_2 (1:1, 4 mL) for 30 min followed by washing with CH_2Cl_2 (5 mL). A fresh portion of TFA–CH_2Cl_2 (1:1, 4 mL) was added to the resin and after additional 30 min the resin was drained, washed with CH_2Cl_2 (5 mL) and all the fractions were pooled and concentrated *in vacuo*. Excess TFA was removed by co-evaporation with toluene to give the crude linear peptide **2.60** (34 mg), which was used without further purification.

(*Z*)-Ethyl-6-((2*R*,5*R*,8*R*,11*R*,12*S*)-8-(4-hydroxybenzyl)-2-isopropyl-5,12-dimethyl-3,6,9,13-tetraoxo-1,4,7,10-tetraazacyclotridecan-11-yl)hex-4-enoate (2.61)

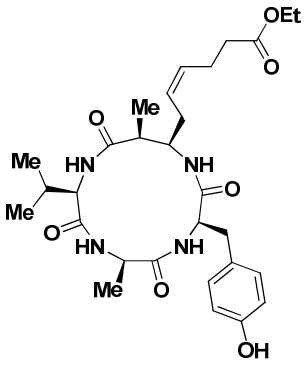

The crude linear peptide **2.60** (34 mg, 0.045 mmol) was dissolved in DMF (180 mL ≈ 0.25 mM) and *i*Pr_2NEt (102 μL, 0.58 mmol, 13 equiv) and HATU (45 mg, 0.12 mmol, 2.7 equiv) were added. The solution was stirred for 2 hours and the reaction mixture was concentrated and added EtOAc (220 mL). The organic phase was washed with aq. HCl (1.0 M, 3 × 10 mL) and concentrated to afford the crude cyclic peptide **2.61** (61 mg) as a brown oil, which was used without further purification.

Azumamide C [(*Z*)-6-((2*R*,5*R*,8*R*,11*R*,12*S*)-8-(4-Hydroxybenzyl)-2-isopropyl-5,12-dimethyl-3,6,9,13-tetraoxo-1,4,7,10-tetraazacyclotridecan-11-yl)hex-4-enoic acid]

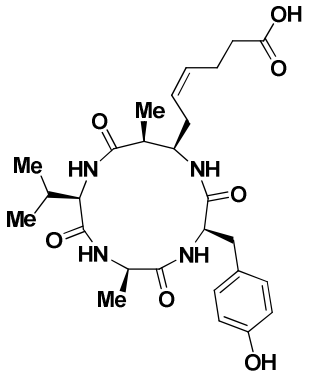

LiOH (49 mg, 2.0 mmol, 35 equiv) in water (5.0 mL) was added to the crude cyclic peptide **2.61** (61 mg) in THF (5.0 mL). The solution was stirred for 16 hours and concentrated *in vacuo*. The resulting residue was dissolved in THF–H_2O (1:1), 10 mL) by adding a few drops of TFA and then purification by preparative HPLC afforded azumamide C (2.2 mg, 9%, 8 steps) as a white solid. $[\alpha]_D$: +49° (*c* = 0.14, MeOH) Litt;[229] $[\alpha]_D$: +21° (*c* = 0.1, MeOH); ^{1}H NMR (500 MHz, CD_3OH) δ 8.08 (d, *J* = 7.7 Hz, 1H), 7.99 (d, *J* = 8.4 Hz, 1H), 7.84 (s, 1H), 7.62 (d, *J* = 8.1 Hz, 1H), 7.01 (d, *J* = 8.4 Hz, 2H), 6.67 (d, *J* = 8.4 Hz, 2H), 5.48 (t, *J* = 8.8 Hz, 1H), 5.38 (dt, *J* = 10.7, 7.0 Hz, 1H), 4.29 (pentet, *J* = 7.3 Hz 1H), 4.16 (m, 1H), 4.01 (m, 1H), 3.58 (m, 1H), 3.15 (dd, *J*= 13.7, 10.2 Hz 1H), 3.00 (dd, *J* = 13.7 Hz and 6.0 Hz, 1H), 2.72 (m, 1H), 2.67 (m, 1H) 2.39 (m, 5H), 1.29 (d, *J* = 7.2 Hz, 3H), 1.27 (d, *J* = 7.3 Hz, 3H), 0.95 (d, *J* = 6.0 Hz, 3H), 0.93 (d, *J* = 6.0 Hz, 3H). HRMS (ESI-TOF): *m/z* calcld. for $C_{27}H_{38}N_4O_7H^+$: 531.2819; found: 531.2815 $[M+H]^+$. HPLC gradient C, t_R = 11.04 min (>95%).

(*R*)-2-((2*S*,3*R*)-(*Z*)-3-((*R*)-2-((*R*)-2-Aminopropanamido)-3-phenylpropanamido)-9-ethoxy-2-methyl-9-oxonon-5-enamido)propanoic acid (2.64)

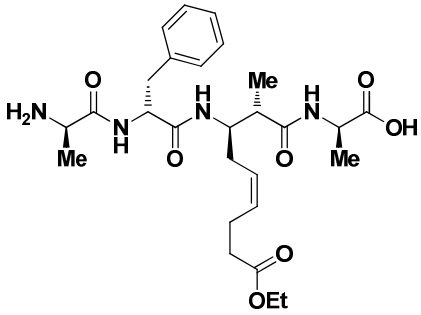

Polystyrene 2-chlorotrityl-bound Fmoc-(D)Ala (118 mg, 0.096 mmol) was added to a fritted syringe and swelled with CH_2Cl_2 before the Fmoc group was removed with piperidine–DMF (1:4, 4 mL, 2 × 30 min) and DBU–piperidine–DMF (2:2:96, 4 mL, 30 min). The resin was then washed with DMF (×3), MeOH (×3), CH_2Cl_2 (×3). β-Amino acid **2.51** (49 mg, 105 μmol, 1.1 equiv) in DMF (2.0 mL) was preincubated for 5 min with *i*Pr_2NEt (43 μL, 249 μmol, 2.6 equiv) and PyBOP (65 mg, 125 μmol, 1.3 equiv) and added to the resin. The reaction was allowed to proceed on a rocking table for 16 hours. A Kaiser test showed incomplete coupling and the resin treated with β-amino acid **2.51** (15 mg, 32 μmol), *i*Pr_2NEt (15 μL, 83 μmol, 2.6 equiv) and PyBOP (22 mg, 42 μmol, 1.3 equiv) for another 16 hours. The resin was then washed with DMF (×3), MeOH (×3), and CH_2Cl_2 (×3) and the Fmoc group was removed with piperidine–DMF (1:4, 4 mL, 2 × 25 min) and DBU–piperidine–DMF (2:2:96, 4 mL, 30 min). The resin was washed with DMF (×3), MeOH (×3), and CH_2Cl_2 (×3) before addition of a preincubated solution of Fmoc-(D)Phe-OH (148 mg, 382 μmol, 3.0 equiv), 2,6-lutidine (88 μL, 762 μmol, 6.0 equiv) and HATU (143 mg, 376 μmol, 3.0 equiv) in DMF (2 mL). The coupling was allowed to proceed on a rocking table for 2 hours. The resin was then washed with DMF (×3), MeOH (×3), and CH_2Cl_2 (×3) and the Fmoc group was removed with piperidine–DMF (1:4, 4 mL, 2 × 25 min) and DBU–piperidine–DMF (2:2:96, 4 mL, 30 min). After washing [DMF (×3), MeOH (×3), and CH_2Cl_2 (×3)], a preincubated solution of Fmoc-(D)Ala-OH (119 mg, 382 μmol, 3.0 equiv), 2,6-lutidine (88 μL, 762 μmol, 6.0 equiv) and HATU (143 mg, 376 μmol, 3.0 equiv) in DMF (2 mL) was added to the resin. The coupling was allowed to proceed on a rocking table for 15 hours. After washing, the Fmoc group was removed with piperidine–DMF (1:4, 4 mL, 2 × 25 min) and DBU–piperidine–DMF (2:2:96, 4 mL, 30 min) and the resin was washed again [DMF (×3), MeOH (×3), and CH_2Cl_2 (×3)]. After cleavage from the resin with TFA–CH_2Cl_2 (1:1, 2 × 4 mL, 30 min) the solvent was removed under a stream of argon and precipitation with diethyl ether afforded the TFA salt of the crude linear peptide **2.64** (84 mg, >99%) as a pale yellow solid. UPLC-MS gradient B, t_R = 1.06 min (purity >95%)

(*Z*)-ethyl-6-((2*R*,5*R*,8*R*,11*R*,12*S*)-8-Benzyl-2,5,12-trimethyl-3,6,9,13-tetraoxo-1,4,7,10-tetraazacyclotridecan-11-yl)hex-4-enoate (2.65)

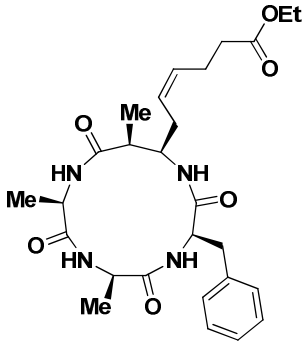

The crude linear peptide **2.64** (79 mg, 0.12 mmol) was dissolved in DMF (250 mL ≈ 0.5 mM) and *i*Pr_2NEt (170 μL, 0.98 mmol, 8.0 equiv) and HATU (51 mg, 0.13 mmol, 1.1 equiv) were added successively. The solution was stirred for 19 hours and concentrated. To the oily residue was added EtOAc (150 mL). A precipitate was observed as the organic phase was acidified with aq. HCl (1.0 M, 20 mL). The precipitate was dissolved in CH_2Cl_2 (150 mL) and washed with aq. HCl (1.0 M, 20 mL). The organic phases were pooled, concentrated, and purified by VLC to afford a residue **2.65** (22.7 mg), which was found not to be pure by ^{1}H NMR (residual *i*Pr_2NEt was observed; yield based on ^{1}H NMR = 19%). The residue was used without further purification. HPLC gradient B, t_R = 1.45 min.

Azumamide D [(*Z*)-6-((2*R*,5*R*,8*R*,11*R*,12*S*)-8-Benzyl-2,5,12-trimethyl-3,6,9,13-tetraoxo-1,4,7,10-tetraazacyclotridecan-11-yl)hex-4-enamide]

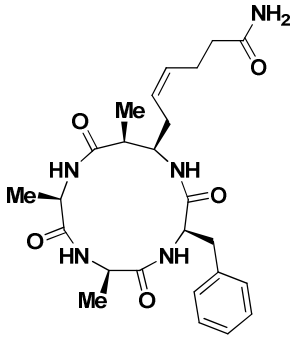

LiOH (53 mg, 2.21 mmol, 50 equiv) in water (5.0 mL) was added to a stirred solution of the impure cyclic peptide **2.65** (22.7 mg, approx. 0.044 mmol) in THF (3 mL). After 4 hours the organic solvent was removed *in vacuo* and the water (0.5 mL) was added to the aqueous, which was then acidified with 1 M HCl (2 mL) and extracted with EtOAc (4 × 2 mL). The organic phases were dried ($MgSO_4$), filtered, and concentrated to give the crude acid (53 mg), which was used without further purification. To a solution of the crude acid (11 mg, 23 μmol) in CH_2Cl_2–DMF (8:1, 2.3 mL) was added HOBt (10 mg, 66 μmol, 3.0 equiv), DIC (10 μL, 66 μmol, 3.0 equiv) and *i*Pr_2NEt (15 μL, 88 μmol, 4.0 equiv). After 5 minutes NH_3–dioxane (0.5 M, 0.22 mL, 110 μmol, 5.0 equiv) was added. After 1 hour NH_3–dioxane (0.5 M, 0.22 mL, 110 μmol, 5.0 equiv) was added. After stirring for 18 hours additional DMF (0.5 mL) followed by NH_3–MeOH (2.0 M, 0.11 mL, 230 μmol, 10 equiv) was added. After additionally 5 hours DIC (7 μL, 46 μmol, 2.0 equiv) was added. The next day NH_3–MeOH (2.0 M, 0.06 mL, 111 μmol, 5.0 equiv) was added and the mixture was stirred for 10 days. Finally, DIC (3.4 μL, 23 μmol, 1.0 equiv) followed by NH_3–MeOH (2.0 M, 0.055 mL, 210 μmol, 5.0 equiv) was added and after 2 days the mixture was concentrated, dissolved in MeCN–H_2O (2:1) and purified by preparative HPLC to afford azumamide D (1.2 mg, 4%, 11 steps) as a white solid. $[\alpha]_D$: +32° (*c* = 0.08, MeOH) Litt;[229] $[\alpha]_D$: +25° (*c* = 0.1, MeOH); 1H NMR (500 MHz, CD_3OH) δ 8.03 (d, *J* = 7.8 Hz, 1H), 8.01 (d, *J* = 8.8 Hz, 1H) 7.94 (d, *J* = 6.8 Hz, 1H), 7.58 (s, 1H), 7.32 (d, *J* = 7.5 Hz, 1H), 7.25–7.14 (m, 5H), 6.75 (s, 1H), 5.47 (m, 1H), 5.39 (m, 1H), 4.35 (m, 1H), 4.19 (m, 1H) 4.17– 4.11 (m, 2H), 3.09 (m, 2H), 2.69 (m, 1H), 2.62 (m, 1H), 2.41 (m, 2H), 2.28 (m, 1H), 1.47 (d, *J* = 7.4 Hz, 3H), 1.28 (d, *J* = 7.4 Hz, 3H), 1.22 (d, *J* = 7.3 Hz, 3H). HRMS (ESI-TOF): *m/z* calcld. for $C_{25}H_{35}N_5O_5H^+$: 486.2716; found: 486.2710 $[M+H]^+$. HPLC gradient C, t_R = 10.55 min (>95%).

(2*R*,5*R*,8*S*,11*S*,12*R*)-(*Z*)-12-Amino-2-benzyl-8-isopropyl-5,11-dimethyl-4,7,10,18-tetraoxo-19-oxa-3,6,9-triazahenicos-14-en-1-oic acid (2.67)

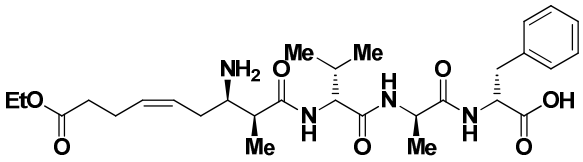

Polystyrene 2-chlorotrityl-bound Fmoc-(D)Val-(D)Ala-(D)-Phe (0.41 g, 0.21 mmol) was added to a fritted syringe and swelled with CH_2Cl_2 before the Fmoc group was removed with piperidine–DMF (1:4, 4 mL, 2 × 25 min) and DBU–piperidine–DMF (2:2:96, 4 mL, 30 min). The resin was then washed with DMF (×3), MeOH (×3), and CH_2Cl_2 (×3).

β-Amino acid **2.51** (100 mg, 0.21 mmol, 1.05 equiv) in DMF (3.0 mL) was preincubated for 5 min with *i*Pr_2NEt (90 μL, 0.52 mmol, 2.4 equiv) and PyBOP (134 mg, 0.26 mmol, 1.2 equiv) and added to the resin. The reaction was allowed to proceed on a rocking table for 16 hours. The resin was then washed [DMF (×3), MeOH (×3), and CH_2Cl_2 (×3)] and the Fmoc group was removed with piperidine–DMF (1:4, 4 mL, 2 × 25 min) followed by DBU–piperidine–DMF (2:2:96, 4 mL, 30 min). After washing [DMF (×3), MeOH (×3), and CH_2Cl_2 (×3)], the resin was cleaved with TFA–CH_2Cl_2 (1:1, 2 × 4 mL, 30 min each) and all the fractions were pooled in a Falcon tube. The solvent was removed under a stream of argon and precipitation with diethyl ether afforded the TFA salt of the linear peptide **2.67** (124 mg, 90%) as a pale yellow solid. UPLC-MS gradient A, t_R = 1.19 min (93% purity as determined by the HPLC UV trace).

(*Z*)-Ethyl-6-((2*R*,5*R*,8*R*,11*R*,12*S*)-8-benzyl-2-isopropyl-5,12-dimethyl-3,6,9,13-tetraoxo-1,4,7,10-tetraazacyclotridecan-11-yl)hex-4-enoate (Table 2-3, entry 1, 2.68)

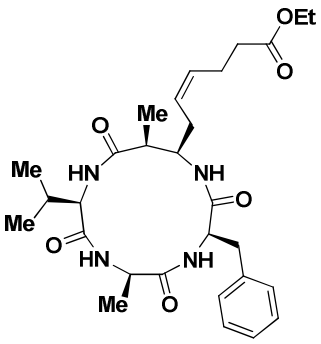

The crude linear peptide **2.67** (120 mg, 0.18 mmol) was dissolved in DMF (450 mL ≈ 0.4 mM) and *i*Pr_2NEt (248 μL, 1.42 mmol, 8.0 equiv) and HATU (74 mg, 0.20 mmol, 2.1 equiv) were added. The solution was stirred for 21 hours and then added *i*Pr_2NEt (125 μL, 0.71 mmol, 4.0 equiv) and HATU (34 mg, 0.09 mmol, 0.5 equiv). After additionally 3 hours of stirring the reaction mixture was concentrated and added EtOAc (250 mL). The organic phase was washed with aq. HCl (1.0 M, 10 mL) and the aqueous phase was extracted with CH_2Cl_2 (2 × 50 mL). The organic phases were pooled, concentrated and purified by VLC to afford a residue **2.68** (36.6 mg), which was found not to be pure by ^{1}H NMR (residual *i*Pr_2NEt was observed; yield based on ^{1}H NMR, 23%). The residue was used without further purification. HPLC gradient B, t_R = 1.84 min.

The same peptide was obtained using the slow addition cyclization protocol (Table 11, entry 5).

The crude linear peptide **2.67** (61 mg, 0.09 mmol) was dissolved in CH_2Cl_2–DMF (10:1, 24 mL) and added dropwise over 3.5 hours to a solution of HATU (69 mg, 0.18 mmol, 2.0 equiv) and *i*Pr_2NEt (71 μL, 0.41 mmol, 4.5 equiv) in CH_2Cl_2 (12 mL). After the addition, additional HATU (33 mg, 0.09 mmol, 1.0 equiv) and *i*Pr_2NEt (35 μL, 0.20 mmol, 2.3 equiv) was added. The solution was stirred for 16 hours and concentrated. The brown residue was dissolved in CH_2Cl_2 (30 mL) and washed with aq. HCl (0.25 M, 10 mL) and the aqueous phase were extracted with CH_2Cl_2 (3 × 20 mL). The combined organic phases were washed with sat. aq. $NaHCO_3$ (15 mL), brine (15 mL) dried (Na_2SO_4), filtered, and concentrated. Purification by VLC afforded a residue **2.66** (19 mg), which was found not to be sufficiently pure by ^{1}H NMR (residual *i*Pr_2NEt was observed).

Azumamide E [(*Z*)-6-((2*R*,5*R*,8*R*,11*R*,12*S*)-8-Benzyl-2-isopropyl-5,12-dimethyl-3,6,9,13-tetraoxo-1,4,7,10-tetraazacyclotridecan-11-yl)hex-4-enoic acid]

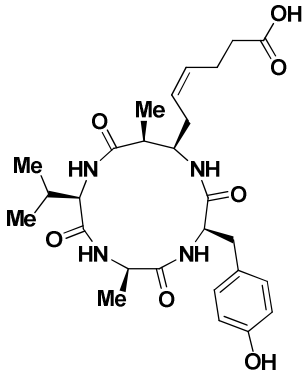

LiOH (18.5 mg, 0.77 mmol, 39 equiv) in water (4 mL) was added to a stirred solution of the impure cyclic peptide **2.68** (10.5 mg, approx. 0.02 mmol) in THF (4 mL). After 1 hour, LiOH (10 mg, 0.42 mmol, 21 equiv) in water (1 mL) was added and after 2 hours LiOH (5.0 mg, 0.21 mmol, 1.0 equiv) in water (0.5 mL) was added. The solution was stirred for 16 h and another portion of LiOH (6.0 mg, 0.25 mmol, 1.3 equiv) in water (0.5 mL) was added. After additionally 2.5 hours of stirring the organic solvent was removed *in vacuo*. The aqueous phase was acidified with 1 M HCl and extracted with EtOAc (4 × 25 mL). The combined organic phases were dried (Na_2SO_4), filtered, and concentrated. The resulting residue was dissolved in MeCN–water [(3:2), 2.5 mL] and purified by preparative HPLC to afford azumamide E (4.3 mg, 15%, 6 steps) as a white solid. $[\alpha]_D$: +66° (*c* = 0.2, MeOH) Litt;[229] $[\alpha]_D$: +53° (*c* = 0.1, MeOH); 1H NMR (500 MHz, CD_3OH) δ 8.10 (d, *J* = 7.7 Hz, 1H), 7.95 (d, *J* = 8.8 Hz, 1H), 7.84 (bs, 1H), 7.63 (d, *J* = 8.4 Hz, 1H), 7.28–7.16 (m, 5H), 5.48 (m, 1H), 5.37 (m, 1H), 4.28 (pentet, *J* = 7.5 Hz, 1H), 4.16 (m, 1H), 4.08 (m, 1H), 3.59 (m, 1H), 3.25 (dd, *J* = 13.6 Hz and 10.4 Hz, 1H), 3.11 (dd, *J* = 13.6 Hz and 6.1 Hz, 1H), 2.72 (m, 1H), 2.68 (m, 1H), 2.39 (d, *J* = 1.7 Hz, 6H), 2.39 (m, 6H), 1.28 (d, *J* = 7.1 Hz, 3H), 1.27 (d, *J* = 7.4 Hz, 3H), 0.94 (m, 6H). HRMS (ESI-TOF): *m/z* calcld. for $C_{27}H_{38}N_4O_6H^+$: 515.2869; found: 515.2869 $[M+H]^+$. HPLC gradient C, t_R = 12.53 min (>95%).

Experimental for chapter 3

Biochemical profiling

Assay Materials

See experimental for chapter 2.

In Vitro Histone Deacetylase Inhibition Assays

For inhibition of recombinant human HDACs the dose–response experiments with internal controls were performed in black low binding NUNC 96-well microtiter plates. Dilution series (3-fold dilution, 6 concentrations) were prepared in HDAC assay buffer from 5–10 mM DMSO stock solutions. The appropriate dilution of inhibitor (5 μL of 5 $\times$ the desired final concentration) was added to each well followed by HDAC assay buffer (10 μL) containing substrate [*Ac-Leu-Gly-Lys(Ac)-AMC* (20 μM) for HDAC1, 2, and 3; (32 μM) for HDAC6 and (40 μM) for HDAC11; (200 μM) for HDAC8; and *Ac-Arg-His-Lys(Ac)-Lys(Ac)-AMC* (50 μM) for HDAC10]. Finally, a solution of the appropriate HDAC (10 μL) was added and the plate was incubated at 37 °C for 30 min. Final HDAC concentrations: HDAC1: 6 ng/μL, HDAC2: 1 or 2 ng/μL, HDAC3: 0.2 ng/μL, HDAC6: 2.4 or 3.6 ng/μL, HDAC8: 0.1 or 0.2 ng/μL, HDAC10: 10 or 14 ng/μL and HDAC11: 10 ng/μL. Then trypsin (25 μL, 0.4 mg/mL) was added and the assay development was allowed to proceed for 15–30 min at room temperature, before the plate was read using a Perkin Elmer Enspire plate reader with excitation at 360 nm and detecting emission at 460 nm. Each assay was performed in duplicate. The data were analyzed as described in chapter 2.

NMR solution structures

NMR

NMR spectra were acquired using standard pulse sequences on a Unity Inova 500 by Varian (499.9 MHz for ^{1}H, 125.7 MHz for ^{13}C) or a Bruker Avance 800 MHz spectrometer (798.9 MHz for ^{1}H and 200.9 MHz for ^{13}C) located at the Danish Instrument Centre for NMR Spectroscopy of Biological Macromolecules at Carlsberg Laboratory.

The deuterated solvent used for all compounds was DMSO-d_6. For homonuclear 2D experiments 4096 data points were recorded in the direct dimension and 512 in the indirect dimension. Typical d1 times were from 2 to 4 seconds, and 8 seconds. The T1 times were investigated for a model compound and all nuclei were found to have T1's below 2 seconds. All *J*-couplings were extracted from the 1D ^{1}H spectra. Distances were obtained from 2D NOESY or ROESY experiments using the initial rate approximation (IRA).[230,231] The linear range was increased by the method suggested by Krishnamurthy et al.[232] Mixing time was 150 ms for all compounds. Prior different mixing times were used to construct buildup curves to ensure that only crosspeaks which fitted the IRA were used. The *J*-couplings from angles were calculated by the Karplus equation for peptides.[233]

It should be noted that it was tried to obtain NMR spectra in D_2O to better simulate a biological environment. This was not possible due to solubility problems. Up to 15 % DMSO-d_6 was added but a concentration that made it possible to obtain spectra was not reached.

Simulations

Simulations were conducted using the program Maestro (Version 9.3.515, MMshare Version 2.1.515) from the Schrödinger suite. Conformational searches in implicit solvents (DMSO and H_2O) were run by MacroModel (version 9.9, Schrödinger, LLC, New York, NY, 2012) using the force fields OPLS2005 and MMFFs. The natural compound was altered to avoid very stable interactions with the ring amide functionalities, as this structure was not supported by the NMR data. The side β^3-side chain amide was thus exchanged with a methyl group. Monte Carlo torsional sampling was used to generate the structures and the minimization method was PRCG. Only conformations within 20 kJ/mol of the found "global" minimum were considered. DMSO was treated as a constant dielectric constant of 47.0. Both solvents and force fields gave similar results, and the distances and torsion angles were optimized by applying constraints on the side groups of valine and the aromatic amino acid residue according to the observed *J*-couplings. The constraints were implemented by calculating the appropriate angles from *J*-couplings, using the structural knowledge obtained from NOE/ROEs. This angle was allowed to differ by 10 degrees and was governed by a force constant of 50 kJ/mol.

The structures obtained as well as structures from non-restricted minimizations were placed in the center of a cubic box of 45x45x45 $Å^3$, and explicit water was added using the program Desmond (Desmond Molecular Dynamics System, version 3.1, D. E. Shaw Research, New York, NY, 2012. Maestro-Desmond Interoperability Tools, version 3.1, Schrödinger, New York, NY, 2012) and the force field OPLS2005.[234] Berendsen coupling was used for temperature and pressure control.[235] The system was minimized by steepest decent to remove unwanted overlaps of atoms. The system was then heated from 30 K to 300 K in two steps; 30 to 100 K in 100 ps and 100 to 300 K in 200 ps. This was done with temperature coupling (tT=0.1 ps). The resulting system was held at 300 K and 1 bar with temperature and pressure couplings (tT=0.1 ps, tP=0.5 ps) and simulations of 10 ns was conducted. Structures were recorded every 20 ps.

Material and methods

General

All chemicals and solvents were analytical grade and used without further purification. Vacuum liquid chromatography (VLC) was performed on silica gel 60 (particle size 0.015−0.040μm). UPLC−MS analyses were performed on a Waters Acquity ultra high-performance liquid chromatography system. A gradient with eluent I (0.1% HCOOH in water) and eluent II (0.1% HCOOH in acetonitrile) rising linearly from 0% to 95% of II during t = 0.00–2.50 min was applied at a flow rate of 1 mL/min (gradient A) or during t = 0.00–5.20 min (gradient B). Analytical HPLC was performed on a [150 mm × 4.6 mm, C_{18} Phenomenex Luna column (3 μm)] using an Agilent 1100 LC system equipped with a UV detector. A gradient, C, with eluent III (95:5:0.1, water−MeCN−TFA) and eluent IV (0.1% TFA in acetonitrile) rising linearly from 0% to 95% of IV during t = 2−20 min was applied at a flow rate of 1 mL/min. Preparative reversed-phase HPLC was performed on a [250 mm × 20 mm, C_{18} Phenomenex Luna column (5 μm, 100 Å)] using an Agilent 1260 LC system equipped with a diode array UV detector and an evaporative light scattering detector (ELSD). A gradient C with eluent III and eluent IV) rising linearly from 0% to 95% of IV during t = 5−45 min was applied at a flow rate of 20 mL/min. 1D and 2D NMR spectra were recorded on a Varian INOVA 500 MHz instrument, a Bruker Ascend 400 MHz or a Varian Mercury 300 instrument. All spectra were recorded at 298 K. For the Varian INOVA 500 MHz instrument and the Varian Mercury 300 instrument 1D NMR spectra were recorded at 499.9 MHz and 300

MHz for 1H and 100 MHz and 75 MHz for 13C, respectively. The correlation spectroscopy (COSY) spectra were recorded with a relaxation delay of 1.5 sec before each scan, a spectral width of 6k × 6k, collecting 8 FIDs and 1k × 512 data points. Heteronuclear single quantum coherence (HSQC) spectra were recorded with a relaxation delay of 1.5 sec before each scan, a spectral width of 6k × 25k, collecting 16 FIDs and 1k × 128 datapoints. Heteronuclear 2-bond correlation (H2BC) spectra were recorded with a relaxation delay of 1.5 sec before each scan, a spectral width of 4k × 35k, collecting 16 FIDs at 295 K and 1k × 256 datapoints. Heteronuclear multiple-bond correlation (HMBC) spectra were recorded with a relaxation delay of 1.5 sec before each scan, a spectral width of 6k × 35 k, collecting 32 FIDs and 1k × 256 datapoints. Finally, on the Bruker Ascend 400 MHz the 1D NMR spectra were recorded at 400 MHz for 1H and 100 MHz for 13C. The correlation spectroscopy (COSY) spectra were recorded with a relaxation delay of 1.5 sec before each scan, a spectral width of 3k × 3k, collecting 4 FIDs and 1k × 128 data points. The heteronuclear single quantum coherence (HSQC) spectra were recorded with a relaxation delay of 1.5 sec before each scan, a spectral width of 4800 × 16600, collecting 4 FIDs and 1k × 256 datapoints. Chemical shifts are reported in ppm relative to deuterated solvent peaks as internal standards (δH, DMSO-d_6 2.50 ppm; δC, DMSO-d_6 39.52 ppm, δH, CD_3OH 3.30 ppm, δH, $CDCl_3$ 7.26 ppm; δC, $CDCl_3$ 77.16 ppm). Coupling constants (*J*) are given in hertz (Hz). Multiplicities of ^{1}H NMR signals are reported as follows: s, singlet; d, doublet; t, triplet; q, quartet; m, multiplet.

General method for Mannich reactions

A solution of LDA (2.1–3.1 equiv) was added dropwise to a solution of the ester (2.0 – 3.0 equiv) in dry THF at – 78 °C. After stirring for 30 min Ti(O-*i*Pr)$_3$Cl (4.2 equiv) in dry THF was added dropwise. The orange solution was stirred for 30 min and the imine (1.0 equiv) in dry THF was added dropwise. The mixture was stirred for 3 h or until TLC showed full conversion of the imine. The mixture was quenched with sat. aq. NH_4Cl and allowed to warm up to room temperature. Water was added and the mixture decanted into a separatory funnel. The remaining Ti precipitate was added EtOAc–water (1:1) and stirred vigorously for 5 min before being added to the separatory funnel. The aqueous phase was extracted with EtOAc and the combined organic phases were washed again with water, dried ($MgSO_4$), filtered, and concentrated *in vacuo*.

***tert*-butyl 3-((*R*)-1,1-dimethylethylsulfinamido)-5-((triisopropylsilyl)oxy)pentanoate (Table 3-2, entry 2)**

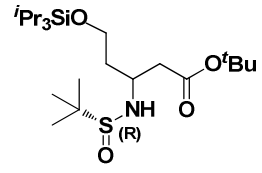

The general procedure was followed using imine **2.14** (187 mg, 0.56 mmol), *tert*-butyl acetate (0.15 mL, 1.12 mmol), LDA (1.8 M, 0.65 mL, 1.17 mmol) and Ti(O-*i*Pr)$_3$Cl (0.60 mL, 2.35 mmol). Diastereoselectivity was determined by ^{1}H NMR integration of the crude reaction mixture (3*R*/3*S*; 74:26). The diastereomers could not be separated by VLC and the purification afforded a mixture of diastereomers as a pale yellow oil (171 mg, 68%).

4-methoxybenzyl 3-((R)-1,1-dimethylethylsulfinamido)hexanoate (Table 3-2, entry 4)

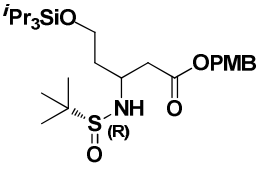

The general procedure was followed using imine **2.14** (169 mg, 0.51 mmol), PMB acetate (0.16 mL, 1.01 mmol), LDA (1.0 M, 1.1 mL, 1.07 mmol) and Ti(O-*i*Pr)$_3$Cl (0.53 mL, 2.13 mmol). To accomplish full conversion of the imine, additional enolate was prepared as above using PMB acetate (90 μL, 0.56 mmol), LDA (0.6 mL, 0.60 mmol) and Ti(O-*i*Pr)$_3$Cl (0.3 mL, 1.21 mmol) and added to the reaction mixture. Diastereoselectivity was determined by ^{1}H NMR integration of the crude reaction mixture (82:18).

tert-butyl 3-((*R*)-1,1-dimethylethylsulfinamido)-5-((triisopropylsilyl)oxy)pentanoate (Table 3-2, entry 3)

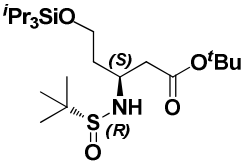

A solution of *tert*-butyl acetate (106 μL, 0.79 mmol, 2.0 equiv) in dry THF (6 mL) was cooled to – 78 °C and added LDA (1.0 M, 0.83 mL, 0.83 mmol, 2.1 equiv) over 5 minutes. After 30 minutes HMPA (0.22 mL, 1.26 mmol, 3.2 equiv) was added and after additional 30 minutes of stirring imine **2.14** (131 mg, 0.39 mmol) in dry THF (0.5 mL) was added dropwise. After 45 minutes the reaction was quenched with sat. aq. NH_4Cl (50 μL) and allowed to warm to room temperature. The reaction mixture was diluted with ethyl acetate (50 mL) and washed with water (10 mL). The aqueous phase was extracted again with ethyl acetate (30 mL) and the combined organic phases were dried ($MgSO_4$), filtered, and concentrated in *in vacuo*. Diastereoselectivity was determined by ^{1}H NMR integration of the crude reaction mixture (3*R*/3*S*; 28:72). Purification by VLC afforded the major 3*S* diastereomer (34 mg, 19%) as well as a fraction containing a mixture of diastereomers (74 mg, 42%). Characterization of major diastereomer: $\alpha_{[D]}$= –37 ° (CH_2Cl_2); ^{1}H NMR (300 MHz, $CDCl_3$) δ 4.07 (d, *J* = 6.5 Hz, 1H), 3.93–3.74 (m, 3H), 2.58 (dd, *J* = 15.8, 6.4 Hz, 1H) 2.47 (dd, *J* = 15.8, 6.4 Hz, 1H), 1.90 (m, 2H), 1.43 (s, 9H), 1.18 (s, 9H), 1.11–0.99 (m, 21H); ^{13}C NMR (75 MHz, $CDCl_3$) δ 171.0, 80.9, 60.9, 55.7, 52.2, 42.1, 37.9, 28.3, 22.8, 18.2, 12.0. HRMS (ESI-TOF): *m/z* calcld. for $C_{22}H_{47}NO_4SSiH^+$: 450.3068; found: 450.3106 $[M+H]^+$.

(*R*)-ethyl 3-((*R*)-1,1-dimethylethylsulfinamido)-5-((triisopropylsilyl)oxy)pentanoate (Table 3-2, entry 1, 3.25)

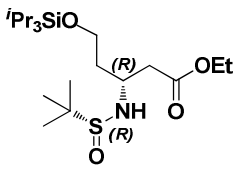

The general procedure was followed using imine **2.14** (0.99 g, 2.97 mmol), ethyl acetate (0.59 mL, 6.0 mmol), LDA (1.0 M, 6.25 mL, 6.30 mmol) and Ti(O-*i*Pr)$_3$Cl (3.00 mL, 12.5 mmol). Only one diastereomer was observed in the ^{1}H NMR and the crude mixture (1.17 g, 94%) was used without further purification. ^{1}H NMR (300 MHz, $CDCl_3$) δ 4.32 (d, *J* = 8.9 Hz, 1H), 4.13 (q, *J* = 7.1 Hz, 2H), 3.78 (m, 1H), 2.89 (dd, *J* = 16.2 and 5.3 Hz, 1H), 2.64 (dd, *J* = 16.2 and 5.0 Hz, 1H), 1.66–1.87 (m, 2H), 1.25 (t, *J* = 7.1 Hz, 3H), 1.21 (s, 9H), 1.04 (m, 21H); ^{13}C NMR (75 MHz, $CDCl_3$) δ 172.3, 60.7, 60.0, 56.0, 51.1, 40.5, 38.5, 22.8, 18.2, 14.3, 12.0; HRMS (ESI-TOF): *m/z* calcld. for $C_{20}H_{43}NO_4SSiNa^+$: 444.2574; found: 444.2584 $[M+Na]^+$.

(*R*)-tert-butyl 3-((*R*)-1,1-dimethylethylsulfinamido)-5-((triisopropylsilyl)oxy)pentanoate (3.26)

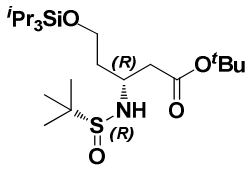

LiOH (98 mg, 4.1 mmol, 1.5 equiv) in water (25 mL) was added to a stirred solution of ethyl ester **3.25** (1.12 g, 2.66 mmol) in THF (25 mL). After 1 hour of stirring additional LiOH (190 mg, 7.9 mmol, 3.0 equiv) in water (8 mL) was added and the solution stirred for 16 h. The mixture was concentrated *in vacuo* and added CH_2Cl_2 (50 mL) and water (30 mL). The pH was adjusted to approximately 2 with HCl (2 M, ≈ 5 mL) and the aqueous phase was extracted with CH_2Cl_2 (60 mL) before the combined organic phases were dried ($MgSO_4$) and concentrated *in vacuo* to afford the acid (1.21 g) as an orange oil. The crude acid was used without further purification. ^{1}H NMR (300 MHz, $CDCl_3$) δ 4.83 (d, *J* = 9.4 Hz, 1H), 3.86–3.70 (m, 3H), 2.96 (dd, *J* = 17.0, 4.6 Hz, 1H), 2.55 (dd, *J* = 17.0, 4.2 Hz, 1H), 1.94 (m, 1H), 1.77 (m, 1H), 1.25 (s, 9H), 1.12–0.94 (m, 21H); ^{13}C NMR (75 MHz, $CDCl_3$) δ 173.8, 59.9, 56.7, 51.6, 39.8, 38.4, 23.0, 18.2, 12.1.

Boc_2O (0.815 g, 3.73 mmol, 1.4 equiv) and DMAP (98 mg, 0.80 mmol, 0.3 equiv) were added to a solution of the crude acid (1.2 g, 2.66 mmol,) in *tert*-butanol (30 mL) and the resulting solution was stirred under N_2 for 16 h. To ensure complete protection of the amino group, Boc_2O (200 mg, 0.92 mmol, 0.3 equiv) was added

and after additional 1.5 h of stirring the mixture was concentrated and the *tert*-butanol was removed by co-evaporation with MeOH (× 3). Purification by VLC afforded the *tert*-butyl ester **3.26** (0.611 g, 44%, 3 steps) as a clear oil. $\alpha_{[D]}$= –20 ° (CH_2Cl_2); ^{1}H NMR (300 MHz, $CDCl_3$) δ 4.31 (d, *J* = 8.6 Hz, 1H), 3.88–3.67 (m, 3H), 2.79 (dd, *J* = 15.9, 5.3 Hz, 1H), 2.56 (dd, *J* = 15.9, 5.1 Hz, 1H), 1.87–1.71 (m, 2H), 1.44 (s, 9H), 1.21 (s, 10H), 1.05 (s, 21H); ^{13}C NMR (75 MHz, $CDCl^3$) δ 171.7, 81.3, 60.1, 56.0, 51.3, 41.8, 38.4, 28.3, 22.9, 18.3, 12.1; HRMS (ESI-TOF): *m/z* calcld. for $C_{22}H_{47}NO_4SSiNa^+$: 472.2887; found: 472.2881 $[M+Na]^+$.

(*R*)-*tert*-butyl 3-((*R*)-1,1-dimethylethylsulfinamido)-5-hydroxypentanoate (3.27)

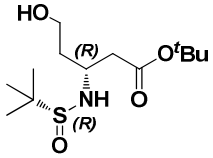

Glacial acetic acid (62 μL, 1.08 mmol, 1.0 equiv) and TBAF (1.0 M, 2.16 mL, 2.16 mmol, 2.0 equiv) was added to a solution of silyl ether **3.26** (0.485 g, 1.08 mmol) in dry THF (20 mL) at 0 °C. After stirring for 15 min the cooling was removed and the stirring continued for 1 hour before the mixture was quenched with methoxy trimethylsilane (0.5 mL, 3.63 mmol, 3.4 equiv). The reaction mixture was concentrated and purification by VLC afforded alcohol **3.27** (0.298 g, 94%) as colorless oil. Upon refrigeration white needle shaped crystals formed. α[D]= –28.6° (CH_2Cl_2); mp 62–64 °C; ^{1}H NMR (300 MHz, $CDCl_3$) δ 4.39 (d, *J* = 7.9 Hz, 1H), 3.76 (m, 3H), 2.70 (dd, *J* = 16.0, 5.8 Hz, 3H), 2.58 (dd, *J* = 16.0, 5.4 Hz, 1H (H-2B), overlapped with O**H**), 1.87 (m, 1 H), 1.75 (m, 1H), 1.43 (s, 9H), 1.20 (s, 9H); ^{13}C NMR (75 MHz, $CDCl_3$) δ 171.3, 81.4, 60.1, 56.1, 51.7, 41.6, 37.8, 28.2, 22.8; HRMS (ESI-TOF): *m/z* calcld. for $C_{13}H_{27}NO_4SH^+$: 294.1734; found: 294.1725 $[M+H]^+$.

(*R,Z*)-9-*tert*-butyl 1-ethyl 7-((*R*)-1,1-dimethylethylsulfinamido)non-4-enedioate (3.29)

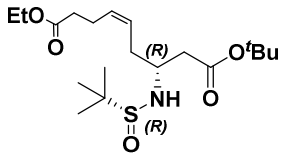

$NaHCO_3$ (178 mg, 2.1 mmol, 1.5 equiv) was added to a stirred solution of the alcohol **3.27** (415 mg, 1.4 mmol) in dry CH_2Cl_2 (18 mL). After cooling to 0 °C, Dess-Martin periodinane reagent (0.90 g, 2.1 mmol, 1.5 equiv) was added to the solution. After 40 min. sat. aq. thiosulfate (20 mL) and sat. aq. $NaHCO_3$ (20 mL) were added and after stirring for 5 min the aqueous phase was extracted with CH_2Cl_2 (140 mL + 100 mL). The combined organic phases were washed with sat. $NaHCO_3$ (70 mL), brine (70 mL), dried ($MgSO_4$), filtered, and concentration *in vacuo* to afford the aldehyde **3.28** (376 mg) as a pale yellow oil. The aldehyde was used immediately without further purification.

A flame dried round-bottomed flask was charged with (4-ethoxy-4-oxobutyl)triphenylphosphonium bromide (1.32 g, 2.89 mmol, 2.0 equiv) and the Wittig reagent dried over high vacuum for 18 hours. Under N_2 the Wittig reagent was dissolved in THF (25 mL) and cooled to –78 °C. KHMDS (0.5 M, 5.37 mL, 2.69 mmol, 1.9 equiv) was added dropwise and the resulting orange solution was stirred for 30 min. The aldehyde **3.28** (376 mg, 1.41 mmol) in dry THF (5 mL) was added dropwise over 10 min and after 30 min of stirring at –78 °C, the reaction was quenched with water (0.1 mL) and the cooling was removed, allowing the reaction mixture to warm up to room temperature. Water (45 mL) was added and the aqueous phase extracted with EtOAc (150 mL + 60 mL). The combined organic phases were dried ($MgSO_4$), filtered, and concentrated *in vacuo*. Purification by VLC afforded the alkene **3.29** (175 mg, 32%, 2 steps) as a pale yellow oil. $\alpha_{[D]}$= –47.2 ° (CH_2Cl_2); ^{1}H NMR (300 MHz, $CDCl_3$) δ 5.45 (m, 2H), 4.19 (d, *J* = 7.1 Hz, 1H), 4.12 (q, *J* = 7.1 Hz, 2H), 3.59 (m, 1H), 2.63 (dd, *J* = 15.9, 5.2 Hz, 1H), 2.49 (dd, *J* = 15.9, 6.0 Hz, 1H), 2.35 (m, 6H), 1.45 (s, 9H), 1.25 (t, *J* = 7.1 Hz, 3H), 1.20 (s, 9H); ^{13}C NMR (75 MHz, CDC_3) δ 173.1, 171.2, 130.6, 126.5, 81.5, 71.2, 60.5, 53.4, 41.0, 34.2, 33.1, 28.3, 23.1, 22.8, 14.4; HRMS (ESI-TOF): *m/z* calcld. for $C_{19}H_{35}NO_5SH^+$: 390.2309 ; found: 390.2310 $[M+H]^+$.

(*R,Z*)-3-((*tert*-butoxycarbonyl)amino)-9-ethoxy-9-oxonon-5-enoic acid (3.31)

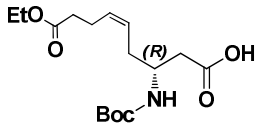

TFA (5 mL) was added to a solution of *tert*-butyl ester **3.29** (170 mg, 0.34 mmol) in dry CH_2Cl_2 (5 mL) under argon at 0 °C. After 2 hours the cooling was removed and the mixture allowed to warm up to room temperature. After stirring for an additional hour the mixture was concentrated and TFA was removed by co-evaporation with CH_2Cl_2–toluene (1:1, 10 mL × 3) and CH_2Cl_2–hexane (1:1, 10 mL × 2) to afford a mixture of the *N*-sulfinyl protected β-amino acid, the β-amino acid containing the free amine and the starting material (152 mg). To ensure complete conversion of the starting material, TFA (5 mL) was added to a solution of the crude residue in dry CH_2Cl_2 (5 mL) under argon at 0 °. After stirring for 1 h the mixture was concentrated and TFA was removed by co-evaporation with CH_2Cl_2–toluene (1:1, 10 mL × 3) and CH_2Cl_2–hexane 1:1, 10 mL × 2) to afford a mixture of the *N*-sulfinyl protected β-amino acid and the β-amino acid containing the free amine (185 mg). To a solution of the crude mixture (185 mg, 0.44 mmol) in dioxane (10 mL) and water (0.10 mL) was added HCl (4.0 M in dioxane, 0.2 mL, 0.77 mmol, 1.8 equiv). After 1 h, TLC showed full conversion and the mixture was concentrated to afford the deprotected β-amino acid chloride salt (152 mg) as a yellow oil.

To a solution of the crude β-amino acid (150 mg, 0.44 mmol) in dry CH_2Cl_2 (11 mL) was added *i*Pr_2NEt (0.23 mL, 1.31 mmol, 3.0 equiv) and Boc_2O (197 mg, 0.90 mmol, 2.0 equiv) in dry CH_2Cl_2 (1 mL) under argon and the mixture was stirred for 6 hours. To ensure complete protection of the amino group, Boc_2O (100 mg, 0.045 mmol, 1.0 equiv) was added and after stirring for additional 16 h the reaction mixture was concentrated *in vacuo* and purification by VLC (0.2% acetic acid in the eluent) afforded the β-amino acid **3.31** (75 mg, 52%, 3 steps) as a yellow oil after co-evaporation of residual acetic acid with CH_2Cl_2–heptane (1:1, 10 mL × 2). $\alpha_{[D]}$= –5.4 ° (CH_2Cl_2); ^{1}H NMR (300 MHz, $CDCl_3$) δ 5.43 (m, 2H), 5.15 (brs, 1H), 4.12 (q, *J* = 7.1 Hz, 1H), 3.95 (brs, 1H), 2.57 (d, *J* = 5.3 Hz, 1H), 2.35 (m, 6H), 1.43 (s, 9H), 1.24 (t, *J* = 7.1 Hz, 3H); ^{13}C NMR (75 MHz, $CDCl_3$) δ 176.2, 173.4, 155.6, 131.0, 126.5, 79.6, 60.6, 47.5, 38.7, 34.1, 32.2, 28.5, 22.9, 14.4; HRMS (ESI-TOF): *m/z* calcld. for $C_{16}H_{27}NO_6H^+$: 330.1911; found: 330.1919 $[M+H]^+$.

(*R,Z*)-3-((((9H-fluoren-9-yl)methoxy)carbonyl)amino)-9-ethoxy-9-oxonon-5-enoic acid (3.30)

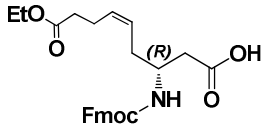

TFA (5 mL) was added to a solution of *tert*-butyl ester **3.29** (217 mg, 0.56 mmol) in dry CH_2Cl_2 (5 mL) at 0 °C. After 15 min the cooling was removed and the mixture allowed to warm up to room temperature. After stirring for an additional 1 hour and 45 minutes the reaction mixture was concentrated and residual TFA was removed by co-evaporation with CH_2Cl_2–toluene (1:1, 10 mL × 3) and CH_2Cl_2–hexane (1:1, 10 mL) to afford the crude acid.

To a solution of the crude acid (0.56 mmol) in dioxane (10 mL) was added HCl (4.0 M in dioxane, 0.35 mL, 1.39 mmol, 2.5 equiv). After 3 hours the mixture was concentrated to afford the deprotected β-amino acid chloride salt (218 mg) as a yellow oil.

A solution of the crude β-amino acid in water (5.0 mL) was added Na_2CO_3 (0.24 g, 2.24 mmol, 4.0 equiv) and cooled to 0° C. Fmoc-O-succinimide (0.23 g, 0.67 mmol, 1.2 equiv) in 1,4-dioxane (1.0 mL) was added dropwise and the cooling removed. After 45 minutes water (25 mL) was added and the mixture cooled to 0° C. After acidification with concentrated HCl (pH 1–2) the aqueous layer was extracted with ethyl acetate (3 × 60 mL). The combined organic phases were dried (Na_2SO_4), filtered, and concentrated. Purification of the crude residue by VLC (0.2% acetic acid in the eluent) afforded β-amino acid **3.30** (124 mg, 49%, 3 steps) as a white solid after co-evaporation of residual acetic acid with CH_2Cl_2–toluene (1:1, 3 × 10 mL). $\alpha_{[D]}$= –6.0 ° (CH_2Cl_2); ^{1}H NMR (400 MHz, $CDCl_3$) δ 7.74 (d, *J* = 7.5 Hz, 2H), 7.58 (d, *J* = 7.5 Hz, 2H), 7.38 (t, *J* = 7.4 Hz, 2H),

7.29 (t, *J* = 7.4, Hz, 2H), 5.56 (d, *J* = 8.5 Hz, 1H), 5.52–5.35 (m, 2H), 4.35 (d, *J* = 6.9 Hz, 2H), 4.21 (d, *J* = 6.9 Hz, 1H), 4.11 (m, 3H), 2.61 (m, 2H), 2.47 – 2.23 (m, 6H), 1.20 (t, *J* = 7.0 Hz, 3H). ^{13}C NMR (101 MHz, $CDCl_3$) δ 176.4, 173.5, 156.2, 144.0, 141.4, 131.2, 127.8, 127.1, 126.4, 125.2, 120.1, 66.9, 60.7, 48.2, 47.3, 38.7, 33.9, 32.0, 22.8, 14.3. HRMS (ESI-TOF): *m/z* calcld. for $C_{26}H_{29}NO_6H^+$: 452.2069; found: 452.2068 $[M+H]^+$.

4-methoxybenzyl 3-((R)-1,1-dimethylethylsulfinamido)-2,2-dimethylhexanoate (Table 3-1, entry 1)

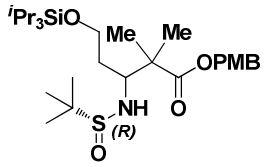

The general procedure was followed using imine **2.14** (185 mg, 0.56 mmol), PBM isobutyrate (0.30 g, 1.40 mmol), LDA (1.2 M, 1.21 mL, 1.44 mmol) and Ti(O-*i*Pr)$_3$Cl (0.63 mL, 2.50 mmol). Diastereoselectivity was determined by ^{1}H NMR integration of the crude reaction mixture (65:35). Purification by VLC afforded the major diastereomer (140 mg, 47%) and the minor diastereomer (40 mg, 13%) as well as a fraction containing a mixture (23 mg, 8.0 %). Characterization of major diastereomer; ^{1}H NMR (300 MHz, $CDCl_3$) δ 7.26 (d, *J* = 8.1 Hz, 2H), 6.87 (d, *J* = 8.6 Hz, 2H), 5.11 (d, *J* = 11.9 Hz, 1H), 4.99 (d, J= 11.9 Hz, 1H), 4.16 (d, *J* = 8.7 Hz, 1H), 3.80 (s, 3H), 3.72 (m, 2H), 3.37 (t, *J* = 9.5 Hz, 1H), 1.82 (m, 1H), 1.37 (m, 1H), 1.31 (s, 3H), 1.25 (s, 3H), 1.14 (s, 9H), 1.03 (m, 21H). ^{13}C NMR (75 MHz, $CDCl_3$) δ 176.4, 159.7, 130.0, 128.7, 128.0, 114.1, 66.3, 60.3, 56.5, 55.4, 48.1, 36.1, 23.1, 22.9, 21.6, 18.2, 12.0. HRMS (ESI-TOF): *m/z* calcld. for $C_{28}H_{51}NO_5SSiH^+$: 542.3335; found: 542.3337 $[M+H]^+$.

Ethyl 3-((R)-1,1-dimethylethylsulfinamido)-2,2-dimethylhexanoate (Table 3-1, entry 2)

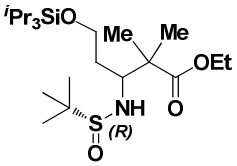

The general procedure was followed using imine **2.14** (160 mg, 0.48 mmol), ethyl isobutyrate (0.13 mL, 0.96 mmol), LDA (1.8 M, 0.56 mL, 1.01 mmol) and Ti(O-*i*Pr)$_3$Cl (0.51 mL, 2.02 mmol). Diastereoselectivity was determined by ^{1}H NMR integration of the crude reaction mixture (64:36). Purification by VLC afforded the major diastereomer (64 mg, 29%) and the minor diastereomer (37 mg, 17%) as well as a fraction containing a mixture (56 mg, 26%). Characterization of major diastereomer; ^{1}H NMR (300 MHz, $CDCl_3$) δ 4.23 (d, *J* = 8.6 Hz, 1H), 4.20–4.07 (m, 2H), 3.74 (m, 2H), 3.38 (ddd, *J* = 10.4, 8.7, 1.8 Hz, 1H), 1.82 (m, 1H), 1.42 (m, 1H), 1.30 (s, 3H), 1.25 (t, *J* = 7.2 Hz, 3H), 1.24 (s, 3H), 1.22 (s, 9H), 1.03 (m, 21H). ^{13}C NMR (75 MHz, $CDCl_3$) δ 177.0, 60.9, 60.8, 60.2, 56.6, 46.4, 36.7, 24.9, 23.4, 23.2, 18.1, 14.3, 12.0. HRMS (ESI-TOF): *m/z* calcld. for $C_{22}H_{47}NO_4SSiH^+$: 450.3074; found: 450.3081 $[M+H]^+$.

Ethyl 5-(benzyloxy)-3-((R)-1,1-dimethylethylsulfinamido)-2,2-dimethylpentanoate (Table 3-1, entry 5)

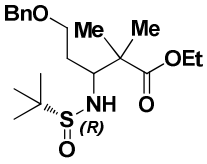

The general procedure was followed using imine **2.14** (186 mg, 0.70 mmol), ethyl isobutyrate (0.23 mL, 1.74 mmol), LDA (1.3 M, 1.40 mL, 1.81 mmol) and Ti(O-*i*Pr)$_3$Cl (0.79 mL, 3.13 mmol). Diastereoselectivity was determined by ^{1}H NMR integration of the crude reaction mixture (53:47). The diastereomers could not be separated by VLC and afforded a mixture of diastereomers (209 mg, 78%).

***tert*-butyl 3-((R)-1,1-dimethylethylsulfinamido)-5-((4-methoxybenzyl)oxy)-2,2-dimethylpentanoate (Table 3-1, entry 6)**

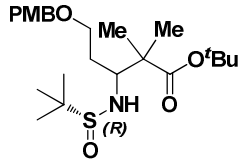

The general procedure was followed using imine **2.14** (166 mg, 0.56 mmol), *tert*-isobutyrate (0.21 g, 1.40 mmol), LDA (1.3 M, 1.12 mL, 1.45 mmol) and Ti(O-*i*Pr)$_3$Cl (0.63 mL, 2.51 mmol). Diastereoselectivity was determined by ^{1}H NMR integration of the

crude reaction mixture (83:17). The diastereomers could not be separated by VLC and afforded a mixture of diastereomers (172 mg, 70%).

Ethyl 3-((R)-1,1-dimethylethylsulfinamido)-5-((4-methoxybenzyl)oxy)-2,2-dimethylpentanoate (Table 3-1, 7)

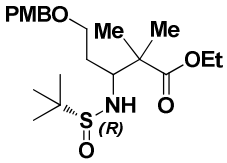

The general procedure was followed using imine **2.14** (183 mg, 0.56 mmol), ethyl isobutyrate (0.21 mL, 0.87 mmol), LDA (1.3 M, 1.23 mL, 1.60 mmol) and Ti(O-*i*Pr)$_3$Cl (0.70 mL, 2.77 mmol). Diastereoselectivity was determined by ^{1}H NMR integration of the crude reaction mixture (66:33). The diastereomers could not be separated by VLC and afforded a mixture of diastereomers (208 mg, 77%).

(*R*)-*tert*-butyl 3-((*S*)-1,1-dimethylethylsulfinamido)-2,2-dimethylhexanoate (Table 3-1, entry 4, 3.12)

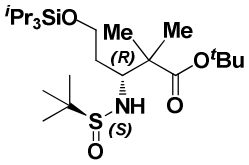

A solution of LDA (1.3 M in THF, 4.3 mL, 5.6 mmol, 2.6 equiv) was added dropwise over 10 min to *tert*-butyl isobutyrate (0.76 g, 5.3 mmol, 2.5 equiv) in dry THF (15 mL) at –78 °C. After stirring for 45 min Ti(O-*i*Pr)$_3$Cl (2.4 mL, 9.5 mmol, 4.5 equiv) in dry THF (2.5 mL) was added dropwise. The resulting orange solution was stirred for 45 min and the imine **2.35** (0.70 g, 2.1 mmol) in dry THF (2.5 mL) was added over 15 minutes. After stirring for 30 min at –78 °C the flask raised allowing cooling only on the bottom of the flask. After additional 20 min of stirring, TLC showed full conversion of the imine, and the mixture was quenched with sat. aq. NH_4Cl (0.1 mL) and allowed to warm up to room temperature. Water (60 mL) was added and the mixture decanted into a separatory funnel containing EtOAc (120 mL). The remaining residue was added EtOAc (15 mL) and water (15 mL) and stirred vigorously for 5 min before added to the separatory funnel. After separation the aqueous phase was extracted with EtOAc (120 mL) and the combined organic phases were washed with brine (100 mL), dried (Na_2SO_4), filtered, and concentrated *in vacuo*. Diastereoselectivity was determined by ^{1}H NMR integration of the crude reaction mixture (3*R*/3*S*; 84:16). Purification by VLC afforded the 3*R* diastereomer **3.12** as a colorless oil (0.584 g, 58%), as well as a fraction containing a mixture of diastereomers (68 mg, 7%) and the 3*S* diastereomer (194 mg, 19%). Characterization data for the (3*R*)-diastereisomer. $\alpha_{[D]}$= 39.3° (CH_2Cl_2); ^{1}H NMR (300 MHz, $CDCl_3$) δ 3.93 (dd, *J* = 7.6, 5.2 Hz, 2H), 3.54–3.34 (m, 2H), 1.89 (m, 1H), 1.52 (m, 1H), 1.44 (s, 9H), 1.21 (s, 9H), 1.13 (s, 3H), 1.11 (s, 3H), 1.05 (m, 21H). ^{13}C NMR (75 MHz, $CDCl_3$) δ 175.8, 80.7, 60.5, 60.3, 56.6, 48.5, 36.6, 28.2, 23.3, 23.1, 22.5, 18.2, 12.1. HRMS (ESI-TOF): *m/z* calcld. for $C_{24}H_{51}NO_4SSiH^+$: 478.3381; found: 478.3387 $[M+H]^+$.

(*R*)-*tert*-butyl 3-((*S*)-1,1-dimethylethylsulfinamido)-2,2-dimethylhexanoate (Table 3-1, entry 3)

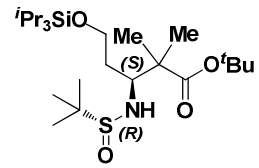

The general procedure was followed using imine **2.14** (172 mg, 0.52 mmol), *tert*-butyl isobutyrate (0.186 g, 1.29 mmol), LDA (1.2 M, 1.03 mL, 1.34 mmol) and Ti(O-*i*Pr)$_3$Cl (0.58 mL, 2.32 mmol). Diastereoselectivity was determined by ^{1}H NMR integration of the crude reaction mixture (3*R*/3*S*; 8:92). Purification by VLC afforded the major diastereomer (88 mg, 36%) and a fraction containing a mixture of diastereomers (25 mg, 10%). Characterization of major diastereomer; $\alpha_{[D]}$= –43.3 ° (CH_2Cl_2); ^{1}H NMR (300 MHz, $CDCl_3$) δ 3.93 (dd, *J* = 7.6, 5.2 Hz, 2H), 3.44 (m, 2H), 1.88 (m, 1H), 1.51 (m, 1H), 1.43 (s, 9H), 1.21 (s, 9H), 1.13 (s, 3H), 1.11 (s, 3H), 1.05 (m, 21H). ^{13}C NMR (75 MHz, $CDCl_3$) δ 175.8, 80.7, 60.5, 60.3, 56.6, 48.5, 36.6, 28.2, 23.3, 23.1, 22.5, 18.2, 12.1. HRMS (ESI-TOF): *m/z* calcld. for $C_{24}H_{51}NO_4SSiH^+$: 478.3381; found: 478.3400 $[M+H]^+$.

(*S*)-*tert*-butyl 3-((*R*)-1,1-dimethylethylsulfinamido)-5-hydroxy-2,2-dimethylpentanoate (S5)

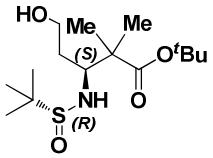

TBAF (1.0 M, 0.36 mL, 0.36 mmol, 2.0 equiv) was added over 10 min to a stirred solution of silyl ether from Table 13, entry 7 (86 mg, 0.18 mmol) and AcOH (10.3 μL, 0.18 mmol, 1.0 equiv) in THF (8 mL) at 0 °C under N_2. After stirring for 30 min the cooling was removed. After stirring for 1 h at room temperature TBAF (20 μL, 20 μmol, 0.06 equiv) was added and after additional 20 minutes of stirring the mixture was concentrated and purified by VLC to afford alcohol **S5** (49.3 mg, 85%) as a white solid. $\alpha_{[D]}$= –20.0° (CH_2Cl_2); ^{1}H NMR (300 MHz, $CDCl_3$) δ 4.29 (bs, 1H), 3.80 (m, 2H), 3.58 (m, 2H), 1.75 (m, 1H), 1.59 (m, 1H), 1.42 (s, 9H), 1.24 (s, 9H), 1.11 (s, 3H), 1.06 (s, 3H). ^{13}C NMR (75 MHz, $CDCl_3$) δ 175.6, 80.9, 62.0, 60.3, 56.8, 48.5, 34.5, 28.2, 23.2, 23.0, 21.6. HRMS (ESI-TOF): *m/z* calcld. for $C_{15}H_{31}NO_4SH^+$: 322.2047; found: 322.2056 $[M+H]^+$.

(*R*)-*tert*-butyl 3-((*S*)-1,1-dimethylethylsulfinamido)-5-hydroxy-2,2-dimethylpentanoate (3.13)

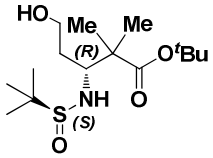

TBAF (1.0 M, 2.4 mL, 2.4 mmol, 2.0 equiv) was added over 10 min to a stirred solution of silyl ether **3.12** (0.56 g, 1.2 mmol) and AcOH (68 μL, 1.2 mmol, 1.0 equiv) in THF (20 mL) at 0 °C under N_2. After stirring for 10 min the cooling was removed. After stirring for 30 min TBAF (0.20 mL, 0.20 mmol, 0.17 equiv) was added and after additionally 15 min of stirring the mixture was concentrated and purified by VLC to afford alcohol **3.13** (318 mg, 84%) as a colorless oil. Upon refrigeration needle shaped crystals formed. $\alpha_{[D]}$= 19.2° (CH_2Cl_2); mp 81–82 °C; ^{1}H NMR (300 MHz, $CDCl_3$) δ 4.29 (t, *J*= 7.2 Hz, 1H), 3.82 (m, 2H), 3.60 (m, 2H), 1.76 (m, 1H), 1.60 (m, 1H), 1.44 (s, 9H), 1.26 (s, 9H), 1.13 (s, 3H), 1.08 (s, 3H). ^{13}C NMR (75 MHz, $CDCl_3$) δ 175.5, 80.8, 62.0, 60.3, 56.7, 48.5, 34.5, 28.2, 23.1, 23.0, 21.3.HRMS (ESI-TOF): *m/z* calcld. for $C_{15}H_{31}NO_4SH^+$: 322.2047; found: 322.2058 $[M+H]^+$.

(*R,Z*)-9-tert-butyl 1-ethyl 7-((*S*)-1,1-dimethylethylsulfinamido)-8,8-dimethylnon-4-enedioate (3.15)

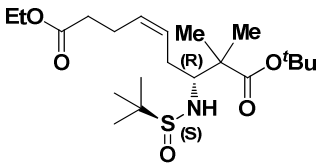

$NaHCO_3$ (125 mg, 1.5 mmol, 1.5 equiv) and Dess-Martin periodinane reagent (645 mg, 1.5 mmol, 1.5 equiv) were added to a stirred solution of alcohol **3.13** (315 mg, 0.98 mmol) in dry CH_2Cl_2 (15 mL) at 0 °C under N_2. After 20 min the flask was raised from the cooling bath allowing cooling on the bottom of the flask. After 20 min the cooling bath was removed and after stirring for 20 min sat. aq. $Na_2S_2O_3$ (10 mL) and sat. aq. $NaHCO_3$ (10 mL) were added and the aqueous phase was extracted with CH_2Cl_2 (2 × 65 mL). The combined organic layers were washed with sat. aq. $NaHCO_3$ (35 mL), brine (35 mL), dried (Na_2SO_4), filtered, and concentrated *in vacuo* to afford the crude aldehyde **3.14** (331 mg) as a pale yellow oil, which was used immediately without further purification.

A flame dried round-bottomed flask was charged with (4-ethoxy-4-oxobutyl)triphenylphosphonium bromide (0.913 g, 1.9 mmol, 2.0 equiv) and the Wittig was reagent dried over high vacuum for 24 hours. The Wittig reagent was the dissolved in dry THF (13 mL) under argon and cooled to –78 °C. KHMDS (0.5 M, 3.65 mL, 1.8 mmol, 1.9 equiv) was added dropwise and the resulting orange solution was stirred for 30 min before the crude aldehyde 3.14 (331 mg, 0.96 mmol) in dry THF (3.0 mL) was added dropwise. After 16 hours, while gradually allowing the mixture to warm to room temperature, the reaction mixture was concentrated and water (30 mL) was added. The aqueous phase was extracted with EtOAc (2 × 70 mL). The combined organics were washed with brine (40 mL), dried (Na_2SO_4), filtered, and concentrated *in vacuo*. Purification by VLC afforded alkene **3.15** as a pale yellow oil (222 mg, 54%, 2 steps). $\alpha_{[D]}$= 42.9° (CH_2Cl_2); ^{1}H NMR (300 MHz, $CDCl_3$) δ 5.59 (dt, *J* = 11.2, 7.0 Hz, 1H), 5.46 (m, 1H), 4.09 (q, *J*= 7.1 Hz, 2H), 3.42 (m, 1H), 3.32 (d, *J* = 7.4 Hz,

1H), 2.30 (m, 6H), 1.43 (s, 9H), 1.20 (s, 9H), 1.15 (s, 3H), 1.10 (s, 3H). ^{13}C NMR (75 MHz, $CDCl_3$) δ 175.6, 173.2, 130.2, 127.5, 80.8, 62.4, 60.4, 56.6, 48.6, 34.0, 30.6, 28.1, 23.7, 23.1, 23.0, 21.4, 14.4.
HRMS (ESI-TOF): *m/z* calcld. for $C_{21}H_{39}NO_5SH^+$: 418.2622; found: 418.2642 $[M+H]^+$.

(*R,Z*)-3-((tert-butoxycarbonyl)amino)-9-ethoxy-2,2-dimethyl-9-oxonon-5-enoic acid (3.16)

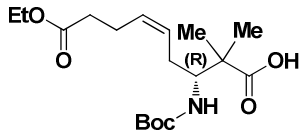

TFA (5 mL, 126 equiv) was added to a solution of *tert*-butyl ester **3.15** (220 mg, 0.52 mmol) in dry CH_2Cl_2 (5 mL) at 0 °C and the mixture allowed to warm to room temperature. After 2 hours the mixture was concentrated and excess TFA was removed by co-evaporation with toluene–CH_2Cl_2 (1:1, 10 mL × 3) and hexane–CH_2Cl_2 (1:1, 10 mL × 2) to afford the crude acid (224 mg).

HCl in dioxane (4.0 M, 0.20 mL, 0.79 mmol, 1.5 equiv) was added to a solution of crude sulfinyl protected amine in 1,4-dioxane (8.0 mL). After 2 hours additional HCl in dioxane (0.05 mL, 0.4 equiv) was added and after 30 minutes the mixture was concentrated to afford the crude unprotected β-amino acid (219 mg).
To a solution of the crude β-amino (219 mg) in dry CH_2Cl_2 (7 mL) and *i*Pr_2NEt (0.37 mL, 2.1 mmol, 4.0 equiv) was added Boc_2O (235 mg, 1.1 mmol, 2.0 equiv) in dry CH_2Cl_2 (2 mL) under argon. After 20 hours the reaction mixture was concentrated and *i*Pr_2NEt was removed by co-evaporation with toluene. Purification of the crude residue VLC (0.2% acetic acid in the eluent) afforded **3.16** (114 mg, 61%, 3 steps) as a colorless oil after co-evaporation of residual acetic acid with CH_2Cl_2–toluene (1:1, 10 mL × 3). $\alpha_{[D]}$= –40.9 °; ^{1}H NMR (300 MHz, $CDCl_3$) δ 5.42 (m, 2H), 4.98 (d, *J* = 10.5 Hz, 1H), 4.12 (q, *J* = 7.1, Hz, 2H), 3.73 (td, *J* = 10.5, 3.4 Hz, 1H), 2.49–2.08 (m, 7H), 1.41 (s, 9H), 1.28–1.20 (m, 9H). ^{13}C NMR (75 MHz, $CDCl_3$) δ 182.4, 173.5, 156.4, 129.9, 127.6, 79.3, 60.6, 57.0, 46.5, 34.2, 29.2, 28.5, 23.5, 22.9 (×2), 14.4. HRMS (ESI-TOF): *m/z* calcld. for $C_{18}H_{31}NO_6H^+$: 358.2230; found: 358.2240 $[M+H]^+$.

(2*R*,5*R*,8*R*,12*R*,*Z*)-12-amino-2-benzyl-8-isopropyl-5-methyl-4,7,10,18-tetraoxo-19-oxa-3,6,9-triazahenicos-14-en-1-oic acid (3.32)

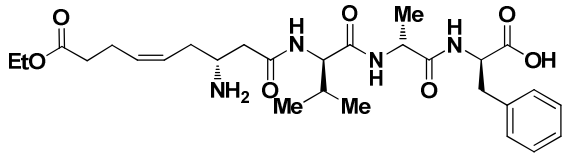

Polystyrene 2-chlorotrityl-bound Fmoc-(D)Val–(D)Ala–(D)Phe (224 mg, 0.11 mmol, 1.5 equiv) was added to a fritted syringe and the Fmoc group was removed with piperidine–DMF (1:4, 4 mL, 2 × 25 min) and DBU–piperidine–DMF (2:2:96, 4 mL, 30 min). The resin was then washed with DMF (×3), MeOH (×3), CH_2Cl_2 (×3). β-amino acid **3.31** (24.6 mg, 0.075 mmol) in DMF (2.2 mL) was preincubated for 5 min with 2,6-lutidine (26 μL, 0.22 mmol, 3.0 equiv) and HATU (44 mg, 0.12 mmol, 1.5 equiv) before addition to the resin and the reaction was allowed to proceed on a rocking table for 16 hours. After washing [DMF (×3), MeOH (×3), CH_2Cl_2 (×3)] the resin was treated with TFA–CH_2Cl_2 (1:1, 4 mL) for 1 h followed by washing with CH_2Cl_2 (5 mL). A fresh portion of TFA–CH_2Cl_2 (1:1, 4 mL) was added to the resin and after additional 30 min the resin was drained and all the fractions were pooled and concentrated *in vacuo* to provide the linear peptide as an oily residue. Precipitation with diethyl ether afforded the TFA salt of the linear peptide **3.32** (45 mg, 91%) as a white solid. UPLC-MS gradient A, t_R = 1.36 min, *m/z* calcld. for $C_{28}H_{42}N_4O_7H^+$: 547.3; found: 547.4 $[M+H]^+$.

(*Z*)-ethyl-6-((2*R*,5*R*,8*R*,11*R*)-8-benzyl-2-isopropyl-5-methyl-3,6,9,13-tetraoxo-1,4,7,10-tetraazacyclotridecan-11-yl)hex-4-enoate (3.33)

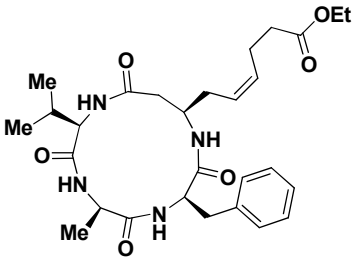

The linear peptide **3.32** (45 mg, 0.068 mmol) was dissolved in DMF (200 mL ≈ 0.34 mM) and *i*Pr_2NEt (131 μL, 0.75 mmol, 10 equiv) and HATU (57 mg, 0.15 mmol, 2.2 equiv) were added. The solution was stirred for 16 hours and the reaction mixture was concentrated. The residue was taken up in EtOAc (200 mL), which afforded a white precipitate (HOAt). The EtOAc was decanted off and washed with aq. HCl (1.0 M, 10 mL × 3) and concentrated to afford the cyclic peptide **3.33** (127 mg) as a brown oil. UPLC-MS gradient A t_R = 1.87 min, m/z calcld. for $C_{28}H_{40}N_4O_6$: 529.3; found: 529.4 $[M+H]^+$.

(*Z*)-6-((2*R*,5*R*,8*R*,11*R*)-8-benzyl-2-isopropyl-5-methyl-3,6,9,13-tetraoxo-1,4,7,10-tetraazacyclotridecan-11-yl)hex-4-enoic acid (3.01)

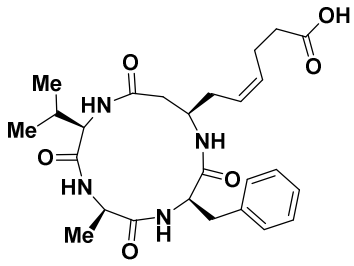

LiOH (38 mg, 1.59 mmol, 23 equiv) in water (5 mL) was added to the cyclic peptide **3.33** (127 mg, 0.068 mmol) in THF (5 mL). To ensure a pH value above 10, additional LiOH (21 mg, 0.88 mmol, 13.0 equiv) was added and the solution was stirred for 16 h. The mixture was concentrated *in vacuo* and dissolved in DMF–MeCN (8:2, 3.0 mL) before purification by preparative HPLC afforded β^2-desmethyl azumamide E (**3.01**) (8.1 mg, 21%, 5 steps) as a white solid. Two conformations are observed in a 94:6 ratio. Characterization is given for the major conformation. ^{1}H NMR (799 MHz, DMSO) δ 12.08 (s, 1H), 7.86 (d, *J* = 6.8 Hz, 1H), 7.66 (d, *J* = 9.0 Hz, 1H), 7.43 (d, *J* = 9.0 Hz, 1H), 7.35 (d, *J* = 6.6 Hz, 1H), 7.28 (m, 2H), 7.16–7.23 (m, 3H), 5.48 (m, 1H), 5.37 (dt, *J* = 10.5, 7.4 Hz, 1H), 4.30–4.21 (m, 2H), 3.93 (dd, *J* = 7.2, 3.6 Hz, 1H), 3.81 (t, *J* = 6.7 Hz, 1H), 2.95 (dd, *J* = 13.8, 5.8 Hz, 1H), 2.82 (dd, *J* = 13.8, 9.5 Hz, 1H), 2.50 (m, 1H), 2.29 (m, 7H), 1.94 (m, 1H), 1.15 (d, *J* = 7.3 Hz, 3H), 0.94 (d, *J* = 6.8 Hz, 3H), 0.91 (d, *J* = 6.8 Hz, 3H). HRMS (ESI-TOF): *m/z* calcld. for $C_{26}H_{36}N_4O_6H^+$: 501.2708; found: 501.2713 $[M+H]^+$. HPLC gradient C, t_R = 11.70 min (>95%).

(2*R*,5*R*,8*R*,12*R*,*Z*)-12-amino-2-(4-hydroxybenzyl)-8-isopropyl-5-methyl-4,7,10,18-tetraoxo-19-oxa-3,6,9-triazahenicos-14-en-1-oic acid (3.34)

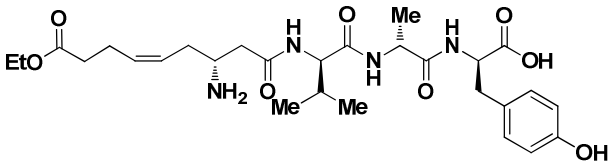

Polystyrene 2-chlorotrityl-bound Fmoc-(D)Val–(D)Ala–(D)Tyr (187 mg, 0.10 mmol, 1.0 equiv) was added to a fritted syringe and the Fmoc group was removed with piperidine–DMF (1:4, 4 mL, 2 × 30 min) and DBU–piperidine–DMF (2:2:96, 4 mL, 30 min). The resin was then washed with DMF (×3), MeOH (×3), CH_2Cl_2 (×3). β-amino acid **3.30** (51 mg, 0.11 mmol, 1.1 equiv) in DMF (1.8 mL) was preincubated for 5 min with 2,6-lutidine (36 μL, 0.31 mmol, 3.0 equiv) and HATU (59 mg, 0.16 mmol, 1.5 equiv) before addition to the resin and the reaction was allowed to proceed on a rocking table for 16 hours. After washing [DMF (×3), MeOH (×3), CH_2Cl_2 (×3)] the resin was added piperidine–DMF (1:4, 4 mL, 2 × 30 min) and DBU–piperidine–DMF (2:2:96, 4 mL, 30 min). The resin was then washed with DMF (×3), MeOH (×3), CH_2Cl_2 (×3) and treated with TFA–CH_2Cl_2 (1:1, 4 mL) for 45 min followed by washing with CH_2Cl_2 (5 mL). A fresh portion of TFA–CH_2Cl_2 (1:1, 4 mL) was added to the resin and after additional 45 min the resin was drained and all the fractions were pooled and concentrated *in vacuo* to provide the linear peptide as an oily residue. Precipitation with diethyl ether afforded the TFA salt of the linear peptide **3.34** (72 mg, 100 %)

as a white solid. ^{1}H NMR (400 MHz, MeOD) δ 7.04 (d, *J* = 8.5 Hz, 2H), 6.68 (d, *J* = 8.5 Hz, 2H), 5.63 (m, 1H), 5.43 (m, 1H), 4.56 (dd, *J* = 7.7, 5.4 Hz, 1H), 4.39 (q, *J* = 7.1 Hz, 1H), 4.18 (d, *J* = 6.7 Hz, 1H), 4.12 (q, *J* = 7.1 Hz, 2H) 3.56 (m, 1H), 3.07 (dd, *J* = 14.0, 5.4 Hz, 1H), 2.92 (dd, *J* = 14.0, 7.7 Hz, 1H), 2.73 (dd, *J* = 16.5, 4.3 Hz, 1H), 2.57 (dd, *J* = 16.5, 8.5 Hz, 1H), 2.50–2.33 (m, 6H), 2.05 (octet, *J* = 6.8 Hz, 1H), 1.33 (d, *J* = 7.1 Hz, 3H), 1.24 (t, *J* = 7.1 Hz, 3H), 0.94 – 0.91 (m, 6H). UPLC-MS gradient B, t_R = 1.10 min, *m/z* calcld. for $C_{28}H_{42}N_4O_8H^+$: 563.3; found: 563.3 $[M+H]^+$.

(*Z*)-ethyl-6-((2*R*,5*R*,8*R*,11*R*)-8-(4-hydroxybenzyl)-2-isopropyl-5-methyl-3,6,9,13-tetraoxo-1,4,7,10-tetraazacyclotridecan-11-yl)hex-4-enoate (3.36a)

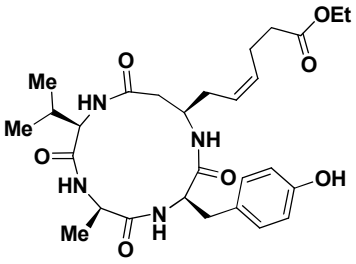

The linear peptide **3.34** (67 mg, 0.099 mmol) was dissolved in DMF (240 mL ≈ 0.4 mM) and *i*Pr$_2$NEt (138 μL, 0.79 mmol, 8.0 equiv) and HATU (57 mg, 0.15 mmol, 1.5 equiv) were added. The solution was stirred for 16 hours and the reaction mixture was concentrated. Purification by VLC afforded the cyclic peptide (22 mg). ^{1}H NMR showed a mixture of the cyclic peptide **3.36a** and an unidentified impurity. The cyclic peptide was used without further purification. UPLC-MS gradient B, t_R = 1.60 min, *m/z* calcld. for $C_{28}H_{42}N_4O_8H^+$: 545.3; found: 545.3 $[M+H]^+$

(*Z*)-6-((2*R*,5*R*,8*R*,11*R*)-8-(4-hydroxybenzyl)-2-isopropyl-5-methyl-3,6,9,13-tetraoxo-1,4,7,10-tetraazacyclotridecan-11-yl)hex-4-enoic acid (3.02)

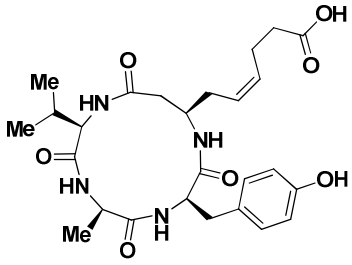

LiOH (44 mg, 1.84 mmol, 50 equiv) in water (4 mL) was added to the cyclic peptide **3.36a** (20 mg, 0.037 mmol) in THF (4 mL). After 17 hours the mixture was concentrated *in vacuo* and dissolved in DMF–MeCN–water (2:1:2, 2.5 mL) and purified by preparative HPLC to afford β^2-desmethyl azumamide C (**3.02**) (11.2 mg, 22%, 5 steps) as a white solid. Two conformations are observed in a 92:8 ratio. Characterization is given for the major conformation. ^{1}H NMR (500 MHz, DMSO) δ 7.87 (d, *J* = 6.9 Hz, 1H), 7.56 (d, *J* = 9.7 Hz, 1H), 7.43 (d, *J* = 9.8 Hz, 1H), 7.25 (d, *J* = 7.0 Hz, 1H), 6.95 (d, *J* = 8.4 Hz, 2H), 6.65 (d, *J* = 8.4 Hz, 2H), 6.52 (bs, 1H), 5.47 (m, 1H), 5.37 (m, 1H), 4.28 (dq, *J* = 9.7, 7.4 Hz, 1H), 4.16 (m, 1H), 3.93 (m, 1H), 3.81 (t, *J* = 6.6 Hz, 1H), 2.82 (dd, *J* = 13.9, 5.7 Hz, 1H), 2.70 (dd, *J* = 13.9, 9.3 Hz, 1H), 2.47 (m, 1H), 2.27 (m, 7H), 1.95 (m, 1H), 1.16 (d, *J* = 7.3 Hz, 3H), 0.93 (d, *J* = 6.9 Hz, 3H), 0.91 (d, *J* = 6.9 Hz, 3H). HRMS: *m/z* calcld. for $C_{26}H_{36}N_4O_7H^+$: 517.2657; found: 517.2658 $[M+H]^+$. HPLC gradient C, t_R = 10.11 min (>95%).

(2*R*,5*R*,8*R*,12*R*,*Z*)-12-amino-2-((1-(*tert*-butoxycarbonyl)-1H-indol-3-yl)methyl)-8-isopropyl-5-methyl-4,7,10,18-tetraoxo-19-oxa-3,6,9-triazahenicos-14-en-1-oic acid (3.35)

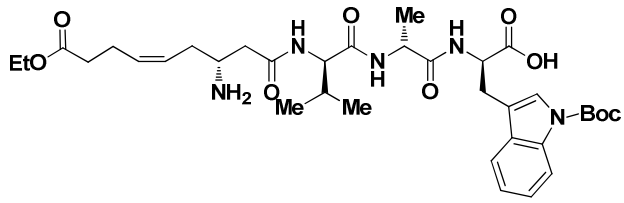

Polystyrene 2-chlorotrityl-bound Fmoc-(D)Val–(D)Ala–(D)Trp(*N*-Boc) (193 mg, 0.10 mmol, 1.0 equiv) was added to a fritted syringe and the Fmoc group was removed with piperidine–DMF (1:4, 4 mL, 2 × 30 min) and DBU–piperidine–DMF (2:2:96, 4 mL, 30 min). The resin was then washed with DMF (×3), MeOH (×3), CH_2Cl_2 (×3). β-amino acid **3.30** (49 mg, 0.11 mmol, 1.1 equiv) in DMF (1.8 mL) was preincubated for 5 min with 2,6-lutidine (34 μL, 0.30 mmol, 3.0 equiv) and HATU (57 mg, 0.15 mmol, 1.5 equiv) before addition

to the resin and the reaction was allowed to proceed on a rocking table for 16 hours. After washing [DMF (×3), MeOH (×3), CH_2Cl_2 (×3)] the resin was added piperidine–DMF (1:4, 4 mL, 2 × 30 min) and DBU–piperidine–DMF (2:2:96, 4 mL, 30 min). The resin was then washed with DMF (×3), MeOH (×3), CH_2Cl_2 (×3) and treated with CH_2Cl_2–AcOH–triflouroethanol (6:2:2, 1.5 mL) for 2 hours followed by washing with CH_2Cl_2 (3 mL). A fresh portion of CH_2Cl_2–AcOH–triflouroethanol (6:2:2, 1.5 mL) was added to the resin and after additional 2 hours the resin was drained and all the fractions were pooled and concentrated *in vacuo* to provide the linear peptide as an oily residue. Residual AcOH was removed by co-evaporation with toluene (3 × 10 mL) to afford the TFA salt of the linear peptide **3.35** (37 mg, 47%) as a white solid. ^{1}H NMR (400 MHz, MeOD) δ 8.05 (d, *J* = 8.0 Hz, 1H), 7.65 (d, *J* = 7.3 Hz, 1H), 7.46 (s, 1H), 7.22 (m, 2H), 5.61 (m, 1H), 5.41 (m, 1H), 4.43 (t, *J* = 5.5 Hz, 1H), 4.31 (q, *J* = 7.1 Hz, 1H), 4.11 (m, 3H), 3.54 (m, 1H), 3.36 (m, 1H(overlapped with solvent signal)), 3.20 (m, 1H), 2.68 (dd, *J* = 16.4, 4.3 Hz, 1H), 2.56 (dd, *J* = 16.4, 9.3 Hz, 1H), 2.40 (m, 6H), 2.00 (m, 1H), 1.66 (s, 9H), 1.30 (d, *J* = 9.4 Hz, 3H), 1.24 (t, *J* = 7.1 Hz, 3H), 0.90 (m, 6H). UPLC-MS gradient B, t_R = 1.84 min, *m/z* calcld. for $C_{35}H_{51}N_5O_9H^+$: 686.4; found: 686.0 $[M+H]^+$.

tert-butyl-3-(((3*R*,6*R*,9*R*,13*R*)-13-((*Z*)-6-ethoxy-6-oxohex-2-en-1-yl)-9-isopropyl-6-methyl-2,5,8,11-tetraoxo-1,4,7,10-tetraazacyclotridecan-3-yl)methyl)-1H-indole-1-carboxylate (3.36b)

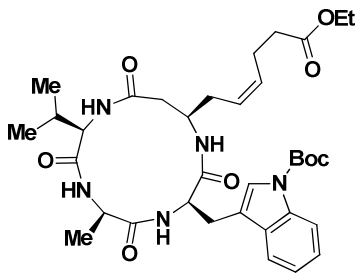

The linear peptide **3.35** (35 mg, 0.051 mmol) was dissolved in DMF (130 mL ≈ 0.4 mM) and *i*Pr$_2$NEt (71 μL, 0.41 mmol, 10 equiv) and HATU (29 mg, 0.77 mmol, 1.5 equiv) were added. The solution was stirred for 16 hours and the reaction mixture was concentrated. Purification by VLC afforded the cyclic peptide (30 mg) as a white amorphous solid. ^{1}H NMR showed a mixture of the cyclic peptide (**3.36b**) and an unidentified impurity. The cyclic peptide was used without further purification. UPLC-MS gradient B, t_R = 2.52 min, *m/z* calcld. for $C_{35}H_{49}N_5O_8H^+$: 668.4; found: 668.4 $[M+H]^+$.

(*Z*)-6-((2*R*,5*R*,8*R*,11*R*)-8-((1H-indol-3-yl)methyl)-2-isopropyl-5-methyl-3,6,9,13-tetraoxo-1,4,7,10-tetraazacyclotridecan-11-yl)hex-4-enoic acid (3.03)

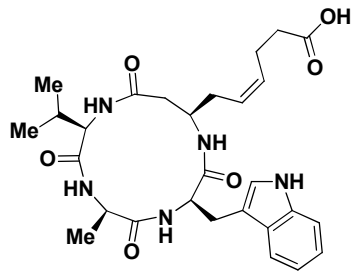

LiOH (54 mg, 2.25 mmol, 50 equiv) in water (4 mL) was added to the impure cyclic peptide **3.36b** (30 mg, 0.045 mmol) in THF (4 mL). After 17 hours the THF was removed *in vacuo* and the aqueous phase was acidified to pH 1–2 with 2M HCl and extracted with CH_2Cl_2 (3 × 50 mL) and EtOAc (2 × 40 mL). All the organic fractions were pooled and concentrated *in vacuo*. The residue was taken up in CH_2Cl_2 (6 mL) and added TFA (6 mL). After 1 hour the solvent was removed *in vacuo* and the residue was dissolved in DMF–MeCN–water (1:2:2, 2.5 mL) and purified by preparative HPLC to afford the acid **3.03** (2.6 mg, 5%, 6 steps) as a white solid. Two conformations are observed in a 97:3 ratio. Characterization is given for the major conformation. ^{1}H NMR (500 MHz, DMSO) δ 12.08 (bs, 1H), 10.87 (bs, 1H), 7.83 (m, 1H), 7.51 (m, 3H), 7.33 (d, *J* = 8.1 Hz, 1H), 7.27 (m, 1H), 7.08 (s, 1H), 7.06 (t, *J* = 7.8 Hz, 1H), 6.97 (t, *J* = 7.4 Hz, 1H), 5.47 (m, 1H), 5.33 (m, 1H), 4.36 (m, 1H), 4.30 (m, 1H), 3.92 (m, 1H), 3.82 (t, *J* = 6.5 Hz, 1H), 3.01 (m, 2H), 2.45 (m, 1H), 2.33–2.14 (m, 7H), 1.94 (m, 1H), 1.15 (d, *J* = 7.3 Hz, 3H), 0.92 (d, *J* = 7.4 Hz, 3H), 0.90 (d, *J* = 7.4 Hz, 3H). HRMS (ESI-TOF):: *m/z* calcld. for $C_{28}H_{37}N_5O_6H^+$: 540.2817; found: 540.2814 $[M+H]^+$. HPLC gradient C, t_R = 10.53 min (>95%).

(2*R*,5*R*,8*R*,12*R*,*Z*)-12-amino-2-benzyl-8-isopropyl-5,11,11-trimethyl-4,7,10,18-tetraoxo-19-oxa-3,6,9-triazahenicos-14-en-1-oic acid (3.48)

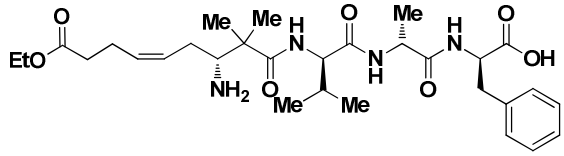

Polystyrene 2-chlorotrityl-bound Fmoc-(D)Val–(D)Ala–(D)Phe (239 mg, 0.12 mmol, 1.5 equiv) was added to a fritted syringe and the Fmoc group was removed with piperidine–DMF (1:4, 4 mL, 2 × 25 min) and DBU–piperidine–DMF (2:2:96, 4 mL, 30 min). The resin was then washed with DMF (×3), MeOH (×3), CH_2Cl_2 (×3). β-amino acid **3.16** (28.5 mg, 0.080 mmol) in DMF (2.0 mL) was preincubated for 5 min with *i*Pr_2NEt (42 μL, 0.24 mmol, 3.0 equiv) and HATU (46 mg, 0.12 mmol, 1.5 equiv) before addition to the resin and the reaction was allowed to proceed on a rocking table for 16 hours. After washing [DMF (×3), MeOH (×3), CH_2Cl_2 (×3)] the resin was treated with TFA–CH_2Cl_2 (1:1, 4 mL) for 1 h followed by washing with CH_2Cl_2 (5 mL). A fresh portion of TFA–CH_2Cl_2 (1:1, 4 mL) was added to the resin and after additional 30 min the resin was drained and all the fractions were pooled and concentrated *in vacuo* to provide the linear peptide as an oily residue. Precipitation with diethyl ether afforded the TFA salt of the linear peptide **3.48** (83 mg) as a white solid. UPLC-MS gradient B, t_R = 1.35 min, *m/z* calcld. for $C_{30}H_{46}N_4O_7H^+$: 575.3; found: 575.3 $[M+H]^+$.

(*Z*)-ethyl-6-((2*R*,5*R*,8*R*,11*R*)-8-benzyl-2-isopropyl-5,12,12-trimethyl-3,6,9,13-tetraoxo-1,4,7,10-tetraazacyclotridecan-11-yl)hex-4-enoate (S6)

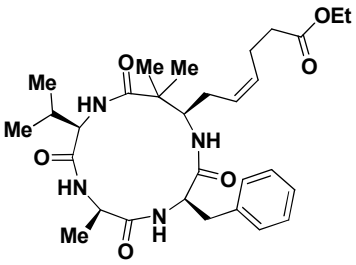

The linear peptide **3.48** (35 mg, 0.08 mmol) was dissolved in DMF (200 mL ≈ 0.4 mM) and *i*Pr_2NEt (140 μL, 0.80 mmol, 10 equiv) and HATU (61 mg, 0.16 mmol, 2.0 equiv) were added. The solution was stirred for 16 hours and the reaction mixture was concentrated and added EtOAc (200 mL), which afforded a white precipitate (HOAt). The EtOAc was decanted off and washed with aq. HCl (1.0 M, 10 mL × 3) and concentrated to afford the crude cyclic peptide **S6** (76 mg) as a brown oil. UPLC-MS gradient B, t_R = 1.92 min, *m/z* calcld. for $C_{32}H_{51}N_4O_6H^+$: 557.7; found: 557.2 $[M+H]^+$.

(*Z*)-6-((2*R*,5*R*,8*R*,11*R*)-8-benzyl-2-isopropyl-5,12,12-trimethyl-3,6,9,13-tetraoxo-1,4,7,10-tetraazacyclotridecan-11-yl)hex-4-enoic acid (3.51)

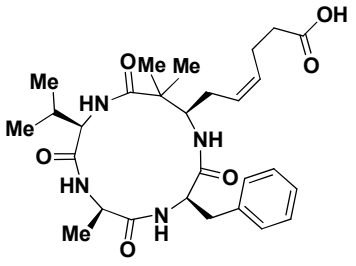

LiOH (67 mg, 2.79 mmol, 35 equiv) in water (5 mL) was added to the impure cyclic peptide **S6** (30 mg, 0.08 mmol) in THF (5 mL). After 16 hours the mixture was concentrated *in vacuo* and and the residue was dissolved in DMF and purified by preparative HPLC to afford the acid **3.51** (2.6 mg, 4%, 5 steps) as a white solid. Two conformations are observed in a 91:9 ratio. Characterization is given for the major conformation. ^{1}H NMR (500 MHz, DMSO) δ 8.04 (bs, 1H), 7.38 (bs, 1H), 7.27–7.11 (m, 6H), 7.05 (d, *J* = 9.5 Hz, 1H), 5.16 (m, 1H), 4.99 (m, 1H), 4.40 (m, 1H), 4.14 (dq, *J* = 8.4, 7.9 Hz, 1H), 4.05 (m, 1H), 3.70 (dd, *J*= 10.1, 8.7 Hz, 1H), 3.00 (dd, *J* = 13.6, 8.0 Hz, 2H), 2.70 (dd, *J* = 13.6, 6.6 Hz, 1H), 2.16 (m, 5H), 2.01 (m, 2H), 1.15–1.3 (m, 6H), 1.04 (s, 3H), 0.85–0.84 (m, 6H). HRMS (ESI-TOF): *m/z* calcld. for $C_{28}H_{40}N_4O_6Na^+$: 551.2840; found: 551.2839 $[M+Na]^+$. HPLC gradient C, t_R = 12.94 min (>95%).

(2*R*,5*R*,8*R*,12*R*,*Z*)-12-amino-2-(4-hydroxybenzyl)-8-isopropyl-5,11,11-trimethyl-4,7,10,18-tetraoxo-19-oxa-3,6,9-triazahenicos-14-en-1-oic acid (3.49)

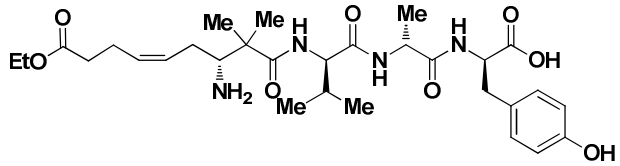

Polystyrene 2-chlorotrityl-bound Fmoc-(D)Val–(D)Ala–(D)Tyr (279 mg, 0.14 mmol, 1.5 equiv) was added to a fritted syringe and the Fmoc group was removed with piperidine–DMF (1:4, 4 mL, 2 × 25 min) and DBU–piperidine–DMF (2:2:96, 4 mL, 30 min). The resin was then washed with DMF (×3), MeOH (×3), CH_2Cl_2 (×3). *β*-amino acid **3.16** (33 mg, 0.082 mmol) in DMF (2.0 mL) was preincubated for 5 min with *i*Pr_2NEt (45 μL, 0.28 mmol, 3.0 equiv) and COMU (61 mg, 0.14 mmol, 1.5 equiv) before addition to the resin and the reaction was allowed to proceed on a rocking table for 16 hours. After washing [DMF (×3), MeOH (×3), CH_2Cl_2 (×3)] the resin was treated with TFA–CH_2Cl_2 (1:1, 4 mL) for 30 min followed by washing with CH_2Cl_2 (5 mL). A fresh portion of TFA–CH_2Cl_2 (1:1, 4 mL) was added to the resin and after additional 30 min the resin was drained and all the fractions were pooled and concentrated *in vacuo* to provide the linear peptide (**3.49**) as an oily residue (141 mg). UPLC-MS gradient B, t_R = 1.17 min, *m/z* calcld. for $C_{30}H_{46}N_4O_8H^+$: 591.3; found: 591.3 $[M+H]^+$.

(*Z*)-ethyl 6-((2*R*,5*R*,8*R*,11*R*)-8-(4-hydroxybenzyl)-2-isopropyl-5,12,12-trimethyl-3,6,9,13-tetraoxo-1,4,7,10-tetraazacyclotridecan-11-yl)hex-4-enoate (S7)

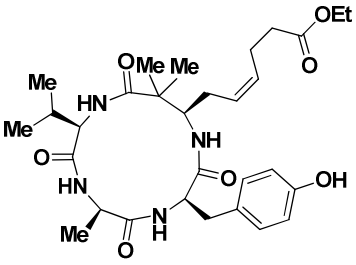

The linear peptide **3.48** (35 mg, 0.092 mmol) was dissolved in DMF (230 mL ≈ 0.4 mM) and *i*Pr_2NEt (159 μL, 0.92 mmol, 10 equiv) and HATU (70 mg, 0.19 mmol, 2.0 equiv) were added. The solution was stirred for 16 hours and the reaction mixture was concentrated and added EtOAc (200 mL). The EtOAc was decanted off and washed with aq. HCl (1.0 M, 10 mL × 3) and concentrated to afford the crude cyclic peptide **S7** (123 mg) as a brown oil. UPLC-MS gradient B, t_R = 1.72 min, *m/z* calcld. for $C_{30}H_{43}N_4O_7^-$: 571.3; found: 571.3 $[M-H]^-$.

(*Z*)-6-((2*R*,5*R*,8*R*,11*R*)-8-(4-hydroxybenzyl)-2-isopropyl-5,12,12-trimethyl-3,6,9,13-tetraoxo-1,4,7,10-tetraazacyclotridecan-11-yl)hex-4-enoic acid (3.52)

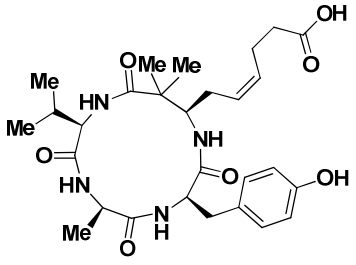

LiOH (77 mg, 3.2 mmol, 35 equiv) in water (5 mL) was added to the impure cyclic peptide **S7** (123 mg, 0.08 mmol) in THF (5 mL). After 20 hours the mixture was concentrated *in vacuo* and and the residue was dissolved in DMF and purified by preparative HPLC to afford the acid **3.52** (1.0 mg, 2%, 5 steps) as a white solid. Two conformations are observed in a 89:11 ratio. Characterization is given for the major conformation. ^{1}H NMR (500 MHz, DMSO) δ 8.03 (d, *J* = 8.6 Hz, 1H), 7.29 (d, *J* = 8.6 Hz, 1H), 7.19 (d, *J* = 8.3 Hz, 1H), 7.00 (d, *J* = 9.9 Hz, 1H), 6.95 (d, *J* = 8.4 Hz, 2H), 6.60 (d, *J* = 8.4 Hz, 2H), 5.19 (m, 1H), 5.01 (m, 1H), 4.32 (q, *J* = 8.0 Hz, 1H), 4.13 (pentet, *J* = 7.0 Hz, 1H), 4.04 (m, 1H), 3.69 (t, *J* = 10.1, 8.3 Hz, 1H), 2.87 (dd, *J* = 13.7, 8.0 Hz, 1H), 2.57 (dd, *J* = 13.7, 6.6 Hz, 1H), 2.18 (m, 5H), 2.00 (m, 2H), 1.15 (m, 6H), 1.03 (s, 3H), 0.84 (m, 6H). HRMS (ESI-TOF): *m/z* calcld. for $C_{28}H_{40}N_4O_7H^+$: 545.2970; found: 545.2968 $[M+H]^+$. HPLC gradient C, t_R = 11.36 min (>95%).

(2*R*,5*R*,8*R*,12*R*,*Z*)-12-amino-2-((1-(tert-butoxycarbonyl)-1H-indol-3-yl)methyl)-8-isopropyl-5,11,11-trimethyl-4,7,10,18-tetraoxo-19-oxa-3,6,9-triazahenicos-14-en-1-oic acid (3.50)

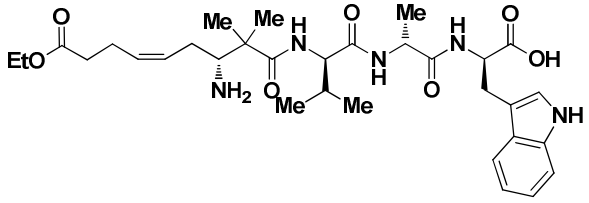

Polystyrene 2-chlorotrityl-bound Fmoc-(D)Val–(D)Ala–(D)Trp(Boc-*N*-indol) (142 mg, 0.072 mmol) was added to a fritted syringe and the Fmoc group was removed with piperidine–DMF (1:4, 4 mL, 2 × 25 min) and DBU–piperidine–DMF (2:2:96, 4 mL, 30 min). The resin was then washed with DMF (×3), MeOH (×3), CH_2Cl_2 (×3). β-amino acid **3.16** (28.4 mg, 0.079 mmol) in DMF (1.8 mL) was preincubated for 5 min with *i*Pr_2NEt (37.7 μL, 0.22 mmol, 3.0 equiv) and HATU (41 mg, 0.11 mmol, 1.5 equiv) before addition to the resin and the reaction was allowed to proceed on a rocking table for 17 hours. After washing [DMF (×3), MeOH (×3), CH_2Cl_2 (×3)] the resin was treated with with TFA–CH_2Cl_2 (1:1, 4 mL) for 30 min followed by washing with CH_2Cl_2 (5 mL). A fresh portion of TFA–CH_2Cl_2 (1:1, 4 mL) was added to the resin and after additional 30 min the resin was drained and all the fractions were pooled and concentrated *in vacuo*. Precipitation with diethyl ether afforded the TFA salt of the linear peptide **3.50** (43 mg) as a white solid. UPLC-MS gradient B, t_R = 1.30 min, *m/z* calcld. for $C_{32}H_{47}N_5O_7H^+$: 614.3; found: 614.4 $[M+H]^+$.

(*Z*)-ethyl-6-((2*R*,5*R*,8*R*,11*R*)-8-((1H-indol-3-yl)methyl)-2-isopropyl-5,12,12-trimethyl-3,6,9,13-tetraoxo-1,4,7,10-tetraazacyclotridecan-11-yl)hex-4-enoate (S8)

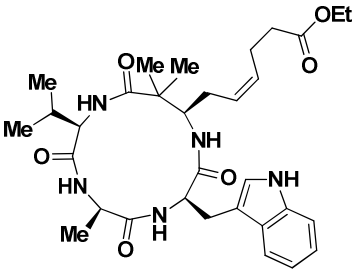

The linear peptide **3.50** (43 mg, 0.059 mmol) was dissolved in DMF (150 mL ≈ 0.4 mM) and *i*Pr_2NEt (51.4 μL, 0.30 mmol, 5.0 equiv) and HATU (34 mg, 0.089 mmol, 1.5 equiv) were added. The solution was stirred for 17 hours and the reaction mixture was concentrated to afford the crude cyclic peptide. Purification by VLC afforded a fraction containing the cyclic peptide **S8** (13 mg) which was found not to be pure by ^{1}H NMR. A fraction containing dimer (17 mg) was obtained as well. The impure cyclic peptide was used without further purification. UPLC-MS gradient B, t_R = 1.72 min, *m/z* calcld. for $C_{32}H_{45}N_5O_6H^+$: 595.3; found: 596.5 $[M+H]^+$.

(*Z*)-6-((2*R*,5*R*,8*R*,11*R*)-8-((1H-indol-3-yl)methyl)-2-isopropyl-5,12,12-trimethyl-3,6,9,13-tetraoxo-1,4,7,10-tetraazacyclotridecan-11-yl)hex-4-enoic acid (3.53)

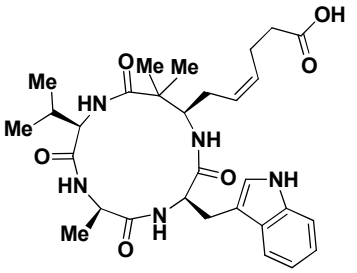

LiOH (26 mg, 1.09 mmol, 50 equiv) in water (4 mL) was added to the impure cyclic peptide **S8** (13 mg, 0.022 mmol) in THF (4 mL). After 18 hours the mixture was concentrated *in vacuo* and the residue was dissolved in MeCN–water–DMF (2:2:1, 2.5 mL) and purified by preparative HPLC to afford the acid **3.53** (2.6 mg, 6%, 5 steps) as a white solid. Two conformations are observed in a 92:8 ratio. Characterization is given for the major conformation ^{1}H NMR (500 MHz, DMSO) δ 7.74 (d, *J* = 8.6 Hz, 1H), 7.53 (d, *J* = 7.8 Hz, 1H), 7.39 (d, *J* = 8.3 Hz, 1H), 7.32 (d, *J* = 8.1 Hz, 2H), 3.95 (td, *J* = 9.5, 4.1 Hz, 1H), 3.71 (dd, *J* = 10.0, 8.5 Hz 1H), 3.08 (d, *J* = 7.6 Hz, 2H), 2.36–2.17 (m, 6H), 2.08 (m, 2H), 1.32 (s, 3H), 1.23 (d, *J* = 7.3 Hz, 3H), 1.09 (s, 3H), 0.88 (d, *J* = 6.9 Hz, 3H), 0.87 (d, *J* = 7.0 Hz, 3H).). HRMS (ESI-TOF): *m/z* calcld. for $C_{32}H_{47}N_5O_6H^+$: 568.3130; found: 568.3135 $[M+H]^+$. HPLC gradient C, t_R = 11.57 min (>95%).

(*S*,*E*)-*N*-butylidene-2-methylpropane-2-sulfinamide (3.60)

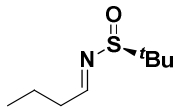

A solution of butyraldehyde (0.80 mL, 8.91 mmol, 2.0 equiv) in dry CH_2Cl_2 (1.0 mL) was added dropwise to a solution of dried $CuSO_4$ (3.6 g, 22.6 mmol, 5.0 equiv) and (*S*)-(-)-2-methyl-2-propanesulfinamide (0.54 g, 4.46 mmol) in dry CH_2Cl_2 (7 mL). After stirring vigorously for 20 hours the reaction mixture was filtered through a pad of Celite and the filter cake washed with CH_2Cl_2. The organic phase was concentrated *in vacuo* and purification by VLC afforded *tert*-butanesulfinyl imine **3.60** as a colorless oil (0.72 g, 92 %). Spectral data was in accordance with that found in the literature.[236] 300 MHz, $CDCl_3$) δ 8.03 (t, *J* = 4.7 Hz, 1H), 2.46 (td, *J* = 7.3, 4.7 Hz, 2H), 1.63 (h, *J* = 7.4 Hz, 2H), 1.16 (s, 9H), 0.95 (t, *J* = 7.4 Hz, 3H); ^{13}C NMR (75 MHz, $CDCl_3$) δ 169.7, 56.5, 38.1, 22.5, 19.0, 13.9.

(2*S*,3*R*)-*tert*-butyl 3-((*S*)-1,1-dimethylethylsulfinamido)-2-methylhexanoate (3.61)

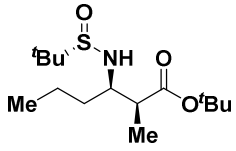

A solution of LDA (1.5 M in THF, 5.0 mL, 7.5 mmol, 2.6 equiv) was added dropwise over 5 min to a solution of HMPA (1.5 mL, 8.6 mmol, 5.7 equiv) at –78 °C. After 15 min *tert*-butyl propionate (1.1 mL, 7.3 mmol, 2.5 equiv) was added dropwise and after stirring for additionally 30 min imine **3.60** (0.51 g, 2.90 mmol) in dry THF (2.0 mL) was added dropwise. After 2 hours the reaction was quenched with sat. aq. NH_4Cl and warmed to rt. The mixture was added 1 M HCl (20 mL) and extracted with EtOAc (2 x 60 mL). The combined organic phases were washed with brine (40 mL), dried ($MgSO_4$), filtered, and concentrated *in vacuo*. Diastereoselectivity was determined by ^{1}H NMR integration of the crude reaction mixture (65:25:8:2). Purification by silica gel chromatography afforded **3.61** (335 mg, 38%) as needle-like crystals. A fraction containing a mixture of diastereomers (200 mg, 23%) was obtained as well. Characterization data for the major diastereomer. $\alpha_{[d]}$= 55.0 °; ^{1}H NMR (300 MHz, $CDCl_3$) δ 3.52 (m, 1H), 3.13 (d, *J* = 8.1 Hz, 1H), 2.46 (m, 1H), 1.46 – 1.60 (m, 2H), 1.42 (s, 9H), 1.18 (s, 9H), 1.07 (d, *J* = 7.1 Hz, 3H), 0.91 (t, *J* = 6.9 Hz, 3H); ^{13}C NMR (75 MHz, $CDCl_3$) δ 173.8, 80.7, 59.0, 56.3, 45.2, 36.6, 28.2, 22.9, 19.4, 13.9, 11.8. HRMS (ESI-TOF): *m/z* calcld. for $C_{15}H_{31}NO_3H^+$: 306.2103; found: 306.2110 $[M+H]^+$.

(2*S*,3*R*)-methyl 3-(((benzyloxy)carbonyl)amino)-2-methylhexanoate (3.67)

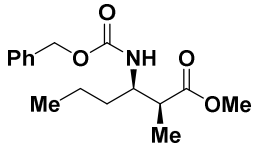

A solution of β-amino ester **3.61** (190 mg, 0.62 mmol) in MeOH (5.0 mL) was added 4 M HCl in dioxane (4.7 mL, 18.8 mmol, 30 equiv). After stirring for 22 hours the mixture was concentrated. ^{1}H NMR showed a mixture of the fully deprotected β-amino acid and amine deprotected methyl ester. To ensure full conversion to the methyl ester the crude product was dissolved in MeOH (5.0 mL) and cooled to 0 °C. Thionyl chloride (70 μL, 0.94 mmol, 1.5 equiv) was added dropwise under argon. After 10 min the mixture was heated to reflux and stirred for 20 hours before additional thionyl chloride (70 μL, 0.94 mmol, 1.5 equiv) was added. After 2.5 hours of stirring the mixture was concentrated and re-dissolved in MeOH (5.0 mL). Thionyl chloride (90 μL, 1.23 mmol, 2.0 equiv) was added at 0 °C and the mixture stirred for 22 hours at room temperature, before concentration afforded the crude amine.

The crude amine was dissolved in aq. sat. $NaHCO_3$–ethyl acetate (1:1, 6.0 mL) and added benzylchloroformate (133 μL, 0.93 mmol, 1.5 equiv). After 18 hours of vigorously stirring the phases were separated and the aqueous layer was diluted with water (5 mL) and extracted with ethyl acetate (2 × 5 mL). The combined organic phases were washed with 1 M HCl (6 mL) and brine (6 mL), dried (Na_2SO_4), filtered, and concentrated *in vacuo*. Purification with VLC afforded the β-amino ester **3.67** in 37%, over three steps. $\alpha_{[D]}$= –39 ° ($CHCl_3$, c= 0.99), $\alpha_{[D]litt.}$= –34 ° ($CHCl_3$, c= 1.0); ^{1}H NMR (400 MHz, $CDCl_3$) δ 7.3 –7.28 (m, 5H), 5.09 (s, 2H), 4.95 (d, *J* =

9.7 Hz, 1H), 3.93–3.82 (m, 1H), 3.67 (s, 3H), 2.65 (m, 1H), 1.43 (m, 1H), 1.31 (m, 1H), 1.15 (d, *J* = 7.2 Hz, 3H), 0.91 (t, *J* = 6.6 Hz, 3H); ^{13}C NMR (101 MHz, $CDCl_3$) δ 175.0, 156.2, 136.7, 128.6, 128.2, 128.2, 66.8, 53.2, 51.9, 44.1, 34.2, 19.6, 13.9, 13.2.
The spectral data was in accordance with the data report in the literature.[204]

(2S,3R)-3-((((9H-fluoren-9-yl)methoxy)carbonyl)amino)-2-methylhexanoic acid (3.57)

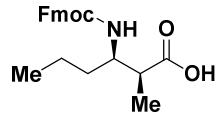

A solution of *β*-amino ester **3.61** (224 mg, 0.73 mmol) in dry CH_2Cl_2 (5.0 mL) was added TFA (5 mL). After 25 hours the solution was concentrated and residual TFA was removed by co-evaporation with toluene (3 × 10 mL). The crude residue was dissolved in dioxane and 4 M HCl in dioxane (0.55 mL, 2.2 mmol, 3.0 equiv) was added. After 1.5 hour the mixture was concentrated. The crude fully deprotected *β*-amino acid was suspended in water (5 mL) and added Na_2CO_3 (311 mg, 2.93, 4.0 equiv) followed by Fmoc-O-succinimide (297 mg, 0.88 mmol, 1.2 equiv) in DMF (3.0 mL) at 0 °C. The cooling was removed and DMF (2 mL) was added. After 1.5 hours, water (5.0 mL) was added and after additionally 1.5 hours of stirring the reaction mixture was diluted with water (60 mL) and extracted with Et_2O (15 mL). After acidification with concentrated HCl, until pH ≈ 1–2, the aqueous layer was extracted with ethyl acetate (3 × 75 mL). The combined organic phases were dried ($MgSO_4$), filtered, and concentrated *in vacuo*. Purification of the crude residue by VLC (0.2% acetic acid in the eluent) afforded *β*-amino acid **3.57** (66 mg, 25%, 3 steps) as a white solid after co-evaporation of residual acetic acid with CH_2Cl_2–toluene (1:1, 3 × 10 mL). $\alpha_{[D]}$= 1.0 ° (MeOH); ^{1}H NMR (300 MHz, DMSO) δ 12.19 (s, 1H), 7.86 (d, *J* = 7.4 Hz, 2H), 7.66 (dd, *J* = 7.3, 2.9 Hz, 2H), 7.38 (t, *J* = 7.4 Hz, 2H), 7.30 (d, *J* = 7.4, 2H), 7.05 (d, *J* = 9.5 Hz, 1H), 4.31 (m, 2H), 4.18 (t, *J* = 6.7 Hz, 1H), 3.58 (m, 1H), 2.28 (m, 1H), 1.22 (m, 4H), 0.95 (d, *J* = 6.9 Hz, 3H), 0.79 (t, *J* = 6.9 Hz, 3H). ^{13}C NMR (75 MHz, DMSO) δ 176.2, 156.2, 143.9, 140.8, 127.6, 127.1, 127.0, 125.2, 125.2, 120.1, 65.0, 52.4, 46.9, 44.4, 35.0, 18.8, 14.0, 13.7. HRMS (ESI-TOF): *m/z* calcld. for $C_{22}H_{25}NO_4H^+$: 368.1862; found: 368.1863 $[M+H]^+$.

(R)-2-((R)-2-((R)-2-((2S,3R)-3-amino-2-methylhexanamido)-3-methylbutanamido)propanamido)-3-(4-hydroxyphenyl)propanoic acid (3.68)

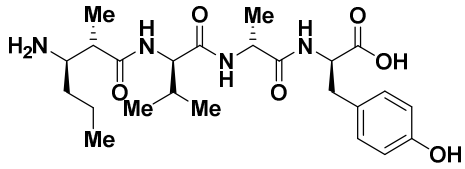

Polystyrene 2-chlorotrityl-bound Fmoc-(D)Val–(D)Ala–(D)Tyr (140mg, 0.11 mmol) was added to a fritted syringe and the Fmoc group was removed with piperidine–DMF (1:4, 4 mL, 2 × 30 min) and DBU–piperidine–DMF (2:2:96, 4 mL, 30 min). The resin was then washed with DMF (×3), MeOH (×3), CH_2Cl_2 (×3). *β*-amino acid **3.57** (43 mg, 0.12 mmol, 1.1 equiv) in DMF (2.0 mL) was preincubated for 5 min with 2,6-lutidine (37 *μ*L, 0.32 mmol, 3.0 equiv) and HATU (61 mg, 0.16 mmol, 1.5 equiv) before addition to the resin and the reaction was allowed to proceed on a rocking table for 17 hours. After washing [DMF (×3), MeOH (×3), CH_2Cl_2 (×3)] the resin was treated with TFA–CH_2Cl_2 (1:1, 4 mL) for 30 min followed by washing with CH_2Cl_2 (5 mL). A fresh portion of TFA–CH_2Cl_2 (1:1, 4 mL) was added to the resin and after additional 30 min the resin was drained and all the fractions were pooled and concentrated *in vacuo* to provide the linear peptide as an oily residue. Precipitation with diethyl ether afforded the TFA salt of the linear peptide **3.68** (53 mg, 84%) as a white solid. UPLC-MS gradient A, t_R = 0.84 min, *m/z* calcld. for $C_{24}H_{38}N_4O_6H^+$: 478.3; found: 479.3 $[M+H]^+$.

(3R,6R,9R,12S,13R)-3-(4-hydroxybenzyl)-9-isopropyl-6,12-dimethyl-13-propyl-1,4,7,10-tetraazacyclotridecane-2,5,8,11-tetraone (3.56)

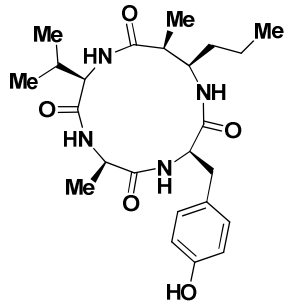

The linear peptide **3.68** (50 mg, 0.084 mmol) was dissolved in DMF (200 mL ≈ 0.4 mM) and *i*Pr_2NEt (73 μL, 0.42 mmol, 5 equiv) and HATU (48 mg, 0.13 mmol, 1.5 equiv) were added. The solution was stirred for 19 hours and the reaction mixture was concentrated. The residue was taken up in CH_2Cl_2 (80 mL) and washed with aq. HCl (1.0 M, 15 mL × 2) and the aqueous phase was re-extracted with CH_2Cl_2 (50 mL). The combined organics were washed with brine (25 mL), dried ($MgSO_4$), filtered, and concentrated. The residue was dissolved in DMF (2.5 mL) and purified by preparative HPLC to afford the cyclic peptide **3.56** (2.7 mg, 7%, 5 steps) as a white solid. Two conformations are observed in an 88:12 ratio. Characterization is given for the major conformation. ^{1}H NMR (500 MHz, DMSO) δ 7.67 (d, *J* = 8.8 Hz, 1H), 7.55 (d, *J* = 9.0 Hz, 1H), 7.46 (d, *J* = 8.4 Hz, 1H), 6.96 (d, *J* = 8.3 Hz, 2H), 6.63 (d, *J* = 8.4 Hz, 2H), 4.14 (p, , *J* = 7.3 Hz, 1H), 4.07 (p, *J* = 8.8 Hz, 1H), 3.99 (m, 1H), 3.67 (t, *J* = 9.4 Hz 1H), 2.89 (dd, *J* = 13.7, 7.2 Hz, 1H), 2.81 (dd, *J* = 13.7, 9.0 Hz, 1H), 2.54 (m, 1H), 2.16 (m, 1H), 1.64 (m, 1H), 1.36 (m, 1H), 1.20 (m, 6H), 0.87 (m, 6H). HRMS (ESI-TOF): *m/z* calcld. for $C_{24}H_{35}N_4O_5H^+$: 461.2765; found: 461.2754 $[M+H]^+$. HPLC gradient C, t_R = 11.14 min (>95%).

Experimental for chapter 4

Material and methods

General

Solvents and piperidine were obtained from SDS and all chemicals were analytical grade and used without further purification. Analytical HPLC-PDA was performed on a Waters instrument comprising a separation module (Waters 2695), an automatic injector, a photodiode array detector (Waters 996 or Waters 2998) and a system controller (Millenium^{31} login). The columns used were Xbridge C18 reversed-phase analytical column (2.5 × mm × 4.6mm × 75mm) and Xbridge BEH130 C18 reversed-phase analytical column (3.5 mm × 4.6mm × 100 mm). Ultraviolet detection was at 220 and 254 nm, and linear gradients of acetonitrile (MeCN) (+0.036% TFA) into H_2O (+0.045% TFA) were run at a 1 mL/min flow rate over 8 min.

HPLC-MS analysis was performed on a Waters instrument comprising a separation module (Waters 2695),

an automatic injector, a photodiode array detector (Waters 2998), a Waters Micromass ZQ spectrometer and, a system controller (Masslynx v4.1). The column used was a Sunfire C18 reversed-phase analytical column (3.5 × 2.1 × 100mm). Ultraviolet detection was at 220 and 254 nm, and linear gradients of MeCN

(+0.07% formic acid) into H_2O (+0.1% formic acid) were run at a 0.3 mL/min flow rate over 8 min.

NMR. ^{1}H NMR and ^{13}C NMR spectra were recorded on a Varian MERCURY 400 (400 MHz for ^{1}H NMR, 100 MHz for ^{13}C NMR) spectrometer. Chemical shifts are reported in ppm relative to deuterated solvent peaks as internal standards (δH, DMSO-d_6 2.50 ppm; δC, DMSO-d_6 39.52 ppm, δH, CD_3OH 3.30 ppm, δH, $CDCl_3$ 7.26 ppm; δC, $CDCl_3$ 77.16 ppm). Coupling constants (*J*) are given in hertz (Hz). Multiplicities of ^{1}H NMR signals are reported as follows: s, singlet; d, doublet; t, triplet; q, quartet; m, multiplet.

Benzo[b]thiophen-2-yl(3,4-dimethoxyphenyl)methanol (4.13)

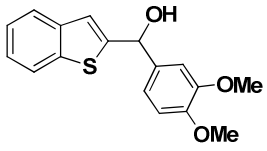

Butyl lithium (7.5 mL, 18.8 mmol, 1.3 equiv) was added dropwise to a solution of benzothiophene (2.0 g, 14.2 mmol) in dry THF (10 mL) at 0 °C under nitrogen. After 30 minutes, 3,4-dimethoxybenzaldehyde (3.1 g, 18.5 mmol, 1.3 equiv) in dry THF (10 mL) was added dropwise over 10 min. After 15 minutes the cooling bath was removed and after stirring for 3.5 hours at room temperature the mixture was cooled to 0 °C and quenched with sat. aq. NH_4Cl (20 mL). The layers were separated and the aqueous phase was extracted with ethyl acetate (2 × 20 mL) and the combined organics were dried ($MgSO_4$), filtered, and concentrated *in vacuo*. Purification by silica gel chromatography (hexane/ethyl acetate, 2:1) afforded the alcohol **4.13** (3.89 g, 92%) as a white solid. ^{1}H NMR (400 MHz, $CDCl_3$) δ 7.78 (d, *J* = 8.0 Hz, 1H), 7.69 (*J* = 7.4 Hz, 1H), 7.30 (pd, *J* = 7.2, 1.4 Hz, 2H), 7.12 (s, 1H), 7.03 (m, 2H), 6.87 (d, *J* = 8.1 Hz, 1H), 6.08 (bs, 1H), 3.89 (s, 3H), 3.88 (s, 3H). ^{13}C NMR (100 MHz, $CDCl_3$) δ 1493, 149.1, 149.0, 140.0, 139.5, 135.4, 124.4, 124.3, 123.7, 122.5, 121.2, 119.0, 111.0, 109.7, 72.9, 56.0, 56.0.

2-((3,4-dimethoxyphenyl)(hydroxy)methyl)benzo[b]thiophene 1,1-dioxide (4.16)

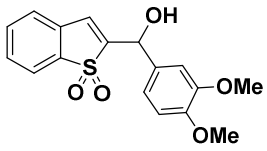

To a solution of benzothiophene alcohol **4.13** (1.0 g, 3.33 mmol) in MeOH–2-propanol (5:1, 30 mL) was added MMPP (2.31 g, 4.66 mmol, 1.3 equiv) in small portions. Over the same period of time water (7.0 mL) was added in small portions. After stirring for 15 hours the suspension was filtered and concentrated. The

concentrate was added ethyl acetate (100 mL) and sat. aq. $NaHCO_3$ (25 mL) and stirred for 10 minutes until all was dissolved. The layers were separated and the organic phase was washed with sat. aq. $NaHCO_3$ (2 × 15 mL), water (15 mL), brine (15 mL), dried ($MgSO_4$), and concentrated *in vacuo* to afford the sulfone **4.16** (0.95 g, 86%) as a yellow crystalline solid. ^{1}H NMR (400 MHz, $CDCl_3$) δ 7.71 (d, *J* = 7.2 Hz, 1H), 7.53 (td, *J* = 7.5, 1.3 Hz, 1H), 7.48 (td, *J* = 7.7, 1.2 Hz, 1H) 7.28 (d, *J* = 7.7, 1H), 7.04 (m, 2H), 6.91 (d, *J* = 8.0 Hz, 1H), 6.72 (bs, 1H), 5.88 (bs, 1H), 3.90 (m, 6H), 2.72 (bs, 1H). ^{13}C NMR (100 MHz, $CDCl_3$) δ 149.4, 149.3, 146.4, 137.6, 133.8, 131.9, 130.5, 130.3, 127.9, 125.3, 121.6, 119.3, 111.2, 109.9, 68.5, 56.1, 56.0.

1-(benzo[b]thiophen-2-yl)propan-1-ol (4.14)

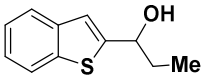

Butyl lithium (15.5 mL, 38.7 mmol, 1.3 equiv) was added dropwise to a solution of benzothiophene (4.0 g, 29.8 mmol) in dry THF (12 mL) at 0 °C under nitrogen. After 30 minutes propionaldehyde (2.8 mL, 38.7 mmol, 1.3 equiv) in dry THF (5 mL) was added dropwise over 10 min. After 15 minutes the cooling bath was removed and after stirring 2 hours at room temperature the mixture was cooled to 0 °C and quenched with sat. aq. NH_4Cl (20 mL). The layers were separated and the aqueous phase was extracted with ethyl acetate (2 × 30 mL) and the combined organics were dried ($MgSO_4$), filtered, and concentrated *in vacuo*. Purification by silica gel chromatography (hexane/ethyl acetate, 4:1) afforded the alcohol **4.14** (4.80 g, 84%) as a pale yellow oil, which crystalized upon storage. ^{1}H NMR (400 MHz, $CDCl_3$) δ 7.75 (d, *J* = 7.7 Hz, 1H), 7.65 (d, *J* = 8.0 1H), 7.28 (td, *J* = 7.2, 1.2 Hz, 1H), 7.24 (*J* = 7.1, 1.3 Hz, 1H), 4.84 (t, *J* = 6.6 Hz, 1H), 2.33 (bs, 1H), 1.86 (m, 2H), 0.93 (t, *J* = 7.4 Hz, 3H). ^{13}C NMR (100 MHz, $CDCl_3$) δ 149.4, 139.6, 139.4, 124.3, 124.2, 123.5, 122.6, 120.3, 72.4, 32.0, 10.1.

2-(1-hydroxypropyl)benzo[b]thiophene 1,1-dioxide (4.17)

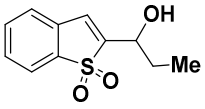

To a solution of benzothiophene alcohol **4.14** (2.0 g, 10.4 mmol) in MeOH (50 mL) was added MMPP (7.2 g, 14.6 mmol, 1.4 equiv) in small portions. Over the same period of time, water (15 mL) was added in small portions. After stirring for 16 hours the suspension was filtered and concentrated. The solid was added ethyl acetate (150 mL) and sat. aq. $NaHCO_3$ (35 mL) and stirred for 10 minutes until all was dissolved. The layers were separated and the organic phase was washed with sat. aq. $NaHCO_3$ (2 × 30 mL), water (30 mL), brine (30 mL), dried ($MgSO_4$), and concentrated *in vacuo* to afford the sulfone **4.17** (1.83 g, 79%) as a white solid. ^{1}H NMR (400 MHz, $CDCl_3$) δ 7.69 (d, *J* = 7.6 Hz, 1H), 7.54 (td, *J* = 7.5, 1.2 Hz, 1H), 7.48 (td, *J* = 7.6, 1.1 Hz, 1H), 7.33 (d, *J* = 7.4 Hz, 1H), 7.04 (dd, *J* = 1.4, 1.0 Hz, 1H), 4.78 (m, 1H), 2.26 (bs, 1H), 2.04 (m, 1H), 1.91 (m, 1H), 1.07 (t, *J* = 7.4 Hz, 3H). ^{13}C NMR (100 MHz, $CDCl_3$) δ 146.8, 137.5, 133.8, 130.8, 130.1, 126.5, 125.1, 121.5, 68.0, 29.1, 9.5.

***N*-(1-(benzo[b]thiophen-2-yl)propyl)-1H-imidazole-1-carboxamide (4.20)**

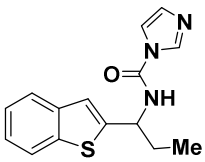

To a solution of carbonyldiimidazole (0.51 g, 3.12 mmol, 1.4 equiv) in dry CH_2Cl_2 (5 mL) was added a solution of alcohol **4.14** (0.42 g, 2.17 mmol) in dry CH_2Cl_2 (3 mL) over 5 min under argon. After 1.5 hours of stirring the reaction mixture was diluted with CH_2Cl_2 (50 mL) and washed with water (2 × 10 mL), dried ($MgSO_4$), filtered, and concentrated *in vacuo* to afford the carbonyl imidazole **4.20** (0.61 g, 98%). ^{1}H NMR (400 MHz, $CDCl_3$) δ 8.08 (s, 1H), 7.73 (m, 1H), 7.67 (m, 1H), 7.35 (t, *J* = 1.5 Hz, 1H), 7.29 (s, 1H), 7.26 (m, 2H), 6.98 (m, 1H), 6.11 (t, *J* = 7.0 Hz, 1H) 2.15 (sekstet, *J* = 7.4 Hz, 1H), 2.06 (sekstet, *J* = 7.4 Hz, 1H), 0.97 (t, *J* = 7.4 Hz, 3H). ^{13}C NMR (100 MHz, $CDCl_3$) δ 148.1, 141.4, 139.6, 138.9, 137.2, 130.8, 125.1, 124.7, 124.1, 123.9, 122.5, 117.2, 78.0, 29.1, 10.0.

1-(benzo[b]thiophen-2-yl)propyl benzylcarbamate (4.22)

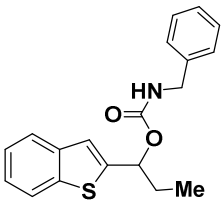

To a solution of carbonylimidazole **4.20** (127 mg, 0.44 mmol) in dry CH_2Cl_2 (2 mL) was added a solution of benzyl amine (60 μL, 0.55 mmol, 1.2 equiv) and Et_3N (75 μL, 0.55 mmol, 1.2 equiv) in dry CH_2Cl_2 (1 mL). After stirring for 15 hours DMAP (3.2 mg, 0.03 mmol, 0.06 equiv) was added followed by benzyl amine (50 μL, 0.46 mmol, 1.0 equiv) and the mixture was heated to 35 °C. After stirring for 20 hours the mixture was diluted with ethyl acetate (20 mL) and washed with sat. aq. NH_4Cl (2 × 10 mL), water (10 mL), dried ($MgSO_4$), filtered, and concentrated *in vacuo*. Purification by silica gel chromatography (hexane/ethyl acetate, 6:1) afforded the carbamate **4.22** (89 mg, 62%) as a white solid. ^{1}H NMR (400 MHz, $CDCl_3$) δ 7.76 (d, *J* = 7.8 Hz, 1H), 7.68 (d, *J* = 7.3 Hz, 1H), 7.25 (m, *J* = 7H), 5.95 (t, *J* = 6.9 Hz, 1H), 5.14 (bs, 1H), 4.31 (m, 3H), 1.97 (dtd, *J* = 20.9, 13.8, 6.8 Hz, 3H), 0.95 (t, *J* = 7.4 Hz, 3H). ^{13}C NMR (100 MHz, $CDCl_3$) δ 155.9, 144.7, 139.5, 139.4, 138., 128.7 (× 2), 127.6, 127.5, 124.4, 124.3, 123.8, 122.5, 122.3, 74.1, 45.2 29.6, 10.0.

benzo[b]thiophen-2-yl(3,4-dimethoxyphenyl)methyl 1H-imidazole-1-carboxylate (4.19)

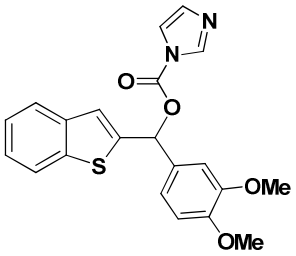

To a suspension of alcohol **4.13** (0.50 g, 3.1 mmol, 1.4 equiv) in dry CH_2Cl_2 (5 mL) was added a solution of alcohol (0.66 g, 2.2 mmol) in dry CH_2Cl_2 (3 mL) over 5 min under argon. After 2 hours of stirring the reaction mixture was diluted with CH_2Cl_2 (30 mL) and washed with water (2 × 10 mL), dried ($MgSO_4$), filtered, and concentrated *in vacuo.* Purification by silica gel chromatography (ethyl acetate) afford the carbonyl imidazole **4.19** (0.51 g, 59%) as a clear oil. ^{1}H NMR (400 MHz, $CDCl_3$) δ 7.78 (m, 1H), 7.70 (m, 1H), 7.59 (s, 1H), 7.35 (m, 2H), 7.13 (t, *J* = 1.1 Hz, 1H), 7.03 (s, 1H), 6.99 (t, *J* = 1.3 Hz, 1H), 6.86 (d, *J* = 8.2 Hz, 1H), 6.79 (m, 2H), 6.69 (s, 1H), 3.90 (s, 3H), 3.81 (s, 3H). ^{13}C NMR (101 MHz, $CDCl_3$) δ 149.6, 149.5, 143.3, 140.3, 139.1, 137.2, 131.0, 129.4, 125.2, 124.9, 124.3, 124.1, 122.5, 120.2 (×2), 119.2, 111.3, 110.8, 61.3, 56.1, 56.1.

7-((1-(benzo[b]thiophen-2-yl)propyl)amino)-4-methyl-2H-chromen-2-one (4.21)

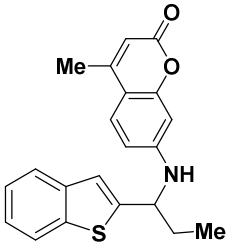

To a solution of carbonyl imidazole **4.19** (25 mg, 0.09 mmol) in dry DMF (2 mL) was added 7-amino-4-methylcoumarin (30 mg, 0.17 mmol, 2.0 equiv) and the solution heated to 100 °C. After stirring for 16 hours, the reaction mixture was diluted with ethyl acetate (40 mL) and washed with sat. aq. NH_4Cl (2 × 15 mL), water (15 mL), dried ($MgSO_4$), filtered, and concentrated *in vacuo*. Purification by silica gel chromatography (hexane/ethyl acetate, 2:1) afforded the amine **4.21** (10 mg, 30%) as a white solid. ^{1}H NMR (400 MHz, DMSO) δ 7.83 (d, *J* = 8.2 Hz, 1H), 7.75 (d, *J* = 7.2 Hz, 1H), 7.40 (m, 2H), 7.29 (m, 2H), 7.22 (d, *J* = 7.1 Hz, 1H), 6.71 (dd, *J* = 8.8, 2.3 Hz, 1H), 6.47 (d, *J* = 2.2 Hz, 1H), 5.89 (d, *J* = 1.1 Hz, 1H), 4.79 (m, 1H), 2.26 (d, *J* = 1.1 Hz, 4H), 1.92 (m, 2H), 0.98 (t, *J* = 7.3 Hz, 3H). ^{13}C NMR (100 MHz, DMSO) δ 160.9, 155.4, 154.0, 151.8, 149.7, 139.6, 138.5, 126.1, 124.5, 124.1, 123.4, 122.6, 121.3, 111.0 (×2), 109.5, 108.1, 54.7, 30.4, 18.1, 11.0.

benzo[b]thiophen-2-ylmethanol (4.15)

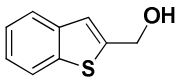

Butyl lithium (11.6 mL, 29.1 mmol, 1.3 equiv) was added over 10 minutes to a solution of benzothiophene (3.0 g, 22.4 mmol) in dry THF (15 mL) at –20 °C under nitrogen. After 50 minutes of stirring the solution was cooled to –78 °C and paraformaldehyde (4.7 g, 157 mmol, 7.0 equiv) was added in small portions over 5 min. The mixture was allowed to warm to room temperature over 15 hours

and quenched with 2M HCl (15 mL). The mixture was extracted with Et_2O (3 × 25 mL) and the combined organic phases were washed with brine (25 mL), dried ($MgSO_4$), filtered, and concentrated *in vacuo*. Purification by silica gel chromatography (hexane/ethyl acetate, 4:1) afforded the alcohol **4.15** (2.64 g, 72%) as a white solid. The spectral data was in accordance with that previously reported.[237] ^{1}H NMR (400 MHz, $CDCl_3$) δ 7.82 (d, *J* = 7.5 Hz, 1H), 7.72 (d, *J* = 7.5 Hz, 1H), 7.38–7.29 (m, 2H), 7.17 (d, *J* = 0.8 Hz, 1H), 4.89 (d, *J* = 0.9 Hz, 2H), 2.50 (bs, 1H). ^{13}C NMR (100 MHz, $CDCl_3$) δ 144.9, 140.0, 139.6, 124.4, 124.3, 123.6, 122.6, 121.6, 88.7, 64.5, 60.9.

2-(hydroxymethyl)benzo[b]thiophene 1,1-dioxide (4.18)

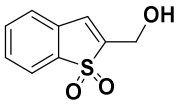

To a solution of benzothiophene alcohol **4.15** (1.0 g, 6.1 mmol) in MeOH (7.5 mL) was added MMPP (4.25 g, 8.5 mmol, 1.4 equiv) in small portions at 0 °C. Over the same period of time water (3.5 mL) was added in small portions. After stirring this suspension for 15 minutes the cooling bath was removed and the resulting clear solution was stirred at room temperature for 2 hours and concentrated *in vacuo*. The residue was added CH_2Cl_2 (35 mL) and sat. aq. $NaHCO_3$ (20 mL) and stirred for 10 minutes until all was dissolved. The layers were separated and the organic phase was washed with sat. aq. $NaHCO_3$ (2 × 20 mL), brine (15 mL), water (20 mL), dried ($MgSO_4$), and concentrated *in vacuo* to afford the sulfone **4.18** (0.80 g, 67%) as a white solid. The spectral data was in accordance with that previously reported.[237] ^{1}H NMR (400 MHz, $CDCl_3$) δ 7.69 (d, *J* = 7.3 Hz, 1H), 7.51 (td, *J* = 7.5, 1.2 Hz, 1H), 7.45 (td, *J* = 7.5, 1.2 Hz, 1H), 7.29 (m, 2H), 7.05 (m, 1H), 4.68 (d, *J* = 1.6 Hz, 2H), 2.81 (bs, 1H). ^{13}C NMR (100 MHz, $CDCl_3$) δ 143.7, 137.3, 133.9, 130.9, 130.1, 127.2, 125.3, 121.5, 55.7.

1-(1,1-dioxidobenzo[b]thiophen-2-yl)propyl (4-methyl-2-oxo-2H-chromen-7-yl)carbamate (4.25)

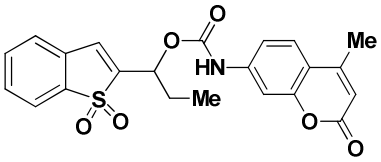

A solution of AMC (50 mg, 0.29 mmol) and Et_3N (0.4 mL, 2.90 mmol, 10 equiv) in dry CH_2Cl_2 (5 mL) was cooled to 0 °C and added a solution of triphosgene (126 mg, 0.43 mmol, 1.5 equiv) in dry THF (2 mL) over 30 minutes under nitrogen. After stirring for an additional hour the reaction mixture was added alcohol **4.17** (96 mg, 0.43 mmol, 1.5 equiv). After stirring for 2 hours the reaction mixture was diluted with CH_2Cl_2 (20 mL) and concentrated *in vacuo*. Purification by silica gel chromatography (hexane/ethyl acetate, 1:1) afforded the carbamate **4.25** (38 mg, 31%) as a yellow solid. ^{1}H NMR (400 MHz, DMSO) δ 7.86 (dd, *J* = 7.5, 0.8 Hz, 1H), 7.74–7.69 (m, 2H), 7.66 (s, 1H), 7.65–7.59 (m, 2H), 7.56 (d, *J* = 2.0 Hz, 1H), 7.47 (dd, *J* = 8.7, 2.1 Hz, 1H), 6.25 (d, *J* = 1.2 Hz, 1H), 5.75 (t, *J* = 6.4 Hz, 1H), 2.39 (d, *J* = 1.2 Hz, 3H), 2.06 (m, 2H), 1.02 (t, *J* = 7.3 Hz, 3H). ^{13}C NMR (100 MHz, DMSO) δ 160.0, 153.8, 153.1, 152.3, 142.5, 141.2, 136.7, 134.3, 130.8, 129.8, 129.3, 126.0 (×2), 121.1, 114.5, 114.4, 112.0, 104.6, 70.5, 26.1, 18.0, 9.4.

(3,4-dimethoxyphenyl)(1,1-dioxidobenzo[b]thiophen-2-yl)methyl-(4-methyl-2-oxo-2H-chromen-7-yl)carbamate (4.24)

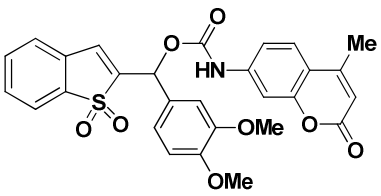

A solution of AMC (50 mg, 0.29 mmol) and Et_3N (0.4 mL, 2.90 mmol, 10 equiv) in dry CH_2Cl_2 (5 mL) was cooled to 0 °C and added a solution of triphosgene (126 mg, 0.43 mmol, 1.5 equiv) in dry THF (2 mL) over 30 minutes under nitrogen. After stirring for an additional hour the reaction mixture was added alcohol **4.16** (143 mg, 0.43 mmol, 1.5 equiv). After stirring for 19 hours the reaction mixture was diluted with CH_2Cl_2 (20 mL) and concentrated *in vacuo*. Purification by silica gel chromatography (hexane/ethyl acetate, 1:1) afforded the carbamate **4.24** (6 mg, 4%)

as a yellow solid. Additional impure fractions were collected. ^{1}H NMR (400 MHz,$CDCl_3$) δ 7.72 (dd, *J* = 6.8, 1.2 Hz, 1H), 7.57–7.47 (m, 3H), 7.44 (d, *J* = 2.1 Hz, 1H), 7.39 (m, 2H), 7.29 (*J* = 7.3 Hz, 1H), 7.12 (dd, *J* = 8.3, 2.0 Hz, 1H), 7.09 (d, *J* = 2.0 Hz, 1H), 6.92 (d, *J* = 8.3 Hz, 1H), 6.88 (d, *J* = 1.7 Hz, 1H), 6.77 (s, 1H), 6.18 (d, *J* = 1.2 Hz, 1H), 3.91 (s, 3H), 3.90 (s, 3H), 2.39 (d, *J* = 1.2 Hz, 3H). ^{13}C NMR (100 MHz, DMSO) δ 160.0, 153.8, 153.2, 151.8, 149.4, 148.8, 142.3, 142.0, 136.8, 134.3, 130.9, 129.9, 129.6, 128.2, 126.3, 126.1 (×2), 121.4, 121.2, 120.1, 114.7, 112.1, 111.7, 111.2, 69.9, 55.6, 55.6, 18.0.

1-(benzo[b]thiophen-2-yl)propyl (4-methyl-2-oxo-2H-chromen-7-yl)carbamate (4.26)

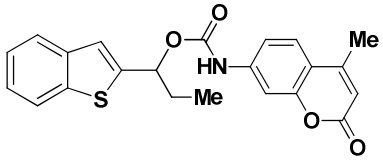

A solution of AMC (200 mg, 1.14 mmol) and Et_3N (1.59 mL, 11.4 mmol, 10 equiv) in dry CH_2Cl_2 (20 mL) was cooled to 0 °C and added a solution of triphosgene (0.51 g, 1.71 mmol, 1.5 equiv) in dry THF (4 mL) over 30 minutes under nitrogen. After stirring for an additional hour the alcohol **5.14** (285 mg, 1.48 mmol, 1.3 equiv) in dry THF (2 mL) was added dropwise. After stirring for 1 hour and 15 minutes the reaction mixture was diluted with CH_2Cl_2 (20 mL) and concentrated *in vacuo*. Purification by silica gel chromatography (hexane/ethyl acetate, 4:1) afforded the carbamate **4.26** (142 mg, 32%) as a white solid. ^{1}H NMR (400 MHz, $CDCl_3$) δ 7.81 (d, *J* = 7.5 Hz, 1H), 7.75 (dd, *J* = 6.8, 2.3 Hz, 1H), 7.50 (d, *J* = 8.6 Hz, 1H), 7.41 (d, *J* = 2.1 Hz, 1H), 7.39–7.29 (m, 4H), 6.92 (bs, 1H), 6.18 (d, *J* = 1.2 Hz, 1H), 6.05 (t, *J* = 7.0 Hz, 1H), 2.39 (d, *J* = 1.2 Hz, 3H), 2.13 (m, 1H), 2.04 (m, 1H), 1.03 (t, *J* = 7.4 Hz, 3H). ^{13}C NMR (100 MHz, $CDCl_3$) δ 161.2, 154.6, 152.3 (×2), 143.5, 141.4, 139.6, 139.3, 125.5, 124.8, 124.6, 124.0, 123.1, 122.6, 115.8, 114.5, 113.4, 106.1, 75.0, 29.5, 18.7, 10.1.

7 References

1. Bednar, J.; Horowitz, R. A.; Grigoryev, S. A.; Carruthers, L. M.; Hansen, J. C.; Koster, A. J.; Woodcock, C. L., Nucleosomes, linker DNA, and linker histone form a unique structural motif that directs the higher-order folding and compaction of chromatin. *Proceedings of the National Academy of Sciences* **1998,** *95* (24), 14173-14178.
2. Schalch, T.; Duda, S.; Sargent, D. F.; Richmond, T. J., X-ray structure of a tetranucleosome and its implications for the chromatin fibre. *Nature* **2005,** *436* (7047), 138-141.
3. Luger, K.; Mader, A. W.; Richmond, R. K.; Sargent, D. F.; Richmond, T. J., Crystal structure of the nucleosome core particle at 2.8 A resolution. *Nature* **1997,** *389* (6648), 251-260.
4. Kornberg, R. D., Chromatin Structure: A Repeating Unit of Histones and DNA. *Science* **1974,** *184* (4139), 868-871.
5. Olins, A. L.; Olins, D. E., Spheroid Chromatin Units (ν Bodies). *Science* **1974,** *183* (4122), 330-332.
6. Annunziato, A., DNA Packaging: Nucleosomes and Chromatin. *Nature Education* **2008**. 1(1):26
7. Bird, A., DNA methylation patterns and epigenetic memory. *Genes & Development* **2002,** *16* (1), 6-21.
8. Brownell, J. E.; Zhou, J.; Ranalli, T.; Kobayashi, R.; Edmondson, D. G.; Roth, S. Y.; Allis, C. D., Tetrahymena Histone Acetyltransferase A: A Homolog to Yeast Gcn5p Linking Histone Acetylation to Gene Activation. *Cell* **1996,** *84* (6), 843-851.
9. Strahl, B. D.; Allis, C. D., The language of covalent histone modifications. *Nature* **2000,** *403* (6765), 41-45.
10. Bannister, A. J.; Kouzarides, T., Reversing histone methylation. *Nature* **2005,** *436* (7054), 1103-1106.
11. Barski, A.; Cuddapah, S.; Cui, K.; Roh, T. Y.; Schones, D. E.; Wang, Z.; Wei, G.; Chepelev, I.; Zhao, K., High-Resolution Profiling of Histone Methylations in the Human Genome. *Cell* **2007,** *129* (4), 823-837.
12. Suzuki, T.; Terashima, M.; Tange, S.; Ishimura, A., Roles of histone methyl-modifying enzymes in development and progression of cancer. *Cancer Science* **2013,** *104* (7), 795-800.
13. Albert, M.; Helin, K., Histone methyltransferases in cancer. *Seminars in Cell & Developmental Biology* **2010,** *21* (2), 209-220.
14. Glozak, M. A.; Sengupta, N.; Zhang, X.; Seto, E., Acetylation and deacetylation of non-histone proteins. *Gene* **2005,** *363*, 15-23.
15. Walia, H.; Chen, H. Y.; Sun, J. M.; Holth, L. T.; Davie, J. R., Histone Acetylation Is Required to Maintain the Unfolded Nucleosome Structure Associated with Transcribing DNA. *Journal of Biological Chemistry* **1998,** *273* (23), 14516-14522.
16. Bauer, W. R.; Hayes, J. J.; White, J. H.; Wolffe, A. P., Nucleosome Structural Changes Due to Acetylation. *Journal of Molecular Biology* **1994,** *236* (3), 685-690.
17. Chuang, D. M.; Leng, Y.; Marinova, Z.; Kim, H. J.; Chiu, C.-T., Multiple roles of HDAC inhibition in neurodegenerative conditions. *Trends in Neurosciences* **2009,** *32* (11), 591-601.
18. Taunton, J.; Hassig, C. A.; Schreiber, S. L., A Mammalian Histone Deacetylase Related to the Yeast Transcriptional Regulator Rpd3p. *Science* **1996,** *272* (5260), 408-411.
19. Gao, L.; Cueto, M. A.; Asselbergs, F.; Atadja, P., Cloning and Functional Characterization of HDAC11, a Novel Member of the Human Histone Deacetylase Family. *Journal of Biological Chemistry* **2002,** *277* (28), 25748-25755.
20. Gray, S. G.; Ekström, T. J., The Human Histone Deacetylase Family. *Experimental Cell Research* **2001,** *262* (2), 75-83.
21. Imai, S.; Guarente, L., Ten years of NAD-dependent SIR2 family deacetylases: implications for metabolic diseases. *Trends in Pharmacological Sciences* **2010,** *31* (5), 212-220.
22. Gregoretti, I.; Lee, Y.-M.; Goodson, H. V., Molecular Evolution of the Histone Deacetylase Family: Functional Implications of Phylogenetic Analysis. *Journal of Molecular Biology* **2004,** *338* (1), 17-31.
23. Zhang, Y.; Ng, H. H.; Erdjument-Bromage, H.; Tempst, P.; Bird, A.; Reinberg, D., Analysis of the NuRD subunits reveals a histone deacetylase core complex and a connection with DNA methylation. *Genes & Development* **1999,** *13* (15), 1924-1935.
24. You, A.; Tong, J. K.; Grozinger, C. M.; Schreiber, S. L., CoREST is an integral component of the CoREST- human histone deacetylase complex. *Proceedings of the National Academy of Sciences* **2001,** *98* (4), 1454-1458.
25. Zhang, Y.; Iratni, R.; Erdjument-Bromage, H.; Tempst, P.; Reinberg, D., Histone Deacetylases and SAP18, a Novel Polypeptide, Are Components of a Human Sin3 Complex. *Cell* **1997,** *89* (3), 357-364.
26. Knoepfler, P. S.; Eisenman, R. N., Sin Meets NuRD and Other Tails of Repression. *Cell* **1999,** *99* (5), 447-450.
27. Lagger, G.; O'Carroll, D.; Rembold, M.; Khier, H.; Tischler, J.; Weitzer, G.; Schuettengruber, B.; Hauser, C.; Brunmeir, R.; Jenuwein, T.; Seiser, C., Essential function of histone deacetylase 1 in proliferation control and CDK inhibitor repression. *EMBO Journal* **2002,** *21* (11), 2672-2681.
28. Taplick, J.; Kurtev, V.; Kroboth, K.; Posch, M.; Lechner, T.; Seiser, C., Homo-oligomerisation and nuclear localisation of mouse histone deacetylase 1. *Journal of Molecular Biology* **2001,** *308* (1), 27-38.

29. Hassig, C. A.; Tong, J. K.; Fleischer, T. C.; Owa, T.; Grable, P. G.; Ayer, D. E.; Schreiber, S. L., A role for histone deacetylase activity in HDAC1-mediated transcriptional repression. *Proceedings of the National Academy of Sciences* **1998,** *95* (7), 3519-3524.
30. Yang, W. M.; Tsai, S. C.; Wen, Y. D.; Fejér, G.; Seto, E., Functional Domains of Histone Deacetylase-3. *Journal of Biological Chemistry* **2002,** *277* (11), 9447-9454.
31. Takami, Y.; Nakayama, T., N-terminal Region, C-terminal Region, Nuclear Export Signal, and Deacetylation Activity of Histone Deacetylase-3 Are Essential for the Viability of the DT40 Chicken B Cell Line. *Journal of Biological Chemistry* **2000,** *275* (21), 16191-16201.
32. Guenther, M. G.; Barak, O.; Lazar, M. A., The SMRT and N-CoR Corepressors Are Activating Cofactors for Histone Deacetylase 3. *Molecular and Cellular Biology* **2001,** *21* (18), 6091-6101.
33. Fischle, W.; Dequiedt, F.; Fillion, M.; Hendzel, M. J.; Voelter, W.; Verdin, E., Human HDAC7 Histone Deacetylase Activity Is Associated with HDAC3 in Vivo. *Journal of Biological Chemistry* **2001,** *276* (38), 35826-35835.
34. Fischle, W.; Dequiedt, F.; Hendzel, M. J.; Guenther, M. G.; Lazar, M. A.; Voelter, W.; Verdin, E., Enzymatic Activity Associated with Class II HDACs Is Dependent on a Multiprotein Complex Containing HDAC3 and SMRT/N-CoR. *Molecular Cell* **2002,** *9* (1), 45-57.
35. Bradner, J. E.; West, N.; Grachan, M. L.; Greenberg, E. F.; Haggarty, S. J.; Warnow, T.; Mazitschek, R., Chemical phylogenetics of histone deacetylases. *Nature Chemical Biology* **2010,** *6* (3), 238-243.
36. Verdin, E.; Dequiedt, F.; Kasler, H. G., Class II histone deacetylases: versatile regulators. *Trends in Genetics* **2003,** *19* (5), 286-293.
37. Grozinger, C. M.; Schreiber, S. L., Regulation of histone deacetylase 4 and 5 and transcriptional activity by 14-3-3-dependent cellular localization. *Proceedings of the National Academy of Sciences* **2000,** *97* (14), 7835-7840.
38. Kao, H. Y.; Verdel, A.; Tsai, C. C.; Simon, C.; Juguilon, H.; Khochbin, S., Mechanism for Nucleocytoplasmic Shuttling of Histone Deacetylase 7. *Journal of Biological Chemistry* **2001,** *276* (50), 47496-47507.
39. Wang, A. H.; Kruhlak, M. J.; Wu, J.; Bertos, N. R.; Vezmar, M.; Posner, B. I.; Bazett-Jones, D. P.; Yang, X. J., Regulation of Histone Deacetylase 4 by Binding of 14-3-3 Proteins. *Molecular and Cellular Biology* **2000,** *20* (18), 6904-6912.
40. Kirsh, O.; Seeler, J. S.; Pichler, A.; Gast, A.; Muller, S.; Miska, E.; Mathieu, M.; Harel-Bellan, A.; Kouzarides, T.; Melchior, F.; Dejean, A., The SUMO E3 ligase RanBP2 promotes modification of the HDAC4 deacetylase. *EMBO Journal* **2002,** *21* (11), 2682-2691.
41. Yang, X. J.; Grégoire, S., Class II Histone Deacetylases: from Sequence to Function, Regulation, and Clinical Implication. *Molecular and Cellular Biology* **2005,** *25* (8), 2873-2884.
42. Biel, M.; Wascholowski, V.; Giannis, A., Epigenetics—An Epicenter of Gene Regulation: Histones and Histone-Modifying Enzymes. *Angewandte Chemie International Edition* **2005,** *44* (21), 3186-3216.
43. Guardiola, A. R.; Yao, T. P., Molecular Cloning and Characterization of a Novel Histone Deacetylase HDAC10. *Journal of Biological Chemistry* **2002,** *277* (5), 3350-3356.
44. Hubbert, C.; Guardiola, A.; Shao, R.; Kawaguchi, Y.; Ito, A.; Nixon, A.; Yoshida, M.; Wang, X. F.; Yao, T.-P., HDAC6 is a microtubule-associated deacetylase. *Nature* **2002,** *417* (6887), 455-458.
45. Frye, R. A., Characterization of Five Human cDNAs with Homology to the Yeast SIR2 Gene: Sir2-like Proteins (Sirtuins) Metabolize NAD and May Have Protein ADP-Ribosyltransferase Activity. *Biochemical and Biophysical Research Communications* **1999,** *260* (1), 273-279.
46. Imai, S.-i.; Armstrong, C. M.; Kaeberlein, M.; Guarente, L., Transcriptional silencing and longevity protein Sir2 is an NAD-dependent histone deacetylase. *Nature* **2000,** *403* (6771), 795-800.
47. Olsen, C. A., Expansion of the Lysine Acylation Landscape. *Angewandte Chemie International Edition* **2012,** *51* (16), 3755-3756.
48. Banks, A. S.; Kon, N.; Knight, C.; Matsumoto, M.; Gutiérrez-Juárez, R.; Rossetti, L.; Gu, W.; Accili, D., SirT1 Gain of Function Increases Energy Efficiency and Prevents Diabetes in Mice. *Cell Metabolism* **2008,** *8* (4), 333-341.
49. Longo, V. D.; Kennedy, B. K., Sirtuins in Aging and Age-Related Disease. *Cell* **2006,** *126* (2), 257-268.
50. Fournel, M.; Bonfils, C.; Hou, Y.; Yan, P. T.; Trachy-Bourget, M. C.; Kalita, A.; Liu, J.; Lu, A. H.; Zhou, N. Z.; Robert, M. F.; Gillespie, J.; Wang, J. J.; Ste-Croix, H.; Rahil, J.; Lefebvre, S.; Moradei, O.; Delorme, D.; MacLeod, A. R.; Besterman, J. M.; Li, Z., MGCD0103, a novel isotype-selective histone deacetylase inhibitor, has broad spectrum antitumor activity in vitro and in vivo. *Molecular Cancer Therapeutics* **2008,** *7* (4), 759-768.
51. Vickers, C. J.; Olsen, C. A.; Leman, L. J.; Ghadiri, M. R., Discovery of HDAC Inhibitors That Lack an Active Site Zn2+-Binding Functional Group. *ACS Medicinal Chemistry Letters* **2012,** *3* (6), 505-508.
52. Crabb, S. J.; Howell, M.; Rogers, H.; Ishfaq, M.; Yurek-George, A.; Carey, K.; Pickering, B. M.; East, P.; Mitter, R.; Maeda, S.; Johnson, P. W.; Townsend, P.; Shin-ya, K.; Yoshida, M.; Ganesan, A.; Packham, G., Characterisation of the in

vitro activity of the depsipeptide histone deacetylase inhibitor spiruchostatin A. *Biochemical pharmacology* **2008,** *76* (4), 463-475.
53. Kanao, K.; Mikami, S.; Mizuno, R.; Shinojima, T.; Murai, M.; Oya, M., Decreased Acetylation of Histone H3 in Renal Cell Carcinoma: A Potential Target of Histone Deacetylase Inhibitors. *The Journal of Urology* **2008,** *180* (3), 1131-1136.
54. Beumer, J. H.; Tawbi, H., Role of histone deacetylases and their inhibitors in cancer biology and treatment. *Current clinical pharmacology* **2010,** *5* (3), 196-208.
55. Bolden, J. E.; Peart, M. J.; Johnstone, R. W., Anticancer activities of histone deacetylase inhibitors. *Nature Review Drug Discovery* **2006,** *5* (9), 769-784.
56. Taylor, R. C.; Cullen, S. P.; Martin, S. J., Apoptosis: controlled demolition at the cellular level. *Nature Review Molecular Cell Biology* **2008,** *9* (3), 231-241.
57. Fandy, T. E.; Shankar, S.; Ross, D. D.; Sausville, E.; Srivastava, R. K., Interactive effects of HDAC inhibitors and TRAIL on apoptosis are associated with changes in mitochondrial functions and expressions of cell cycle regulatory genes in multiple myeloma. *Neoplasia* **2005,** *7* (7), 646-57.
58. Nakata, S.; Yoshida, T.; Horinaka, M.; Shiraishi, T.; Wakada, M.; Sakai, T., Histone deacetylase inhibitors upregulate death receptor 5/TRAIL-R2 and sensitize apoptosis induced by TRAIL/APO2-L in human malignant tumor cells. *Oncogene* **2004,** *23* (37), 6261-6271.
59. Fulda, S., Histone deacetylase (HDAC) inhibitors and regulation of TRAIL-induced apoptosis. *Experimental Cell Research* **2012,** *318* (11), 1208-1212.
60. Stypula-Cyrus, Y.; Damania, D.; Kunte, D. P.; Cruz, M. D.; Subramanian, H.; Roy, H. K.; Backman, V., HDAC Up-Regulation in Early Colon Field Carcinogenesis Is Involved in Cell Tumorigenicity through Regulation of Chromatin Structure. *PLOS ONE* **2013,** *8* (5), e64600.
61. Kawai, H.; Li, H.; Avraham, S.; Jiang, S.; Avraham, H. K., Overexpression of histone deacetylase HDAC1 modulates breast cancer progression by negative regulation of estrogen receptor α. *International Journal of Cancer* **2003,** *107* (3), 353-358.
62. Nakagawa, M.; Oda, Y.; Eguchi, T.; Aishima, S. I.; Yao, T.; Hosoi, F.; Basaki, Y.; Ono, M.; Kuwano, M.; Tanaka, M., Expression profile of class I histone deacetylases in human cancer tissues. *Oncology reports* **2007,** *18* (4), 769-774.
63. Ropero, S.; Esteller, M., The role of histone deacetylases (HDACs) in human cancer. *Molecular Oncology* **2007,** *1* (1), 19-25.
64. Peart, M. J.; Smyth, G. K.; van Laar, R. K.; Bowtell, D. D.; Richon, V. M.; Marks, P. A.; Holloway, A. J.; Johnstone, R. W., Identification and functional significance of genes regulated by structurally different histone deacetylase inhibitors. *Proceedings of the National Academy of Sciences* **2005,** *102* (10), 3697-3702.
65. Marks, P. A.; Richon, V. M.; Rifkind, R. A., Histone Deacetylase Inhibitors: Inducers of Differentiation or Apoptosis of Transformed Cells. *Journal of the National Cancer Institute* **2000,** *92* (15), 1210-1216.
66. Zhao, Y.; Lu, S.; Wu, L.; Chai, G.; Wang, H.; Chen, Y.; Sun, J.; Yu, Y.; Zhou, W.; Zheng, Q.; Wu, M.; Otterson, G. A.; Zhu, W. G., Acetylation of p53 at Lysine 373/382 by the Histone Deacetylase Inhibitor Depsipeptide Induces Expression of p21Waf1/Cip1. *Molecular and Cellular Biology* **2006,** *26* (7), 2782-2790.
67. Condorelli, F.; Gnemmi, I.; Vallario, A.; Genazzani, A. A.; Canonico, P. L., Inhibitors of histone deacetylase (HDAC) restore the p53 pathway in neuroblastoma cells. *British Journal of Pharmacology* **2008,** *153* (4), 657-668.
68. Sandor, V.; Senderowicz, A.; Mertins, S.; Sackett, D.; Sausville, E.; Blagosklonny, M. V.; Bates, S. E., P21-dependent G1arrest with downregulation of cyclin D1 and upregulation of cyclin E by the histone deacetylase inhibitor FR901228. *British journal of cancer* **2000,** *83* (6), 817-825.
69. Choudhary, C.; Kumar, C.; Gnad, F.; Nielsen, M. L.; Rehman, M.; Walther, T. C.; Olsen, J. V.; Mann, M., Lysine Acetylation Targets Protein Complexes and Co-Regulates Major Cellular Functions. *Science* **2009,** *325* (5942), 834-840.
70. Bertrand, P., Inside HDAC with HDAC inhibitors. *European Journal of Medicinal Chemistry* **2010,** *45* (6), 2095-2116.
71. Montgomery, R. L.; Davis, C. A.; Potthoff, M. J.; Haberland, M.; Fielitz, J.; Qi, X.; Hill, J. A.; Richardson, J. A.; Olson, E. N., Histone deacetylases 1 and 2 redundantly regulate cardiac morphogenesis, growth, and contractility. *Genes & Development* **2007,** *21* (14), 1790-1802.
72. Bhaskara, S.; Chyla, B. J.; Amann, J. M.; Knutson, S. K.; Cortez, D.; Sun, Z. W.; Hiebert, S. W., Deletion of Histone Deacetylase 3 Reveals Critical Roles in S Phase Progression and DNA Damage Control. *Molecular Cell* **2008,** *30* (1), 61-72.
73. Haberland, M.; Montgomery, R. L.; Olson, E. N., The many roles of histone deacetylases in development and physiology: implications for disease and therapy. *Nature Reviews Genetics* **2009,** *10* (1), 32-42.
74. Minucci, S.; Pelicci, P. G., Histone deacetylase inhibitors and the promise of epigenetic (and more) treatments for cancer. *Nature Reviews Cancer* **2006,** *6* (1), 38-51.

75. Gottlicher, M.; Minucci, S.; Zhu, P.; Kramer, O. H.; Schimpf, A.; Giavara, S.; Sleeman, J. P.; Lo Coco, F.; Nervi, C.; Pelicci, P. G.; Heinzel, T., Valproic acid defines a novel class of HDAC inhibitors inducing differentiation of transformed cells. *EMBO Journal* **2001,** *20* (24), 6969-6978.
76. Abel, T.; Zukin, R. S., Epigenetic targets of HDAC inhibition in neurodegenerative and psychiatric disorders. *Current Opinion in Pharmacology* **2008,** *8* (1), 57-64.
77. Hockly, E.; Richon, V. M.; Woodman, B.; Smith, D. L.; Zhou, X.; Rosa, E.; Sathasivam, K.; Ghazi-Noori, S.; Mahal, A.; Lowden, P. A. S.; Steffan, J. S.; Marsh, J. L.; Thompson, L. M.; Lewis, C. M.; Marks, P. A.; Bates, G. P., Suberoylanilide hydroxamic acid, a histone deacetylase inhibitor, ameliorates motor deficits in a mouse model of Huntington's disease. *Proceedings of the National Academy of Sciences* **2003,** *100* (4), 2041-2046.
78. Tsankova, N. M.; Berton, O.; Renthal, W.; Kumar, A.; Neve, R. L.; Nestler, E. J., Sustained hippocampal chromatin regulation in a mouse model of depression and antidepressant action. *Nature Neuroscience* **2006,** *9* (4), 519-525.
79. Pontiki, E.; Hadjipavlou-Litina, D., Histone Deacetylase Inhibitors (HDACIs). Structure—Activity Relationships: History and New QSAR Perspectives. *Medicinal Research Reviews* **2012,** *32* (1), 1-165.
80. Tanaka, M.; Levy, J.; Terada, M.; Breslow, R.; Rifkind, R. A.; Marks, P. A., Induction of erythroid differentiation in murine virus infected eythroleukemia cells by highly polar compounds. *Proceedings of the National Academy of Sciences* **1975,** *72* (3), 1003-1006.
81. Breslow, R.; Jursic, B.; Yan, Z. F.; Friedman, E.; Leng, L.; Ngo, L.; Rifkind, R. A.; Marks, P. A., Potent cytodifferentiating agents related to hexamethylenebisacetamide. *Proceedings of the National Academy of Sciences* **1991,** *88* (13), 5542-5546.
82. Richon, V. M.; Webb, Y.; Merger, R.; Sheppard, T.; Jursic, B.; Ngo, L.; Civoli, F.; Breslow, R.; Rifkind, R. A.; Marks, P. A., Second generation hybrid polar compounds are potent inducers of transformed cell differentiation. *Proceedings of the National Academy of Sciences* **1996,** *93* (12), 5705-5708.
83. Richon, V. M.; Emiliani, S.; Verdin, E.; Webb, Y.; Breslow, R.; Rifkind, R. A.; Marks, P. A., A class of hybrid polar inducers of transformed cell differentiation inhibits histone deacetylases. *Proceedings of the National Academy of Sciences* **1998,** *95* (6), 3003-3007.
84. Kelly, W. K.; Richon, V. M.; O'Connor, O.; Curley, T.; MacGregor-Curtelli, B.; Tong, W.; Klang, M.; Schwartz, L.; Richardson, S.; Rosa, E.; Drobnjak, M.; Cordon-Cordo, C.; Chiao, J. H.; Rifkind, R.; Marks, P. A.; Scher, H., Phase I Clinical Trial of Histone Deacetylase Inhibitor: Suberoylanilide Hydroxamic Acid Administered Intravenously. *Clinical Cancer Research* **2003,** *9* (10), 3578-3588.
85. Vannini, A.; Volpari, C.; Filocamo, G.; Casavola, E. C.; Brunetti, M.; Renzoni, D.; Chakravarty, P.; Paolini, C.; De Francesco, R.; Gallinari, P.; Steinkühler, C.; Di Marco, S., Crystal structure of a eukaryotic zinc-dependent histone deacetylase, human HDAC8, complexed with a hydroxamic acid inhibitor. *Proceedings of the National Academy of Sciences* **2004,** *101* (42), 15064-15069.
86. Finnin, M. S.; Donigian, J. R., Structures of a histone deacetylase homologue bound to the TSA and SAHA inhibitors. *Nature* **1999,** *401* (6749), 188-193.
87. Bottomley, M. J.; Lo Surdo, P.; Di Giovine, P.; Cirillo, A.; Scarpelli, R.; Ferrigno, F.; Jones, P.; Neddermann, P.; De Francesco, R.; Steinkühler, C.; Gallinari, P.; Carfí, A., Structural and Functional Analysis of the Human HDAC4 Catalytic Domain Reveals a Regulatory Structural Zinc-binding Domain. *Journal of Biological Chemistry* **2008,** *283* (39), 26694-26704.
88. Schuetz, A.; Min, J.; Allali-Hassani, A.; Schapira, M.; Shuen, M.; Loppnau, P.; Mazitschek, R.; Kwiatkowski, N. P.; Lewis, T. A.; Maglathin, R. L.; McLean, T. H.; Bochkarev, A.; Plotnikov, A. N.; Vedadi, M.; Arrowsmith, C. H., Human HDAC7 Harbors a Class IIa Histone Deacetylase-specific Zinc Binding Motif and Cryptic Deacetylase Activity. *Journal of Biological Chemistry* **2008,** *283* (17), 11355-11363.
89. Cole, K. E.; Dowling, D. P.; Boone, M. A.; Phillips, A. J.; Christianson, D. W., Structural Basis of the Antiproliferative Activity of Largazole, a Depsipeptide Inhibitor of the Histone Deacetylases. *Journal of the American Chemical Society* **2011,** *133* (32), 12474-12477.
90. Somoza, J. R.; Skene, R. J.; Katz, B. A.; Mol, C.; Ho, J. D.; Jennings, A. J.; Luong, C.; Arvai, A.; Buggy, J. J.; Chi, E.; Tang, J.; Sang, B. C.; Verner, E.; Wynands, R.; Leahy, E. M.; Dougan, D. R.; Snell, G.; Navre, M.; Knuth, M. W.; Swanson, R. V.; McRee, D. E.; Tari, L. W., Structural Snapshots of Human HDAC8 Provide Insights into the Class I Histone Deacetylases. *Structure* **2004,** *12* (7), 1325-1334.
91. Millard, Christopher J.; Watson, Peter J.; Celardo, I.; Gordiyenko, Y.; Cowley, Shaun M.; Robinson, Carol V.; Fairall, L.; Schwabe, John W. R., Class I HDACs Share a Common Mechanism of Regulation by Inositol Phosphates. *Molecular Cell* **2013,** *51* (1), 57-67.
92. Watson, P. J.; Fairall, L.; Santos, G. M.; Schwabe, J. W. R., Structure of HDAC3 bound to co-repressor and inositol tetraphosphate. *Nature* **2012,** *481* (7381), 335-340.

93. Furumai, R.; Komatsu, Y.; Nishino, N.; Khochbin, S.; Yoshida, M.; Horinouchi, S., Potent histone deacetylase inhibitors built from trichostatin A and cyclic tetrapeptide antibiotics including trapoxin. *Proceedings of the National Academy of Sciences* **2001,** *98* (1), 87-92.
94. Vanommeslaeghe, K.; Proft, F. D.; Loverix, S.; Tourwé, D.; Geerlings, P., Theoretical study revealing the functioning of a novel combination of catalytic motifs in histone deacetylase. *Bioorganic & Medicinal Chemistry* **2005,** *13* (12), 3987-3992.
95. Suzuki, N.; Suzuki, T.; Ota, Y.; Nakano, T.; Kurihara, M.; Okuda, H.; Yamori, T.; Tsumoto, H.; Nakagawa, H.; Miyata, N., Design, Synthesis, and Biological Activity of Boronic Acid-Based Histone Deacetylase Inhibitors. *Journal of Medicinal Chemistry* **2009,** *52* (9), 2909-2922.
96. Suzuki, T.; Matsuura, A.; Kouketsu, A.; Hisakawa, S.; Nakagawa, H.; Miyata, N., Design and synthesis of non-hydroxamate histone deacetylase inhibitors: identification of a selective histone acetylating agent. *Bioorganic & Medicinal Chemistry* **2005,** *13* (13), 4332-4342.
97. Jones, P.; Bottomley, M. J.; Carfí, A.; Cecchetti, O.; Ferrigno, F.; Lo Surdo, P.; Ontoria, J. M.; Rowley, M.; Scarpelli, R.; Schultz-Fademrecht, C.; Steinkühler, C., 2-Trifluoroacetylthiophenes, a novel series of potent and selective class II histone deacetylase inhibitors. *Bioorganic & Medicinal Chemistry Letters* **2008,** *18* (11), 3456-3461.
98. Chou, C. J.; Herman, D.; Gottesfeld, J. M., Pimelic Diphenylamide 106 Is a Slow, Tight-binding Inhibitor of Class I Histone Deacetylases. *Journal of Biological Chemistry* **2008,** *283* (51), 35402-35409.
99. Lauffer, B. E. L.; Mintzer, R.; Fong, R.; Mukund, S.; Tam, C.; Zilberleyb, I.; Flicke, B.; Ritscher, A.; Fedorowicz, G.; Vallero, R.; Ortwine, D. F.; Gunzner, J.; Modrusan, Z.; Neumann, L.; Koth, C. M.; Lupardus, P. J.; Kaminker, J. S.; Heise, C. E.; Steiner, P., Histone Deacetylase (HDAC) Inhibitor Kinetic Rate Constants Correlate with Cellular Histone Acetylation but Not Transcription and Cell Viability. *Journal of Biological Chemistry* **2013,** *288* (37), 26926-26943.
100. Newkirk, T. L.; Bowers, A. A.; Williams, R. M., Discovery, biological activity, synthesis and potential therapeutic utility of naturally occurring histone deacetylase inhibitors. *Natural product reports* **2009,** *26* (10), 1293-1320.
101. Bieliauskas, A. V.; Pflum, M. K. H., Isoform-selective histone deacetylase inhibitors. *Chemical Society Reviews* **2008,** *37* (7), 1402-1413.
102. Estiu, G.; Greenberg, E.; Harrison, C. B.; Kwiatkowski, N. P.; Mazitschek, R.; Bradner, J. E.; Wiest, O., Structural Origin of Selectivity in Class II-Selective Histone Deacetylase Inhibitors. *Journal of Medicinal Chemistry* **2008,** *51* (10), 2898-2906.
103. Boissinot, M.; Inman, M.; Hempshall, A.; James, S. R.; Gill, J. H.; Selby, P.; Bowen, D. T.; Grigg, R.; Cockerill, P. N., Induction of differentiation and apoptosis in leukaemic cell lines by the novel benzamide family histone deacetylase 2 and 3 inhibitor MI-192. *Leukemia Research* **2012,** *36* (10), 1304-1310.
104. Park, J.-H.; Jung, Y.; Kim, T. Y.; Kim, S. G.; Jong, H. S.; Lee, J. W.; Kim, D. K.; Lee, J. S.; Kim, N. K.; Kim, T. Y.; Bang, Y. J., Class I Histone Deacetylase-Selective Novel Synthetic Inhibitors Potently Inhibit Human Tumor Proliferation. *Clinical Cancer Research* **2004,** *10* (15), 5271-5281.
105. KrennHrubec, K.; Marshall, B. L.; Hedglin, M.; Verdin, E.; Ulrich, S. M., Design and evaluation of 'Linkerless' hydroxamic acids as selective HDAC8 inhibitors. *Bioorganic & Medicinal Chemistry Letters* **2007,** *17* (10), 2874-2878.
106. Moradei, O. M.; Mallais, T. C.; Frechette, S.; Paquin, I.; Tessier, P. E.; Leit, S. M.; Fournel, M.; Bonfils, C.; Trachy-Bourget, M. C.; Liu, J.; Yan, T. P.; Lu, A. H.; Rahil, J.; Wang, J.; Lefebvre, S.; Li, Z.; Vaisburg, A. F.; Besterman, J. M., Novel Aminophenyl Benzamide-Type Histone Deacetylase Inhibitors with Enhanced Potency and Selectivity. *Journal of Medicinal Chemistry* **2007,** *50* (23), 5543-5546.
107. Siliphaivanh, P.; Harrington, P.; Witter, D. J.; Otte, K.; Tempest, P.; Kattar, S.; Kral, A. M.; Fleming, J. C.; Deshmukh, S. V.; Harsch, A.; Secrist, P. J.; Miller, T. A., Design of novel histone deacetylase inhibitors. *Bioorganic & Medicinal Chemistry Letters* **2007,** *17* (16), 4619-4624.
108. Frey, R. R.; Wada, C. K.; Garland, R. B.; Curtin, M. L.; Michaelides, M. R.; Li, J.; Pease, L. J.; Glaser, K. B.; Marcotte, P. A.; Bouska, J. J.; Murphy, S. S.; Davidsen, S. K., Trifluoromethyl Ketones as Inhibitors of Histone Deacetylase. *Bioorganic & Medicinal Chemistry Letters* **2002,** *12* (23), 3443-3447.
109. Jones, P.; Altamura, S.; De Francesco, R.; Gallinari, P.; Lahm, A.; Neddermann, P.; Rowley, M.; Serafini, S.; Steinkühler, C., Probing the Elusive Catalytic Activity of Vertebrate Class IIa Histone Deacetylases. *Bioorganic & Medicinal Chemistry Letters* **2008,** *18* (6), 1814-1819.
110. Ontoria, J. M.; Altamura, S.; Di Marco, A.; Ferrigno, F.; Laufer, R.; Muraglia, E.; Palumbi, M. C.; Rowley, M.; Scarpelli, R.; Schultz-Fademrecht, C.; Serafini, S.; Steinkühler, C.; Jones, P., Identification of Novel, Selective, and Stable Inhibitors of Class II Histone Deacetylases. Validation Studies of the Inhibition of the Enzymatic Activity of HDAC4 by Small Molecules as a Novel Approach for Cancer Therapy. *Journal of Medicinal Chemistry* **2009,** *52* (21), 6782-6789.

111. Singh, S. B.; Zink, D. L.; Polishook, J. D.; Dombrowski, A. W.; Darkin-Rattray, S. J.; Schmatz, D. M.; Goetz, M. A., Apicidins: Novel Cyclic Tetrapeptides as Coccidiostats and Antimalarial Agents from *Fusarium pallidoroseum*. *Tetrahedron Letters* **1996,** *37* (45), 8077-8080.
112. Singh, S. B.; Zink, D. L.; Liesch, J. M.; Dombrowski, A. W.; Darkin-Rattray, S. J.; Schmatz, D. M.; Goetz, M. A., Structure, Histone Deacetylase, and Antiprotozoal Activities of Apicidins B and C, Congeners of Apicidin with Proline and Valine Substitutions. *Organic Letters* **2001,** *3* (18), 2815-2818.
113. von Bargen, K. W.; Niehaus, E. M.; Bergander, K.; Brun, R.; Tudzynski, B.; Humpf, H.-U., Structure Elucidation and Antimalarial Activity of Apicidin F: An Apicidin-like Compound Produced by *Fusarium fujikuroi*. *Journal of Natural Products* **2013,** *76* (11), 2136-2140.
114. Singh, S. B.; Zink, D. L.; Liesch, J. M.; Mosley, R. T.; Dombrowski, A. W.; Bills, G. F.; Darkin-Rattray, S. J.; Schmatz, D. M.; Goetz, M. A., Structure and Chemistry of Apicidins, a Class of Novel Cyclic Tetrapeptides without a Terminal α-Keto Epoxide as Inhibitors of Histone Deacetylase with Potent Antiprotozoal Activities. *The Journal of organic chemistry* **2002,** *67* (3), 815-825.
115. Darkin-Rattray, S. J.; Gurnett, A. M.; Myers, R. W.; Dulski, P. M.; Crumley, T. M.; Allocco, J. J.; Cannova, C.; Meinke, P. T.; Colletti, S. L.; Bednarek, M. A.; Singh, S. B.; Goetz, M. A.; Dombrowski, A. W.; Polishook, J. D.; Schmatz, D. M., Apicidin: A novel antiprotozoal agent that inhibits parasite histone deacetylase. *Proceedings of the National Academy of Sciences* **1996,** *93* (23), 13143-13147.
116. Mou, L.; Singh, G., Synthesis of (S)-2-amino-8-oxodecanoic acid (Aoda) and apicidin A. *Tetrahedron Letters* **2001,** *42* (37), 6603-6606.
117. Kranz, M.; Murray, P. J.; Taylor, S.; Upton, R. J.; Clegg, W.; Elsegood, M. R. J., Solution, solid phase and computational structures of apicidin and its backbone-reduced analogs. *Journal of Peptide Science* **2006,** *12* (6), 383-388.
118. Shute, R. E.; Kawai, M.; Rich, D. H., Conformationally Constrained Biologically Active Peptides: Tentative Identification of the Antimitogenic Bioactive Confomer of the Naturally Occurring Cyclic Tetrapeptides. *Tetrahedron* **1988,** *44* (3), 685-695.
119. Horne, W. S.; Olsen, C. A.; Beierle, J. M.; Montero, A.; Ghadiri, M. R., Probing the Bioactive Conformation of an Archetypal Natural Product HDAC Inhibitor with Conformationally Homogeneous Triazole-modified Cyclic Tetrapeptides. *Angewandte Chemie International Edition* **2009,** *48* (26), 4718-4724.
120. Gu, W.; Cueto, M.; Jensen, P. R.; Fenical, W.; Silverman, R. B., Microsporins A and B: new histone deacetylase inhibitors from the marine-derived fungus *Microsporum* cf. *gypseum* and the solid-phase synthesis of microsporin A. *Tetrahedron* **2007,** *63* (28), 6535-6541.
121. Kawai, M.; Rich, D. H.; Walton, J. D., The structure and conformation of HC-toxin. *Biochemical and Biophysical Research Communications* **1983,** *111* (2), 398-403.
122. Kawai, M.; Rich, D. H., Total Synthesis of the Cyclic Tetrapeptide, HC-Toxin. *Tetrahedron Letters* **1983,** *24* (48), 5309-5312.
123. Taunton, J.; Collins, J. L.; Schreiber, S. L., Synthesis of Natural and Modified Trapoxins, Useful Reagents for Exploring Histone Deacetylase Function. *Journal of the American Chemical Society* **1996,** *118* (43), 10412-10422.
124. Rasmussen, J. B.; Scheffer, R. P., Isolation and Biological Activities of Four Selective Toxins from *Helminthosporium carbonum*. *Plant physiology* **1988,** *86* (1), 187-191.
125. Closse, A.; Huguenin, R., Isolierung und Strukturaufklärung von Chlamydocin. *Helvetica Chimica Acta* **1974,** *57* (3), 533-545.
126. Flippen, J. L.; Karle, I. L., Conformation of the cyclic tetrapeptide dihydrochlamydocin. Iabu-L-Phe-D-Pro-LX, and experimental values for 3 → 1 intramolecular hydrogen bonds by X-ray diffraction. *Biopolymers* **1976,** *15* (6), 1081-1092.
127. Nishino, N.; Jose, B.; Shinta, R.; Kato, T.; Komatsu, Y.; Yoshida, M., Chlamydocin–hydroxamic acid analogues as histone deacetylase inhibitors. *Bioorganic & Medicinal Chemistry* **2004,** *12* (22), 5777-5784.
128. Nakai, H.; Nagashima, K.; Itazaki, H., Structure of a new cyclotetrapeptide trapoxin A. *Acta Crystallographica Section C* **1991,** *47* (7), 1496-1499.
129. Itazaki, H.; Nagashima, K.; Sugita, K.; Yoshida, H.; Kawamura, Y.; Yasuda, Y.; Matsumoto, K.; Ishii, K.; Uotani, N.; Nakai, H., Isolation and structural elucidation of new cyclotetrapeptides, trapoxins A and B, having detransformation activities as antitumor agents. *The Journal of antibiotics* **1990,** *43* (12), 1524-1532.
130. Montero, A.; Beierle, J. M.; Olsen, C. A.; Ghadiri, M. R., Design, Synthesis, Biological Evaluation, and Structural Characterization of Potent Histone Deacetylase Inhibitors Based on Cyclic α/β-Tetrapeptide Architectures. *Journal of the American Chemical Society* **2009,** *131* (8), 3033-3041.
131. Kijima, M.; Yoshida, M.; Sugita, K.; Horinouchi, S.; Beppu, T., Trapoxin, an antitumor cyclic tetrapeptide, is an irreversible inhibitor of mammalian histone deacetylase. *Journal of Biological Chemistry* **1993,** *268* (30), 22429-35.

132. Mwakwari, S. C.; Patil, V.; Guerrant, W.; Oyelere, A. K., Macrocyclic histone deacetylase inhibitors. *Current Topics in Medicinal Chemistry* **2010,** *10* (14), 1423-1440.
133. Furumai, R.; Matsuyama, A.; Kobashi, N.; Lee, K. H.; Nishiyama, M.; Nakajima, H.; Tanaka, A.; Komatsu, Y.; Nishino, N.; Yoshida, M.; Horinouchi, S., FK228 (Depsipeptide) as a Natural Prodrug That Inhibits Class I Histone Deacetylases. *Cancer research* **2002,** *62* (17), 4916-4921.
134. Bowers, A.; West, N.; Taunton, J.; Schreiber, S. L.; Bradner, J. E.; Williams, R. M., Total synthesis and biological mode of action of largazole: a potent class I histone deacetylase inhibitor. *Journal of the American Chemical Society* **2008,** *130* (33), 11219-11222.
135. Nakao, Y.; Yoshida, S.; Matsunaga, S.; Shindoh, N.; Terada, Y.; Nagai, K.; Yamashita, J. K.; Ganesan, A.; van Soest, R. W. M.; Fusetani, N., Azumamides A–E: Histone Deacetylase Inhibitory Cyclic Tetrapeptides from the Marine Sponge *Mycale izuensis*. *Angewandte Chemie International Edition* **2006,** *45* (45), 7553-7557.
136. Maulucci, N.; Chini, M. G.; Di Micco, S.; Izzo, I.; Cafaro, E.; Russo, A.; Gallinari, P.; Paolini, C.; Nardi, M. C.; Casapullo, A.; Riccio, R.; Bifulco, G.; De Riccardis, F., Molecular Insights into Azumamide E Histone Deacetylases Inhibitory Activity. *Journal of the American Chemical Society* **2007,** *129* (10), 3007-3012.
137. Izzo, I.; Maulucci, N.; Bifulco, G.; De Riccardis, F., Total Synthesis of Azumamides A and E. *Angewandte Chemie International Edition* **2006,** *45* (45), 7557-7560.
138. Wen, S.; Carey, K. L.; Nakao, Y.; Fusetani, N.; Packham, G.; Ganesan, A., Total Synthesis of Azumamide A and Azumamide E, Evaluation as Histone Deacetylase Inhibitors, and Design of a More Potent Analogue. *Organic Letters* **2007,** *9* (6), 1105-1108.
139. Chandrasekhar, S.; Rao, C. L.; Seenaiah, M.; Naresh, P.; Jagadeesh, B.; Manjeera, D.; Sarkar, A.; Bhadra, M. P., Total Synthesis of Azumamide E and Sugar Amino Acid-Containing Analogue. *The Journal of organic chemistry* **2008,** *74* (1), 401-404.
140. Wang, D.; Helquist, P.; Wiest, O., Zinc Binding in HDAC Inhibitors: A DFT Study. *The Journal of organic chemistry* **2007,** *72* (14), 5446-5449.
141. Lahm, A.; Paolini, C.; Pallaoro, M.; Nardi, M. C.; Jones, P.; Neddermann, P.; Sambucini, S.; Bottomley, M. J.; Lo Surdo, P.; Carfí, A.; Koch, U.; De Francesco, R.; Steinkühler, C.; Gallinari, P., Unraveling the hidden catalytic activity of vertebrate class IIa histone deacetylases. *Proceedings of the National Academy of Sciences* **2007,** *104* (44), 17335-17340.
142. Njardarson, J. T.; Gaul, C.; Shan, D.; Huang, X. Y.; Danishefsky, S. J., Discovery of Potent Cell Migration Inhibitors through Total Synthesis: Lessons from Structure−Activity Studies of (+)-Migrastatin. *Journal of the American Chemical Society* **2004,** *126* (4), 1038-1040.
143. Hintermann, T.; Seebach, D., A Useful Modification of the Evans Auxiliary: 4-Isopropyl-5,5-diphenyloxazolidin-2-one. *Helvetica Chimica Acta* **1998,** *81* (11), 2093-2126.
144. Nagula, G.; Huber, V. J.; Lum, C.; Goodman, B. A., Synthesis of α-Substituted β-Amino Acids Using Pseudoephedrine as a Chiral Auxiliary. *Organic Letters* **2000,** *2* (22), 3527-3529.
145. Lee, H. S.; Park, J. S.; Kim, B. M.; Gellman, S. H., Efficient synthesis of enantiomerically pure β^2-amino acids via chiral isoxazolidinones. *The Journal of Organic Chemistry* **2003,** *68* (4), 1575-1578.
146. Juaristi, E.; Quintana, D., Preparation and Assignment of Configuration of 1-benzoyl- (2S)-tert-butyl-3-methyl-perhydropyrimidin-4-one. Useful Starting Material for the Enantioselective Synthesis of α-Substituted β-Amino Acids. *Tetrahedron: Asymmetry* **1992,** *3* (6), 723-726.
147. Davies, H. M. L.; Venkataramani, C., Catalytic Enantioselective Synthesis of β^2-Amino Acids. *Angewandte Chemie International Edition* **2002,** *41* (12), 2197-2199.
148. Ponsinet, R.; Chassaing, G.; Vaissermann, J.; Lavielle, S., Diastereoselective Synthesis of β^2-Amino Acids. *European Journal of Organic Chemistry* **2000,** *2000* (1), 83-90.
149. Plucińska, K.; Liberek, B., Synthesis of diazoketones derived from α-amino acids; problem of side reactions. *Tetrahedron* **1987,** *43* (15), 3509-3517.
150. Kaseda, T.; Kikuchi, T.; Kibayashi, C., Enantioselective total synthesis of (+)-(S)-dihydroperiphylline. *Tetrahedron Letters* **1989,** *30* (34), 4539-4542.
151. El Marini, A.; Roumestant, M. L.; Viallefont, P.; Razafindramboa, D.; Bonato, M.; Follet, M., Synthesis of Enantiomerically Pure β- and γ-Amino Acids from Aspartic and Glutamic Acid Derivatives. *Synthesis* **1992,** *1992* (11), 1104-1108.
152. Hawkins, J. M.; Lewis, T. A., An asymmetric ammonia synthon for Michael additions. *The Journal of organic chemistry* **1992,** *57* (7), 2114-2121.
153. Lubell, W. D.; Kitamura, M.; Noyori, R., Enantioselective synthesis of β-amino acids based on BINAP—ruthenium(II) catalyzed hydrogenation. *Tetrahedron: Asymmetry* **1991,** *2* (7), 543-554.

154. Hsiao, Y.; Rivera, N. R.; Rosner, T.; Krska, S. W.; Njolito, E.; Wang, F.; Sun, Y.; Armstrong, J. D.; Grabowski, E. J. J.; Tillyer, R. D.; Spindler, F.; Malan, C., Highly Efficient Synthesis of β-Amino Acid Derivatives via Asymmetric Hydrogenation of Unprotected Enamines. *Journal of the American Chemical Society* **2004,** *126* (32), 9918-9919.
155. Weiner, B.; Szymanski, W.; Janssen, D. B.; Minnaard, A. J.; Feringa, B. L., Recent advances in the catalytic asymmetric synthesis of β-amino acids. *Chemical Society Reviews* **2010,** *39* (5), 1656-1691.
156. Mannich, C.; Krösche, W., Ueber ein Kondensationsprodukt aus Formaldehyd, Ammoniak und Antipyrin. *Archiv der Pharmazie* **1912,** *250* (1), 647-667.
157. Arend, M.; Westermann, B.; Risch, N., Modern Variants of the Mannich Reaction. *Angewandte Chemie International Edition* **1998,** *37* (8), 1044-1070.
158. Hong, C. Y.; Kado, N.; Overman, L. E., Asymmetric synthesis of either enantiomer of opium alkaloids and morphinans. Total synthesis of (-)- and (+)-dihydrocodeinone and (-)- and (+)-morphine. *Journal of the American Chemical Society* **1993,** *115* (23), 11028-11029.
159. Knight, S. D.; Overman, L. E.; Pairaudeau, G., Asymmetric Total Syntheses of (-)- and (+)-Strychnine and the Wieland-Gumlich Aldehyde. *Journal of the American Chemical Society* **1995,** *117* (21), 5776-5788.
160. Kim, S. M.; Yang, J. W., Organocatalytic asymmetric synthesis of β^3-amino acid derivatives. *Organic & Biomolecular Chemistry* **2013,** *11* (29), 4737-4749.
161. Wenzel, A. G.; Jacobsen, E. N., Asymmetric Catalytic Mannich Reactions Catalyzed by Urea Derivatives: Enantioselective Synthesis of β-Aryl-β-Amino Acids. *Journal of the American Chemical Society* **2002,** *124* (44), 12964-12965.
162. Jones, C. R.; Dan Pantoş, G.; Morrison, A. J.; Smith, M. D., Plagiarizing Proteins: Enhancing Efficiency in Asymmetric Hydrogen-Bonding Catalysis through Positive Cooperativity. *Angewandte Chemie International Edition* **2009,** *48* (40), 7391-7394.
163. Yang, J. W.; Chandler, C.; Stadler, M.; Kampen, D.; List, B., Proline-catalysed Mannich reactions of acetaldehyde. *Nature* **2008,** *452* (7186), 453-455.
164. Kano, T.; Yamaguchi, Y.; Maruoka, K., A Designer Axially Chiral Amino Sulfonamide as an Efficient Organocatalyst for Direct Asymmetric Mannich Reactions of N-Boc-Protected Imines. *Angewandte Chemie International Edition* **2009,** *48* (10), 1838-1840.
165. Ma, Z.; Zhao, Y.; Jiang, N.; Jin, X.; Wang, J., Stereoselective nucleophilic addition of chiral lithium enolates to (N-tosyl)imines: enantioselective synthesis of β-aryl-β-amino acid derivatives. *Tetrahedron Letters* **2002,** *43* (17), 3209-3212.
166. Tang, T. P.; Ellman, J. A., Asymmetric Synthesis of β-Amino Acid Derivatives Incorporating a Broad Range of Substitution Patterns by Enolate Additions to tert-Butanesulfinyl Imines. *The Journal of organic chemistry* **2002,** *67* (22), 7819-7832.
167. Robak, M. T.; Herbage, M. A.; Ellman, J. A., Synthesis and Applications of tert-Butanesulfinamide. *Chemical Reviews* **2010,** *110* (6), 3600-3740.
168. Davis, F. A.; Zhou, P.; Reddy, G. V., Asymmetric Synthesis and Reactions of cis-N-(p-Toluenesulfinyl)aziridine-2-carboxylic Acids. *The Journal of organic chemistry* **1994,** *59* (12), 3243-3245.
169. Davies, S. G.; Garrido, N. M.; Ichihara, O.; Walters, L. A. S., Asymmetric syntheses of β-phenylalanine, α-methyl-β-phenylalanines and derivatives. *Journal of the Chemical Society, Chemical Communications* **1993,** (14), 1153-1155.
170. Hawkins, J. M.; Lewis, T. A., Asymmetric Synthesis of Erythro and Threo α-Substituted β-Amino Esters. *The Journal of organic chemistry* **1994,** *59* (3), 649-652.
171. Yang, J. W.; Stadler, M.; List, B., Proline-Catalyzed Mannich Reaction of Aldehydes with N-Boc-Imines. *Angewandte Chemie International Edition* **2007,** *46* (4), 609-11.
172. Mitsumori, S.; Zhang, H.; Ha-Yeon Cheong, P.; Houk, K. N.; Tanaka, F.; Barbas, C. F., Direct Asymmetric anti-Mannich-Type Reactions Catalyzed by a Designed Amino Acid. *Journal of the American Chemical Society* **2006,** *128* (4), 1040-1041.
173. Morimoto, H.; Lu, G.; Aoyama, N.; Matsunaga, S.; Shibasaki, M., Lanthanum Aryloxide/Pybox-Catalyzed Direct Asymmetric Mannich-Type Reactions Using a Trichloromethyl Ketone as a Propionate Equivalent Donor. *Journal of the American Chemical Society* **2007,** *129* (31), 9588-9589.
174. Seebach, D.; Sifferlen, T.; Mathieu, P. A.; Häne, A. M.; Krell, C. M.; Bierbaum, D. J.; Abele, S., CD Spectra in Methanol of β-Oligopeptides Consisting of β-Amino Acids with Functionalized Side Chains, with Alternating Configuration, and with Geminal Backbone Substituents – Fingerprints of New Secondary Structures? *Helvetica Chimica Acta* **2000,** *83* (11), 2849-2864.
175. Seebach, D.; Sifferlen, T.; Bierbaum, D. J.; Rueping, M.; Jaun, B.; Schweizer, B.; Schaefer, J.; Mehta, A. K.; O'Connor, R. D.; Meier, B. H.; Ernst, M.; Glättli, A., Isotopically Labelled and Unlabelled β-Peptides with Geminal

Dimethyl Substitution in 2-Position of Each Residue: Synthesis and NMR Investigation in Solution and in the Solid State. *Helvetica Chimica Acta* **2002,** *85* (9), 2877-2917.
176. Ihori, Y.; Yamashita, Y.; Ishitani, H.; Kobayashi, S., Chiral Zirconium Catalysts Using Multidentate BINOL Derivatives for Catalytic Enantioselective Mannich-Type Reactions; Ligand Optimization and Approaches to Elucidation of the Catalyst Structure. *Journal of the American Chemical Society* **2005,** *127* (44), 15528-15535.
177. Kobayashi, S.; Arai, K.; Shimizu, H.; Ihori, Y.; Ishitani, H.; Yamashita, Y., A Novel Dinuclear Chiral Niobium Complex for Lewis Acid Catalyzed Enantioselective Reactions: Design of a Tridentate Ligand and Elucidation of the Catalyst Structure. *Angewandte Chemie International Edition* **2005,** *44* (5), 761-764.
178. Chen, Z.; Morimoto, H.; Matsunaga, S.; Shibasaki, M., A Bench-Stable Homodinuclear Ni2−Schiff Base Complex for Catalytic Asymmetric Synthesis of α-Tetrasubstituted anti-α,β-Diamino Acid Surrogates. *Journal of the American Chemical Society* **2008,** *130* (7), 2170-2171.
179. Chowdari, N. S.; Suri, J. T.; Barbas, C. F., Asymmetric Synthesis of Quaternary α- and β-Amino Acids and β-Lactams via Proline-Catalyzed Mannich Reactions with Branched Aldehyde Donors. *Organic Letters* **2004,** *6* (15), 2507-2510.
180. White, C. J.; Yudin, A. K., Contemporary strategies for peptide macrocyclization. *Nature Chemistry* **2011,** *3* (7), 509-524.
181. Thakkar, A.; Trinh, T. B.; Pei, D., Global analysis of peptide cyclization efficiency. *ACS Combinatorial Science* **2013,** *15* (2), 120-129.
182. Crimmins, M. T.; DeBaillie, A. C., Enantioselective total synthesis of bistramide A. *Journal of the American Chemical Society* **2006,** *128* (15), 4936-7.
183. Hjelmgaard, T.; Faure, S.; Lemoine, P.; Viossat, B.; Aitken, D. J., Rapid Assembly of the Polyhydroxylated β-Amino Acid Constituents of Microsclerodermins C, D, and E. *Organic Letters* **2008,** *10* (5), 841-844.
184. Fujisawa, T.; Kooriyama, Y.; Shimizu, M., Switchover of Diastereofacial Selectivity in the Condensation Reaction of Optically Active N-Sulfinimine with Ester Enolate. *Tetrahedron Letters* **1996,** *37* (22), 3881-3884.
185. Kuduk, S. D.; DiPardo, R. M.; Chang, R. K.; Ng, C.; Bock, M. G., Reversal of diastereoselection in the addition of Grignard reagents to chiral 2-pyridyl tert-butyl (Ellman) sulfinimines. *Tetrahedron Letters* **2004,** *45* (35), 6641-6643.
186. Barrow, J. C.; Ngo, P. L.; Pellicore, J. M.; Selnick, H. G.; Nantermet, P. G., A facile three-step synthesis of 1,2-amino alcohols using the Ellman homochiral tert-butylsulfinamide. *Tetrahedron Letters* **2001,** *42* (11), 2051-2054.
187. Ferreira, F.; Audouin, M.; Chemla, F., Influence of HMPA on the Stereochemical Outcome of the Addition of a Racemic Allenylzinc onto Enantiopure N-tert-Butanesulfinimines: Stereoselective Access to Enantiopure cis-Ethynylaziridines. *Chemistry – A European Journal* **2005,** *11* (18), 5269-5278.
188. Bharatam, P. V.; Uppal, P.; Kaur, A.; Kaur, D., Theoretical investigation on the conformational preferences of sulfinimines. *Journal of the Chemical Society, Perkin Transactions 2* **2000,** (1), 43-50.
189. Shintani, R.; Ikehata, K.; Hayashi, T., Synthesis of Nine-Membered Azlactones by Palladium-Catalyzed Ring-Expansion of γ-Methylidene-δ-valerolactones with Aziridines. *The Journal of Organic Chemistry* **2011,** *76* (11), 4776-4780.
190. Ireland, R. E.; Wipf, P.; Armstrong, J. D., Stereochemical Control in the Ester Enolate Claisen Rearrangement. 1. Stereoselectivity in Silyl Ketene Acetal Formation. *The Journal of Organic Chemistry* **1991,** *56* (2), 650-657.
191. Denmark, S. E.; Beutner, G. L.; Wynn, T.; Eastgate, M. D., Lewis Base Activation of Lewis Acids: Catalytic, Enantioselective Addition of Silyl Ketene Acetals to Aldehydes. *Journal of the American Chemical Society* **2005,** *127* (11), 3774-3789.
192. Ireland, R. E.; Mueller, R. H.; Willard, A. K., The Ester Enolate Claisen Eearrangement. Stereochemical Control through Stereoselective Enolate Formation. *Journal of the American Chemical Society* **1976,** *98* (10), 2868-2877.
193. Busch-Petersen, J.; Corey, E. J., Sterically shielded secondary N-tritylamines and N-tritylamide bases, readily available and useful synthetic reagents. *Tetrahedron Letters* **2000,** *41* (15), 2515-2518.
194. Villadsen, J. S.; Stephansen, H. M.; Maolanon, A. R.; Harris, P.; Olsen, C. A., Total Synthesis and Full Histone Deacetylase Inhibitory Profiling of Azumamides A–E as Well as β2- epi-Azumamide E and β3-epi-Azumamide E. *Journal of Medicinal Chemistry* **2013,** *56* (16), 6512-6520.
195. Perlman, Z. E.; Bock, J. E.; Peterson, J. R.; Lokey, R. S., Geometric diversity through permutation of backbone configuration in cyclic peptide libraries. *Bioorganic & Medicinal Chemistry Letters* **2005,** *15* (23), 5329-5334.
196. Tang, Y. C.; Xie, H.B.; Tian, G. l.; Ye, Y. H., Synthesis of cyclopentapeptides and cycloheptapeptides by DEPBT and the influence of some factors on cyclization. *The Journal of Peptide Research* **2002,** *60* (2), 95-103.
197. Madsen, A. S.; Olsen, C. A., Profiling of Substrates for Zinc-Dependent Lysine Deacylase Enzymes: HDAC3 Exhibits Decrotonylase Activity *in Vitro*. *Angewandte Chemie International Edition* **2012,** *51* (36), 9083-7.
198. Madsen, A. S.; Olsen, C. A., Substrates for Efficient Fluorometric Screening Employing the NAD-Dependent Sirtuin 5 Lysine Deacylase (KDAC) Enzyme. *Journal of Medicinal Chemistry* **2012,** *55* (11), 5582-5590.

199. Nielsen, T. K.; Hildmann, C.; Dickmanns, A.; Schwienhorst, A.; Ficner, R., Crystal Structure of a Bacterial Class 2 Histone Deacetylase Homologue. *Journal of Molecular Biology* **2005,** *354* (1), 107-120.
200. Tonlolo, C.; Benedetti, E., The polypeptide 310-helix. *Trends in Biochemical Sciences* **1991,** *16* (0), 350-353.
201. Melnik, M.; Cozak, D., Titanium Coordination Compounds: Classification and Analysis of Crystallographic and Structural Data. *Reviews in Inorganic Chemistry* **1986,** *8* (3-4), 221-286.
202. Carter, D. C.; Moore, R. E.; Mynderse, J. S.; Niemczura, W. P.; Todd, J. S., Structure of majusculamide C, a cyclic depsipeptide from Lyngbya majuscula. *The Journal of organic chemistry* **1984,** *49* (2), 236-241.
203. Alvarado, C.; Díaz, E.; Guzmán, Á., Total synthesis of ulongamide A, a cyclic depsipeptide isolated from marine cyanobacteria Lyngbya sp. *Tetrahedron Letters* **2007,** *48* (4), 603-607.
204. Wilson, J. E.; Casarez, A. D.; MacMillan, D. W. C., Enantioselective Aldehyde α-Nitroalkylation via Oxidative Organocatalysis. *Journal of the American Chemical Society* **2009,** *131* (32), 11332-11334.
205. Humphrey, J. M.; Aggen, J. B.; Chamberlin, A. R., Total Synthesis of the Serine-Threonine Phosphatase Inhibitor Microcystin-LA. *Journal of the American Chemical Society* **1996,** *118* (47), 11759-11770.
206. Samy, R.; Kim, H. Y.; Brady, M.; Toogood, P. L., Total Synthesis of Motuporin and 5-[l-Ala]-Motuporin. *The Journal of organic chemistry* **1999,** *64* (8), 2711-2728.
207. Bai, R.; Bates, R. B.; Hamel, E.; Moore, R. E.; Nakkiew, P.; Pettit, G. R.; Sufi, B. A., Lyngbyastatin 1 and Ibu-epilyngbyastatin 1: Synthesis, Stereochemistry, and NMR Line Broadening. *Journal of Natural Products* **2002,** *65* (12), 1824-1829.
208. Rodríguez, J.; Fernández, R.; Quiñoá, E.; Riguera, R.; Debitus, C.; Bouchet, P., Onchidin: a cytotoxic depsipeptide with C2 symmetry from a marine mollusc. *Tetrahedron Letters* **1994,** *35* (49), 9239-9242.
209. de Silva, E. D.; Williams, D. E.; Andersen, R. J.; Klix, H.; Holmes, C. F. B.; Allen, T. M., Motuporin, A Potent Protein Phosphatase Inhibitor Isolated from the Papua New Guinea Sponge Theonella swinhoei Gray. *Tetrahedron Letters* **1992,** *33* (12), 1561-1564.
210. Luesch, H.; Williams, P. G.; Yoshida, W. Y.; Moore, R. E.; Paul, V. J., Ulongamides A−F, New β-Amino Acid-Containing Cyclodepsipeptides from Palauan Collections of the Marine Cyanobacterium Lyngbya sp. *Journal of Natural Products* **2002,** *65* (7), 996-1000.
211. Zolot, R. S.; Basu, S.; Million, R. P., Antibody-drug conjugates. *Nature Reviews Drug Discovery* **2013,** *12* (4), 259-260.
212. Sievers, E. L.; Senter, P. D., Antibody-Drug Conjugates in Cancer Therapy. *Annual Review of Medicine* **2013,** *64* (1), 15-29.
213. Senter, P. D.; Sievers, E. L., The discovery and development of brentuximab vedotin for use in relapsed Hodgkin lymphoma and systemic anaplastic large cell lymphoma. *Nature Biotechnology* **2012,** *30* (7), 631-637.
214. Jones, D. P.; Carlson, J. L.; Samiec, P. S.; Sternberg Jr, P.; Mody Jr, V. C.; Reed, R. L.; Brown, L. A. S., Glutathione measurement in human plasma: Evaluation of sample collection, storage and derivatization conditions for analysis of dansyl derivatives by HPLC. *Clinica Chimica Acta* **1998,** *275* (2), 175-184.
215. Luo, J. L.; Hammarqvist, F.; Andersson, K.; Wernerman, J., Skeletal muscle glutathione after surgical trauma. *Annals of surgery* **1996,** *223* (4), 420-7.
216. Meister, A., Glutathione metabolism and its selective modification. *Journal of Biological Chemistry* **1988,** *263* (33), 17205-17208.
217. Meister, A.; Anderson, M. E., Glutathione. *Annual Review of Biochemistry* **1983,** *52* (1), 711-760.
218. Carpino, L. A.; Philbin, M.; Ismail, M.; Truran, G. A.; Mansour, E. M. E.; Iguchi, S.; Ionescu, D.; El-Faham, A.; Riemer, C.; Warrass, R.; Weiss, M. S., New Family of Base- and Nucleophile-Sensitive Amino-Protecting Groups. A Michael-Acceptor-Based Deblocking Process. Practical Utilization of the 1,1-Dioxobenzo[*b*]thiophene-2-ylmethyloxycarbonyl (Bsmoc) Group. *Journal of the American Chemical Society* **1997,** *119* (41), 9915-9916.
219. Santi, D. V.; Schneider, E. L.; Reid, R.; Robinson, L.; Ashley, G. W., Predictable and tunable half-life extension of therapeutic agents by controlled chemical release from macromolecular conjugates. *Proceedings of the National Academy of Sciences* **2012,** *109* (16), 6211-6.
220. D'Addona, D.; Bochet, C. G., Preparation of carbamates from amines and alcohols under mild conditions. *Tetrahedron Letters* **2001,** *42* (31), 5227-5229.
221. Kim, S.-B.; Cho, D.-G., HgII-Selective Fluorescent Indicator: One-Step Synthesis. *European Journal of Organic Chemistry* **2012,** *2012* (13), 2495-2498.
222. Thiemann, T.; Fujii, H.; Ohira, D.; Arima, K.; Li, Y.; Mataka, S., Cycloaddition of thiophene S-oxides to allenes, alkynes and to benzyne. *New Journal of Chemistry* **2003,** *27* (9), 1377-1384.
223. Khodaei, M. M.; Bahrami, K.; Karimi, A., H_2O_2/Tf_2O System: An Efficient Oxidizing Reagent for Selective Oxidation of Sulfanes. *Synthesis* **2008,** *2008* (EFirst), 1682-1684.

224. Pouzet, P.; Erdelmeier, I.; Dansette, P. M.; Mansuy, D., Synthesis of (4-chlorophenyl)-(1-oxo-1λ4-benzo[*b*]thien-2-yl)methanone and study of its reactivity towards sulfur- and oxygen-containing nucleophiles. *Tetrahedron* **1998,** *54* (49), 14811-14824.
225. Inks, E. S.; Josey, B. J.; Jesinkey, S. R.; Chou, C. J., A Novel Class of Small Molecule Inhibitors of HDAC6. *ACS Chemical Biology* **2011,** *7* (2), 331-339.
226. Nielsen, L.; Lindsay, K. B.; Faber, J.; Nielsen, N. C.; Skrydstrup, T., Stereocontrolled Synthesis of Methyl Silanediol Peptide Mimics. *The Journal of Organic Chemistry* **2007,** *72* (26), 10035-10044.
227. Chowdhury, P. S.; Gupta, P.; Kumar, P., Enantioselective synthesis of decarestrictine J. *Tetrahedron Letters* **2009,** *50* (51), 7188-7190.
228. Hernández, D.; Lindsay, K. B.; Nielsen, L.; Mittag, T.; Bjerglund, K.; Friis, S.; Mose, R.; Skrydstrup, T., Further Studies toward the Stereocontrolled Synthesis of Silicon-Containing Peptide Mimics. *The Journal of Organic Chemistry* **2010,** *75* (10), 3283-3293.
229. Nakao, Y.; Yoshida, S.; Matsunaga, S.; Shindoh, N.; Terada, Y.; Nagai, K.; Yamashita, J. K.; Ganesan, A.; van Soest, R. W.; Fusetani, N., Azumamides A-E: histone deacetylase inhibitory cyclic tetrapeptides from the marine sponge Mycale izuensis. *Angewandte Chemie International Edition* **2006,** *45* (45), 7553-7.
230. Bothner-By, A. A.; Stephens, R. L.; Lee, J.; Warren, C. D.; Jeanloz, R. W., Structure determination of a tetrasaccharide: transient nuclear Overhauser effects in the rotating frame. *J. Am. Chem. Soc.* **1984,** *106* (3), 811-813.
231. Kessler, H.; Griesinger, C.; Kerssebaum, R.; Wagner, K.; Ernst, R. R., Separation of cross-relaxation and J cross-peaks in 2D rotating-frame NMR spectroscopy. *Journal of the American Chemical Society* **1987,** *109* (2), 607-609.
232. Hu, H.; Krishnamurthy, K., Revisiting the initial rate approximation in kinetic NOE measurements. *Journal of Magnetic Resonance* **2006,** *182* (1), 173-177.
233. Pardi, A.; Billeter, M.; Wüthrich, K., Calibration of the angular dependence of the amide proton-C^{α} proton coupling constants, $^{3}J_{HN\alpha}$, in a globular protein: Use of $^{3}J_{HN\alpha}$ for identification of helical secondary structure. *Journal of Molecular Biology* **1984,** *180* (3), 741-751.
234. Shivakumar, D.; Williams, J.; Wu, Y.; Damm, W.; Shelley, J.; Sherman, W., Prediction of Absolute Solvation Free Energies using Molecular Dynamics Free Energy Perturbation and the OPLS Force Field. *Journal of Chemical Theory and Computation* **2010,** *6* (5), 1509-1519.
235. Berendsen, H. J. C.; Postma, J. P. M.; van Gunsteren, W. F.; DiNola, A.; Haak, J. R., Molecular dynamics with coupling to an external bath. *The Journal of chemical physics* **1984,** *81* (8), 3684-3690.
236. Davis, F. A.; Nolt, M. B.; Wu, Y.; Prasad, K. R.; Li, D.; Yang, B.; Bowen, K.; Lee, S. H.; Eardley, J. H., Asymmetric Synthesis of β-Amino Carbonyl Compounds with N-Sulfinyl β-Amino Weinreb Amides. *The Journal of Organic Chemistry* **2005,** *70* (6), 2184-2190.
237. Carpino, L. A.; Ismail, M.; Truran, G. A.; Mansour, E. M. E.; Iguchi, S.; Ionescu, D.; El-Faham, A.; Riemer, C.; Warrass, R., The 1,1-Dioxobenzo[*b*]thiophene-2-ylmethyloxycarbonyl (Bsmoc) Amino-Protecting Group. *The Journal of Organic Chemistry* **1999,** *64* (12), 4324-4338.

Appendix

Accepted manuscripts

1. Villadsen, J. S.; Stephansen, H. M.; Maolanon, A. R.; Harris, P.; Olsen, C. A., Total Synthesis and Full Histone Deacetylase Inhibitory Profiling of Azumamides A–E as Well as β2- epi-Azumamide E and β3-epi-Azumamide E. *Journal of Medicinal Chemistry* **2013,** *56* (16), 6512-6520.

Manuscripts in preparation

2. Maolanon, A. R; Villadsen, J. S.; Hoeck, C.; Gotfredsen, C. H.; Harris, P; Olsen, C. A., Structural editing of the azumamide scaffold: Synthesis and structure–activity relationships, (manuscript in preparation)

Journal of Medicinal Chemistry

Article

pubs.acs.org/jmc

Total Synthesis and Full Histone Deacetylase Inhibitory Profiling of Azumamides A−E as Well as β^2- *epi*-Azumamide E and β^3-*epi*-Azumamide E

Jesper S. Villadsen, Helle M. Stephansen, Alex R. Maolanon, Pernille Harris, and Christian A. Olsen*

Department of Chemistry, Technical University of Denmark, Kemitorvet 207, Kongens Lyngby DK-2800, Denmark

Supporting Information

ABSTRACT: Cyclic tetrapeptide and depsipeptide natural products have proven useful as biological probes and drug candidates due to their potent activities as histone deacetylase (HDAC) inhibitors. Here, we present the syntheses of a class of cyclic tetrapeptide HDAC inhibitors, the azumamides, by a concise route in which the key step in preparation of the noncanonical disubstituted β-amino acid building block was an Ellman-type Mannich reaction. By tweaking the reaction conditions during this transformation, we gained access to the natural products as well as two epimeric homologues. Thus, the first total syntheses of azumamides B−D corroborated the originally assigned structures, and the synthetic efforts enabled the first full profiling of HDAC inhibitory properties of the entire selection of azumamides A−E. This revealed unexpected differences in the relative potencies within the class and showed that azumamides C and E are both potent inhibitors of HDAC10 and HDAC11.

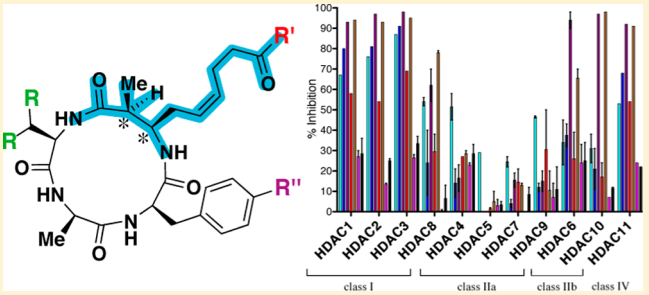

INTRODUCTION

Macrocyclic peptides have played important roles in the field of epigenetics due to their potent activities as inhibitors of histone deacetylase (HDAC) enzymes. One of the two HDAC targeting drugs (**1**[1] and **3**) that are approved by the U.S. Food and Drug Administration (FDA) for clinical treatment of cutaneous T-cell lymphoma is the macrocyclic natural product romidepsin (**3**).[2] Furthermore, a cyclic tetrapeptide, trapoxin,[3] played an instrumental role in the first isolation of a mammalian HDAC enzyme.[4,5] Thus, this class of inhibitors holds promise as tool compounds as well as potential drug candidates targeting HDACs.[6−9]

Though clearly bearing an overall resemblence to the classical cyclic tetrapeptide HDAC inhibitors [including, for example, apicidin (**4**)],[10] the azumamides (**5**−**9**) are structurally unique in that their extended Zn^{2+}-coordinating amino acid (shown in yellow in Figure 1) is a disubstituted β-amino acid.[11] Furthermore, we found the azumamides interesting due to the relatively strong potencies reported for azumamide E against class I HDACs[12] in spite of its weak Zn^{2+}-coordinating carboxylic acid functionality.[13] Previously, azumamide A[14,15] and azumamide E[12,14−16] have been prepared by multistep chemical syntheses, but only azumamide E was tested against recombinant HDAC isoforms 1−9.[12] Furthermore, in vitro profiling with recombinant HDACs has witnessed important new developments since the publication of those results.[17,18] We therefore found it relevant to explore the properties of these macrocycles in more detail by preparing the complete selection of natural products (**5**−**9**), and profiling their activities against the full panel of recombinant human Zn^{2+}-dependent HDAC enzymes, HDAC1−11.

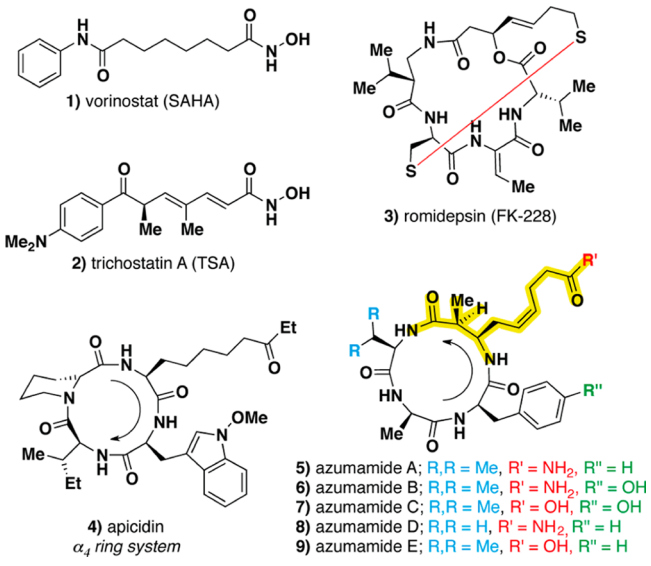

Figure 1. Structures of archetypical HDAC inhibitors (**1**−**4**) and target azumamides **5**−**9**.

As total syntheses of azumamides B−D had not been reported previously, this work would also allow unequivocal validation of the proposed structures.[11]

For syntheses of the azumamides, we envisaged two significant challenges: first, efficient stereoselective synthesis

Received: June 6, 2013
Published: July 18, 2013

of the disubstituted β-amino acid, and second, the macrocyclization step, which is known to be difficult for small cyclic peptides in general[19] and furthermore proved challenging in previously reported syntheses of azumamide analogues.[12]

RESULTS AND DISCUSSION

Building Block Synthesis. For our synthesis of the β-amino acid building block, we chose a diastereoselective Ellman-type Mannich reaction to set the stereochemistry, as also previously reported by Ganesan and co-workers.[15] However, to avoid having this important transformation at a late stage in our synthetic route, we decided to optimize this reaction between a propionate ester and a simple imine as shown in eq 1.

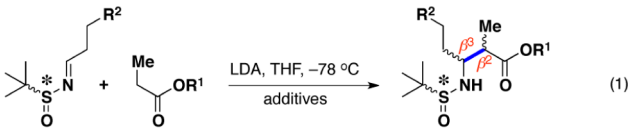

R1 and R2 are defined in Table 1.

This should give an intermediate with the correct stereochemistry (2*S*,3*R*), which could be readily elaborated to give the desired β-amino acid by robust organic synthetic transformations (vide infra). Mannich reactions between ester enolates and chiral sulfinylimines have been studied extensively,[20,21] and using previously reported conditions as our starting point we conducted an optimization study as outlined in Table 1. The *tert*-butyl ester showed superior selectivity (entry 5) compared to the less bulky methyl, ethyl, allyl, and PMB esters (entries 1−4), and furthermore, the methyl ester did not proceed to completion in our hands. Somewhat surprisingly, however, the major diastereoisomer in entry 5 proved to have (2*S*,3*S*) configuration as determined by X-ray crystallography upon desilylation (Figure 2).

This indicates that the pathway leading to our major isomer did not proceed through the six-membered Zimmerman−Traxler-type transition state,[22] which has been proposed to be responsible for the diastereoselectivity with similar substrates.[20,23] By using HMPA as an additive instead of a Lewis acid, this reaction has previously been shown to proceed through a different transition state,[20] and indeed we saw the same product distribution when using HMPA and $TiCl(O^iPr)_3$ as additives with our substrates (entries 5 and 6). This indicates that the six-membered transition state, where coordination of

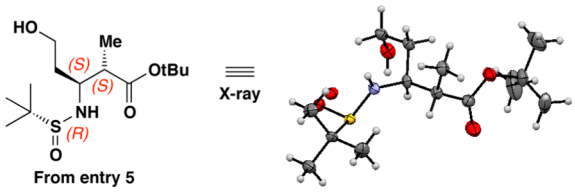

Figure 2. X-ray crystal structure of the (2*S*,3*S*) precursor obtained by desilylation of the major product in entry 5 of Table 1.

titanium is crucial, is highly unlikely to play a significant role in the formation of our major isomer. This is not in agreement with the diastereoselectivities observed with the substrates reported by Ganesan and co-workers.[15] Thus, to address whether the steric bulk of the triisopropylsilyl ether was responsible for interrupting the six-membered transition state, we performed the reaction with different means of protecting the alcohol (entries 7−9). No significant effect was observed, however, indicating instead that the steric bulk of the *tert*-butyl ester caused the predominance of a different transition state when using our substrates. This is also in agreement with the original study by Tang and Ellman[20] where the level of selectivity decreased for 2,3-disubstituted β-amino acids when the bulk of the ester increased from methyl to *tert*-butyl.

Because we were interested in taking advantage of solid-phase synthesis methods to prepare the linear tetrapeptide azumamide precursors with a minimum of chromatographic purification steps, we were keen on keeping the acid-labile *tert*-butyl ester protecting group, which would allow easy protecting group manipulation to give an Fmoc-protected β-amino acid building block. Hence, instead of substituting this protecting group, we decided to optimize the Mannich reaction conditions to deliver the desired stereochemistry. First, we changed the stereochemistry of the sulfinylimine to the *R*-enantiomer, which expectedly furnished the enantiomer of entries 5−9 (2*R*,3*R*) as the major isomer (entry 10). We then hypothesized that the configuration of the 2-position would be sensitive to the *E*/*Z* configuration of the enolate. Using Ireland's conditions for forming the enolate in the presence of HMPA,[24,25] we achieved >80% *Z*-isomer, which gratifyingly afforded the (2*S*,3*R*) product as major isomer (entry 11). Under the developed conditions, we prepared compound **12**, which was further elaborated to give Fmoc-protected β-amino acid **16** in 15% overall yield with just four column chromatographic purification steps from compound **10** (Scheme 1).

Table 1. Optimization of Stereochemical Outcome of the Mannich Reaction Shown in Equation 1

entry	auxiliary*	R^1	R^2	additive	enolate[a]	dr[b]	major isomer
1	*R*	Me	$OSi(^iPr)_3$	$TiCl(O^iPr)_3$	*E*	47:39:10:4	ND[c]
2	*R*	Et	$OSi(^iPr)_3$	$TiCl(O^iPr)_3$	*E*	49:29:11:11	ND
3	*R*	allyl	$OSi(^iPr)_3$	$TiCl(O^iPr)_3$	*E*	46:34:10:10	ND
4	*R*	PMB	$OSi(^iPr)_3$	$TiCl(O^iPr)_3$	*E*	46:33:11:10	ND
5	*R*	^{t}Bu	$OSi(^iPr)_3$	$TiCl(O^iPr)_3$	*E*	60:26:8:6	(2*S*,3*S*)[d]
6	*R*	^{t}Bu	$OSi(^iPr)_3$	HMPA	*E*	71:15:14:0	(2*S*,3*S*)
7	*R*	^{t}Bu	OBn	$TiCl(O^iPr)_3$	*E*	70:18:12:0	ND
8	*R*	^{t}Bu	OPMB	$TiCl(O^iPr)_3$	*E*	77:13:10:0	(2*S*,3*S*)
9	*R*	^{t}Bu	$OSi(Et)_3$	$TiCl(O^iPr)_3$	*E*	75:21:4:0	(2*S*,3*S*)[d]
10	*S*	^{t}Bu	$OSi(^iPr)_3$	HMPA	*E*	77:18:5:0	(2*R*,3*R*)[e]
11	*S*	^{t}Bu	$OSi(^iPr)_3$	HMPA[f]	*Z*	64:25:8:2	(2*S*,3*R*)[g]

[a]Major configuration of the enolate as determined by NMR and by trapping with ^{t}BuMe$_2$SiCl. [b]Diastereomeric ratio determined by ^{1}H NMR. [c]ND = not determined. [d]Determined by X-ray crystallography on its desilylated homologue. [e]Determined spectroscopically by comparison with its enantiomer from entries 5 and 9. [f]HMPA (5.4 equiv) was added prior to the substrate to obtain the (*Z*)-enolate (>80%). [g]Determined by comparison of spectroscopic data of the fully elaborated Boc-protected β-amino acid with previously reported data.[12]

dx.doi.org/10.1021/jm4008449 | J. Med. Chem. 2013, 56, 6512−6520

Scheme 1. Synthesis of β-Amino Acid Building Block 16.[a]

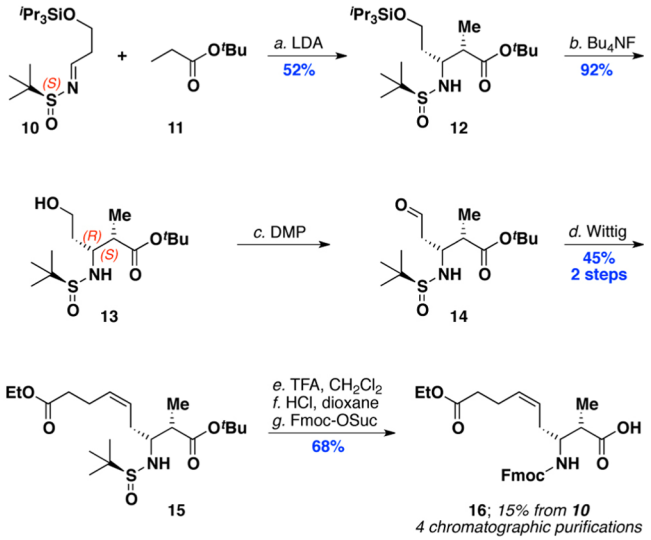

[a]Reagents and conditions: (a) HMPA (6.4 equiv), LDA (2.6 equiv), **11** (2.5 equiv), THF, −78 °C, 30 min; then **10**, −78 °C, 30 min. (b) AcOH (1.0 equiv), Bu_4NF (2.0 equiv), THF, 0 °C → rt, 1.5 h. (c) $NaHCO_3$ (1.5 equiv), Dess−Martin periodinane (1.4 equiv), dry CH_2Cl_2, 0 °C → rt, 1.5 h. (d) KHMDS (1.9 equiv), Ph_3PBr-$(CH_2)_3COOEt$ (2.0 equiv), THF, −78 °C → rt, 18 h. (e) TFA−CH_2Cl_2 (1:1, 10 mL, 80 equiv), 0 °C → rt, 3 h. (f) HCl (4.0 M in dioxane, 3.0 equiv), dioxane, 3 h. (g) Na_2CO_3 (4.0 equiv), Fmoc-OSuc (1.2 equiv), dioxane−H_2O, 0 °C → rt, 2 h.

The Boc-protected homologue of **16** was also prepared to confirm the (2*S*,3*R*) stereochemistry by comparison of spectroscopic data (optical rotation and NMR) with those previously reported (Figure S1 in Supporting Information).[12] Furthermore, the β^2- and β^3-epimeric building blocks were prepared by elaboration of the major isomers from entries 10 and 5, respectively (see Supporting Information for details). Although the achieved diastereomeric ratios were not particularly impressive, this strategy very nicely provided the correct stereochemistry along with two novel β-amino acids, enabling investigation of the biochemical effect of stereochemical configuration at these two chiral centers.

Cyclic Peptide Synthesis. Because three different points of cyclization had been reported for azumamide E and since these were all performed with different coupling reagents,[12,14,15] we performed cyclization experiments using a simplified model peptide to address the issue. Not too surprisingly, this showed that macrolactamizations with the most sterically hindered amino acids at the C-terminal were particularly poor, resulting in significant amounts of N-terminal guanidinylation, incomplete cyclization, epimerization, and/or dimerization (Table S1 in Supporting Information). Thus, we prepared the linear tetrapeptides **17**, **19**, and **21** on solid support by standard Fmoc solid-phase synthesis using β-amino acid **16** and commercially available Fmoc-D-amino acids.

In Scheme 2A, the cyclization was then performed at the β-amino acid position and in Scheme 2B at the alanine residue, whereas the preparation of azumamide D (**8**) was achieved by cyclization between the two least sterically challenging alanine residues (Scheme 2C). After cleavage from the 2-chlorotrityl polystyrene resin with dilute TFA, the linear tetramers were ring-closed by use of HATU under dilute conditions (0.4−0.5 mM),[26−29] and furthermore slow addition of the linear peptide by syringe pump to a solution of Hünig's base and HATU, as described by Ganesan and co-workers,[15] was tested. Judging from LC−MS analyses of the reaction mixtures, we could not observe any significant differences between the cyclization yields obtained with the different methods. Although all the couplings proceeded satisfactorily, with full conversion of linear peptides and minor amounts of the corresponding dimers as the only observed byproducts, the resulting overall isolated yields were relatively low (~10%). We ascribe this to difficulties during purification of the macrocyclic products by preparative reversed-phase HPLC caused by poor water solubility, as we were able to recover more material by purifying the macrocycles by column chromatography. Unfortunately, however, this did not provide the final compounds in satisfyingly high purity for the bioassays, and thus the final compounds were all subjected to preparative reversed-phase HPLC purification although this resulted in a loss of material. Carbodiimide-mediated amidation of the side chain was attempted for conversion of **7** to **6** and **23** to **8**, but the reaction was slow and gave varying yields (**6** vs **8**, Scheme 2). Instead, HATU-mediated coupling was attempted for conversion of **9** to **5**, and this proved faster and gave an acceptable yield (**5**). Spectral data of all the natural products **5**−**9** were in excellent agreement with those originally reported for the azumamides isolated from natural sources,[5] thus corroborating the original structural assignment (Figures S2−S6 in Supporting Information). Finally, the two epimeric β-amino acid building blocks were applied in analogous syntheses of β^3-*epi*-azumamide E (**26**) and β^2-*epi*-azumamide E (**29**) as shown in Scheme 3.

HDAC Screening. As an initial test of the HDAC inhibitory potency of all seven compounds, we first screened against the full panel of recombinant human HDACs at two compound concentrations (50 μM and 5 μM). Protocols for HDAC1−9 were adapted from Bradner et al.,[18] using the fluorogenic Ac-LeuGlyLys(Ac)-AMC substrate for HDAC1−3 and 6 while using the Ac-LeuGlyLys(tfa)-AMC substrate for HDAC4, 5, and 7−9. For HDAC10 we used the tetrapeptide Ac-ArgThr-Lys(Ac)Lys(Ac)-AMC,[30] which was recently reported to perform well with this enzyme.[31] Finally, for HDAC11, we also used Ac-LeuGlyLys(Ac)-AMC as substrate.[32]

The site-specifically epimerized compounds exhibited no activity as previously reported for an analogue having both stereocenters inverted.[7] It was not surprising that **26** was inactive, but it is noteworthy that the subtle change of inverting the stereochemistry of a single methyl group in **29** had such a detrimental effect across the entire selection of enzymes (Figure 3). Furthermore, none of the compounds **5**−**9** were able to inhibit class IIa HDAC activity against a trifluoroacetylated substrate (Figure 3).

Inhibitor K_i Values. Next, we performed dose−response experiments for all compound−HDAC combinations that gave above 50% inhibition in the initial assay (Figure S7 and Table S2 in Supporting Information). The obtained IC_{50} values were converted to K_i values by use of the Cheng−Prusoff equation $[K_i = IC_{50}/(1 + [S]/K_m)]$ with the assumption of a standard fast-on−fast-off mechanism of inhibition. Reported K_m values were applied for the calculations except HDAC10, where we determined the K_m for the used substrate to be 1.5 ± 0.2 μM (Figure 4).

Low potencies were recorded against HDACs 6 and 8, which is in accordance with previous data for azumamide E (Table 2);[6] however, compounds **7** and **9** were both potent inhibitors of HDACs 10 and 11. Although they are classified together

dx.doi.org/10.1021/jm4008449 | J. Med. Chem. 2013, 56, 6512−6520

Scheme 2. Synthesis of Azumamides A–E by Solid-Phase Synthesis Followed by Head-to-Tail Macrolactamization in Solution[a]

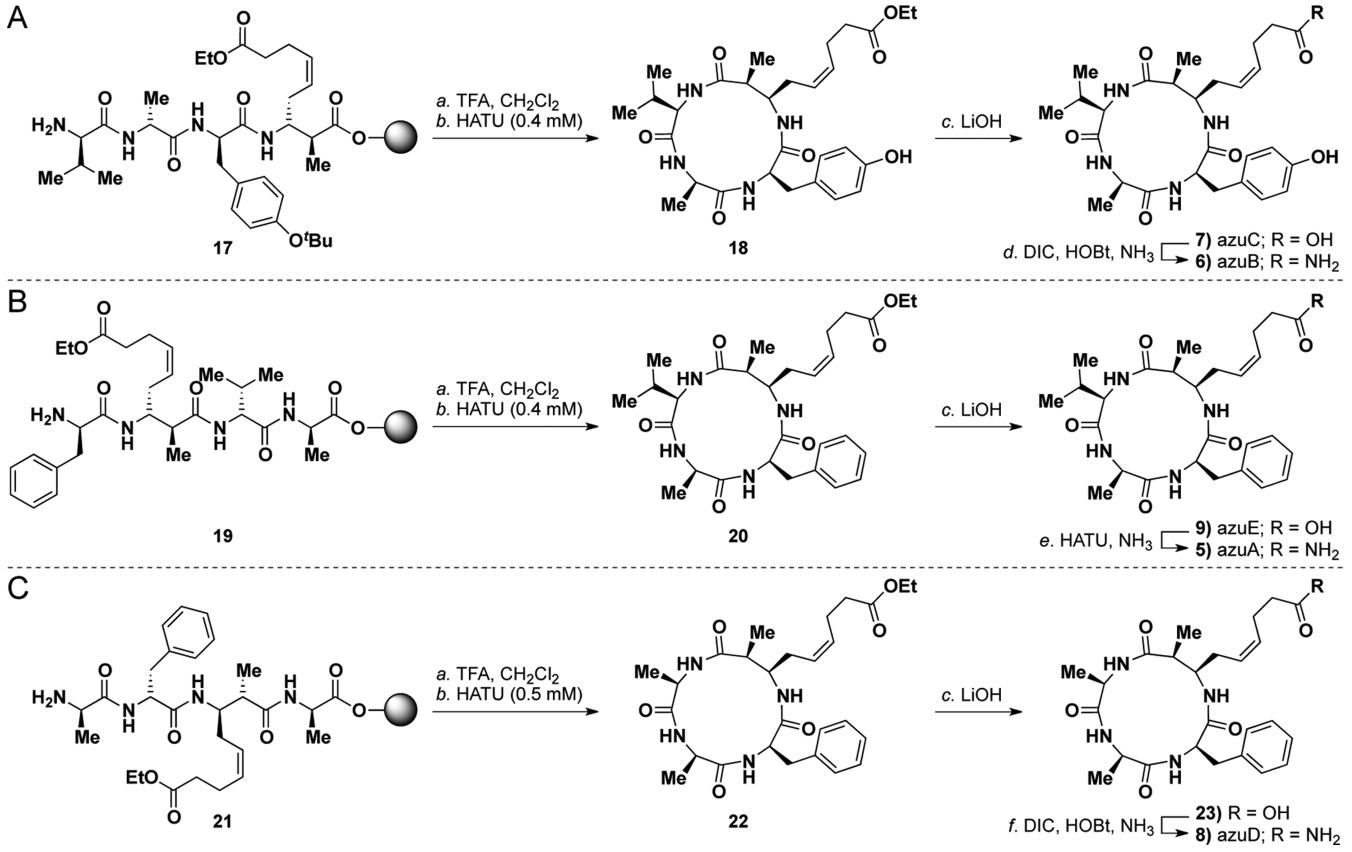

[a]Reagents and conditions: (a) TFA–CH_2Cl_2 (1:1), 2 × 30 min. (b) HATU, $^iPr_2NEt$ (8.0 equiv), DMF (0.4–0.5 mM peptide concn), 17–21 h; then HATU (0.5 equiv), 1–3 h [A, 11% **18** after preparative HPLC; B, 25% **20** after column chromatography; C, 19% **22** after column chromatography]. (c) LiOH, THF–H_2O (1:1). (d) DIC (11 equiv), HOBt (3.0 equiv), $^iPr_2NEt$ (4.0 equiv), NH_3–dioxane (25 equiv), DMF–CH_2Cl_2 (2:1), 5 days, 67%. (e) HATU (2.0 equiv), $^iPr_2NEt$ (5.5 equiv), NH_3–dioxane (25 equiv), DMF, 5.5 h, 40% (for steps c and e). (f) DIC (6.0 equiv), HOBt (3.0 equiv), $^iPr_2NEt$ (4.0 equiv), NH_3–dioxane and NH_3–MeOH (30 equiv), CH_2Cl_2–DMF (2:1), 13 days, 11% (for steps c and f).

Scheme 3. Synthesis of the Two Epimers 26 and 29 of Azumamide E by Solid-Phase Synthesis Followed by Head-to-Tail Macrolactamization in Solution[a]

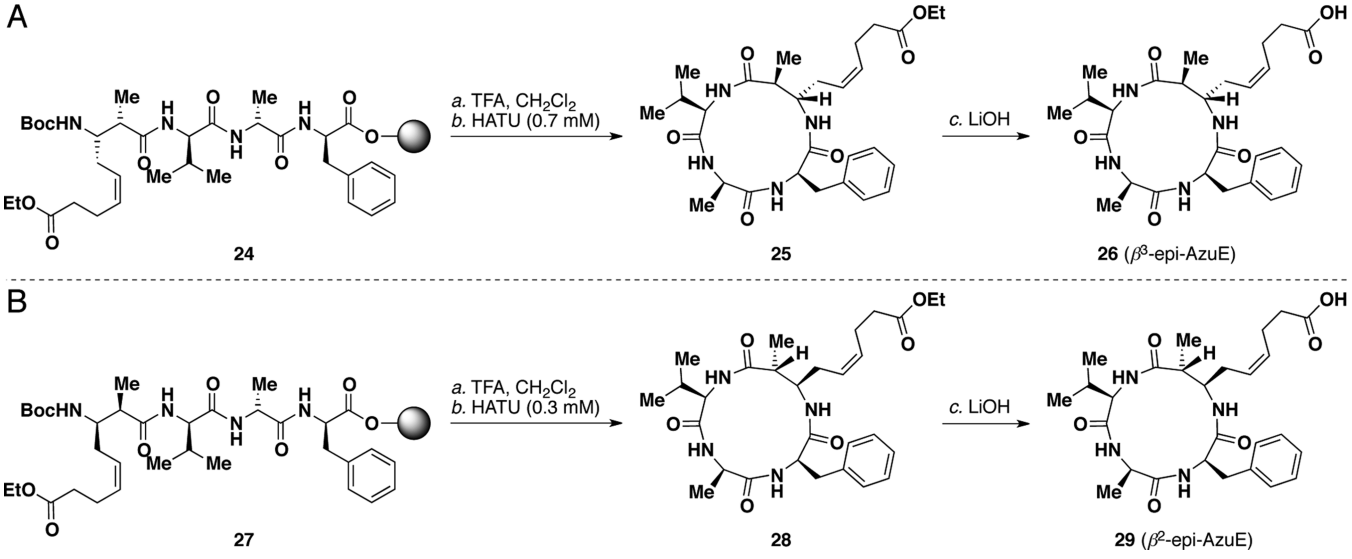

[a]Reagents and conditions: (a) TFA–CH_2Cl_2 (1:1), 2 × 30 min. (b) HATU, $^iPr_2NEt$ (8.0 equiv), DMF (0.3–0.7 mM peptide concn), 17–21 h. (c) LiOH, THF–H_2O (1:1).

(class IIb), HDACs 6 and 10 clearly interact very differently with these inhibitors.

Generally, we found the compounds with a carboxylic acid Zn^{2+}-binding group (**7** and **9**) to be more potent than the

dx.doi.org/10.1021/jm4008449 | J. Med. Chem. 2013, 56, 6512–6520

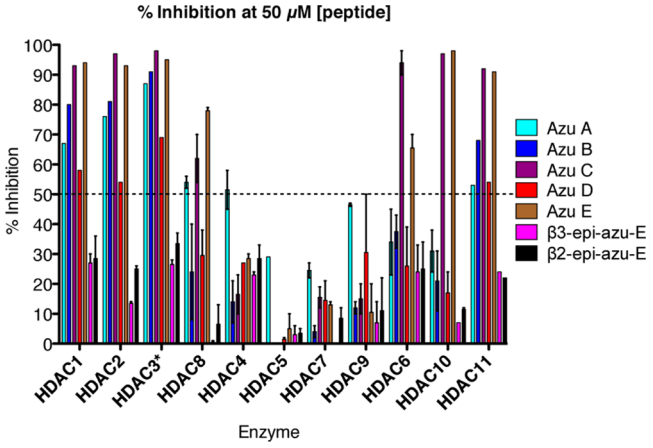

Figure 3. Single-dose HDAC inhibitory screening. Assays were performed at 50 μM (shown) and 5 μM (not shown) peptide concentrations. We chose <50% inhibition at 50 μM as our cutoff to sort away inactive compounds before performing full dose−response experiments. All compound−enzyme combinations that were discarded at this stage were tested in at least two individual assays performed in duplicate. Error bars represent the standard deviation. (*) Fusion protein of GST-tagged HDAC3 with the deacetylase activation domain (DAD) of nuclear receptor corepressor (NCoR1).

carboxamides (**5**, **6**, and **8**), which is in contrast to the originally reported HDAC inhibition data obtained for the natural products against an HDAC-containing cell extract.[5] However, the data presented herein agree with subsequent work from Ganesan and co-workers[15] on azumamide A (**5**) and azumamide E (**9**). We thus show that this applies to all the azumamides, which also confirms that a carboxylate Zn^{2+}-binding group renders HDAC inhibitors significantly more potent than a corresponding carboxamide, as would be expected from literature precendents.[19,26,27] Furthermore, compound **7** was more potent than **9** against HDACs 1−3, 6, 10, and 11, which is also in contrast to the original evaluation that found azuE (**9**) more potent than azuC (**7**) against crude enzymes from K562 cell extract.[5] The tyrosine-containing compound (**7**) exhibited ∼2-fold higher potency against HDACs 1, 3, 6, 10, and 11, whereas the phenylalanine-containing azumamide E (**9**) was only more potent against HDAC8, albeit at micromolar K_i values.

Finally, the inhibition of HDAC11 by azumamides C (**7**) and E (**9**) is, to the best of our knowledge, the first demonstration of potent cyclic peptide inhibitors of this isozyme.[33] Notably, these binding affinities were achieved without the presence of a strong Zn^{2+} chelator, such as hydroxamic acid.

CONCLUSIONS

In summary, we report total syntheses of all five azumamides, including for the first time azumamides B−D, which corroborate the originally proposed structures. Our synthetic route furthermore enabled preparation of site-specifically edited analogues for exploration of structure−activity relationships (SAR).[34−36] The HDAC profiling results show that the β-amino acid residue, present in all the azumamides, is sensitive to even slight modifications. In addition, the original HDAC testing using cell extract indicated that azumamide E was the most

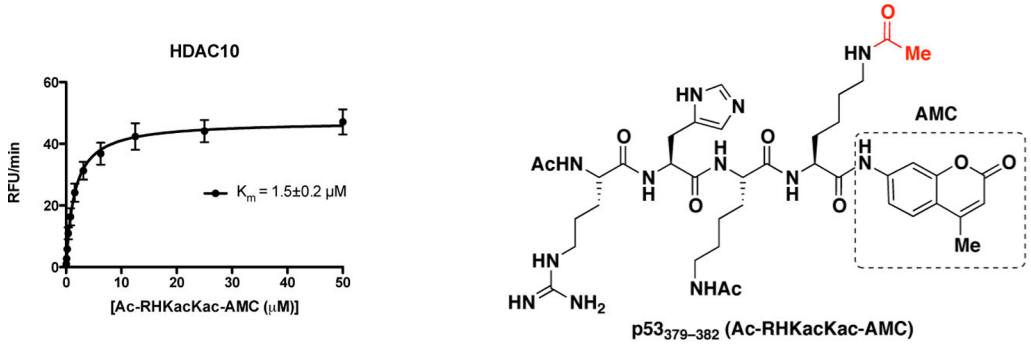

Figure 4. Michaelis−Menten plot for HDAC10.

Table 2. Potencies of Azumamides against Zn^{2+}-Dependent Histone Deacetylases[a]

	K_i values (nM)										
	class I				class IIa				class IIb		class IV
compd	HDAC1	HDAC2	HDAC3[b]	HDAC8	HDAC4	HDAC5	HDAC7	HDAC9	HDAC6	HDAC10	HDAC11
5 (azuA)	>5000	>5000	3200	>5000	52%[c]	IA[d]	IA	IA	IA	IA	>5000
6 (azuB)	5000	3000	3000	IA	IA	IA	IA	IA	IA	IA	>5000
7 (azuC)	32 ± 1	40 ± 20	14 ± 1	>5000	IA	IA	IA	IA	2000	10 ± 4	35 ± 3
8 (azuD)	>5000	>5000	3700	IA	IA	IA	IA	IA	IA	IA	>5000
9 (azuE)	67 ± 7	50 ± 30	25 ± 5	4400	IA	IA	IA	IA	>5000	20 ± 12	60 ± 16
26 (β^3-*epi*-azuE)	IA	IA	IA	IA	IA	IA	IA	IA	IA	IA	IA
29 (β^2-*epi*-azuE)	IA	IA	IA	IA	IA	IA	IA	IA	IA	IA	IA
1 (SAHA)	8 ± 1.5	7 ± 1.5	12 ± 4	700 ± 20	IA	IA	IA	IA	22 ± 9	NT[e]	13 ± 2
3 (FK-228)[f]	0.002	0.038	0.15	0.15	20.5	550	1250	1100	10	NT	NT

[a] IC_{50} values were determined from at least two individual dose−response experiments performed in duplicate (Figure S7 in Supporting Information), and K_i values were calculated from the Cheng−Prusoff equation. [b] Fusion protein of GST-tagged HDAC3 with deacetylase activation domain NCoR1. [c] Percent inhibition at 50 μM inhibitor concentration. [d] IA = inactive (<50% inhibition at 50 μM [inhibitor], Figure 3). [e] NT = not tested. [f] Data from Bradner et al.[18]

dx.doi.org/10.1021/jm4008449 | J. Med. Chem. 2013, 56, 6512−6520

potent of the series, but the comprehensive profiling presented herein shows that azumamide C is in fact ~2-fold more potent than azumamide E against the majority of the isozymes.

By taking advantage of the modular methodologies described in this article and building on the gained SAR information, we are currently investigating collections of azumamide analogues in search of more potent and selective ligands based on this promising scaffold.

EXPERIMENTAL SECTION

General. All chemicals and solvents were analytical-grade and were used without further purification. Vacuum liquid chromatography (VLC) was performed on silica gel 60 (particle size 0.015−0.040 μm). UPLC−MS analyses were performed on a Phenomenex Kinetex column (1.7 μm, 50 × 2.10 mm) by use of a Waters Acquity ultra-high-performance liquid chromatography system. A gradient with eluent I (0.1% HCOOH in water) and eluent II (0.1% HCOOH in acetonitrile) rising linearly from 0% to 95% II during t = 0.00−2.50 min was applied at a flow rate of 1 mL/min (gradient A) or during t = 0.00−5.20 min (gradient B). Analytical HPLC was performed on a Phenomenex Luna column [150 mm × 4.6 mm, C_{18} (3 μm)] by use of an Agilent 1100 LC system equipped with a UV detector. Gradient C, with eluent III (0.1% TFA in water) and eluent IV (0.1% TFA in acetonitrile) rising linearly from 0% to 95% IV during t = 2−20 min, was applied at a flow rate of 1 mL/min. Preparative reversed-phase HPLC was performed on a Phenomenex Luna column [250 mm × 20 mm, C_{18} (5 μm, 100 Å)] by use of an Agilent 1260 LC system equipped with a diode-array UV detector and an evaporative light scattering detector (ELSD). A gradient, with eluent V (95:5:0.1, water−MeCN−TFA) and eluent VI (0.1% TFA in acetonitrile) rising linearly from 0% to 95% IV during t = 5−45 min, was applied at a flow rate of 20 mL/min. All tested compounds were purified to homogeneity and shown by both analytical HPLC (gradient C) and LC−MS (gradient A) to be of more than 95% purity. One- and two-dimensional NMR spectra were recorded on a Varian Mercury 300 instrument or a Varian INOVA 500 MHz instrument. All spectra were recorded at 298 K. Correlation spectroscopy (COSY) spectra were recorded with a relaxation delay of 1.5 s before each scan, a spectral width of 6k × 6k, and eight FIDs and 1k × 512 data points collected. Heteronuclear single quantum coherence (HSQC) spectra were recorded with a relaxation delay of 1.5 s before each scan, a spectral width of 6k × 25k, and 16 FIDs and 1k × 128 data points collected. Heteronuclear two-bond correlation (H2BC) spectra were recorded with a relaxation delay of 1.5 s before each scan, a spectral width of 4k × 35k, and 16 FIDs at 295 K and 1k × 256 data points collected. Heteronuclear multiple-bond correlation (HMBC) spectra were recorded with a relaxation delay of 1.5 s before each scan, a spectral width of 6k × 35k, and 32 FIDs and 1k × 256 data points collected. Chemical shifts are reported in parts per million (ppm) relative to deuterated solvent peaks as internal standards (δH, DMSO-d_6 2.50 ppm; δC, DMSO-d_6 39.52 ppm, δH, CD_3OH 3.30 ppm; δH, $CDCl_3$ 7.26 ppm; δC, $CDCl_3$ 77.16 ppm). Coupling constants (J) are given in hertz (Hz). Multiplicities of ^{1}H NMR signals are reported as follows: s, singlet; d, doublet; t, triplet; q, quartet; m, multiplet.

General Procedure for Mannich Reactions. A solution of LDA (2.1 equiv) was added dropwise to a solution of the ester (2.0 equiv) in dry THF at −78 °C. After the mixture was stirred for 30 min, $Ti(O\text{-}iPr)_3Cl$ (4.2 equiv) in dry THF was added dropwise. The orange solution was stirred for 30 min and the imine (1.0 equiv) in dry THF was added dropwise. The mixture was stirred for 3 h or until thin-layer chromatography (TLC) showed full conversion of the imine. The mixture was quenched with saturated aqueous NH_4Cl and allowed to reach room temperature. Water was added and the mixture was decanted into a separatory funnel. EtOAc−water (1:1) was added to the remaining Ti precipitate, and the mixture was stirred vigorously for 5 min before being added to the separatory funnel. The aqueous phase was extracted with EtOAc and the combined organic phases were washed again with water, dried ($MgSO_4$), filtered, and concentrated in vacuo.

Azumamide A, (*Z*)-6-[(2*R*,5*R*,8*R*,11*R*,12*S*)-8-Benzyl-2-isopropyl-5,12-dimethyl-3,6,9,13-tetraoxo-1,4,7,10-tetraazacyclotridecan-11-yl]hex-4-enamide (5). LiOH (89 mg, 3.72 mmol, 85 equiv) in water (4.0 mL) was added to a stirred solution of the impure cyclic peptide **20** (24.2 mg, approximately 0.045 mmol) in THF (4 mL). After 2.5 h of stirring, the organic solvent was removed in vacuo. The aqueous phase was acidified with 1 M HCl to pH 2 and extracted with EtOAc (4 × 30 mL) and CH_2Cl_2 (40 mL). The organic phases were dried (Na_2SO_4), filtered, and concentrated to afford crude azumamide E, which was used without further purification. Analytical UPLC−MS gradient A, t_R = 1.47 min. To a solution of the above crude azumamide E (≈0.045 mmol) in DMF (3.0 mL) were added HATU (34 mg, 0.09 mmol, 2 equiv), iPr_2NEt (43 μL, 0.25 mmol, 5.5 equiv), and, after 5 min, NH_3−dioxane (0.9 mL, 0.45 mmol, 10 equiv). After 1 h, NH_3−dioxane (0.45 mL, 0.23 mmol, 5 equiv) was added. UPLC−MS analysis showed 50% conversion after 3 h, and HATU (34 mg, 0.09 mmol, 2 equiv) and NH_3−dioxane (0.45 mL, 0.23 mmol, 5 equiv) were added. After an additional 1 h, DMF (1.0 mL) followed by HATU (17 mg, 0.045 mmol, 1 equiv) and NH_3−dioxane (0.45 mL, 0.23 mmol, 5 equiv) were added, and stirring was continued for 1 h before concentration in vacuo. The residue was dissolved in MeCN−H_2O and purified by preperative HPLC to give azumamide A (**5**) (4.8 mg, 12% overall). $[\alpha]_D$ +56° (c = 0.2, MeOH); previously reported[11] $[\alpha]_D$ +33° (c = 0.1, MeOH). ^{1}H NMR (500 MHz, CD_3OH) δ 8.18 (d, J = 8.6 Hz, 1H), 8.16 (d, J = 9.0 Hz, 1H), 7.72 (d, J = 8.2 Hz, 1H), 7.59 (m, 2H), 7.20 (m, 5H), 6.74 (br s, 1H), 5.48 (m, 1H), 5.37 (m, 1H), 4.33 (dt, J = 9.0, 7.0 Hz, 1H), 4.24 (m, 2H), 3.81 (dd, J = 10.4 Hz and 8.4 Hz, 1H), 3.10 (m, 2H), 2.72 (m, 1H), 2.57 (dt, J = 14.1, 6.9 Hz, 1H), 2.41 (m, 2H), 2.27 (m, 4H), 1.30 (d, J = 7.5 Hz, 3H), 1.23 (d, J = 7.3 Hz, 3H), 0.96 (d, J = 6.5 Hz, 3H), 0.94 (d, J = 6.7 Hz, 3H). HRMS (ESI-TOF) m/z calcd for $C_{27}H_{38}N_4O_7H^+$ 514.3029; found 514.3032 $[M + H]^+$. HPLC gradient C, t_R = 11.62 min (>95%).

Azumamide B, (*Z*)-6-[(2*R*,5*R*,8*R*,11*R*,12*S*)-8-(4-Hydroxybenzyl)-2-isopropyl-5,12-dimethyl-3,6,9,13-tetraoxo-1,4,7,10-tetraazacyclotridecan-11-yl]hex-4-enamide (6). An aqueous solution of LiOH (0.5 M, 55 μL, 2.0 mmol, 2.5 equiv) was added to the cyclic peptide **18** (6.1 mg) in THF−H_2O (1:1, 2 mL) at 0 °C. After 30 min the ice bath was removed. Additional portions of LiOH solution (55 μL, 2.0 mmol, 2.5 equiv) were added after 2, 4, and 6 h, and stirring was continued for an additional 19 h to ensure full conversion. Then water (0.5 mL) was added and the organic solvent was removed in vacuo. The aqueous phase was acidified with 1 M HCl and extracted with EtOAc (5 × 20 mL). The organic phase was dried (Na_2SO_4), filtered, and concentrated in vacuo to afford the crude azumamide C, which was used without further purification. To a solution of crude azumamide C (5.8 mg, 10.9 μmol) in DMF (2 mL) were added HOBt (4.4 mg, 33 μmol, 3 equiv), DIC (5.1 μL, 34 μmol, 3 equiv), and iPr_2NEt (7.6 μL, 44 μmol, 4 equiv). After 10 min, NH_3−dioxane (0.5 M, 0.11 mL, 55 μmol, 5 equiv) was added. After 1.5 h, DIC (5 μL, 34 μmol, 3 equiv) was added, followed by NH_3−dioxane (0.5 M, 0.11 mL, 55 μmol, 5 equiv). After the mixture was stirred for 16 h, additional DIC (2 equiv) and NH_3−dioxane (5 equiv) were added, and this procedure was repeated once more after 18 h. Finally, CH_2Cl_2 (1 mL) was added, followed by DIC (3 equiv) and NH_3−dioxane (10 equiv), and after 2 days of stirring at room temperature, the reaction mixture was concentrated, dissolved in MeCN−H_2O (2:1), and purified by preparative HPLC to give azumamide B (**6**) (3.6 mg, 62%, two steps) as a white solid. $[\alpha]_D$ +65° (c = 0.15, MeOH); previously reported[11] $[\alpha]_D$ +45° (c = 0.1, MeOH). ^{1}H NMR (500 MHz, CD_3OH) δ 8.13 (d, J = 7.9 Hz, 1H), 8.00 (d, J = 8.9 Hz, 1H), 7.85 (d, J = 7.2 Hz, 1H), 7.61 (d, J = 8.2 Hz, 1H), 7.01 (d, J = 8.4 Hz, 3H), 6.67 (d, J = 8.4 Hz, 3H), 5.49 (m, 1H), 5.37 (dd, J = 18.0 and 7.3 Hz, 2H), 4.29 (pentet, J = 7.2 Hz, 1H), 4.15 (m, 1H), 4.05 (m, 1H), 3.60 (m, 1H), 3.13 (dd, J = 13.7, 10.1 Hz, 1H), 3.00 (dd, J = 13.8, 6.3 Hz, 1H), 2.70 (m, 2H), 2.36 (ddd, J = 22.3, 21.5, 7.1 Hz, 11H), 1.29 (d, J = 7.2 Hz, 3H), 1.27 (d, J = 7.4 Hz, 3H), 0.95 (d, J = 5.7 Hz, 3H), 0.93 (d, J = 6.0 Hz, 3H). HRMS (ESI-TOF) m/z calcd for $C_{27}H_{39}N_5O_6H^+$ 530.2978; found 530.2973 $[M + H]^+$. HPLC gradient C, t_R = 10.31 min (>95%).

dx.doi.org/10.1021/jm4008449 | J. Med. Chem. 2013, 56, 6512−6520

Azumamide C, (*Z*)-6-[(2*R*,5*R*,8*R*,11*R*,12*S*)-8-(4-Hydroxybenzyl)-2-isopropyl-5,12-dimethyl-3,6,9,13-tetraoxo-1,4,7,10-tetraazacyclotridecan-11-yl]hex-4-enoic Acid (7). LiOH (49 mg, 2.0 mmol, 35 equiv) in water (5.0 mL) was added to the crude cyclic peptide **18** (61 mg) in THF (5.0 mL). The solution was stirred for 16 h and concentrated in vacuo. The resulting residue was dissolved in THF−H_2O (1:1, 10 mL) by adding a few drops of TFA, and then purification by preparative HPLC afforded azumamide C (**7**) (2.2 mg, 9% overall) as a white solid. $[\alpha]_D$ +49° (*c* = 0.14, MeOH); previously reported[11] $[\alpha]_D$ +21° (*c* = 0.1, MeOH). ^{1}H NMR (500 MHz, CD_3OH) δ 8.08 (d, *J* = 7.7 Hz, 1H), 7.99 (d, *J* = 8.4 Hz, 1H), 7.84 (s, 1H), 7.62 (d, *J* = 8.1 Hz, 1H), 7.01 (d, *J* = 8.4 Hz, 2H), 6.67 (d, *J* = 8.4 Hz, 2H), 5.48 (t, *J* = 8.8 Hz, 1H), 5.38 (dt, *J* = 10.7, 7.0 Hz, 1H), 4.29 (pentet, *J* = 7.3 Hz 1H), 4.16 (m, 1H), 4.01 (m, 1H), 3.58 (m, 1H), 3.15 (dd, *J* = 13.7, 10.2 Hz 1H), 3.00 (dd, *J* = 13.7, 6.0 Hz, 1H), 2.72 (m, 1H), 2.67 (m, 1H) 2.39 (m, 5H), 1.29 (d, *J* = 7.2 Hz, 3H), 1.27 (d, *J* = 7.3 Hz, 3H), 0.95 (d, *J* = 6.0 Hz, 3H), 0.93 (d, *J* = 6.0 Hz, 3H). HRMS (ESI-TOF) *m*/*z* calcd for $C_{27}H_{38}N_4O_7H^+$ 531.2819; found 531.2815 $[M + H]^+$. HPLC gradient C, t_R = 11.04 min (>95%).

Azumamide D, (*Z*)-6-[(2*R*,5*R*,8*R*,11*R*,12*S*)-8-Benzyl-2,5,12-trimethyl-3,6,9,13-tetraoxo-1,4,7,10-tetraazacyclotridecan-11-yl]hex-4-enamide (8). LiOH (53 mg, 2.21 mmol) in water (5.0 mL) was added to a stirred solution of the impure cyclic peptide **22** (22.7 mg, approximately 0.044 mmol) in THF (3 mL). After 4 h the organic solvent was removed in vacuo and the water (0.5 mL) was added to the aqueous phase, which was then acidified with 1 M HCl (2 mL) and extracted with EtOAc (4 × 20 mL). The organic phases were dried ($MgSO_4$), filtered, and concentrated to give the crude acid **23**, which was used without further purification. To a solution of the crude acid **23** (≈23 μmol) in CH_2Cl_2−DMF (8:1, 2.3 mL) were added HOBt (10 mg, 66 μmol, 3.0 equiv), DIC (10 μL, 66 μmol, 3 equiv), and iPr$_2$NEt (15 μL, 88 μmol, 4 equiv). After 5 min, NH_3−dioxane (0.5 M, 0.22 mL, 110 μmol, 5 equiv) was added. After 1 h, NH_3−dioxane (0.5 M, 0.22 mL, 110 μmol, 5 equiv) was added. After the mixture was stirred for 18 h, additional DMF (0.5 mL) was added, followed by NH_3−MeOH (2.0 M, 0.11 mL, 230 μmol, 10 equiv). After an additional 5 h, DIC (7 μL, 46 μmol, 2 equiv) was added. The next day NH_3−MeOH (2.0 M, 0.06 mL, 111 μmol, 5 equiv) was added and the mixture was stirred for 10 days. Finally, DIC (3.4 μL, 23 μmol, 1 equiv) was added, followed by NH_3−MeOH (2.0 M, 0.055 mL, 210 μmol, 5 equiv), and after 2 days the mixture was concentrated, dissolved in MeCN−H_2O (2:1), and purified by preparative HPLC to afford azumamide D (**8**) (1.2 mg, 4% overall) as a white solid. $[\alpha]_D$ +32° (*c* = 0.08, MeOH); previously reported[11] $[\alpha]_D$ +25° (*c* = 0.1, MeOH). ^{1}H NMR (500 MHz, CD_3OH) δ 8.03 (d, *J* = 7.8 Hz, 1H), 8.01 (d, *J* = 8.8 Hz, 1H) 7.94 (d, *J* = 6.8 Hz, 1H), 7.58 (s, 1H), 7.32 (d, *J* = 7.5 Hz, 1H), 7.25−7.14 (m, 5H), 6.75 (s, 1H), 5.47 (m, 1H), 5.39 (m, 1H), 4.35 (m, 1H), 4.19 (m, 1H) 4.17− 4.11 (m, 2H), 3.09 (m, 2H), 2.69 (m, 1H), 2.62 (m, 1H), 2.41 (m, 2H), 2.28 (m, 1H), 1.47 (d, *J* = 7.4 Hz, 3H), 1.28 (d, *J* = 7.4 Hz, 3H), 1.22 (d, *J* = 7.3 Hz, 3H). HRMS (ESI-TOF) *m*/*z* calcd for $C_{25}H_{35}N_5O_5H^+$ 486.2716; found 486.2710 $[M + H]^+$. HPLC gradient C, t_R = 10.55 min (>95%).

Azumamide E, (*Z*)-6-[(2*R*,5*R*,8*R*,11*R*,12*S*)-8-Benzyl-2-isopropyl-5,12-dimethyl-3,6,9,13-tetraoxo-1,4,7,10-tetraazacyclotridecan-11-yl]hex-4-enoic Acid (9). LiOH (18.5 mg, 0.77 mmol, 40 equiv) in water (4 mL) was added to a stirred solution of the impure cyclic peptide **20** (10.5 mg, approximately 0.02 mmol) in THF (4 mL). After 1 h, LiOH (10 mg, 0.42 mmol, 20 equiv) in water (1 mL) was added, and after 2 h, LiOH (5.0 mg, 0.21 mmol, 1 equiv) in water (0.5 mL) was added. The solution was stirred for 16 h and another portion of LiOH (6.0 mg, 0.25 mmol, 1.3 equiv) in water (0.5 mL) was added. After an additional 2.5 h of stirring, the organic solvent was removed in vacuo. The aqueous phase was acidified with 1 M HCl and extracted with EtOAc (4 × 25 mL). The combined organic phases were dried (Na_2SO_4), filtered, and concentrated. The resulting residue was dissolved in MeCN−water [(3:2), 2.5 mL] and purified by preparative HPLC to afford azumamide E (**9**) (4.3 mg, 15% overall) as a white solid. $[\alpha]_D$ +66° (*c* = 0.2, MeOH); previously reported[11] $[\alpha]_D$ +53° (*c* = 0.1, MeOH). ^{1}H NMR (500 MHz, CD_3OH) δ 8.10 (d, *J* = 7.7 Hz, 1H), 7.95 (d, *J* = 8.8 Hz, 1H), 7.84 (br s, 1H), 7.63 (d, *J* = 8.4 Hz, 1H), 7.28−7.16 (m, 5H), 5.48 (m, 1H), 5.37 (m, 1H), 4.28 (pentet, *J* = 7.5 Hz, 1H), 4.16 (m, 1H), 4.08 (m, 1H), 3.59 (m, 1H), 3.25 (dd, *J* = 13.6, 10.4 Hz, 1H), 3.11 (dd, *J* = 13.6, 6.1 Hz, 1H), 2.72 (m, 1H), 2.68 (m, 1H), 2.39 (d, *J* = 1.7 Hz, 6H), 2.39 (m, 6H), 1.28 (d, *J* = 7.1 Hz, 3H), 1.27 (d, *J* = 7.4 Hz, 3H), 0.94 (m, 6H). HRMS (ESI-TOF) *m*/*z* calcd for $C_{27}H_{38}N_4O_6H^+$ 515.2869; found 515.2869 $[M + H]^+$. HPLC gradient C, t_R = 12.53 min (>95%).

Assay Materials. HDAC1 (purity >45% by SDS−PAGE according to the supplier), HDAC4 (purity >90% by SDS−PAGE according to the supplier), and HDAC7 (purity >90% by SDS−PAGE according to the supplier) were purchased from Millipore (Temecula, CA). HDAC2 used for dose−response experiments (full length, purity ≥94% by SDS−PAGE according to the supplier), HDAC5 (full length, purity ≥4% by SDS−PAGE according to the supplier), and HDAC8 used for dose−response experiments (purity ≥90% by SDS−PAGE according to the supplier) were purchased from BPS Bioscience (San Diego, CA). HDAC2 used for initial screening experiments (full length, purity 50% by SDS−PAGE according to the supplier), HDAC3−"NCoR1" complex [(purity 90% by SDS−PAGE according to supplier; fusion protein of GST-tagged HDAC3 with the deacetylase activation domain (DAD) of NCoR1 (nuclear receptor corepressor)], HDAC6 (purity >90% by SDS−PAGE according to the supplier), HDAC8 for initial screening experiments (purity >50% by SDS−PAGE according to the supplier), HDAC10 (purity >50% by SDS−PAGE according to the supplier), and HDAC11 (purity >50% by SDS−PAGE according to the supplier) were purchased from Enzo Life Sciences (Postfach, Switzerland). HDAC9 (full length, purity 12% by SDS−PAGE according to the supplier) was purchased from Abnova (Taipei, Taiwan). The HDAC assay buffer consisted of 50 mM Tris-HCl, pH 8.0, 137 mM NaCl, 2.7 mM KCl, 1 mM $MgCl_2$, and bovine serum albumin (0.5 mg/mL). Trypsin [10 000 units/mg;, from bovine pancreas, treated with L-(tosylamido-2-phenyl)ethyl chloromethyl ketone (TPCK)] was from Sigma Aldrich (Steinheim, Germany). All peptides were purified to homogeneity (>95% purity by $HPLC_{230nm}$ via reversed-phase preparative HPLC), and the white fluffy materials obtained by lyophilization were kept at −20 °C. For assaying, peptides were reconstituted in DMSO to give 5−10 mM stock solutions, the accurate concentrations of which were determined by coinjection on HPLC with a standard of known concentration.

In Vitro Histone Deacetylase Inhibition Assays. For inhibition of recombinant human HDACs, dose−response experiments with internal controls were performed in black low-binding Nunc 96-well microtiter plates. Dilution series (3-fold dilution, 10 concentrations) were prepared in HDAC assay buffer from 5−10 mM DMSO stock solutions. The appropriate dilution of inhibitor (10 μL of 5× the desired final concentration) was added to each well followed by HDAC assay buffer (25 μL) containing substrate [Ac-Leu-Gly-Lys(Ac)-AMC, 40 μM for HDAC1−3 and 80 μM for HDAC6 and 11; Ac-Leu-Gly-Lys(Tfa)-AMC, 40 μM for HDAC4, 240 μM for HDAC5, 80 μM for HDAC7, 400 μM for HDAC8, and 160 μM for HDAC9; Ac-Arg-His-Lys(Ac)-Lys(Ac)-AMC, 100 μM for HDAC10]. Finally, a solution of the appropriate HDAC (15 μL) was added and the plate was incubated at 37 °C for 30 min [HDAC1, 150 ng/well; HDAC2, 100 ng/well; HDAC3, 10 ng/well; HDAC4, 2 ng/well; HDAC5, 40 ng/well; HDAC6, 60 ng/well; HDAC7, 2 ng/well; HDAC8, 5 ng/well; HDAC9, 40 ng/well; HDAC10, 500 ng/well; HDAC11, 500 ng/well]. Then trypsin (50 μL, 0.4 mg/mL) was added and the assay development was allowed to proceed for 15−30 min at room temperature, before the plate was read on a Perkin-Elmer Enspire plate reader with excitation at 360 nm and detecting emission at 460 nm. Each assay was performed in duplicate. The data were analyzed by nonlinear regression with GraphPad Prism to afford IC_{50} values from the dose−response experiments, and K_i values were determined from the Cheng−Prusoff equation [$K_i = IC_{50}/(1 + [S]/K_m)$] with the assumption of a standard fast-on−fast-off mechanism of inhibition.

■ ASSOCIATED CONTENT

Supporting Information

Two tables showing cyclization experiments performed on a simplified model peptide and IC_{50} values from dose−response experiments; seven figures showing comparison of ^{1}H and ^{13}C chemical shifts for **S18** with previously reported values, ^{1}H NMR data comparisons for azumamides A−E, and dose−response curves for determination of IC_{50} values for "active" inhibitors; two schemes illustrating synthesis of β^3-epi building block (**S6**) and β^2-epi building block (**S11**); additional text with full experimental details and compound characterization data; and ^{1}H and ^{13}C NMR spectra. A CIF file for the X-ray crystal structures is available (CCDC 933151).This material is available free of charge via the Internet at http://pubs.acs.org.

■ AUTHOR INFORMATION

Corresponding Author

*E-mail cao@kemi.dtu.dk; phone +45-45252105.

Notes

The authors declare no competing financial interest.

■ ACKNOWLEDGMENTS

This work was supported by the Lundbeck Foundation (Young Group Leader Fellowship, C.A.O.), the Danish Independent Research Council−Natural Sciences (Steno Grant 10-080907, C.A.O.), and the Carlsberg Foundation. Novo Nordisk A/S is thanked for a generous donation of peptide coupling reagents used in this work. We thank Ms. Anne Hector and Dr. Charlotte H. Gotfredsen for assistance with NMR spectroscopy and Ms. Tina Gustafsson for technical assistance with UPLC−MS and HRMS. Dr. A. S. Madsen is gratefully acknowledged for assistance with the biochemical assays.

■ ABBREVIATIONS USED

AMC, 7-amino-4-methylcoumarin; Boc, *tert*-butoxycarbonyl; DAD, deacetylase activation domain; DIC, *N*,*N*′-diisopropylcarbodiimide; DMF, *N*,*N*-dimethylformamide; DMSO, dimethyl sulfoxide; ESI, electrospray ionization; FID, free induction decay; Fmoc, fluorenylmethyloxycarbonyl; H3, histone 3 protein; H4, histone 4 protein; HATU, *O*-(7-azabenzotriazol-1-yl)-*N*,*N*,*N*′,*N*′-tetramethyluronium hexafluorophosphate; HDAC, histone deacetylase; HMPA, hexamethylphosphoramide; HOBt, hydroxybenzotriazole; HPLC, high-performance liquid chromatography; KHMDS, potassium hexamethyldisilazide; LDA, lithium diisopropylamide; MS, mass spectrometry; NCoR, nuclear receptor corepressor; NMR, nuclear magnetic resonance; PMB, *p*-methoxybenzyl; rt, room temperature; SDS−PAGE, sodium dodecyl sulfate−polyacrylamide gel electrophoresis; TFA, trifluoroacetic acid; THF, tetrahydrofuran; TOF, time-of-flight; t_R, retention time; UPLC, ultra-high-performance liquid chromatography

■ REFERENCES

(1) Marks, P. A.; Breslow, R. Dimethyl sulfoxide to vorinostat: development of this histone deacetylase inhibitor as an anticancer drug. *Nat. Biotechnol.* **2007**, *25*, 84−90.

(2) Furumai, R.; Matsuyama, A.; Kobashi, N.; Lee, K. H.; Nishiyama, M.; Nakajima, H.; Tanaka, A.; Komatsu, Y.; Nishino, N.; Yoshida, M.; Horinouchi, S. FK228 (depsipeptide) as a natural prodrug that inhibits class I histone deacetylases. *Cancer Res.* **2002**, *62*, 4916−4921.

(3) Kijima, M.; Yoshida, M.; Sugita, K.; Horinouchi, S.; Beppu, T. Trapoxin, an antitumor cyclic tetrapeptide, is an irreversible inhibitor of mammalian histone deacetylase. *J. Biol. Chem.* **1993**, *268*, 22429−22435.

(4) Taunton, J.; Hassig, C. A.; Schreiber, S. L. A mammalian histone deacetylase related to the yeast transcriptional regulator Rpd3p. *Science* **1996**, *272*, 408−411.

(5) Taunton, J.; Collins, J. L.; Schreiber, S. L. Synthesis of natural and modified trapoxins, useful reagents for exploring histone deacetylase function. *J. Am. Chem. Soc.* **1996**, *118*, 10412−10422.

(6) Beumer, J. H.; Tawbi, H. Role of histone deacetylases and their inhibitors in cancer biology and treatment. *Curr. Clin. Pharmacol.* **2010**, *5*, 196−208.

(7) Haberland, M.; Montgomery, R. L.; Olson, E. N. The many roles of histone deacetylases in development and physiology: implications for disease and therapy. *Nat. Rev. Genet.* **2009**, *10*, 32−42.

(8) Kazantsev, A. G.; Thompson, L. M. Therapeutic application of histone deacetylase inhibitors for central nervous system disorders. *Nat. Rev. Drug Discovery* **2008**, *7*, 854−868.

(9) Minucci, S.; Pelicci, P. G. Histone deacetylase inhibitors and the promise of epigenetic (and more) treatments for cancer. *Nat. Rev. Cancer* **2006**, *6*, 38−51.

(10) Darkin-Rattray, S. J.; Gurnett, A. M.; Myers, R. W.; Dulski, P. M.; Crumley, T. M.; Allocco, J. J.; Cannova, C.; Meinke, P. T.; Colletti, S. L.; Bednarek, M. A.; Singh, S. B.; Goetz, M. A.; Dombrowski, A. W.; Polishook, J. D.; Schmatz, D. M. Apicidin: a novel antiprotozoal agent that inhibits parasite histone deacetylase. *Proc. Natl. Acad. Sci. U.S.A.* **1996**, *93*, 13143−13147.

(11) Nakao, Y.; Yoshida, S.; Matsunaga, S.; Shindoh, N.; Terada, Y.; Nagai, K.; Yamashita, J. K.; Ganesan, A.; van Soest, R. W.; Fusetani, N. Azumamides A-E: histone deacetylase inhibitory cyclic tetrapeptides from the marine sponge *Mycale izuensis*. *Angew. Chem., Int. Ed.* **2006**, *45*, 7553−7557.

(12) Maulucci, N.; Chini, M. G.; Micco, S. D.; Izzo, I.; Cafaro, E.; Russo, A.; Gallinari, P.; Paolini, C.; Nardi, M. C.; Casapullo, A.; Riccio, R.; Bifulco, G.; De Riccardis, F. Molecular insights into azumamide E histone deacetylases inhibitory activity. *J. Am. Chem. Soc.* **2007**, *129*, 3007−3012.

(13) Wang, D.; Helquist, P.; Wiest, O. Zinc binding in HDAC inhibitors: a DFT study. *J. Org. Chem.* **2007**, *72*, 5446−5449.

(14) Izzo, I.; Maulucci, N.; Bifulco, G.; De Riccardis, F. Total synthesis of azumamides A and E. *Angew. Chem., Int. Ed.* **2006**, *45*, 7557−7560.

(15) Wen, S.; Carey, K. L.; Nakao, Y.; Fusetani, N.; Packham, G.; Ganesan, A. Total synthesis of azumamide A and azumamide E, evaluation as histone deacetylase inhibitors, and design of a more potent analogue. *Org. Lett.* **2007**, *9*, 1105−1108.

(16) Chandrasekhar, S.; Rao, C. L.; Seenaiah, M.; Naresh, P.; Jagadeesh, B.; Manjeera, D.; Sarkar, A.; Bhadra, M. P. Total synthesis of azumamide E and sugar amino acid-containing analogue. *J. Org. Chem.* **2009**, *74*, 401−404.

(17) Lahm, A.; Paolini, C.; Pallaoro, M.; Nardi, M. C.; Jones, P.; Neddermann, P.; Sambucini, S.; Bottomley, M. J.; Lo Surdo, P.; Carfi, A.; Koch, U.; De Francesco, R.; Steinkuhler, C.; Gallinari, P. Unraveling the hidden catalytic activity of vertebrate class IIa histone deacetylases. *Proc. Natl. Acad. Sci. U.S.A.* **2007**, *104*, 17335−17340.

(18) Bradner, J. E.; West, N.; Grachan, M. L.; Greenberg, E. F.; Haggarty, S. J.; Warnow, T.; Mazitschek, R. Chemical phylogenetics of histone deacetylases. *Nat. Chem. Biol.* **2010**, *6*, 238−243.

(19) White, C. J.; Yudin, A. K. Contemporary strategies for peptide macrocyclization. *Nat. Chem.* **2011**, *3*, 509−524.

(20) Tang, T. P.; Ellman, J. A. Asymmetric synthesis of β-amino acid derivatives incorporating a broad range of substitution patterns by enolate additions to *tert*-butanesulfinyl imines. *J. Org. Chem.* **2002**, *67*, 7819−7832.

(21) Robak, M. T.; Herbage, M. A.; Ellman, J. A. Synthesis and applications of *tert*-butanesulfinamide. *Chem. Rev.* **2010**, *110*, 3600−3740.

(22) Zimmerman, H. E.; Traxler, M. D. The stereochemistry of the Ivanov and Reformatsky reactions. 1. *J. Am. Chem. Soc.* **1957**, *79*, 1920−1923.

(23) Cutter, A. C.; Miller, I. R.; Keily, J. F.; Bellingham, R. K.; Light, M. E.; Brown, R. C. D. Total syntheses of (−)-epilupinine and (−)-tashiromine using imino-aldol reactions. *Org. Lett.* **2011**, *13*, 3988−3991.
(24) Ireland, R. E.; Mueller, R. H.; Willard, A. K. Ester enolate Claisen rearrangement: Stereochemical control through stereoselective enolate formation. *J. Am. Chem. Soc.* **1976**, *98*, 2868−2877.
(25) Oare, D. A.; Heathcock, C. H. Acyclic stereoselection. 47. Stereochemistry of the Michael addition of ester and ketone enolates to α,β-unsaturated ketones. *J. Org. Chem.* **1990**, *55*, 157−172.
(26) Montero, A.; Beierle, J. M.; Olsen, C. A.; Ghadiri, M. R. Design, synthesis, biological evaluation, and structural characterization of potent histone deacetylase inhibitors based on cyclic α/β-tetrapeptide architectures. *J. Am. Chem. Soc.* **2009**, *131*, 3033−3041.
(27) Olsen, C. A.; Ghadiri, M. R. Discovery of potent and selective histone deacetylase inhibitors via focused combinatorial libraries of cyclic $\alpha3\beta$-tetrapeptides. *J. Med. Chem.* **2009**, *52*, 7836−7846.
(28) Vickers, C. J.; Olsen, C. A.; Leman, L. J.; Ghadiri, M. R. Discovery of HDAC inhibitors that lack an active site Zn^{2+}-binding functional group. *ACS Med. Chem. Lett.* **2012**, *3*, 505−508.
(29) Olsen, C. A.; Montero, A.; Leman, L. J.; Ghadiri, M. R. Macrocyclic peptoid-peptide hybrids as inhibitors of class I histone deacetylases. *ACS Med. Chem. Lett.* **2012**, *3*, 749−753.
(30) Madsen, A. S.; Olsen, C. A. Substrates for efficient fluorometric screening employing the NAD-dependent sirtuin 5 lysine deacylase (KDAC) enzyme. *J. Med. Chem.* **2012**, *55*, 5582−5590.
(31) Madsen, A. S.; Olsen, C. A. Profiling of substrates for zinc-dependent lysine deacylase enzymes: HDAC3 exhibits decrotonylase activity in vitro. *Angew. Chem., Int. Ed.* **2012**, *51*, 9083−9087.
(32) Inks, E. S.; Josey, B. J.; Jesinkey, S. R.; Chou, C. J. A novel class of small molecule inhibitors of HDAC6. *ACS Chem. Biol.* **2012**, *7*, 331−337.
(33) Auzzas, L.; Larsson, A.; Matera, R.; Baraldi, A.; Deschenes-Simard, B.; Gianni, G.; Cabri, W.; Bayyistuzzi, G.; Gallo, G.; Ciacci, A.; Vesci, L.; Pisano, C.; Hanessian, S. *J. Med. Chem.* **2010**, *53*, 8387−8399.
(34) Szpilman, A. M.; Carreira, E. M. Probing the biology of natural products: Molecular editing by diverted total synthesis. *Angew. Chem., Int. Ed.* **2010**, *49*, 9592−9628.
(35) Wender, P. A.; Buschmann, N.; Cardin, N. B.; Jones, L. R.; Kan, C.; Kee, J. M.; Kowalski, J. A.; Longcore, K. E. Gateway synthesis of daphnane congeners and their protein kinase C affinities and cell-growth activities. *Nat. Chem.* **2011**, *3*, 615−619.
(36) Wilson, R. M.; Danishefsky, S. J. On the reach of chemical synthesis: creation of a mini-pipeline from an academic laboratory. *Angew. Chem., Int. Ed.* **2010**, *49*, 6032−6056.

Chemical Science

Dynamic Article Links ►

Cite this: DOI: 10.1039/c0xx00000x

www.rsc.org/xxxxxx

EDGE ARTICLE

Structural editing of the azumamide scaffold: Synthesis and structure–activity relationships†

Alex R. Maolanon[a], Jesper S. Villadsen[a], Casper Hoeck[a], Charlotte H. Gotfredsen[a], Pernille Harris[a] and Christian A. Olsen*[,a]

Department of Chemistry, Technical University of Denmark, Kemitorvet 207, DK-2800, Kongens Lyngby, Denmark

Received (in XXX, XXX) Xth XXXXXXXXX 20XX, Accepted Xth XXXXXXXXX 20XX
DOI: 10.1039/b000000x

HDAC inhibitors have been found to be potential anticancer agents and isoform selective HDAC inhibitors could be useful for dissecting the individual biochemical pathways associated with each of these HDAC isoforms. In our pursuit for potent and selective HDAC inhibitors, we designed four series of cyclic tetrapeptide compounds, which are based on the azumamide scaffold. We have probed different modifications in the unique *β*-amino acid moiety and synthesized tryptophan-containing analogs. The biochemical profiling of the azumamide analogs was combined with high-resolution NMR solution structures to correlate the biological activity to specific structural features. We hypothesize that the β^2-methyl group, found in the azumamides, has an important side chain directing function, which guides the zinc-binding side chain towards the active site.

Introduction

Histone deacetylases (HDACs) are a family of enzymes, which play a key role in the epigenetic regulation of important cellular functions. Interestingly, these enzymes can modulate the interactions between the DNA and the histone proteins and affect gene transcription. In the field of cancer research this discovery has encouraged the development of HDAC inhibitors as potential anticancer drugs.[1, 2] Currently, two HDAC targeting drugs (**1** and **4**) are approved by the FDA for clinical treatment of cutaneous T-cell lymphoma. The HDAC family is divided into four classes, where class II is further sub-divided into two groups: class I (HDAC1–3, 8), class IIa (HDAC4, 5, 7, and 9) class IIb (HDAC6 and HDAC10), and class IV (HDAC11).

Macrocyclic peptides (**3, 5a,** and **5b)** and depsipeptides (**4**) have proven to be potent HDAC inhibitors.[3, 4, 5] Azumamide C (**5a**) and azumamide E (**5b)** are macrocyclic tetrapeptides, which demonstrate high activity as HDAC inhibitors in spite of their weak Zn^{2+}-coordinating side chain functionality (COOH).[6] The azumamides are structurally related to apicidin (**3**),[4] but the macrocyclic scaffold has a disubstituted *β*-amino acid. Furthermore the azumamides are unique in having a retro-enantio arrangement, compared to other macrocyclic peptides (e.g. apicidin) where only D-amino acids are found in the ring. The binding mode of macrocyclic peptides and depsipeptides has previously been explored and it is hypothesized that the peptide side chain, bearing the Zn^{2+}-binding group, reaches into the binding pocket through a narrow channel and coordinates a zinc ion.[7, 8] The cyclic peptide core has favorable interactions with the surface of the protein and the presence of an aromatic amino acid in cyclic tetra peptides, related to the azumamides, was found to be important for activity.[9] Furthermore, the interactions between the cyclic peptide core and the surface of the protein seem to be important for isoform selectivity.[10, 11] The biological role of the individual isoforms have not yet been identified and isoform selective HDAC inhibitors could be useful for dissecting the individual biochemical pathways associated with each of these

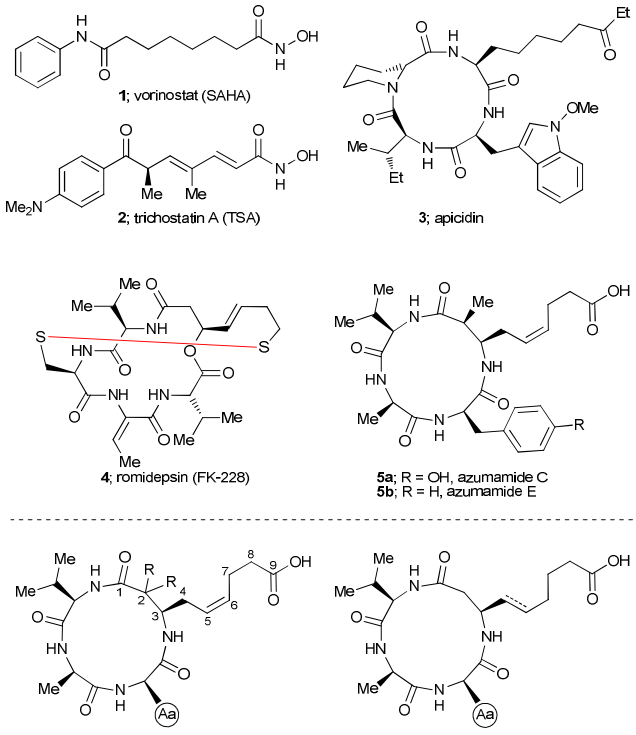

Figure 1. Known HDAC inhibitors (top) and target compounds (bottom)

enzymes. Furthermore, selective inhibitors could be have potential as new drug candidates.[2, 12]

Results and discussion

Design and synthesis

In pursuit of isoform-selective compounds we conducted a structure–activity relationship (SAR) study, where we synthesized a variety of structurally edited azumamides. The structural changes reported for the azumamides are limited to modification of the Zn^{2+}-binding group[13], incorporation of a sugar-amino acid residue[14], and manipulation of the stereochemistry.[7, 15] Our previous work has shown that changes in the stereochemistry of the β-amino acid substituents in azumamide E had a detrimental impact on activity.[15] We therefore set out to explore modifications at the β^2-position, without altering the stereochemistry. Instead we incorporated a dimethylated as well as a desmethylated β-amino acid in the cyclic peptides, **6a-c** and **7a-c**, respectively.

Considering the saturated side chain of **3** and the *trans* olefin in **4**, we speculated that the *cis* olefin in the azumamides would not be essential for activity. To explore this hypothesis, we prepared **8a–c** and **9a–c**, where the required β-amino acids easily could be obtained from commercially available Boc-L-Asp-O^{t}Bu. We recently found that the nature of the aromatic amino acid effects the biological activity.[15] Hence, an indole motif, also present in **3**, was incorporated in our target compounds in addition to Phe and Tyr, which are found in the azumamides.

Building block synthesis

The building block, employed for the synthesis of the dimethylated analogs **6a–c**, was prepared by a method recently developed in our laboratory. The diastereoselective Ellman-type Mannich reaction between the enolate of *tert*-butyl isobutyrate and the enantiomer of sulfinyl imine **10** afforded the desired Mannich product in 58% yield and with a diastereoselectivity of (77:23) in favour of the *R*-isomer.

Table 1. Screening of acetates for the Ellman-type Mannich reaction.

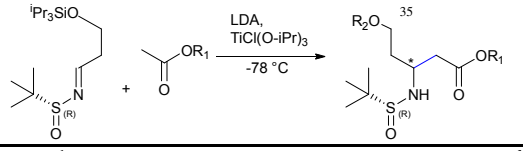

entry	R[1]	additive	d.r.	major isomer, (%)[d]
1	Et	TiCl(O-^{i}Pr)$_3$	>99:1	*3R*[a] (94)[b]
2	^{t}Bu	TiCl(O-^{i}Pr)$_3$	74:26	*3R*[c] (68)
3	^{t}Bu	HMPA	28:72	*3S*[c] (61)
4	PMB	TiCl(O-^{i}Pr)$_3$	82:18	ND

[a] Determined by X-ray crystallography from the desilylated and re-esterified *tert*-butyl ester **19**. [b] Yield is reported for the crude product. [c] Determined spectroscopically by comparison with the crystallized compound from entry 1 (supplementary figure S1).[d] Total yield of all diastereoisomers.

The absolute stereochemistry of the Mannich product was determined by X-ray crystallography upon desilylation with Bu_4NF. The alcohol was elaborated to give the Boc-protected β-amino acid **22** (scheme 3) in 16% overall yield from the sulfinyl imine (Supplementary scheme S1). The desmethylated β-amino

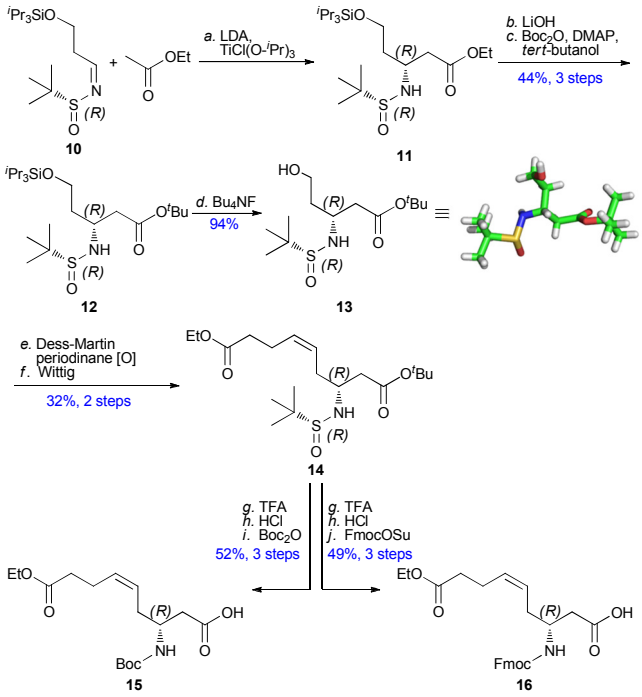

Scheme 1. Reagents and conditions: (a) LDA (2.1 equiv), EtOAc (2.0 equiv), TiCl(O-^{i}Pr)$_3$ (4.2 equiv), THF, –78 ºC, 30 min; then **10**, –78 ºC, 20 min. (b) LiOH (4.5 equiv), THF–water, 17 h. (c) Boc_2O (1.4 equiv), DMAP (0.3 equiv), *tert*-butanol, 16 h, then Boc_2O (0.3 equiv), 15 h (d) AcOH (1.0 equiv), Bu_4NF (2.0 equiv), THF, 0 ºC → rt, 75 min. (e) $NaHCO_3$ (1.5 equiv), Dess-Martin periodinane (1.5 equiv), dry CH_2Cl_2, 0 ºC → rt, 40 min. (f) KHMDS (1.9 equiv), $Ph_3PBr(CH_2)_3COOEt$, (2.0 equiv), THF, –78 ºC → rt, 40 min. (g) TFA–CH_2Cl_2 (1:1, 10 mL, 117–192 equiv), 0 ºC → rt, 2–3 h. (h) HCl (4.0 M in dioxane, 1.8–2.5 equiv), dioxane, 1–3 h. (i) ^{i}Pr$_2$NEt (3.0 equiv), Boc_2O (2.0 equiv), dry CH_2Cl_2, 6 h, then Boc_2O (1.0 equiv), 16 h. (j) Na_2CO_3 (4.0 equiv), FmocOSu (1.2 equiv) water–dioxane (5:1, 6 mL), 0 ºC → rt, 45 min.

acid building blocks **15** (Boc-protected) and **16** (Fmoc-protected) were prepared by a similar route (scheme 1). The Boc-derivative only allows one cyclization site, whereas the introduction of the Fmoc group would allow macrolactamization at all four positions. Initially, an optimization study was conducted, where various acetate enolates were investigated to produce the best diastereomeric ratio and yield in the Mannich reaction (table 1).

It is interesting, that the desired (3*R*) configuration is obtained from the (*R*)-auxillary in the case of *tert*-butyl acetates, whereas the equivalent *tert*-butyl isobutyrate reaction yields the (3*S*) configuration as the major diastereomer. The high dr obtained with ethyl acetate and the switchover in diastereoselectivity induced by the addition of HMPA confirms the hypothesis that the acetate mediated reaction proceeds through a six-membered Zimmerman–Traxler-type transition state, where coordination to titanium is essential for the high diastereoselectivity.[16, 17]

To establish the stereochemistry of the product from entry 1, the compound was re-esterified to the *tert*-butyl ester, since the *tert*-butyl ester alcohols in most cases were crystalline. Gratifyingly, the alcohol **13** crystallized and the stereochemistry was determined by X-ray crystallography. Furthermore, an acid labile protection group for the carboxylic acid was required to obtain orthogonality. This strategy nicely provided the Fmoc- and Boc-protected β-

amino acids **15** and **16** (Scheme 1).

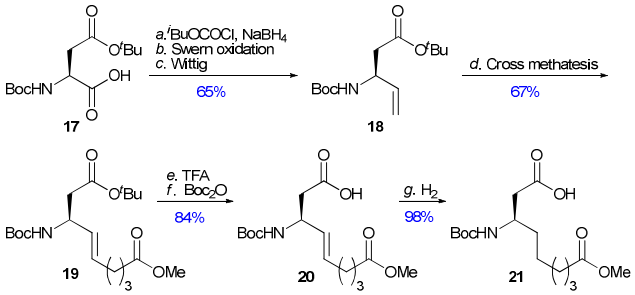

Scheme 2. (a) N-methylmorpholine (1.0 equiv), isobutyl chloroformate (1.0 equiv), $NaBH_4$ (3.0 equiv), MeOH, THF, –30 ºC → rt, 160 min. (b) oxalyl chloride (1.7 equiv), DMSO (3.3 equiv), Et_3N (5.0 equiv.), CH_2Cl_2, –78 ºC → –40 ºC → rt, 2 h. (c) PPh_3CH_3Br (2.2 equiv), KHMDS (0.5 M in toluene) (2.1 equiv), THF, –78 ºC → rt, 4 h. (d) methyl 5-hexenoate (3 equiv), Hoveyda Grubbs 2nd gen. catalyst (0.1 equiv), CH_2Cl_2, 40 ºC, 24h. (e) TFA–CH_2Cl_2 (1:3), 2 h. (f) Boc_2O (1.3 equiv.), $^iPr_2NEt$ (2.6 equiv.), CH_2Cl_2. (g) H_2, Pd/C (1% w/w), THF, 19 h.

The building blocks used to synthesize compound **8a-c** and **9a-c** were prepared from the readily available Boc-L-Asp-O^{t}Bu **17** (scheme 2). Using a slightly modified procedure from Bradner *et al*[18], acid **17** was reduced to the corresponding alcohol and a subsequent Swern oxidation yielded the aldehyde, which was used immediately in a Wittig reaction to produce the terminal alkene **18**. The optimal conditions for the succeeding cross methathesis was found to be Hoveyda-Grubbs 2nd generation catalyst (see table 2), which afforded the *trans* olefin in a good yield. Acidic deprotection followed by reprotection of the amino functionality gave the final building block (**20**) for synthesis of **8** whereas hydrogenation of **20** gave the desired *β*-amino acid **21** for the synthesis of **9** (Scheme 2).

Table 2. Catalyst screening for cross-metathesis.

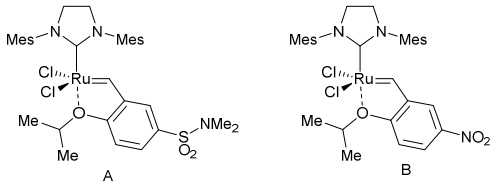

entry	catalyst	yield (%)[a]
1	Grubbs cat. 1st gen., 0.1 equiv	11
2	Grubbs cat. 2nd gen., 0.05 equiv	54
3	Grubbs cat. 2nd gen., 0.1 equiv	62
4	Hoveyda Grubbs cat. 1st gen., 0.1 equiv	12
5	Hoveyda Grubbs cat. 2nd gen., 0.1 equiv	67
6	catalyst A	62
7	catalyst B	52

[a] Isolated trans isomer.

Peptide synthesis

All the synthesized building blocks were coupled to a tripeptide on solid support, which after deprotection and cleavage were cyclized using HATU or COMU under dilute conditions (0.3–0.8 mM). Saponification of the cyclic peptides gave the final compounds (scheme 3). The modest isolated yields for most compounds can be attributed to the difficulties in the cyclization of small rings. Furthermore, solubility problems resulted in problems during the final HPLC purification. The synthesis of the tryptophan analogues proved particularly challenging, revealed by an unsuccessful synthesis of **9c** by the original synthetic route. Changing the point of cyclization had previous shown to have an effect on a simplified linear tetrapeptide.[15] The Boc protection group of **21** was therefore substituted for an Fmoc group, allowing the building block to be loaded directly on to the resin. Even though we expected a better cyclization reaction, using the less hindered and more flexible *β*-amino acid at the C-terminal, we were surprised to find the dramatic effect this alteration had, when we isolated **9c** with a yield of 48% (12 steps) from the Fmoc building block (supplementary scheme S2). This result emphasise the importance of the peptide sequence and its impact on the conformation of the linear tetrapeptide.[19]

Biochemical profiling

All nine desmethylated compounds were characterized with dose–response experiments on recombinant human HDACs. The screening protocols were adapted from Villadsen *et al*.[15] Full profiling was performed on class I, class IIb, and class IV. Low activity at concentrations between 10–100 μM was observed with single experiment data on HDAC4 and HDAC7 for all tested compounds. This result confirms the lack of class IIa activity previously reported with this type of inhibitors and activity towards class IIa was not explored further.[15] Preliminary testing of the dimethylated series (**6a–c**) indicated low activity against class I, class IIb, and class IV. With this in mind, these compounds were only screened at two concentrations (10 and 20 μM, see SI, table S1).

The Phe and Tyr-containing analogs (**6a** and **6b**) were poor inhibitors of HDAC1–3 and no inhibition was observed on HDAC6, HDAC8, HDAC10, and HDAC11 at 20 μM. However, **6c**, containing a tryptophan as the aromatic residue, displayed activity against HDAC1–3 (~50% inhibition at 10 μM). **6c** also inhibited HDAC6, HDAC8, HDAC10, and HDAC11, albeit none of the isoforms were inhibited more than 50% at 20 μM. The positive effect of tryptophan indicates that this aromatic amino acid is superior to Phe and Tyr in establishing favorable interactions with the surface of the HDAC enzymes. Overall, the low activity of **6a–6c** emphasize how sensitive the β^2-position is to modifications. The incorporation of the extra methyl group could induce a change in the overall conformation of the cyclic peptides, which may explain the loss of activity. The second methyl group, which will be located *trans* to the Zn^{2+}-coordinating side chain, could also be involved in a steric clash with the protein, leading to the reduced activity.

The IC_{50} values obtained from the dose–response data on the desmethylated compounds were converted to K_i values using the

Cite this: DOI: 10.1039/c0xx00000x

www.rsc.org/xxxxxx

EDGE ARTICLE

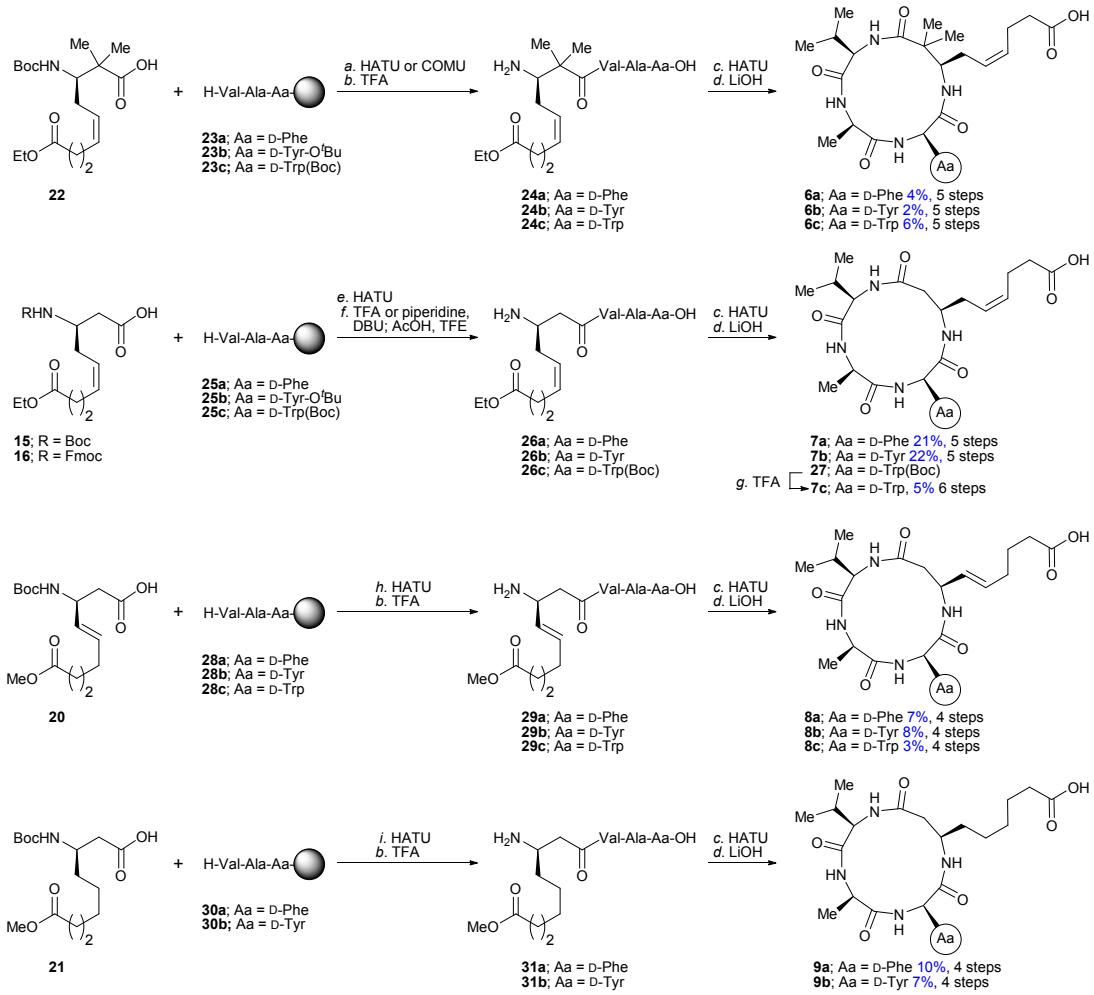

Scheme 3. Reagents and conditions: (*a*) Resin (1.5 equiv), **22** (1.0 equiv)**,** HATU or COMU (1.5 equiv), *i*Pr$_2$NEt (3.0 equiv), DMF, 16 h or **22** (1.1 equiv), resin (1.0 equiv), HATU (1.5 equiv), *i*Pr$_2$NEt (3.0 equiv), DMF, 17 h (*b*) TFA–CH_2Cl_2 (1:1), 2 × 30 min. (*c*) HATU (1.5–2.2 equiv), *i*Pr$_2$NEt (5–10 equiv), DMF (0.4 mM peptide concentration), 16 h. 17–21 h (*d*) LiOH (36–50 equiv), THF–water (1:1), 16–17 h. (*e*) Resin (1.0 or 1.5 equiv), HATU (1.5 equiv), 2,6-lutidine (3.0 equiv), **15** or **16** (1.1 or 1.0 equiv), DMF, 16 h. (*f*) TFA–CH_2Cl_2 (1:1), 2 × 30 min or piperidine–DMF (1:4, 2 × 30 min); DBU–piperidine–DMF (2:2:96, 30 min); AcOH–TFE–CH_2Cl_2 (6:2:2, 1.5 mL), 2 × 2 h. (*g*) TFA–CH_2Cl_2 (1:1), 1 h.

Cheng-Prusoff equation and the K_m values reported previously.[15] The result are shown in table 2. Compounds **7a-c** address the importance of the β^2-methyl group found in the azumamide A and E. The desmethylated analogs show a 3–18-fold decrease in activity towards HDAC1–3. The greatest difference is observed on HDAC3, where **7a** displays an 18–fold reduction in activity compared to azumamide E. A 7–8-fold decrease in activity was observed on HDAC10 and for class IV a 13–14-fold reduction in activity was observed. Based on these results the β^2-methyl group may participate in a favorable hydrophobic interaction with the surface of the protein. However, docking studies of an NMR solution structure of azumamide E into Histone Deacetylase Like Protein (HDLP) did not reveal any interactions for the β^2-methyl group.[7] Instead, the removal of the methyl group could induce changes in the conformation of the cyclic peptide backbone. Conformational changes could alter the orientation (C_3–C_4 vector) of the β^3-side chain and or disrupt the favorable interactions between the macrolactam ring and the protein.[9] Finally, the β^2-methyl group may provide steric direction of the Zn^{2+}-binding side chain towards the 11 Å channel. The methyl group was found to be less important for inhibition of HDAC6 and HDAC8 where the reduction in activity was below 2-fold. Interestingly, these two enzymes were highly sensitive to the nature of the aromatic amino acid. The Tyr and Trp-containing compounds were 2–5-fold more active on HDAC1–3, HDAC10, and HDAC 11 than the corresponding phenylalanine compounds. In contrast to Tyr and Trp, the side chain in Phe is unable to participate in hydrogen bonding to the surface of the enzyme and it could be hypothesized

Cite this: DOI: 10.1039/c0xx00000x

www.rsc.org/xxxxxx

EDGE ARTICLE

Table 1. Activities of desmethylated compounds against selected HDAC enzymes given as K_i values (nM)[a]

	class I				class IIb		class IV
Compound	HDAC1	HDAC2	HDAC3	HDAC8	HDAC6	HDAC10	HDAC11
7a: Phe, cis	300±130	500±70	500±80	6,700±870	>20,000	140±20	900±130
7b: Tyr, cis	200±117	100±35	200±143	>20,000	3,500±360	80±3	400±198
7c: Trp, cis	100±65	100±7	300±78	3000±354	>20,000	70±18	500±357
8a: Phe, unsat.	700±180	900±20	800±160	4,300±1,800	>20,000	>20,000	1,800±300
8b: Tyr, unsat.	400±130	300±140	300±130	>20,000	1,300±480	150±2	700±210
8c: Trp, unsat.	300±40	200±150	300±220	1,700±1,030	2,200±180	130±2	600±300
9a: Phe, sat.	500±200	400±60	400±120	6,400±2900	>20,000	260±80	1200±640
9b: Tyr, sat.	400±340	200±100	100±80	>20,000	2000±1,120	80±40	500±410
9c: Trp, sat.	600±70	800±190	1,200±460	6,100±390	>20,000	190±30	1,600±900

[a]The IC_{50} values were obtained from two individual dose-response experiments.

that the reduced activity of Phe-containing compounds is related to this feature. In contrast, the tyrosine containing compounds failed to inhibit HDAC8 at concentration up to 20 μM, whereas the Phe- and Trp-containing compounds displayed K_i values between ~2–7 μM. The same, but less pronounced, effect were observed in the natural products, where azumamide C was 2-fold more potent than azumamide E on HDAC8. Surprisingly, **8c**, **7c**, and **8a** were more active against HDAC8 than the natural products. In terms of isoform selectivity our data suggest that the incorporation of tyrosine favors the inhibition of HDAC6, with the exception of **8c.**

The β^3-side chain modifications **(8a–c** and **9a–c)** cannot be related directly directly to the azumamides, as the removal of the β^2-methyl group had an important impact on activity. It is currently not known if the modifications are synergistic or antagonistic, but this study shows that the shifted *trans* double bond decrease activity towards HDAC1–3, 10, and 11 with a 1.5–3-fold reduction in activity compared to the *cis*-compounds. In contrast, the *trans* series was more active against HDAC6 and 8.

Introduction of the saturated side chain did not show a clear trend for the Tyr- and Phe-containing compounds. On HDAC1 and 2 the saturated analogs were slightly less active than the corresponding *cis*-compounds, whereas **9a** and **9b** were more active than **7a** and **7b** on HDAC3. **9c** displayed a 2–8-fold reduction in activity against the entire selection of enzymes..

Interestingly, all nine desmethylated analogs are more active against the entire panel of enzymes, than the natural products bearing a carboxyamide as the zinc-binding group (azumamide A, azumamide B, and azumamide D). This can be attributed to the difference in the zinc-binding groups (COOH *vs* $CONH_2$). The carboxylic acid is a stronger zinc-chelator than the carboxyamide[20] and the loss of activity, associated with removal of the methyl group, is regained by having a stronger zinc-chelating functionality.

NMR solution structures

In order to correlate the biochemical data presented above with distinct structural features in the cyclic peptide structures we, elucidated the NMR solution structures of azumamide A[15] and **7b.** In combination with the assay date these structures can provide a powerful tool for establishing important structure activity relationships (SAR). The NMR experiments were performed in DMSO at 295 K and NMR solution structures were obtained using ROESY correlations. An overlay of the two structures is shown in figure 2.

Figure 2. Overlay of NMR solution structures of compound **7b** (carbon: green, hydrogen: white, oxygen: red, nitrogen: blue) and azumamide A (carbon: grey, hydrogen: white, oxygen: red, nitrogen: blue). The β^3-side chain beyond C_6 have been omitted for clarity. The superimposition was made on all atoms in the cyclic peptide backbone

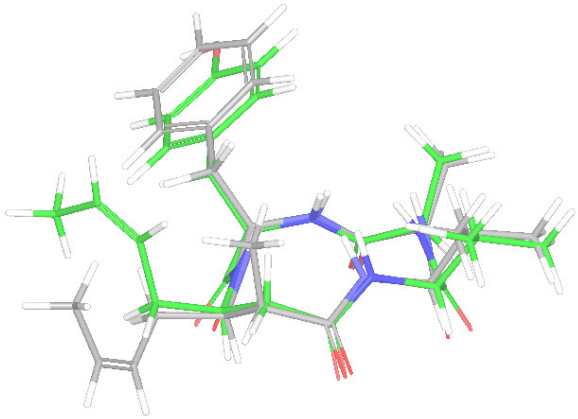

Figure 2 illustrates that the cyclic peptide backbone for azumamide A and **7b** overlay almost perfectly. Based on these structures the removal of the β^2-methyl group does not induce any changes to the conformation of the peptide backbone. This observation excludes the hypothesis that changes in the conformation of the cyclic peptide is responsible for the loss of activity. As mentioned above the C_3–C_4 vector has been found to be important for activity in cyclic peptide HDAC inhibitors. In figure 2, the C_3–C_4 vector of **7b** is only slightly different from the vector found in azumamide A and both vectors are projected in the plane of the cyclic peptide backbone. However, beyond C_4 the two structures appear to be different. In **7b** the C_4–C_5 bond is projected upwards, thus positioning the β^3-side chain above the cyclic peptide backbone. In azumamide A the C_4–C_5 bond is projecting downwards, which positions the side chain in the plane or slightly under the macrolactam ring. It could be hypothesixed that the zinc-binding side chain in azumamide A is forced away from the top face of the ring by the neighboring methyl group. In compound **7b**, lacking the β^2-methyl group, the β^3-side chain is free to occupy the space above the ring and this could explain the difference in the side chain orientations. If this difference should be related to the biological data, it could be hypothesized that β^3-side chain positioning found in azumamide A is optimal for HDAC inhibition.

Docking in HDAC3

In order to explore the hypothesis that the difference in β^3-side chain positioning is responsible for the difference in activity, we are performing a docking study of **7b**, azumamide C, and **6b** in HDAC3. The investigations are ongoing.

Testing in cell lines

The testing is ongoing.

References

1. M. J. Peart, G. K. Smyth, R. K. van Laar, D. D. Bowtell, V. M. Richon, P. A. Marks, A. J. Holloway and R. W. Johnstone, *Proceedings of the National Academy of Sciences of the United States of America*, 2005, **102**, 3697-3702.
2. J. H. Beumer and H. Tawbi, *Current clinical pharmacology*, 2010, **5**, 196-208.
3. A. Bowers, N. West, J. Taunton, S. L. Schreiber, J. E. Bradner and R. M. Williams, *J Am Chem Soc*, 2008, **130**, 11219-11222.
4. S. J. Darkin-Rattray, A. M. Gurnett, R. W. Myers, P. M. Dulski, T. M. Crumley, J. J. Allocco, C. Cannova, P. T. Meinke, S. L. Colletti, M. A. Bednarek, S. B. Singh, M. A. Goetz, A. W. Dombrowski, J. D. Polishook and D. M. Schmatz, *Proceedings of the National Academy of Sciences*, 1996, **93**, 13143-13147.
5. Y. Nakao, S. Yoshida, S. Matsunaga, N. Shindoh, Y. Terada, K. Nagai, J. K. Yamashita, A. Ganesan, R. W. M. van Soest and N. Fusetani, *Angewandte Chemie International Edition*, 2006, **45**, 7553-7557.
6. Y. Nakao, S. Yoshida, S. Matsunaga, N. Shindoh, Y. Terada, K. Nagai, J. K. Yamashita, A. Ganesan, R. W. M. van Soest and N. Fusetani, *Angewandte Chemie*, 2006, **118**, 7715-7719.
7. N. Maulucci, M. G. Chini, S. Di Micco, I. Izzo, E. Cafaro, A. Russo, P. Gallinari, C. Paolini, M. C. Nardi, A. Casapullo, R. Riccio, G. Bifulco and F. De Riccardis, *Journal of the American Chemical Society*, 2007, **129**, 3007-3012.
8. K. E. Cole, D. P. Dowling, M. A. Boone, A. J. Phillips and D. W. Christianson, *Journal of the American Chemical Society*, 2011, **133**, 12474-12477.
9. A. Montero, J. M. Beierle, C. A. Olsen and M. R. Ghadiri, *Journal of the American Chemical Society*, 2009, **131**, 3033-3041.
10. R. Furumai, Y. Komatsu, N. Nishino, S. Khochbin, M. Yoshida and S. Horinouchi, *Proceedings of the National Academy of Sciences*, 2001, **98**, 87-92.
11. A. V. Bieliauskas and M. K. H. Pflum, *Chemical Society Reviews*, 2008, **37**, 1402-1413.
12. S. Minucci and P. G. Pelicci, *Nat Rev Cancer*, 2006, **6**, 38-51.
13. S. Wen, K. L. Carey, Y. Nakao, N. Fusetani, G. Packham and A. Ganesan, *Organic Letters*, 2007, **9**, 1105-1108.
14. S. Chandrasekhar, C. L. Rao, M. Seenaiah, P. Naresh, B. Jagadeesh, D. Manjeera, A. Sarkar and M. P. Bhadra, *The Journal of organic chemistry*, 2008, **74**, 401-404.
15. J. S. Villadsen, H. M. Stephansen, A. R. Maolanon, P. Harris and C. A. Olsen, *Journal of Medicinal Chemistry*, 2013, **56**, 6512-6520.
16. T. P. Tang and J. A. Ellman, *The Journal of organic chemistry*, 2002, **67**, 7819-7832.
17. T. Fujisawa, Y. Kooriyama and M. Shimizu, *Tetrahedron Letters*, 1996, **37**, 3881-3884.
18. A. A. Bowers, T. J. Greshock, N. West, G. Estiu, S. L. Schreiber, O. Wiest, R. M. Williams and J. E. Bradner, *J Am Chem Soc*, 2009.
19. C. J. White and A. K. Yudin, *Nat Chem*, 2011, **3**, 509-524.
20. D. Wang, P. Helquist and O. Wiest, *The Journal of organic chemistry*, 2007, **72**, 5446-5449.